

NON-LINEAR FINITE ELEMENT ANALYSIS
OF
WALL-BEAM STRUCTURES

BY
MD. MONJUR HOSSAIN, BSc. Engg., MSc. Engg.

A THESIS SUBMITTED IN PARTIAL FULFILMENT OF THE
REQUIREMENTS FOR THE DEGREE OF
DOCTOR OF PHILOSOPHY

DEPARTMENT OF CIVIL ENGINEERING
BANGLADESH UNIVERSITY OF ENGINEERING AND TECHNOLOGY
DHAKA

MAY, 1997

DECLARATION

I hereby certify that the work embodied in this thesis is the result of original research performed by me and has not been submitted for a higher degree to any other University.

Md. Monjur Hossain



Affectionately dedicated

to my wife and children
for their sacrifice and forbearance during this research.

ABSTRACT

The composite action between masonry wall and its supporting beam concentrates the vertical loading applied on the top of wall close to the beam supports. This produces bending moments much less than would be expected when the full load is acting directly on the beam. The study of this composite action is of economic importance since if the concept is utilised, a rational design of the beam will be achieved.

This thesis presents a comprehensive material model and its incorporation into non-linear finite element computer model for the analysis of wall-beam structures made with brickwork of solid brick subjected to uniformly distributed load. The program is incremental in nature and capable of reproducing the non-linear behaviour caused by material non-linearity and progressive local cracking and crushing. The program is thus capable of modelling the behaviour of wall-beam structures subjected to non-linear load from first crack to final failure. The material model used in this program is derived from tests on representative samples of brick, mortar and small samples of brickwork.

In the finite element model brick, mortar, concrete and steel are treated as separate materials along with the simulation of actual directional effects of mortar joints. A series of failure criteria have been adopted to model the different modes of failure experienced in the constituent materials. Due to the crack sensitive nature of the problem, particular emphasis has been given to the modelling of cracking and the post-cracking behaviour of the materials, especially the manner in which the local stresses in the fractured region are redistributed.

The results of finite element model have been verified by comparison with experiments on brick masonry wall-beam structures subjected to uniformly distributed load applied at the top and extending over the full length and thickness of the wall. Comparison with published literature reveals that the present method can provide a more comprehensive prediction of behaviour of the wall-beam structure up to failure load.

Sensitivity analyses of the various parameters defining the material model and the boundary conditions have been carried out. With the important parameters thus obtained, the finite element model has been used to carry out a comprehensive parametric study of the behaviour of storey height wall-beams subjected to uniformly distributed load. Based on the findings of this study, design recommendations have been proposed. As the computer program developed can handle general cases with arbitrary geometry, loading and boundary conditions, recommendations for investigations of various other wall-beam structures have been made.

ACKNOWLEDGEMENT

I take this opportunity to express my gratitude to my supervisors Professor M. Azadur Rahman and Professor Sk. Sekender Ali for their invaluable advice and guidance throughout the course of this research. Thanks are also expressed to Professor S. Ahmad and Professor J. R. Choudhury for their participation in some of the tests of wall-beam panel. Mention must also be made of their constructive criticism and comments at various stages of this research program.

Thanks are also due to other faculty members and contemporary research workers of the Department of Civil Engineering who offered their co-operation from time to time.

Thanks are due to the staff of concrete laboratory, structures and materials laboratory, sheet metal shop, wood work shop and central instrument section of this university for their help during the experimental work.

I also extend my sincere appreciation to Professor M. A. Hannan, Director, B I T Khulna, who extended his helping hand and all out co-operation to enable me complete the research.

2.4	Summary	35
CHAPTER 3 ELASTIC FINITE ELEMENT ANALYSIS		37
3.1	Introduction	37
3.2	General Description of Finite Element Method	37
3.3	Two Dimensional Linear Elastic Finite Element Model	40
3.3.1	Selection of Finite Element Mesh	41
3.3.2	Reinforcement of the Supporting Beam	45
3.3.3	Finite Element Discretization and Boundary Condition	49
3.4	Verification of the Computer Model	50
3.4.1	Deflection of a Simply Supported Beam	50
3.4.2	Splitting Test of Brickwork Specimen	51
3.4.3	Comparison of existing Experimental Result	54
3.4.4	Comparison with Analytical Result	55
3.4.5	Comparison of Bending moment in Supporting Beam	60
3.4.6	Comparison with the Empirical Equation	62
3.5	Arching Action	64
3.6	Parametric Study of Wall-Beam Structure	68
3.6.1	Effect of Height of Brick wall	70
3.6.2	Effect of Modulus of Elasticity	72
3.6.2.1	Mortar	72
3.6.2.2	Brick	72
3.6.2.3	Concrete	72
3.6.3	Effect of Depth of Supporting Beam	72
3.6.4	Effect of Reinforcement in Supporting Beam	76
3.6.5	Effect of vertical Edge Columns	79
3.6.6	Effect of Opening in Wall-beam	79
3.6.7	Effect of Support Width	81
3.6.8	Effect of Column Height	83
3.7	Summary	88
CHAPTER 4 BRICK, MORTAR AND BRICK MASONRY PROPERTIES		90
4.1	Introduction	90
4.2	Brick Properties	91
4.2.1	Compressive Strength of Brick	91
4.2.2	Tensile Strength of Brick	92

4.2.3	Deformation Characteristics of Bricks	93
4.2.3.1	Load Parallel to Bed Joint	93
4.2.3.2	Load Normal to Bed Joint	94
4.2.4	Poisson's Ratio of brick	96
4.3	Mortar Properties	97
4.3.1	Compressive Strength of Mortar	98
4.3.2	Tensile Strength of Mortar	98
4.3.3	Deformation Characteristics of Mortar	99
4.3.4	Poisson's Ratio of Mortar	99
4.4	Brick Masonry Tests	100
4.4.1	General	100
4.4.2	Uniaxial Compression Test of Stack Bonded Prism Load Normal to the Bed Joint	102
4.4.3	Deformation Characteristics of Mortar Joint	102
4.4.4	Shear Tests on Brick Masonry with Sloping Bed Joint	105
4.4.5	Simplified Approximation of the Bond failure Surface	108
4.4.5.1	Tensile Bond Strength	109
4.4.5.2	Shear Bond Strength	110
4.5	Properties of Concrete	110
4.6	Summary	113

CHAPTER 5	MATERIAL MODEL FOR NON-LINEAR FINITE ELEMENT ANALYSIS	115
5.1	Introduction	115
5.2	Material Deformation Characteristics	115
5.2.1	Constitutive Relations for Brick and Concrete before Failure	116
5.2.2	Constitutive Relations for Mortar Joint before Failure	118
5.3	Non linearity Due to Progressive Cracking	120
5.3.1	Crack Modelling	120
5.4	Failure Criteria	124
5.4.1	Joint Bond failure	125
5.4.2	Cracking and Crushing of Brick, Mortar and Concrete	125
5.5	Behaviour of the Materials after Failure	128
5.5.1	Stress-Strain Relations after Failure	129
5.5.2	Redistribution of Stresses in the Failure Regions	131

5.5.3	Further Cracking or Crushing of the Cracked Material	133
5.6	Summary	136
CHAPTER 6 NON-LINEAR FINITE ELEMENT PROGRAMS		137
6.1	Introduction	137
6.2	Finite Element Selection	137
6.3	Non-linear Analysis	138
6.3.1	Solution Techniques	139
6.3.2	Solution Method for Incremental-Iterative Procedure	141
6.3.3	Constitutive Equations for the Incremental-Iterative Solution Procedure	141
6.3.4	Convergence Criteria for Iterative Solutions	144
6.4	The Non-linear Finite Element Program	145
6.4.1	Program "WBMGEN"	146
6.5	Summary	149
CHAPTER 7 EXPERIMENTAL VERIFICATION OF THEORETICAL MODEL		150
7.1	Introduction	150
7.2	Tests on Wall-Beam Panels	150
7.2.1	Panel Details	151
7.2.2	Panel Construction	151
7.2.3	Testing of the Panels	154
7.2.4	Modes of Failure	155
7.3	Theoretical Analysis of the Tests	156
7.3.1	Modelling of the Tests	156
7.3.2	Analysis and Results	157
7.4	Comparison of Theory and Experiment	163
7.4.1	Initial Cracking Load	163
7.4.2	Failure Pattern	164
7.4.3	Failure Load	166
7.5	Comparison of Strains	173
7.5.1	Horizontal strains down the centre line of wall-beam	173
7.5.2	Vertical strain along the first brick course	175
7.5.3	Horizontal strain in the supporting beam	176
7.6	Summary	181



CHAPTER 8 SENSITIVITY ANALYSIS OF CRITICAL PARAMETERS 182

8.1	Introduction	182
8.2	Parameters Affecting the Material Model	182
8.2.1	Influence of Elastic Properties of the Constituents	182
8.2.2	Influence of Joint Thickness	188
8.2.3	Influence of Brick Tensile Strength	189
8.2.4	Influence of Mortar Tensile Strength	192
8.2.5	Linear Elastic Fracture Analysis	206
8.2.6	Influence of Joint Bond Strength	207
8.3	Parameters Affecting the Finite Element Analysis	210
8.3.1	Element Type, Size and Subdivisions	210
8.3.2	Boundary Conditions	214
8.4	Summary	216

CHAPTER 9 PARAMETRIC STUDY AND DESIGN RECOMMENDATIONS 205

9.1	Introduction	205
9.2	Finite Element Analysis of Story Height Panel	205
9.3	Parametric Study of Story Height Wall-beam Panel	206
9.4	Design Aspects of Wall-beam Structure	208
9.4.1	Deduction of Non Dimensional Characteristics Parameters	209
9.4.2	Bending Moment in Supporting Beam	210
9.4.3	Tie Force in Supporting Beam	216
9.4.4	Maximum Vertical Stress in Wall	218
9.4.5	Maximum Shear Stress in Wall	220
9.5	Comparison of Results Obtained from the Proposed Design Formula	222
9.5.1	Comparison of Proposed Empirical Formulae with Finite Element Analyses	225
9.5.2	Comparison Between Proposed Empirical formulae and existing formulae	228
9.6	The Design Problem	234
9.6.1	Estimate of Critical Actions	236
9.6.2	Adequacy of Beam Section and Reinforcement	238

9.6.3	Illustration of Economy in Design of Wall-beam Structure	240
9.6.4	Some Additional Practical Considerations for Composite Action of Wall-beam Structure	242
9.7	Summary	255
CHAPTER 10	CONCLUSIONS AND FURTHER RECOMMENDATIONS	258
REFERENCES		262
APPENDIX I	RECTANGULAR AND QM6 ELEMENT	A1
APPENDIX II	BRICK, MORTAR AND BRICK-MASONRY PROPERTIES	A11
APPENDIX III	PROGRAM "WBMGEN"	A30
APPENDIX IV	EXPERIMENTAL VERIFICATION OF THEORETICAL MODEL	A45
APPENDIX V	PARAMETRIC STUDY AND DESIGN RECOMMENDATIONS	A55

NOTATION

The following general terminology has been adopted.

- $\{ \}$ Denotes a column vector
- $[\]$ Denotes a row vector or a matrix
- $[\]^T$ Denotes the transpose of a matrix or a column vector

a_s, a_n	Constant of normal stress defining inelastic stress-strain equation
$[B]$	Strain-displacement transformation matrix
B	Width of support along the span
b_s, b_n	Constants of shear stress defining inelastic stress-strain equation
c_1, c_2	Non dimensional characteristic parameter
D	Equivalent diameter
$[D]$	Material constitutive matrix
$[D_f]$	Modified material constitutive matrix after failure
$\{d\}$	Displacement vector
E	Young's modulus of elasticity
EA	Elastic Analysis
E_{cs}	Secant modulus of elasticity
E_0	Initial tangent modulus
E_t	Instantaneous tangent modulus
F'_m	Compressive strength of masonry
FNH	Fine mesh for non-homogeneous solutions
FR	Clear span ratio
$\{F\}$	Vector of nodal forces
f_m	Maximum vertical stress in wall
f_s	Ultimate shear strength of masonry
f_{bs}	Shear bond strength
G	Shear modulus
H	Height of brick wall
h	Depth of supporting beam
H'	Hardening parameter
I	Moment of inertia of supporting beam
K	Coefficient for maximum tie force in supporting beam
$K1$	Coefficient for maximum moment in supporting beam
$[K]$	Stiffness matrix
L	Length of wall-beam structure
M	Maximum bending moment in supporting beam

MH	Medium size mesh for homogeneous solutions
m	Modular ratio of brick to mortar
NLA	Non-linear Analysis using Strain Softening
P_b	Permissible masonry compressive stress
P_f	Cracking load
P_{st}	Permissible steel bending stress
S	Standard deviation
S_c	Shear stress concentration
T	maximum tie force in supporting beam
T_b	Thickness of brick
T_m	Thickness of mortar
[T]	Transformation matrix
t	Thickness of wall
u	Horizontal displacement
V_c	Vertical stress concentration
v	Vertical displacement
W	Total vertical top loading including wall self weight
w	Intensity of load on top of wall
X	Global co-ordinate (normally horizontal)
Y	Global co-ordinate (normally vertical)
Z	Section modulus of supporting beam
ϵ	Strain
σ	Compressive stress
ψ	Angle of cracking
μ	Co-efficient of friction
η	Natural co-ordinate (normally vertical for rectangular element)
ξ	Natural co-ordinate (horizontal for rectangular element)
τ_m	Maximum shear stress
ν	Poisson's ratio

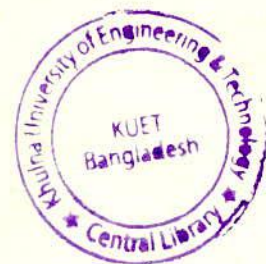
Subscripts

b	Brick
c	Concrete
cr	Cracking
m	Mortar
n	Normal direction
p	Parallel direction

x	X-direction
y	Y-direction
w	masonry or prism
1	Major principal direction
2	Minor principal direction

Superscripts

e	Elastic
p	Plastic
T	Transpose
t	Total



CHAPTER 1

INTRODUCTION

1.1 INTRODUCTION

Masonry wall supported on reinforced concrete or steel beam is a common feature of residential, commercial and factory buildings. Yet the attention of the designers on the wall-beam composite system is very inadequate. Lack of rational analysis and well-defined design procedures, and limited test data are the main reasons behind this; as a result this structural component is over designed in most of the cases. During a series of tests carried out by Building Research Station, U. K., very low amount of anticipated stresses have been observed by Mainstone (1960). It is of course in a broader sense evident that the stress reductions were produced as a result of the composite action between the elements. However, it is necessary to determine how these reductions take place and to what extent.

The wall-beam structure can be categorised as any type of masonry wall that transfers in-plane vertical loads applied on the top of the masonry wall down to the supporting beam. Masonry may be of any combination of materials, e.g. stones, clay bricks, concrete block, lime mortar (calcium silicate) block with mortar made from cement sand of any practical proportion (with or without additives). The supporting member may be reinforced concrete or steel beam. The walls are mainly looked upon as space separator or at best a load transferring media. But when the proper interaction between wall and its supporting beam is considered, the material consumption in the supporting beam can be reduced considerably.

Until recently, it was customary to design beams and lintels carrying brickwork walls so as to be capable of supporting a triangular load of brickwork where the base of the triangle is the span of the beam, provided that the remainder of the brickwork is adequately supported, (see Fig. 1.1). If the wall was carrying any superimposed load above the apex of the triangle, it was not clear what portion if any of the extra load should be taken into account and it was frequently ignored. More conservative approach was to distribute the total superimposed load uniformly on top of the supporting beam. However this is far from the actual behaviour. Since 1952, this traditional concept has become questionable. The theoretical and experimental studies in previous years have resulted in a better understanding of the problem. It was found that due to arching effect (see Fig. 1.2)

in brickwork the brick panel and supporting beam form a composite deep beam, with the supporting beam acting as a tie for the panel as a whole. A greater overall stiffness is thus achieved. As a result a smaller share of the applied load is transmitted to the supporting beam. With this small share of load it was possible to recommend a design moment for the supporting beam as low as $WL/100$. It was also observed that the bending moment induced in the beam depend on the relative stiffness of the beam and wall. Stiffer the beam greater is the amount of load transmitted on the beam at the mid span. Thus for a very flexible supporting beam considerable degree of arching action can be expected to occur in the panel. The bond between the beam and the panel is of prime importance for the proper interaction between wall and the supporting beam. In case of bond failure, the supporting beam at the interface level will carry the superimposed load and the load of the masonry wall as uniformly distributed over the span. As a result the interactive response of the wall-beam disappears.

1.2 BACKGROUND OF RESEARCH

The behaviour of wall-beam structure was first investigated in 1952 by Wood. Later Rosenhaupt (1962) and Burhouse (1969) carried out similar tests. All of them agreed that the moment in the supporting beam of such structure will be much less than if the same load be distributed on the beam. Recently, Annamalai, et.al.,(1984) carried out tests on reinforced brick wall thin lintels to study the composite action. Their experimental results also supported the conclusion made by the previous investigators.

All these investigators observed the concentration of vertical stress near the support that initiated the failure before yielding of supporting beam. They recommended that the moment in the beam supporting the wall was much less than if the load would be uniformly distributed on the span. But these recommendations vary widely from country to country reflecting the empirical nature of the problem. This is possibly due to the size, type and variability in the material properties of the specimens adopted during the experiments.

In the previous years due to the variability in test results the researchers simultaneously worked with the mathematical and computer modelling to model the actual behaviour of wall-beam structure. The analytical works in the field includes the Airy's stress function of Rosenhaupt (1964), variational approach of Coull (1966), the lattice analogy of Colbourne (1969), equivalent stress block of

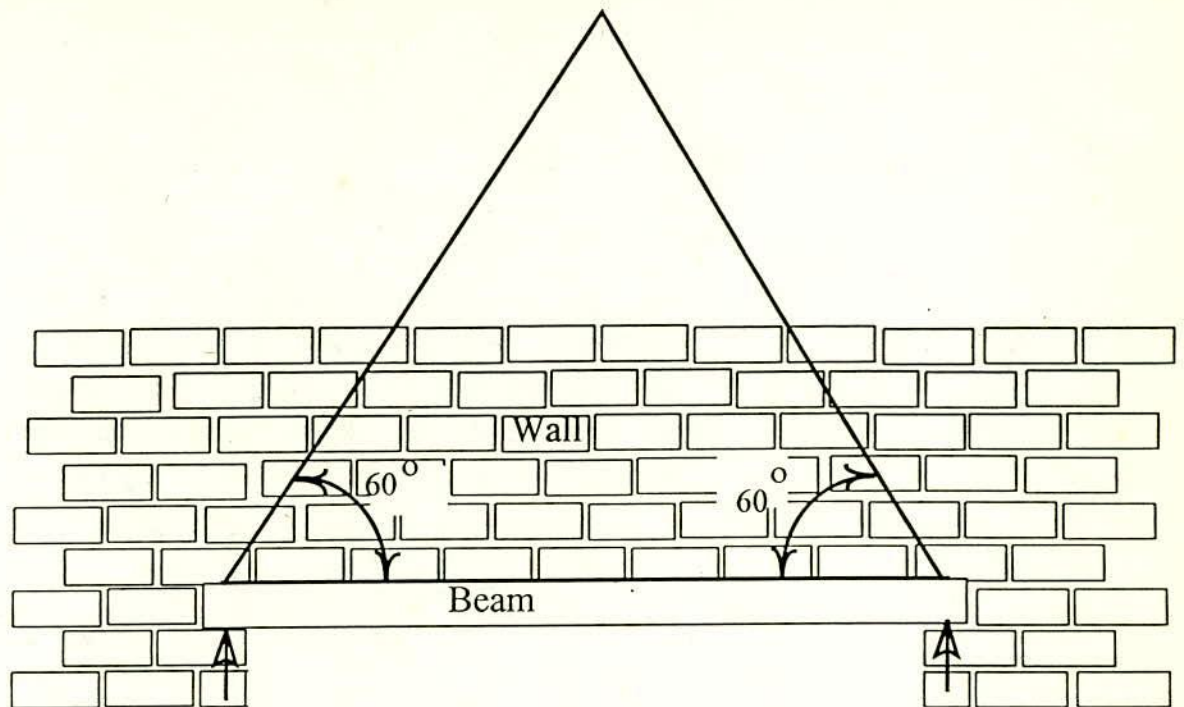


Fig. 1.1 Conventional Concept of Design Load for Supporting Beam of Wall-Beam Structure (e.g. Lintel)

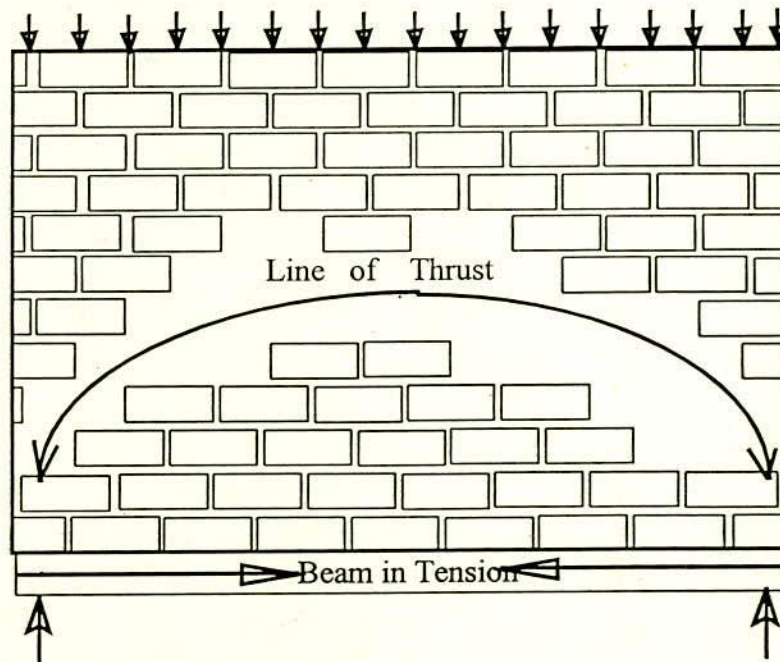


Fig. 1.2 Tied Arch Action of Wall-Beam Structure

Wood and Simms (1969) and shear lag method of Yettram and Hirst (1974). Ramesh et al. (1970) analysed the problem by expressing the displacement in the form of multiple Fourier series and Green (1972) unlike other analysts considered the wall-beam system as a beam on elastic foundation.

With the advent of electronic computer, finite element method of stress analysis for wall-beam structure was adopted by the researchers (Ahmed (1977), Davies and Ahmed (1978), Stafford Smith and Riddington (1977), Yisun et al. (1985) and Kamal (1990)) to make a close study of such highly indeterminate structure.

All the analyses performed at that time were hampered due to lack of representative material model for masonry. In most of the cases the masonry was considered as a homogeneous media with the assumption of isotropic linear elastic behaviour for the constituent material. But in wall-beam structure the brickwork consists of brick and mortar joints (bed joints and header joints). The beam consists of concrete and reinforcement and interface between the wall and supporting beam. All these components behave differently when loaded. Therefore, the idea of considering the brick wall as a homogeneous material cannot fully represent the actual material of the wall-beam. In addition, at failure stage the load response of the structure is non-linear. With this type of elastic model the local behaviour near the support of the wall-beam where the stress gradients are high, cannot be predicted. Moreover, this type of model cannot predict failure load. Therefore, for accurate prediction of failure load the material non-linearity and the non-linearity due to progressive cracking of the component materials must be considered.

Page (1979) proposed a non-linear non-homogeneous finite element model to predict the overall behaviour of wall-beam structures. His model simulated the propagation of the crack, only through the mortar joints. Thus it was incapable of modelling fracture through the bricks that constitute about 90 % of the brickwork. Therefore, the model could not predict the failure load. With the background mentioned above there lies a wide scope for doing research on wall-beam structure.

1.3 OBJECTIVE OF THE RESEARCH

- To develop a computer based finite element model that can analyse the composite behaviour of wall-beam structure from elastic range to ultimate failure.

- To verify and compare the predicted ultimate loads and failure pattern with the experimental results obtained in the laboratory from tests on wall-beam.
- To perform a comprehensive parametric study considering the important parameters involved in the composite behaviour of wall-beam structure.
- Finally, to propose a new design recommendation and to compare with the existing ones.

1.4 ESSENTIAL FEATURES FOR THE ANALYSIS OF WALL-BEAM STRUCTURE

The realistic interaction between masonry wall and its supporting beam have the following features:

1. The thickness of the wall being negligible in comparison to the masonry height and length of the supporting beam and the applied load being in the plane of the wall, a two-dimensional idealisation of the wall-beam is therefore, considered realistic.
2. The mechanical behaviour of most of the component materials is non-linear. A linear elastic approach oversimplifies the problem. A realistic approach must therefore adopt an acceptable stress-strain representation.
3. The wall-beam is non-homogeneous. The component materials have different properties. The assumption of a homogeneous continuum to represent the wall-beam is not realistic. The non-homogeneous nature must therefore be considered in the analysis.
4. The masonry is weak in tension. Local stresses provide tensile bond or shear bond failure. These result in a complete redistribution of stresses within the structure. An iterative analysis should be performed for this.
5. The distribution of stresses at the interface of wall and the supporting beam is complex. The assumption of a simple pressure distribution may not be acceptable. A realistic analysis should therefore be performed to predict the actual stress distribution at the interface.
6. The finite element method is particularly suitable in this case and is adopted here. The brick, mortar joints, supporting beam and the reinforcement of the beam are represented by an assemblage of suitable finite elements and analysed as one complete system. This scheme of analysis is logical and allows for the inclusion of all the essential features of the wall-beam structure.

1.5 ASSUMPTIONS AND LIMITATIONS OF PROPOSED APPROACH

The following assumptions have been made for the proposed finite element analysis of composite behaviour of wall-beam structure.

- The central vertical plane of the wall is continuous at every point before and after distortion and there are no holes in it.
- Perfect integrity exists at the various components of the wall-beam structure.
- Effects of temperature, shrinkage, creep and dynamic loading are ignored.
- Deformation is small in comparison to the wall dimension.
- Concrete is homogeneous and isotropic with reinforcement being modelled separately.
- Bricks and mortar joints are homogeneous and isotropic.
- The material behaviour of the component materials are represented sufficiently accurately by the laboratory tests.
- The material non-linearity and non-linearity due to progressive fracture of the component materials are considered in this investigation. While the geometric non-linearity due to large deformations are excluded.

1.6 METHODOLOGY

In an attempt to investigate the behaviour of wall-beam structure and to recommend a rational design procedure, a survey of the related literature has been made in the next chapter. Some of the analytical approaches are studied in detail in order to delineate the differences among those design approaches, thus enabling a comparison with the findings of the present study.

Comprehensive analysis of a prototype wall-beam structure has been made using finite element technique. In the finite element approach the constituent materials are idealised separately to represent nonhomogeneity. In all the cases four-noded rectangular isoparametric elements have been used to analyse the panel. The analysis is made for several possible parameters in order to determine the critical conditions.

To realistically predict failure, the model must reflect the inelastic nature of the constituents as well as the progressive failure that occurs as the applied load is increased. The material model therefore adopted in the analysis is "microscopic" rather than "macroscopic" in nature with bricks and joints being modelled

separately. This is essential if the high stress gradients and localised failure which occur in wall-beam are to be modelled. The properties needed to define this material model have been obtained from various simple tests on samples of bricks, mortar joints and small brick masonry specimens, thus avoiding the need for more complex testing apparatus. The model incorporates elastic and inelastic deformation characteristics and failure criteria. Series of failure criteria have been adopted to model the different modes of failure experienced in the masonry constituents together with appropriate technique for crack modelling. Due to the nature of the problem, consideration has also been given to the post-cracking behaviour of the materials, particularly the region where the redistribution of stress takes place due to fracture of the component material. Solid clay bricks have been used in conjunction with a mortar consisting of 1 part of cement and 4 parts of sand by volume. Due to the relatively simple nature of the tests required to define the material model, it would not be difficult to reproduce the behaviour of other types of solid masonry.

The adequacy of the finite element model has been verified by comparison with load tests on wall-beam panels made of solid clay brick supported on reinforced concrete beam. The configuration of the wall-beam panel (height, opening and framing) has been varied to produce variations in behaviour and different failure modes. Finite element model has been modified to incorporate strain softening which allows the more gradual release of the stresses in the region of a crack. Sensitivity analyses of the various parameters used in the finite element model have been carried out. These analyses highlight the importance of the accurate evaluation of the modulus of elasticity and the strength parameters of the masonry constituents.

The finite element model was then used to carry out a comprehensive parametric study of the behaviour of storey-height wall subjected to uniformly distributed load. From the results of the parametric study, design rules to predict the ultimate uniformly distributed loads on wall-beam have been proposed.

1.7 STRUCTURE OF THE THESIS

With a view to maintain a systematic way and clarity in the presentation of the study, the structure of the thesis is summarised as follows :

1. A review of the state of the art of the in-plane behaviour of wall-beam structure with particular emphasis on areas significant to this study. (chapter 2)
2. The establishment of critical parameters influencing the behaviour of wall-beam structure subjected to uniformly distributed loads through the use of two-dimensional linear elastic finite element analyses. (chapter 3)
3. The experimental determination of the material parameters from the representative samples of brick, mortar and brick masonry. (chapter 4)
4. The derivation of a material model for the constituents of the wall-beam structure from the tests of step (3). (chapter 5)
5. The development of non-linear finite element model incorporating the material model derived in step (4). (chapter 6)
6. Verification of the proposed finite element model with the results of tests on wall-beam panels. (chapter 7)
7. Sensitivity analysis of the critical parameters of the finite element model. (chapter 8)
8. The application of the finite element model to a parametric study of the behaviour of storey-height wall-beam panels subjected to uniformly distributed load. (chapter 9)
9. Design recommendation for wall-beam structures and comparison with existing formulae. (chapter 9)

CHAPTER 2

REVIEW OF LITERATURE

2.1 INTRODUCTION

A masonry wall and its supporting beam form an integral unit — typically known as wall-beam structure. A study of the interaction between the two components leads to a better understanding of the behaviour of these composite materials. Traditionally, the supporting beam has been treated as a separate member having superimposed load acting at the top of the beam. Thus, any interaction that may take place between the two has been overlooked until recent past. This inherent irrationality of the conventional method ignoring the contribution of the wall results in an uneconomical design of the supporting member.

Wood (1952) for the first time, appreciated the interaction of masonry wall with its supporting beam. A growing interest has since been shown in this field that has become increasingly important with the necessity of building more economic. The masonry wall may be a combination of any of the materials — stones, concrete blocks, clay bricks (burnt and unburned) and lime mortar bricks laid with any of the suitable mortar made from cement and sand with or without lime, lime surki (pulverised clay brick) mortar and mud mortar with or without other indigenous locally used additives. The supporting beams may be of steel or reinforced concrete or concrete encased steel beam. The use of timber or bamboo as supporting beam for wall made of unburned brick or brick with surki can be noticed in rural areas or in old buildings.

Wall-beam structure subjected to in plane uniformly distributed load typically fails by crushing of the masonry block vary close to the end support. The failure mechanism also involves the failure of bond of mortar joint (bed joint and header joint) and the separation of wall from the supporting beam near the centre of the span. In view of the large number of variables in the wall-beam structure, it does not seem realistic to predict its capacity on the basis of experimental data. Therefore, a numerical model capable of predicting in-plane behaviour from elastic level to ultimate failure is required. Since the components of the wall (the mortar joints and the brick) exhibit different deformation characteristics under load, the model should incorporate the material properties of the constituents throughout the

loading history. For the analysis of composite masonry wall-beam structure a thorough knowledge of the deformation characteristics of individual materials and that of the masonry assemblage is important. Since the initiation of crack occurs in very localised area in the region of high stress gradient and approaches to failure in a typical pattern, it seems logical to model brick and joint separately rather than treating the masonry as a continuum with average properties.

This chapter reviews previous literature that have been published on various relevant aspects of this problem. Because, solid clay brickwork has been used in this investigation, review of material properties of clay brick, mortar and brickwork is emphasised. Previous studies, both experimental and analytical, including finite element analysis of wall-beam structure subjected to in-plane loads are then described. This ranges from simple isotropic elastic analysis to sophisticated models that include provisions for non-linear deformation characteristics and progressive local failure. It is shown that design rules for wall beam structure subjected to in-plane loads are empirical, approximate and vary considerably from country to country and in some cases are non conservative, justifying the need for a comprehensive study in this area.

2.2 MATERIAL PROPERTIES

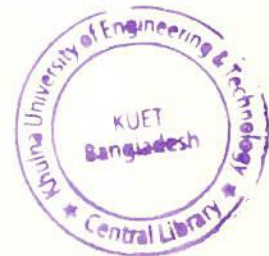
Masonry due to its typical assemblage inherits the properties from its constituents — bricks and the mortar. These constituent materials work compositely yet retaining their own identity and qualitative characteristics. A brief review of material properties relevant to the in-plane composite behaviour of wall-beam is carried out in this section.

2.2.1 Brick Properties

Compressive Strength

Like concrete, the compressive strength test has been traditionally used for brick quality control and specification, since it is easy to perform. It is a good indication of general quality of brick and the compressive capacity of the resulting masonry.

The standard test for determining compressive strength of brick (BDS 208: 1980, Common Building Clay Brick) is influenced by several factors such as



loading rate (Harding et.al., 1973); specimen size (Anderson, 1969; Francis, 1969 and Page, 1984); perforation pattern (West, 1968; West et.al., 1968 and Anderson, 1969) and specimen end conditions (Farrar, 1971; Beech et.al., 1973; Hegemier et.al., 1978 and Page, 1981). Because of the influences of these effects the compressive strength obtained from a standard test is not necessarily the true compressive strength of the material. Despite these differences, however, the nominal compressive strength obtained from the standard test provides a good form of quality control and can be correlated with other brick masonry properties, such as brick masonry compressive strength.

In standard test the result is also influenced by the stiffness of the packing material on top and bottom faces of the specimen and by the frictional resistance imposed by the solid platen producing artificial compressive strength. To minimise the effect of platen restraint several investigators used variable stiffness platens (Newman and Lachance, 1964 and Farrar, 1971) and/or capping materials (Scrivener and Williams, 1971; Beech et.al., 1973 and Harding et.al., 1973). Flexible steel brush platens have also been used successfully for the testing of both concrete (Kupfer et.al., 1969) and masonry (Hegemier et.al., 1978; Page, 1981; and Page, 1983). An indication of the magnitude of the strengthening effect due to platen restraint has also been given by Page, (1984) from compression tests on calcium silicate bricks. Steel brush and solid platens were used in his tests on bricks of varying size and shape. For standard bricks (230 mm × 110 mm × 76 mm) the unconfined compressive strength (with brush platen) was found to be almost half the confined compressive strength (with solid steel platen). The effect should therefore be considered when assessing the compressive strength of a material. Later Page and Marshal (1985) carried out uniaxial unconfined and confined compressive test on calcium silicate bricks and prisms and confirmed the influence of aspect ratio on the evaluation of compressive strength. They derived simple relationship for an aspect ratio correction factor. For unconfined test they used brush platen (as shown in Fig. 2.1) to maintain low resistance to lateral movement.

Tensile Strength

Since final failure very often occurs in biaxial tension split in the brick at the zone of high stress gradient near the support of the wall-beam structure, brick tensile strength has significant influence on the behaviour of such structure. The failure mechanism of solid masonry (as discussed by Hilsdorf, 1969, Khoo and

Hendry, 1973) indicates that the tensile strength of the brick also governs the uniaxial compression test of masonry.

Tensile strength of brick is investigated by various tension tests, e.g. modulus of rupture tests, splitting tests (Double punch or Brazilian tests) and various forms of shear tests including indirect tension.

The effect of size, shape and distribution of perforations on the tensile strength of brick has been studied by West (1968) and Anderson, (1969). Significant reductions in the tensile strength were reported with perforation patterns which produced significant stress concentrations.

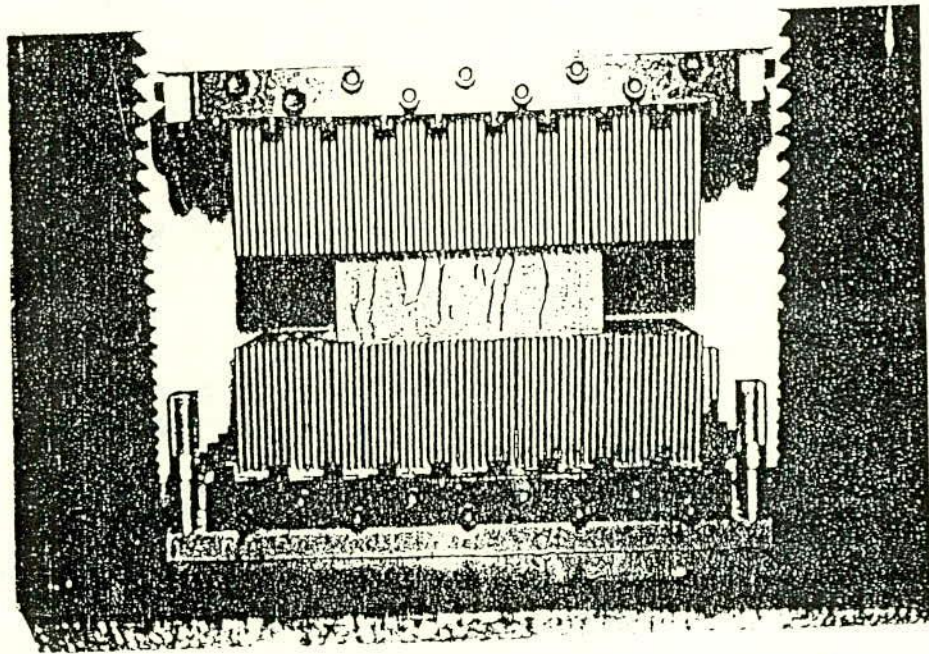


Fig. 2.1 Test Set-up for Unconfined Compressive Strength of Brick
(Page and Marshal, 1985).

Although the lower tensile strength of brick is indirectly the cause of masonry failure in compression, no reliable relationship between brick tensile strength and brick masonry has emerged despite the extensive research. Therefore,

brick compressive strength is still the prime indication of the compressive strength of the masonry.

Other Brick Properties

Most of other properties of brick e.g. brick growth pitting, efflorescence, permeability, dimensional changes etc. do not influence the masonry strength. But brick suction or initial rate of absorption (IRA) significantly affects both compressive and tensile strength of the masonry. It seems that free water on the surface of saturated bricks results in formation of cavities at the brick-mortar interface on drying. These cavities are filled with air resulting in weak bond between brick and mortar. For this phenomenon brickwork built with saturated bricks develops poor adhesion between bricks and mortar and is susceptible to frost damage and other deterioration. On the other hand high IRA of brick hinders hydration of mortar and results in a weak mortar. Some specifications recommend limiting suction rate or alternatively the use of high retentivity mortar to control the extraction of water from the mortar.

2.2.2 Mortar Properties

Mortar in brick masonry has three main functions :

- To provide an even bed for the brick.
- To bond the bricks effectively.
- To seal the joints against weather.

In order to perform the above functions mortar has to possess various properties both in plastic and hardened state.

Workability, water retentivity and early strength of mortar are the required properties in plastic state for proper bond and easiness for work. Good water retention is also required to prevent brick from suction of water from mortar, to prevent bleeding of water from mortar, to prevent stiffening of the mortar bed before placement of the brick and to ensure the retention of sufficient water in the mortar for proper hydration.

Water cement ratio — an important factor which is normally determined by workability in a given mix. The range of water/cement ratio provided by Hendry et.al. (1981) for different grades of mortar for satisfactory workability is shown in

Fig. 2.2 and can be taken as a preliminary guide. Lime is added to these mortars to improve the workability, water retention and bonding properties. In U. K., the type of lime used is designated by BS 890.

In hardened state the required properties are compressive, tensile and the bond strength. Like brick the compressive strength of mortar serves as a good indicator of its quality. Grimm (1975), has expressed the compressive strength of mortar as a function of shape, curing age, air content and initial flow rate of mortar. The response of mortar to the applied load in the masonry structure indicates that the bond between mortar and brick is also very important.

2.2.3 Brick Masonry Properties

Like other structural materials, compressive, tensile and shear strength of masonry are the strength characteristics to ensure satisfactory performance of masonry structures. The deformation characteristics of masonry are also required to assess the stress distributions and relative movements at working loads.

Masonry Compressive Strength

Since brick structures are mainly stressed in compression, the compressive strength of masonry is an important factor. Numerous experimental investigations have been carried out to examine the variables affecting the brickwork strength. The relevant literature was reviewed by Hendry (1981) and Ali (1987). Different formulae have been derived on the basis of elastic analysis of stack bonded prism. Excepting the limitation of the fact that the mortar is not elastic up to failure and that these theories are based on stack bonded prisms, may not be applicable to bonded brickwork, it is observed by Hendry (1981) that the agreement between formulae and test results are favourable, provided the brick strength exceeds the mortar strength.

In practice the compressive strength of brick masonry is determined from approximate relationship between brick strength, mortar type and brick masonry strength or from compressive test on prisms. Finite element analysis of the brick-mortar composite subjected to axial compression, carried by Khoo (1972) revealed that stress concentration occurs at the edge of the brick-mortar interface, causing high stress gradients in both materials in this region. He observed that the edge face of an axially loaded prism, when the width / depth ratio of brick is lower,

contains high values of lateral stresses in the region of stress concentration than the front face section and consequently suggested that the initial tensile cracking of the brick prism will occur along a plane at the edge of the end face in the direction of the brick length resulting a rise in the 'spalling' failure. This phenomenon is frequently observed in prism tests and in the tests of masonry columns under axial load.

Masonry Tensile Strength

The tensile strength of brick masonry is low thus restricting its load carrying capacity. In-plane loading produces a uniform tensile stress through the wall thickness whereas out-of-plane loading produces a non-uniform stress distribution through the wall thickness. Regardless of the loading direction the tensile strength is dependent on the bond characteristics of the brick masonry. Considerable variation in tensile bond strength for any one brick-mortar combination can be expected due to variable nature of the parameters which influence bond strength. In particular the two properties like water retentivity of mortar and the initial rate of absorption of the brick have a marked effect on the bond strength of the resulting masonry. Factors affecting brick masonry bond and hence its tensile strength have been extensively studied and are reviewed elsewhere (Hendry, 1981; Hendry et.al., 1981 and Ali, 1987). Hendry et.al., 1981 observed that grading of sand is important and very fine sands are unfavourable for adhesion. The moisture content of the brick at the time of laying is also important. Both very dry and fully saturated bricks lead to low bond strength.

Under in-plane loading tensile failure may occur either normal or parallel to bed joint depending upon the direction of loading . Tensile failure under inclined loading will normally occur in a stepped manner along bed and header joints. The in-plane masonry tensile strength was first studied by Johnson and Thomson(1969) by using diametral splitting test on circular specimens swan from a wall. Using this technique, by rotating the orientation of bed joint to the splitting force, tensile stress could be applied at varying angles to the jointing direction.

The flexural tensile strength of clay brickwork ranges from about 2.0 to 0.8 MPa in the vertical direction, while the strength in bending across the bed joints being about one third of this (Hendry et.al., 1981).



Masonry Shear Strength

The strength of brickwork in combined shear and compression is of importance in relation to resistance of buildings to lateral forces. The case has been studied by many investigators. They range from tests on small sample of masonry to tests on completely shear wall systems. These tests have been reviewed elsewhere (Sinha and Hendry, 1969; Hendry and Sinha, 1971; Page et.al., (1982) and Hamid and Drysdale, (1980) and more recently by Ali (1987).

From these investigations a simple Coulomb type failure criterion has been proposed as follows:

$$\tau = \tau_0 + \mu\sigma_n \quad (2.1)$$

Where, τ_0 is the shear bond strength at zero pre-compression, μ is a constant often referred to as the frictional coefficient and σ_n is the normal stress.

Hendry et.al. (1981) observed that this relationship holds for values of compression stress up to levels in excess of 2.0 MPa for clay bricks, but eventually the ultimate shear stress must be less than the value given by this formula. In the limit when the compressive stress produces the crushing strength of the brickwork, the shear resistance will fall to zero. They also observed that the shear strength depends on the mortar strength, and for brickwork built with clay bricks of crushing strength between 20 MPa and 50 MPa the value of τ_0 will be approximately 0.3 MPa for strong mortar (cement : lime: sand = 1:1/4:3 by volume) and 0.2 MPa for medium strength mortar (1:1:6). The average value of μ is 0.4. Double frogged or perforated bricks will give higher strength at low pre compression on account of the mechanical key established between bricks and mortar. It is also observed by Sinha (1967) that the degree of saturation of solid clay bricks at the time of laying has an effect on the initial bond strength. The strength is very small and variable in the case of saturated or completely dry bricks.

Samarasinghe (1980) and later Dhanashekar et.al. (1985), determined the influence of the parallel stress (σ_p) on the shear stress/normal stress relationship. From the investigation made by Dhanasekar et.al. (1985) a three dimensional failure surface in terms of σ_n , σ_p and τ was derived from a large number of biaxial test on masonry panels.

Deformation Characteristics of Masonry

Knowledge of stress-strain relationship for brickwork in compression is important in predicting the deflection of masonry structures and further structural design. For the numerical modelling also for the masonry behaviour this property is required. A good number of experimental works have been carried out in the past relating modulus of elasticity of brick masonry to its compressive strength on an empirical basis. These are reviewed by Ali (1987) and Hendry (1981).

The difference between the initial tangent modulus and the secant modulus at two-thirds to three quarters of maximum compressive strength is indicative of the non-linear stress strain relation of the brickwork. The mortar joint in the brickwork mostly undergoes non-linear deformation, while the surface clay burnt bricks often exhibit linear stress-strain characteristics. Some authors (Plowman, 1965; Sahlin, 1971) have related the modulus of elasticity of brick masonry to its compressive strength on an empirical basis, having value between 400 to 1000 times the masonry crushing strength, while Sinha and Pedreschi (1983) suggested a non-linear relationship between the Young's modulus of elasticity of brick masonry and its compressive strength as follows:

$$E_w = 1180(F'_m)^{0.83} \quad (2.2)$$

Dhanasekar et.al. (1985) from their results of biaxial tests on half scale brick masonry panels concluded that the masonry behaves approximately isotropic in elastic range. However in the inelastic range a formulation assuming isotropic behaviour was found to be unsatisfactory.

The studies done by the authors (Lenczner (1971); Lenczner (1973); Lenczner et.al. (1975); Lenczner and Salahuddin (1976) and Wyatt et.al. (1975)) on long term loading which results creep strain in brickwork, have shown that the ratio of long term to instantaneous strain is between 2 and 4. Higher values were found for walls than for piers.

Recently Kawsar (1991) carried out a research on deformation characteristics of brick masonry under compressive load. The study reveals that in case of five brick high prism, the effect of platen restraint is substantially minimised. It was found in his study that the deformation characteristics of masonry can be represented by a parabolic equation of best fit curve which was obtained by minor modification of Saenz's stress-strain relation originally

proposed for axially loaded concrete. Assuming brick, mortar and the assemblage to be elastic he proposed the following formula to predict the initial tangent modulus of brick masonry.

$$E_w = \frac{E_b}{(\mu + \beta\phi)}$$

where, $\mu = \frac{\alpha}{1 + \alpha}$; $\phi = \frac{1}{1 + \alpha}$; $\beta = \frac{E_b}{E_m}$ and $\alpha = \frac{T_b}{T_m}$ (T_b and T_m are thickness of brick and mortar respectively).

2.3 WALL-BEAM STRUCTURE

While the need for an interactive analysis of wall-beam structure is appreciated a few studies are available. Most of these simplify the behaviour of the masonry wall or the supporting beam. This approaches the problem as a two-phase system. The masonry wall is one and the supporting beam is the other. Attempts are then made to account for the interaction between these two phase system by simplified approach. Either the wall is analysed, with the supporting beam being represented by an artificial model or the beam is supported by a continuous elastic foundation and the system is analysed. Some laboratory tests have also been undertaken in the past to account for the influence of important parameters. Though some of the test-results gave valuable information, yet, these laboratory investigations and theoretical analyses are not sufficient to predict the proper interaction between masonry wall and supporting beam. The following articles give a thorough and comprehensive review of experimental investigation and theoretical analyses, of the problem.

2.3.1 Experimental Investigation

Wood (1952) carried out tests to study the composite action of brick panel walls supported on reinforced concrete beams. On the basis of test results he recommended that the bending moment in the supporting beam is equal to $WL/30$ for window and door openings near the support and is equal to $WL/100$ for plain walls or opening in the middle. Wood also proposed another design method for beams supporting walls without openings. The method was based on the deep beam theory, and was referred to as the 'limiting moment-arm method'. It suggests that a limiting moment-arm approximately equal to 0.7 times span for deep beams. For continuous beam the moment-arm is equal to 0.47 times span at the mid span and at the support equal to 0.34 times span. He also recommended that for composite action to occur the depth of the supporting beam be varied from 1/15th

to 1/20th of the span. He also advised that when the superimposed load is applied not on the top of the wall rather at the level of the beam (as the case may often be in conjunction with the load at the top due to floor systems) tensile connectors between wall and beam be used. But he prescribed neither the amount nor the mechanism of providing such connectors.

Rosenhaupt (1962) tested masonry walls on point supported beams under uniformly distributed load. He observed that in addition to crushing of masonry another cause of failure is the vertical shear near the support which is indicated by cracking in vertical direction through the vertical joints. He observed that the shear resistance of the wall depends on the strength of the masonry, the height of the wall and the inclusion of vertical ties. The vertical ties shift the location of the crack away from the support thus reducing the force acting in the ruptured section. Unlike other investigators he found that in the high walls the maximum stress at the supports is approximately four times higher than the external uniformly distributed load acting at the top of the wall.

Later Rosenhaupt and Sokal (1965) published the test results of 2 masonry walls on point supported continuous beams. They observed that the walls behave like a composite diaphragm girder in which the foundation beam acts as a tension tie. They also observed that the reactions at interior supports are much smaller than those of ordinary beams and as a result the external moments are positive throughout the length of the wall. In this case also crushing of the masonry above the support was the main cause of failure of the composite structure.

Plowman et.al. (1967), carried out a series of full scale tests on composite cantilever box beams having reinforced concrete slabs as flanges and reinforced brick walls as webs. The results indicated that in all tests failure was slow and was due to diagonal cracking and crushing of the brickwork in the vertically reinforced specimens and pulling away of the bottom slab in those specimens which are diagonally reinforced. The horizontal reinforcement used in conjunction with vertical steel increased the failure load in these specimens but had no effect on the deflection or the behaviour at working loads. Finally, they suggested that box beams with brickwork webs in corporation with either vertical or diagonal reinforcement can be used as structural units with satisfactory factor of safety.

Burhouse (1969) in his experiments on composite action between brick panel walls and their supporting beam noticed the fact of vertical stress concentration near the support . By measuring the vertical strain and assuming

linear relationship between stress and strain he calculated the ratio of maximum stress to the average applied stress which varied with the applied load. Burhouse obtained this ratio varying from 6.26 to 14.8 in only five tests and cautioned that the permissible loads on wall of wall beam composite should be less than the load derived by CP 111 which assumes a rigid foundation. Like others Burhouse also concluded that for composite action to occur H/L ratio should not be less than 0.6 and with the lower value the sliding at wall-beam interface may occur. From test results he found that the moment arm is approximately equal to one half the wall height.

Stafford Smith et.al. (1978) carried out tests on three full size masonry walls supported on encased steel beams to study the influence of the beam stiffness on the arching effect of the wall and on the ultimate strength of the structure when subjected to vertical load. Their test results revealed that stiffer the beam, the larger the distribution of interaction stresses at the interface and the higher the resulting bending moment. The bending moment obtained was found to be approximately proportional to $4\sqrt{I}$ of the beam. The tie force was found almost independent of the beam stiffness and its magnitude was approximately $W/4$.

Annamalai et.al. (1984) carried out tests on reinforced brick thin lintels having simply supported span of 1.2 m over doors and windows of residential buildings. Tests revealed that moment varied from WL/33 to WL/50 which is comparatively unconservative with respect to the value obtained by Wood. Due to limited number of test data they did not prescribe any coefficient for moment arm. Failures of tests were mostly observed by crushing of bricks over the support followed by shear failure. Among the two types of brick, the wire cut brick walls contributed about 50% increase in composite strength as compared to that of chambered brick walls. They also observed that lintels made of reinforced perforated brickwork (one 6 mm MS rod was provided in each of three elliptical 48 x 32 mm holes with sufficient cover) was adequate in strength for application in residential buildings. In general the reinforced brickwork thin lintels built with solid bricks recommended to have the same strength as reinforced concrete thin lintels besides, giving considerable saving in concrete.

Govindan and Santha Kumar (1985) carried out tests on brick infilled beams to compare the stiffness and load carrying capacity with traditional RCC beams. They observed that the infilled beam is similar to that of the solid beam at low loads before cracking. In the post cracking stages the stiffness of the infill is less

than the stiffness of solid beam by 15 %. The ductility of the infilled beam is 80 % of that of solid beam which is adequate for using them in foundations. They observed that the strength of infill governed the ultimate load and that shear failure preceded the formation of flexural hinge resulting unsatisfactory failure mode. The ultimate load predicted by them compared well with those of observed values.

Experiments performed by Ranjit (1992) on nine wall-beams investigated the composite action between wall and its supporting beam. Wall length, bond pattern and provision for vertical reinforcement in wall-beam were the main variables in his study. Unlike previous investigators he proposed minimum H/L ratio of wall-beam to be 0.5 for proper composite action. He observed better performance for running bonded brickwork in wall-beam composite action in comparison to stack bond for both cases of with or without vertical ties.

The number of variables and their range which influence the stress history until failure of the composite system and the failure modes are so many that experimental investigation covering all these factors is a monumental task and usually associated with expensive instruments and thus increasing the cost of the experiments. The researchers therefore, preferring to consider analytical tools simultaneously with the laboratory investigations for the solution of the wall-beam interaction problem, though they faced restriction about the detailed stress analysis due to the lack of computational facilities and appropriate material model. The available works of some of these researchers are reviewed in the following articles.

2.3.2 Analytical Investigations

Rosenhaupt (1961, 1964) pioneered the analysis of wall-beam structure. In his analysis he neglected the bending rigidity of the supporting beam and assumed that the tensile stresses are concentrated in the supporting beam of the wall which acts solely as a tie beam and compressive stresses are distributed over the whole height of the masonry. The vertical compression forces are transferred by the wall to the supports, where high vertical stresses concentrate. With the above assumption his solution was based on numerical finite difference method using a very coarse mesh. He also concluded that the vertical shear stresses are taken by the masonry part of the wall and the horizontal shear stresses between the supporting beam and the panel, concentrate near the supports.

In 1964 Raab applied the lattice analogy method, proposed by Hrennikoff (1941) to the analysis of composite walls. In the method the continuous material of

the elastic body is replaced by a framework of linear elements. The cross-sectional properties of the bars which comprises the lattices of the frame-work are chosen so as to ensure the framework and the elastic body distort under load in the same manner. He performed the analysis on four different cases of the composite problem and concluded that the assumption made by Rosenhaupt (1964) that the supporting beam has no flexural stiffness can be accepted in many applications with minor modifications.

An alternative numerical approach for the solution of the composite problem was presented by Coull (1966). The analysis was based on the minimization of the strain energy of the system using the variational method. The procedure consisted of expressing the stresses in the wall by a power series in the horizontal direction, the coefficients of the series being the function of the height only. To solve a typical wall on beam problem, Coull chose a simple stress polynomial as a result of which the horizontal and shear stresses had the same form at all levels in the wall. This seems unlikely in practice, however, the accuracy could have been improved if more terms were used which, as Coull pointed out, would be at the expense of extra computational difficulty involved in the solution of the resulting set of simultaneous differential equations. From the analysis he concluded that the wall stresses are mainly affected by the wall height-to-span ratio and the relative stiffness of the wall and beam.

Colbourne (1969) with the help of lattice analogy derived equilibrium equations at interior points, considering the wall beam system homogeneous and elastic. The analogy was then used to derive the equilibrium equations for points near the edges of the wall and for points affected by beam. These equations are identical with the finite difference equations. These equations were solved by computer program to give displacements which were used to find stresses in the wall and stress resultants in the beam. Results were compared with earlier theoretical studies. The method seemed to be useful for beam supporting panels without opening (continuous beams) and for the case when loads are applied at any point of the wall or beam.

Wood and Simms (1969) made a very simple analysis assuming a rectangular stress block at supports as shown in Fig. 2.3. The stress concentration factor C was derived as $L/2X$, where $L = \text{Span}$ and $X = \text{base of the stress block}$. The bending moment was derived from Figure 2.3 as

$$M = WL/K = (W/2) \cdot (X/2) = WX/4 \quad (2.3)$$

where K is moment factor. Simplifying the above equation the relation between moment factor (K), base of the stress block (X) and stress concentration factor (C) was derived as follows:

$$1/K = X/4L = 1/8C \quad (2.4)$$

From this relation for any desired stress concentration factor the corresponding moment factor and the width of the stress block can be obtained. For example, for no composite action (i.e. $K=8$) the value of $C=1$ and $X/L = 1/2$, likewise for maximum composite action (i.e. $K=100$) the value of $C=12.5$ and $X/L = 1/25$. They also proposed that the stress concentration factor due to arching action should not exceed the allowable bearing stress as suggested by CP 111, 1964. This can be mentioned that in the method suggested by Wood and Simms (1969) the moment in the beam is over-estimated while the vertical stress concentration at the wall-beam interface is less than the actual.

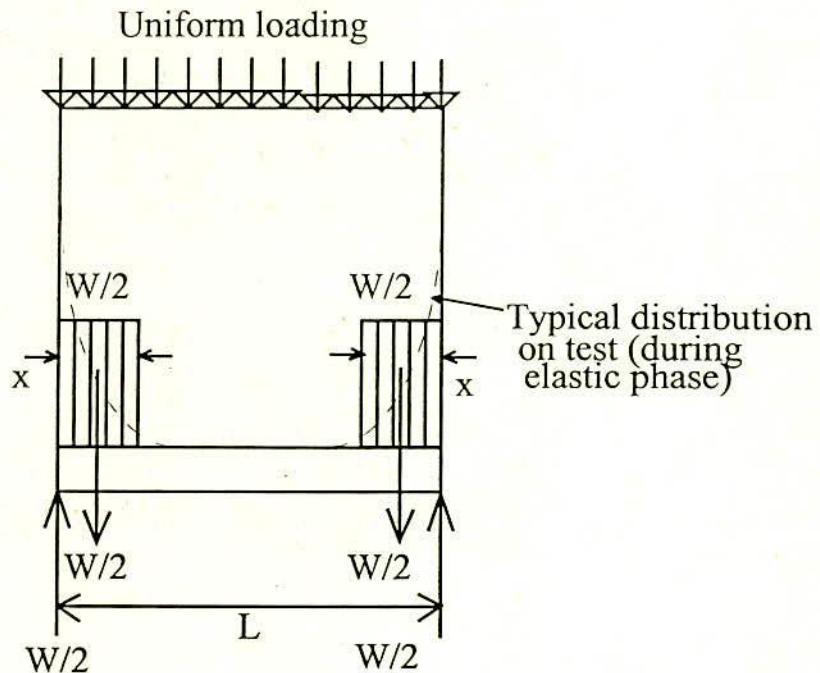


Fig. 2.3 Assumed Equivalent Beam Loading at Failure of Wall
(Wood and Simms, 1969)

Ramesh et.al. (1970) expressed the displacements in the form of multiple Fourier series which satisfied all the boundary conditions of compatibility at wall-beam interface. The method being perfectly general involving no simplifying

assumptions. They suggested that all the boundary conditions will be satisfied if a large number of harmonics in the series are considered. But this is not possible without large computing facility. Their experimental investigations comprised full scale and model tests on brickwork walls on reinforced concrete beams. The tests showed that, the failure load of a wall loaded at the beam level, depends on the amount of reinforcement in the vertical tensile connectors.

Based on the results obtained by Ramesh et.al., Achyutha (1971) proposed an approximate method of analysis for the reinforced wall-beam structure. He assumed the system to be analogous to truss in which the beam was represented by the bottom chord of the truss, and the tensile connectors by the vertical members with length equal to half the wall height. The stresses in the reinforcement of the supporting beam were calculated using the total concrete area including the equivalent concrete area due to steel reinforcement.

Yettram and Hirst (1971) presented a paper describing a numerical method, known as shear-lag method, for the solution of the composite problem. The method consists of dividing the wall into equally spaced vertical stringers. These are assumed to carry the direct load and are connected by shear-carrying panel, acting between them. They showed that the bending moment in the supporting beam substantially increases as the stiffness of the beam increases and for a highly stiff beam the moment may rise to as much as $WL/8$ for a uniformly distributed load applied on the top of the wall.

A more rigorous analytical procedure for the analysis of composite wall, with and without openings was presented by Levy and Spira (1973). The analysis was based on the determination of stress functions using the finite difference method. They also proposed an approximate solution relating the maximum vertical stress in the wall to the relative stiffness parameter. Presence of vertical ties in their study was shown to reduce both the compression in the wall and the bending moment in the supporting beam.

Smith and Riddington in 1973 published a paper in which they proposed a design method for steel beams supporting masonry walls. The method was based on the assumptions that the length of contact between the wall and the beam is governed mainly by relative stiffness parameter $\left(K = \sqrt{\frac{E_w t L^3}{EI}} \right)$. The smaller its value, in other words, the stiffer being the beam, the longer is the length of contact.

In view of this and the results from model tests of plaster walls on steel beams, the following design formula was proposed:

$$I \geq \frac{W^4}{9.5Lt^3P_b^4} \quad (2.5)$$

in which I is the second moment of area of the beam, W is the total load, t is the wall thickness and P_b is the permissible vertical stress in the wall.

In 1976, Chandrashekhara and Jacob presented the results of photoelastic analysis on composite walls, with and without openings. Columbia resin (CR-39) was used to represent the supporting beam and Araldite (CY 230) to represent the wall. The modular ratio obtained by such combination at 115°C was 23.5. The tests showed that the interface stresses depend on the beam stiffness and the presence of opening in the wall.

2.3.3 Finite Element Approach

With the progress of time, the computer based finite element method of stress analysis is adapted by the researchers due to its versatile capacity of handling the various types of problems. In the field of interaction problem of wall-beam structure the finite element is being used since the late sixties. A well-documented finite element analysis supported by experimental studies can be a good replacement of the experiments which often are laborious and expensive.

At the present stage of knowledge numerical simulations are fundamental to provide insight into the structural behaviour and support the derivation of rational design rules. Nevertheless, the step towards the development of reliable and accurate numerical models cannot be performed without a thorough numerical description and a proper validation by comparison with a significant number of experimental results. Non-linear finite element analysis will always be helpful for the validation of the design of complex masonry under complex loading conditions. Masonry is a composite material that consists of units and mortar joints. A detailed analysis of masonry hereby, denoted micro-modelling, must then include representation of units, mortar, and the unit/ mortar interface. The primary aim of micro-modelling is to closely represent masonry from the knowledge of the properties of each constituents and the interface. The necessary experimental data must be obtained from laboratory tests in the constituents and small masonry samples.

In large and practice-oriented analysis the knowledge of the interaction between units and mortar is generally negligible for the global structural behaviour. In these cases a different approach can be used, hereby denoted macro-modelling, where the material is regarded as an anisotropic composite and a relation is established between average masonry strains and average masonry stresses. This clearly a phenomenological approach, meaning that the material parameters must be performed in masonry tests of sufficiently large size under homogeneous state of stress.

Therefore, for efficient execution of the parametric study of wall-beam structure a finite element idealisation is necessary in which the important parameters may be easily varied. The relevant finite element approaches for the solutions of wall-beam structure are reviewed in the following articles.

2.3.3.1 Linear Elastic Finite Element Analysis (Homogeneous Case)

Male and Arbon (1969, 1971) carried out studies using finite element technique to analyse the composite action of masonry wall (solid or with opening) with supporting beam. The beam was idealised by four layers of rectangles, subdivided into triangles. The wall on the other hand was represented by coarser subdivisions. The element used in the program was triangular elements with two degrees of freedom per nodes. From the analysis it was shown that for full composite action to develop, shear stresses across the boundary between wall and beam, must be efficiently transmitted. Moreover, tensile connectors should be provided when the load is applied at the beam level. The presence of a central opening in the wall, was shown not to greatly influence the stress distribution in the wall. However, when the opening was situated near to the supports, very high tensile stresses occurred in the vicinity of the opening. The interaction between wall, footing and soil has also been studied by them, taking into account the swelling of the soil.

The finite element method was also used by Green (1970, 1972) for the analysis of shear walls supported on framed structures. The stiffness matrix of the standard flexural element was modified to include the effect of the horizontal force at the wall-beam boundary. A study of the effect of different parameters on the behaviour of the composite structure was undertaken. These variables included the beam stiffness, the beam support width and the size and position of the opening in the wall. Approximate formulae for the estimation of the behaviour of the wall at its base and of the supporting beam were developed on the basis of this finite

element parameter study. From the analysis, Green estimated the minimum tie force in the beam as $wL/4.4$. The finite support width was found to influence the stress distribution in the wall and the forces in the beam. The stress concentration over the supports was reduced to the order of 1.5, when the finite support width had been introduced. Furthermore, the effect of the central opening in the wall was found to be negligible. The axial force in beams supporting walls with offset openings was however 75 % more. Comparisons were made between the results of finite element analyses and the experimental results on Perspex models and then between finite element idealisation and the approximate formulae. In all the cases agreements are reasonably satisfactory.

In 1974 Saw also applied the finite element method for the analysis of interactive behaviour between walls and their supporting beams. The element used for idealising the wall, was derived from 144 basic rectangular finite elements. The element formulated, termed 'macro' had four corner nodes with two degrees of freedom at each node. In order to combine the beam line elements with those of the wall, the stiffness matrix of the standard line element was modified so as to relate the forces and the displacements at the wall-beam boundary. Results obtained by solving a typical wall on beam problem using a total of 42 nodes with 30 macro elements in conjunction with 5 line elements, were comparable with those obtained by Male and Arbon using a total of 313 nodes with 576 triangular elements. Unlike Male and Arbon he found that horizontal stress varies linearly across the beam depth which was further illustrated by a photo elastic test. He concluded that the use of line element to represent the relatively flexible supporting beam is a better approach than the use of large number of plane elements. He also noted that the beam depth to span ratio has a more pronounced effect on bending moments than the modular ratio of wall to beam and for reasonable range of problem the beam moment increases with a decrease in the beam depth.

Riddington in 1974 made a study on the interaction between walls and their supporting beams, using the finite element method. A finite element program allowing for the automatic generation of separation cracks at the wall-beam interface was developed. This was either achieved by reducing the modulus of elasticity of wall-beam interface elements to zero or separating nodes on the wall-beam interface. The separation crack was formed automatically by first analysing the structure with all nodes connected and then starting from the centre of the beam, the elements above the beam were checked for vertical tensile stresses. If a tension element was found, the analysis and separation were repeated until no

further elements became tensile. By adopting rectangular finite elements with two degrees of freedom per node, for both wall and beam, Riddington carried out parametric study for the composite problem. From the analysis and the result obtained from model tests of plaster and Araldite walls on steel beams together with results from tests conducted at the Building Research Establishment, a simplified design procedure for the composite structure has been proposed.

In 1974 Yettram and Hirst carried out an elastic analysis on the composite action of walls supported on encastre beams and portal frames. They used both the finite element method and the shear lag method previously used by them (1971). In applying the finite element program to a standard wall on beam, the inter-element nodal forces taken as an output was converted to average stress at nodes by dividing by the relevant element edge areas. This method compared favourably with the shear lag method. The analysis revealed that the beam stiffness and the flexural rigidity of the columns, had a considerable influence on the stress pattern of the wall. The effect of the columns was most marked at the ends of the supporting beam, while the mid-span bending moment being affected relatively little.

Stafford Smith and Riddington (1976, 1977) developed a finite element program for the problem using a four-node rectangular element, with two degrees of freedom at each node and with linearly varying displacement functions along the boundaries. The program also allows for tensile cracking at the wall-beam interface. This work confirmed that the total behaviour of the system remains unchanged when the height to length ratio exceeds 0.7. These investigators pointed out that the composite wall-beam is the same type of problem as the beam on and elastic foundation and infilled frame in so far as the distribution of stress between the elements depends on their relative stiffness. Also, in these problems separations of the elements are possible, the lengths remaining in contact being a function of the relative stiffness. It is therefore essential that this parameter should enter into the analysis. Thus representing the length of contact between wall and beam as αL

$$\alpha \propto \sqrt[4]{\left(\frac{EI}{E_w t}\right)} \quad (2.6)$$

where, EI is the flexural rigidity of the beam

E_w is the elastic modulus of the wall material in compression

t is the thickness of the wall

L is the length of the wall

From this,

$$\frac{\alpha}{L} \propto \sqrt[4]{\left(\frac{EI}{E_w t L^3}\right)} \quad \text{or} \quad \frac{\alpha}{L} = \frac{B}{K} \quad (2.7)$$

where $K = \sqrt[4]{(E_w t L^3 / EI)}$ and B is a constant, found as a result of experimental investigation to have an average value of unity, in which case

$$\alpha = \frac{L}{K} \quad (2.8)$$

It will be seen from the above that the stiffer the beam relative to the wall, the longer the length of contact and this in turn increases the bending moment in the beam and reduces the wall stresses. The results of Stafford Smith and Riddington's study covered a wide range of wall-beam combination. It was found that conservative estimates of the stresses in the wall and in the beam could be calculated from the following formulae

$$\text{Maximum stress in wall} = 1.63 \frac{W_w}{Lt} (E_w t L^3 / EI)^{0.28} \quad (2.9)$$

$$\text{Maximum bending moment in beam} = \frac{WL}{4(E_w t L^3 / EI)^{1/3}} \quad (2.10)$$

$$\text{Maximum tie force in beam} = W/3.4 \quad (2.11)$$

The effect of extending the beam into the surrounding brickwork was also examined, and this led to the conclusion that the stresses on both elements would be reduced in this case, although negative bending moments could be induced in the beam near its supports.

Ahmed (1977) carried out a linear elastic finite element study on the composite action between masonry panel and supporting beam. The work included experimental and analytical investigations of the composite behaviour of walls with and without opening and their supporting beams. The computer program he used was 'STRUDL' which is a part of the I.C.E.S. package. For idealisation of the

wall he used rectangular plane stress element type 'PSRCSH' having four corner nodes with only two translational degrees of freedom per node. The element stiffness matrix is computed based on the following displacement function:

$$U = \alpha_1 + \alpha_2 X + \alpha_3 Y + \alpha_4 XY \quad (2.12a)$$

$$V = \alpha_5 + \alpha_6 X + \alpha_7 Y + \alpha_8 XY \quad (2.12b)$$

This function produces linear displacement variation along the edges. The computer output was the displacements, strains, stresses, and principal stresses at the centroid of the element. To represent the supporting beam line elements in bending were used. The basic assumptions of composite action, e.g. the composite beam behaves as a tied arch; the wall taking the compression and the beam acting as a tie are also confirmed by Ahmed (1977). He observed that the maximum bending moment in the beam occurs very near to the supports and the vertical shear extends from the support sections to about one-tenth to one-fifth of the span. He also investigated the influence of size and position of opening in the wall and various support conditions. Based on the theoretical results he proposed an approximate design recommendation.

Stafford-Smith and Riddington (1977) considered the wall as linear elastic homogeneous material supported on simply supported elastic beam. He idealised the wall using four noded rectangular element with two degrees of freedom per node and linearly varying displacement functions along the boundaries. In order to allow cracking along the wall-beam interface for the finite element representation they introduced linkage element along the wall at interface of the wall-beam. Unlike others they introduced finer meshes near the support, and introduced a characteristic parameter, $K = 4\sqrt{\frac{E_w t L^3}{EI}}$, to describe maximum moment and tie force in the beam and stress in the wall. The influence of various physical parameters on the wall stress and deflection of the system has been examined. Model tests made of small size Araldite epoxy resin wall on simply supported beam had also been undertaken to verify the accuracy of the analytical results. He concluded that if beam flexural stiffness is reduced, tie force in the beam, compression and shear stress in the wall above the beam supports increases, with a result of less bending moment. He also observed that restraining of the beam end lowers the peak stress and sagging bending moment at the mid span. The use of fine mesh near the support for the homogeneous solution may be questionable. To

represent homogeneity, the element must have full representation from the component materials, e.g. brick and mortar joint.

Davies and Ahmed (1978) developed approximate method for calculating vertical stress concentration factor, maximum vertical stress in the wall, maximum tension force in the beam, maximum shear stress, maximum bending moment and moment at the centre in terms of flexural stiffness parameter and axial stiffness parameter. The other constants (α, β, γ) associated in the equations were obtainable from graph derived from finite element results depending on H/L values. To derive these constants (α, β, γ) they did not consider the material properties. They observed that the degree of vertical stress concentration in the wall is mainly influenced by a flexural stiffness parameter defined by:

$$R = 4 \sqrt{\frac{H^3 t E_w}{I E_b}} . \text{ For a very slender beam (i.e., for high value of } R) \text{ the stress}$$

distribution is triangular with large vertical stress concentration over the support. For relatively stiff beam (i.e., low R) the contact spreads more with less concentration at the support resulting a third degree parabola and that for intermediate R , is a simple parabola. The moment as proposed by them slightly overestimates when $R > 5$. This may be due to the underestimation of the axial force which they assumed to be linearly distributed, nearly zero at the support to a maximum at the centre. The stress concentration factor as predicted by them compares favourably with lattice analogy of Colbourne (1969) and stress function of Levy and Spira (1973) and the experimental results from full scale tests carried out by Burhouse (1969). Later in 1980 Davies and Ahmed graphically reproduced their approximate (1978) method so that it can be used easily as a design procedure.

Riddington and Stafford-Smith (1978) published a design method for heavily loaded wall-beam structure particularly for masonry wall on steel beam. On the basis of wall-beam relative stiffness, they predicted the distribution of interacting stresses and estimated the maximum wall stresses and beam bending moment. Finally in combination with experimental and theoretical observation for the purpose of design of wall-beam structure, they proposed to select the section of the supporting beam so as to satisfy the following two conditions.

$$I \geq \frac{W^4}{9.5 L t^3 P_b^4} \quad (2.13)$$

and

$$Z \geq \frac{W^2}{3P_{st}P_{bt}} + \frac{W_s L}{8P_{st}} \quad (2.14)$$

which offers a F. S. of 1.33 for maximum compressive stress for wall and F. S. of 1.5 for maximum bending moment in the beam.

2.3.3.2 Linear Elastic Finite Element Analysis (Non Homogeneous Case)

Masonry being non-homogeneous, its realistic representation, for the finite element model should consist of an assemblage of element representing the individual masonry units and the adjacent mortar joints. However, such representation requires considerable amount of effort for the preparation of the input data, as well as an enormous computer storage capacity. Smith et.al. (1970, 1972) used this type of idealisation for the analysis of small brickwork segments under axial compression. They showed that any analysis based on the assumption of a homogeneous material may lead to a substantial underestimation of the maximum stress. Recently, Ali (1987) also adopted non homogeneous idealisation of masonry in his study.

Kamal (1990) developed a linear elastic finite element model to study the composite action of wall beam structure. Isoparametric elements were used in his work to model the bricks, mortar joints, supporting beam and interface elements. The brickwork was modelled both as homogenous and non homogeneous material. He studied with particular emphasis on the variation of vertical stress, shear stress and bending moment due to the variation of H/L ratio, size of the beam, stiffness and wall-beam modular ratio. His observations agreed favourably with previous researchers. He also observed that maximum moment occurs at a distance of about 1/15th of the span from the either supports. In addition he observed that for elastic analysis the brickwork can be considered as a homogenous material provided a finite element contains at least one brick, one vertical joint and bed joint.

2.3.3.3 Non-linear Finite Element Analysis (Homogeneous Case)

All the analyses discussed above have been hampered by the lack of representative material model for masonry. In most cases, isotropic linear elastic behaviour has been assumed, with the masonry being considered as an assemblage of bricks and mortar with average properties.

In 1975 Saw investigated the effect of material non-linearity on the interaction between masonry walls and their supporting beams. The material non-linear behaviour was investigated by the incremental method of initial stress. Results for a typical wall/beam system within linear elastic range were compared with existing solutions. Although the order of magnitude for wall stresses calculated by various methods were found to be comparable but considerable discrepancies were found to exist in the predictions of bending moment for the supporting beam. He emphasised to consider the influence of beam depth to span ratio for a rational design since the effect of this point is ignored in empirical methods. Two failure criteria based on the octahedral shearing stress function have been suggested for use in the elasto-plastic analysis. One for biaxial tension and tension compression stress state, the other for biaxial compression. Elastoplastic finite element solutions are shown to provide good correlation with his experimental results. But he did not propose any design recommendation from this finite element analysis.

2.3.3.4 Non-linear Finite Element Analysis (Non Homogeneous Case)

Page (1979) first proposed a non-linear non homogenous finite element model capable of predicting non-linear deformation and progressive cracking of joints. The non-linear characteristics of the masonry are produced by the non-linear deformation properties of the mortar and the progressive failure and/or slip that occurs in the joints when the shear or tensile bond failure criteria are violated. Although his model was better than the previous analytical models in predicting the stress distribution of deep masonry beams it could not predict final failure which will occur after substantial failure and/or slip in a number of joints and bricks. For accurate prediction of ultimate load a criterion for brick failure would have to be included, since cracks after initiation from mortar joints propagate through the bricks also.

Several attempts to use interfaces for the modelling of masonry were carried out in the last decade with reasonably simple models, (Anthonie,1992; and Lourenco, 1994) for references. In particular, gradual softening behaviour and all failure mechanism, namely tensile, shear and compressive failure, have not been fully included.

Lourenco (1996) carried out a research on different numerical tools and published a comprehensive review on the state-of -art of micro and macro

modelling for the analysis of un reinforced masonry structures. Constitutive micro model including softening and failure mechanism, viz., tensile, shear and compressive failure developed so far have been reviewed. Adequacy of using homogenisation techniques which predicts macro behaviour of composite from the macro properties of masonry was discussed in his work. Validation of models by comparing the predicted behaviour with the behaviour obtained in experiments on different types of structures were also reviewed. He observed that masonry experimental results show typically a wide scatter not only in large structures but also in small tests. The main concern of his work was to demonstrate the ability of the models to capture the behaviour observed in the experiments and not a sharp reproduction of the experimental results in the form of load displacement curve.

The models proposed in the past failed to be widely accepted due to difficulties of formulating robust numerical algorithm and representing satisfactorily the inelastic behaviour. However it is believed that computations beyond the limit load down to a possibly lower residual load are essential to assess the structural safety.

2.4 SUMMARY

A review of literature relevant to this investigation has been presented in this chapter. The properties of brick masonry and similar materials have been reviewed with particular emphasis on the previous investigations (both analytical and experimental) on the composite action of wall-beam structure.

From the literature review, it is clear that much remains unknown about the interaction problem of wall-beam structure. Most experimental investigations have not been comprehensive because of the large number of variables involved. These have illustrated some parameters which are important. Many critical parameters are yet to be investigated. The existing design rules differ widely, which indicates lack of comprehensive information in this area.

Previous theoretical investigations including most of the finite element analyses have been limited due to considering the masonry as a homogeneous material. Those are linear elastic in nature. Due to lack of proper analytical tools and computational facilities available in those days, no attempt was made to model the non-linear characteristics of the constituent materials, consequently having no non-linear fracture model.

It is apparent from the literature that the model for predicting the failure load of wall-beam structure which incorporates non-linearity due to non-linear deformation characteristics of the material and progressive cracking of the constituent materials was not available in the past. If a suitable finite element model could be developed to predict failure of wall-beam structure subjected to uniformly distributed load and concentrated load, a large number of tests could be simulated and the significance of parameters influencing the behaviours of wall-beam could be studied. The need for a large number of tests could then be avoided. This thesis is an attempt to address this problem by developing a model of this nature. In the subsequent chapters, the development and verification of finite element models are described.

CHAPTER 3

ELASTIC FINITE ELEMENT ANALYSIS

3.1 INTRODUCTION

The finite element study outlined in this chapter is aimed at establishing the critical parameters which influence the behaviour of wall-beam structure. Two types of two-dimensional finite element analyses have been used. One assumes masonry to be a homogeneous continuum, the other considers masonry to be an assemblage of elastic bricks and joints each with different material properties (non-homogeneous). The non-homogeneous discretization of masonry for the detailed parametric study is the significant aspect of this chapter. The elastic analysis considering non-homogeneity of the constituent materials made for detailed parametric study of wall-beam structure confirms the results reported by several previous investigators who assumed masonry as a homogeneous material. Since different properties of component materials are incorporated in the present model it became possible to study the effects of constituent materials (brick, mortar, concrete and reinforcing bar) on the interaction behaviour of wall-beam structures. The study in this chapter includes additional parameters which have not been used by previous investigators. Particularly, the support length of the beam and the height of the supporting column carrying the beam of wall-beam structure. The influence of the following parameters on the stress distribution within a wall-beam structure are studied in this chapter: mesh size, height of brick wall, modulus of elasticity of the constituent materials, depth of supporting beam, reinforcement of the supporting beam, opening in the wall and support condition. In the comparison, emphasis has been made on the variation of vertical stress concentration and shear stress concentration at the interface level of wall and the supporting beam. The linear elastic finite element models are used to study the nature of the stress distributions. It should be mentioned here that an elastic analysis may not be adequate to realistically reproduce masonry behaviour for the full range of stress up to failure but very helpful to determine the important factors which influence the interaction behaviour of wall-beam structures.

3.2 GENERAL DESCRIPTION OF FINITE ELEMENT METHOD

The limitations of classical mathematics in solving continuum problems have led to the development of two categories of discretization techniques. In the

first, the differential equations governing the continuum are formed directly and solved by a mathematical discretization method, such as the finite difference approximations. The second method is based on a imaginary division of the continuum into finite elements. This method has become popular particularly among the engineers because of the more physical nature of the discretization.

The present analytical procedure is based on the finite element method. The application of this method has become very common and many texts have been written on the subject (Desai and Abel, 1972; Hinton and Owen, 1977; Zienkiewicz, 1977; Irons and Ahmad, 1980; and Cook, 1981). The finite element method can be thought of as a general method of structural analysis by means of which the solution of a problem in continuum mechanics may be approximated by analysing a structure consisting of an assemblage of properly selected finite elements interconnected at a finite number of joints or nodal points (see Fig. 3.1).

The steps in the finite element approximation of a continuum are summarised below after Zienkiewicz (1977). The continuum is divided by imaginary lines or surfaces into a number of finite elements. These are assumed to be interconnected at discrete number of nodes situated at their boundaries. In the stiffness approach, the displacements of these nodes are the basic unknowns. A set of functions is chosen to describe the internal displacements of the element in terms of the nodal displacements. The internal strains are also expressed in terms of the nodal displacements by using the displacement functions. The state of stress is defined by these and any initial strains. The concentrated forces at the nodes are determined by the equilibrium of the boundary stresses and the distributed loads. This gives the characteristic stiffness relationship of the continuum.

The application of finite element method requires the use of a computer to carry out the numerical processes. The steps in the finite element analysis of a wall-beam structure are described below.

- (a) The brick, the mortar, the supporting beam and the reinforcement are idealised as an assemblage of a number of elements.
- (b) The element displacement functions are chosen to specify the pattern in which the elements deform. On the basis of these displacement functions the element stiffness matrices relating the element nodal forces to the element nodal displacements are evaluated.
- (c) The element stiffness matrices are assembled to develop the overall stiffness matrix of the total structure.

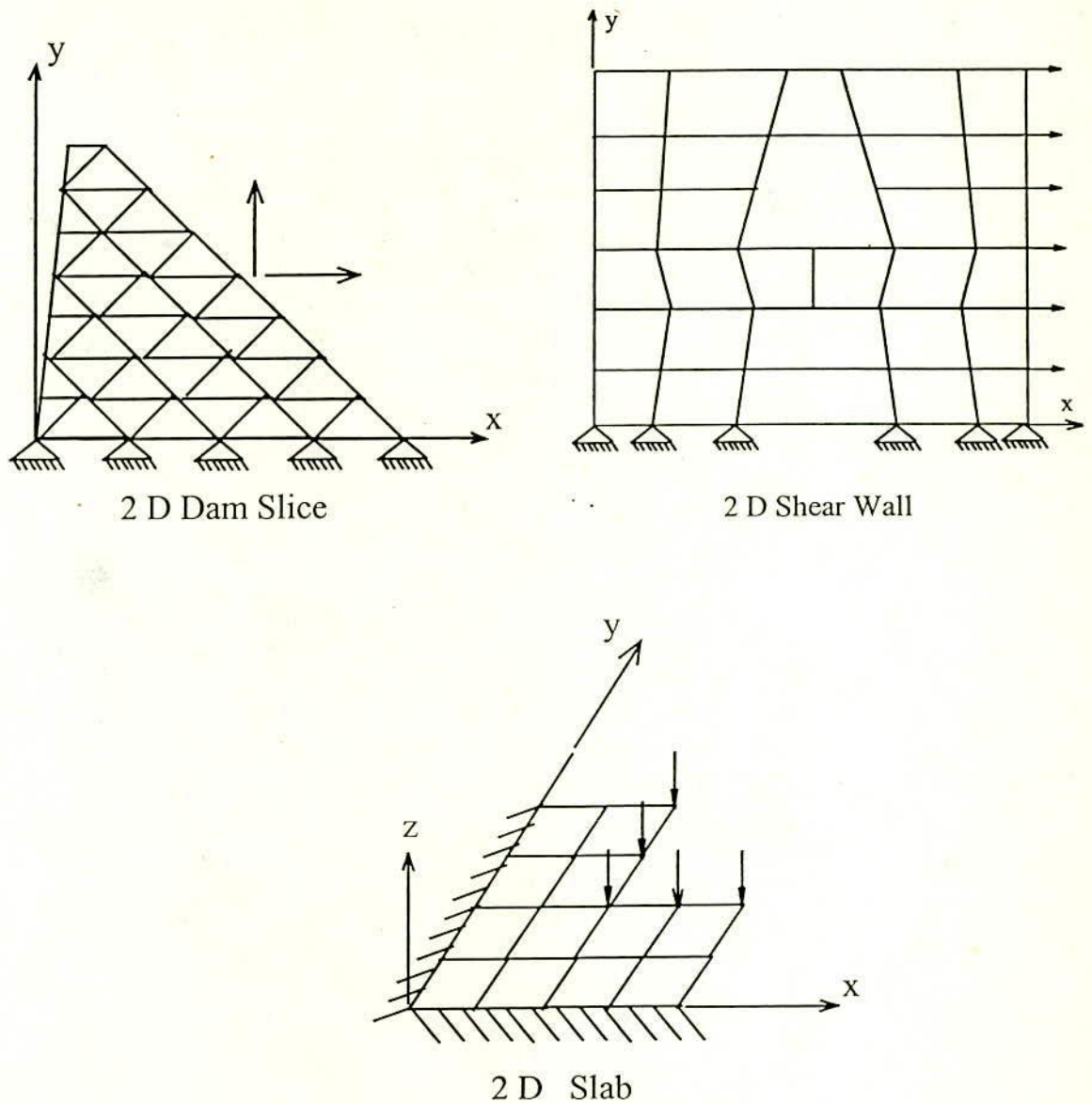


Fig. 3.1 Structure Composed of Two-dimensional Elements

- (d) The joint displacements of the complete system are obtained by solving a set of linear simultaneous equations governing the equilibrium conditions at the nodes. This takes the form:

$$[K]\{\delta\} = \{R\} \quad (3.1)$$

where $\{R\}$ is the vector of applied loads at the joints, $[K]$ is the overall stiffness matrix and $\{\delta\}$ is the vector of unknown joint displacements.

- (e) The joint displacements are used to calculate the other required values such as the strains, the stresses, and the forces at various points in the system.

The accuracy of the finite element method depends on the fineness and the accuracy of the discretization of the continuum. Therefore, each element of the mesh should be chosen carefully to represent the various components of the wall-beam system closely. When a large number of elements are required, the mesh-refinement technique proposed by Anand and Shaw (1980) is useful. The general procedure for the formulation of a finite element model is summarised in the ensuing sections.

3.3 TWO-DIMENSIONAL LINEAR ELASTIC FINITE ELEMENT MODEL

Two types of linear elastic finite element analyses have been performed. One assumes masonry to be a homogeneous continuum, the other models bricks and joints separately. It should be mentioned that, very few experimental investigations on the behaviour of wall-beam structures furnished the detailed material properties. The most extensive series of tests are those of Rosenhaupt (1962) and Wood (1952). However, Rosenhaupt's investigation furnishes the material properties as required in a finite element analysis. Several previous investigators have used the experimental data of Rosenhaupt. Although not representative for normal brick masonry, Rosenhaupt's test values were utilised in this study for the sake of comparison of analytical results. The material properties proposed by Rosenhaupt are typical of light weight brick wall on RCC beam. However, since the model incorporates properties of all constituent materials any brick-mortar combination can be modelled provided their material properties are known.

For the homogeneous case, an elastic modulus of 670 MPa and Poisson's ratio of 0.2 as obtained by Rosenhaupt (1962) were taken for the masonry. For the non-homogeneous case, the finite elements corresponding to bricks and joints were assigned different values of elastic modulus and Poisson's ratio. For brick, modulus of elasticity as obtained by Rosenhaupt (1962) was taken as 1165 MPa. For mortar the modulus of elasticity and Poisson's ratio were assumed to be 500 MPa and 0.17 respectively while the Poisson's ratio of brick was assumed to be 0.184. In the latter part of this analysis the material properties obtained from the extensive

laboratory tests on small burnt clay bricks and brick prisms (discussed in Chapter 4), were incorporated in the model.

The two-dimensional elastic finite element program was adopted for this preliminary study. The frontal method of solution of the equilibrium equations were adopted from Hinton and Owen (1977). In the program most of the data can be generated automatically, including the fine mesh at the locations of higher stress gradient. The nodal displacements, the strains and the stresses at the Gauss points of each element are calculated, as well as the average value at the centre of the element. When the sizes of the meshes are very fine particularly required to represent nonhomogeneity of mortar and brick, Gauss sampling points were not used. Thus a considerable saving in computer time was achieved during nonhomogeneous solutions at the cost of negligible sacrifice of accuracy.

3.3.1 Selection of Finite Element Mesh

Proper representation of brickwork is very important in the finite element analysis of wall-beam structure. In the past the brickwork has been considered as a homogeneous material by majority of the researchers with average properties for both fine and coarse meshes. It should be mentioned that an element should encompass at least a header joint and a bed joint along with a portion of brick to represent the brickwork as a homogeneous continuum. In this chapter the masonry part of wall-beam has been modelled as homogeneous and nonhomogeneous material. Various mesh sizes ranging from very coarse to fine have been used to study the influence of mesh refinement on the analytical results. Coarse meshes of different sizes as shown in Fig. 3.2 to Fig. 3.4 have been used to represent the brickwork as a homogeneous material and the fine mesh shown in Fig. 3.5 has been used to represent the brickwork as a nonhomogeneous material.

Due to symmetry only half of the wall-beam panel has been considered for the finite element analysis. Typical boundary conditions have been shown in Fig. 3.6(a) and the physical and elastic properties of the beam tested by Rosenhaupt is shown in Fig. 3.6(b)

The vertical stress at the interface as obtained by elastic analysis is shown in Fig. 3.7. To keep similarity with previous authors, the vertical compressive stresses at interface is represented by positive sign. The typical vertical stress distribution along the span as shown in Fig. 3.7 agrees favourably with other

authors (Rosenhaupt, 1962; Stafford Smith and Riddington, 1976, 1977; Davies and Ahmed, 1978; Page, 1979 and Kamal, 1990). Fig. 3.7 shows that the stress does not exhibit any considerable variation near the centre of the span irrespective of the size of the mesh used in the analyses. But for a length of $1/4$ th of the span from the supports the variation is quite considerable depending on the size of the mesh and the material characterisation. From these observations it can be concluded that the choice of fine mesh near the supports and the coarse mesh towards the centre of the span can be accepted for the analysis. Since the stresses are concentrated near the support of the wall-beam panel, a nonhomogeneous representation of the material with very fine mesh near the support (see Fig. 3.5 for Mesh FNH) is advisable.

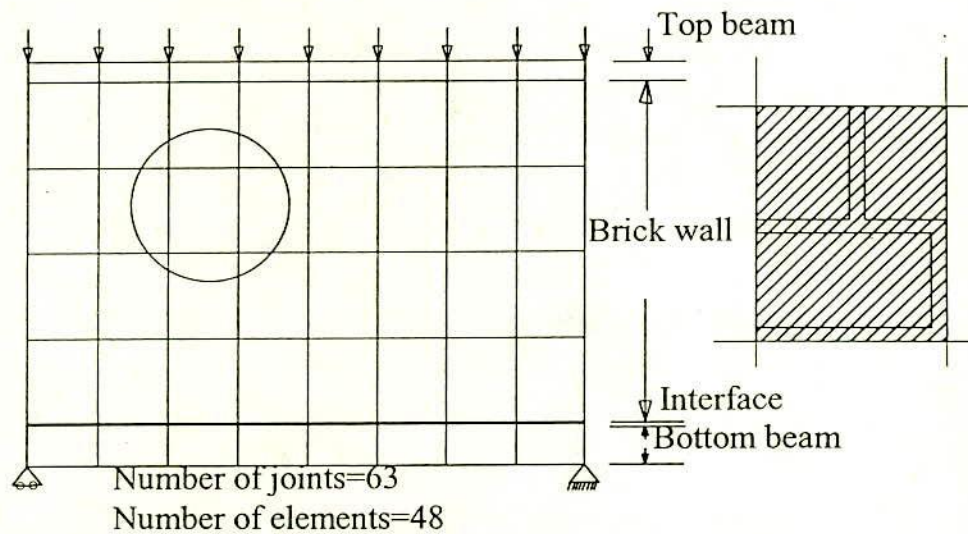


Fig. 3.2 Very Coarse Mesh (XCH) for Homogeneous Analysis

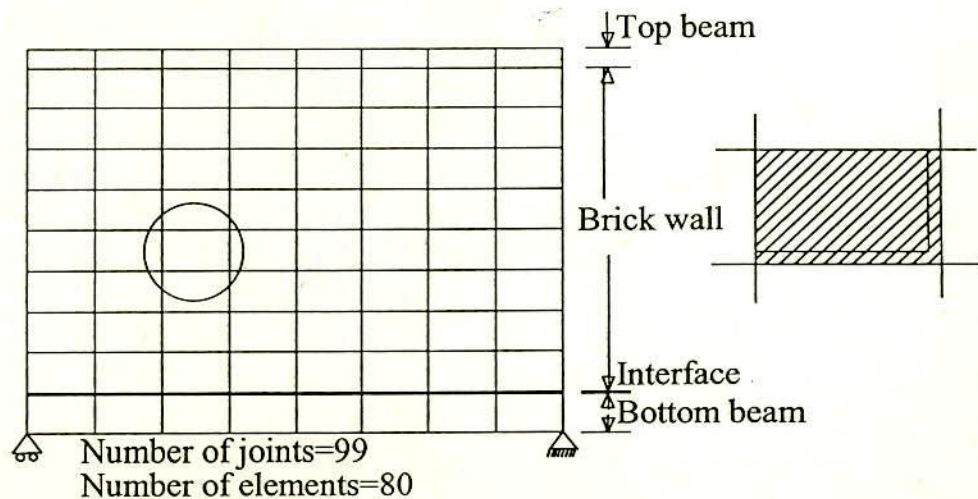


Fig. 3.3 Coarse Mesh (CH) for Homogeneous Analysis

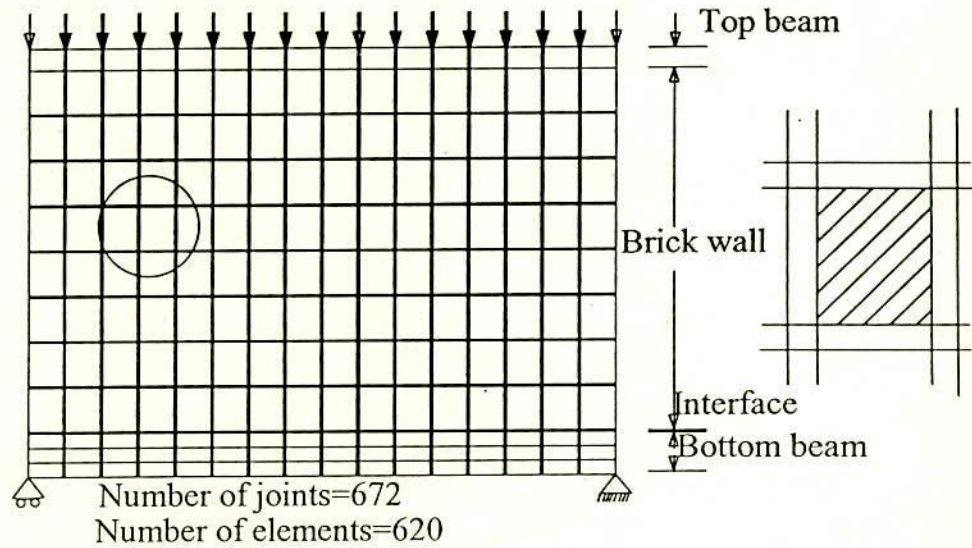


Fig. 3.4 Medium Coarse Mesh (MH)
(Homogeneous)

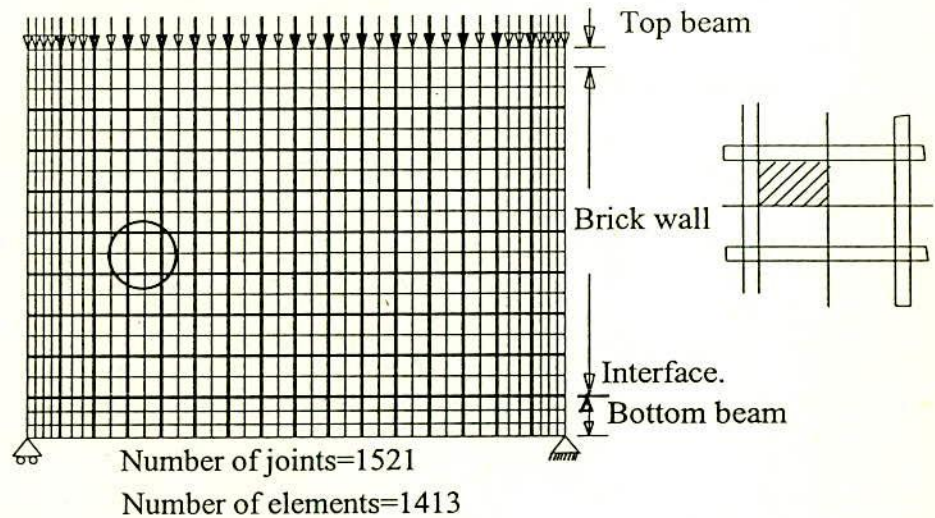


Fig. 3.5 Fine Mesh (FNH)

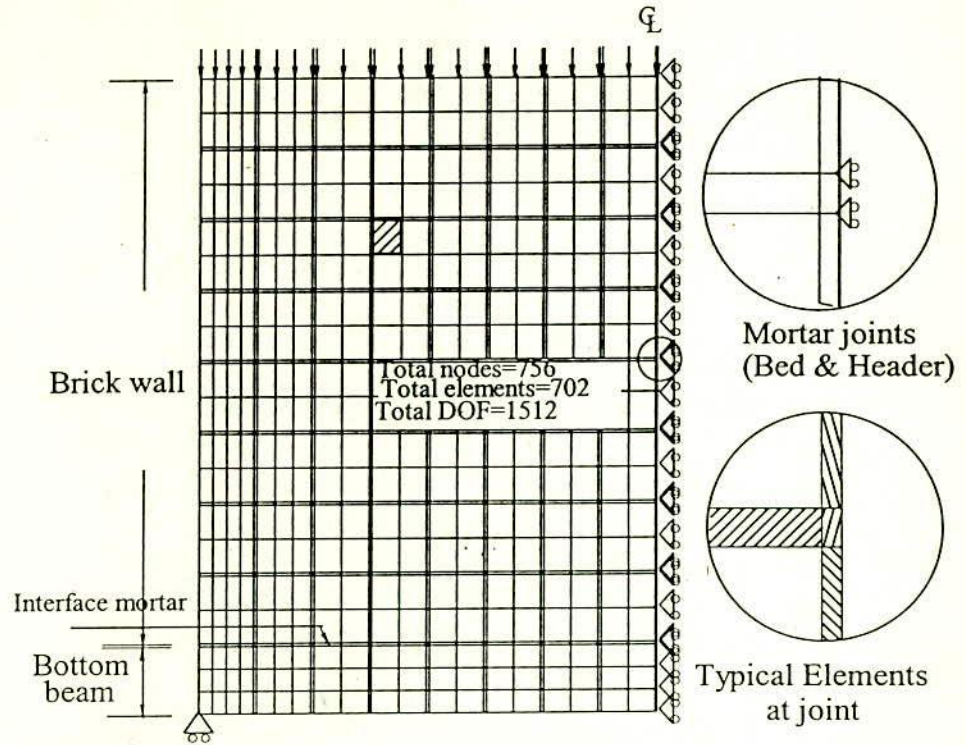


Fig. 3.6 (a) Boundary Condition, Element Discretization and Load Distribution (Uniformly Distributed)

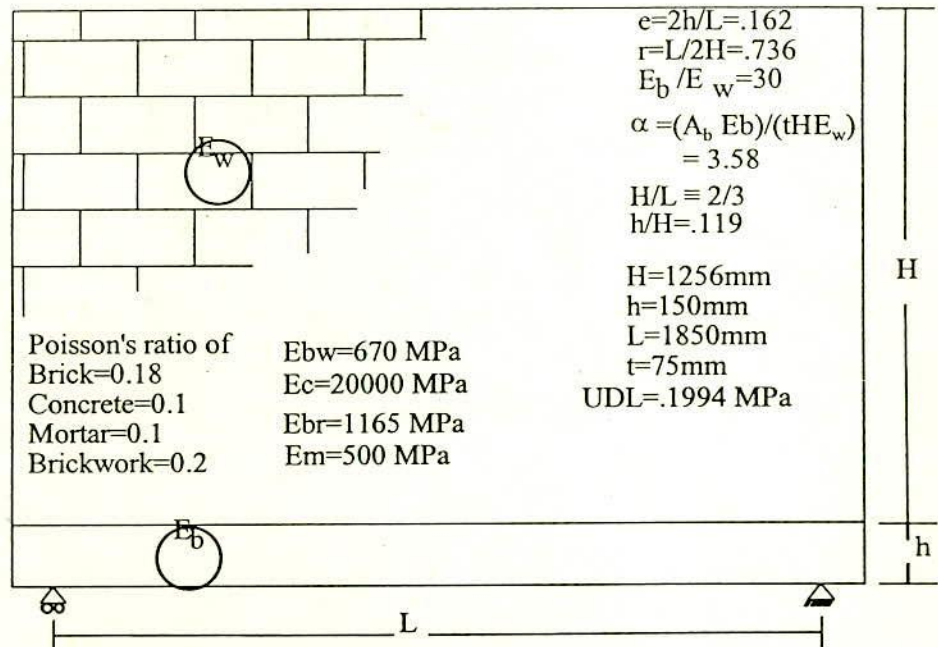


Fig. 3.6 (b) Physical Properties of Beam Tested by Rosenhaupt (1962)

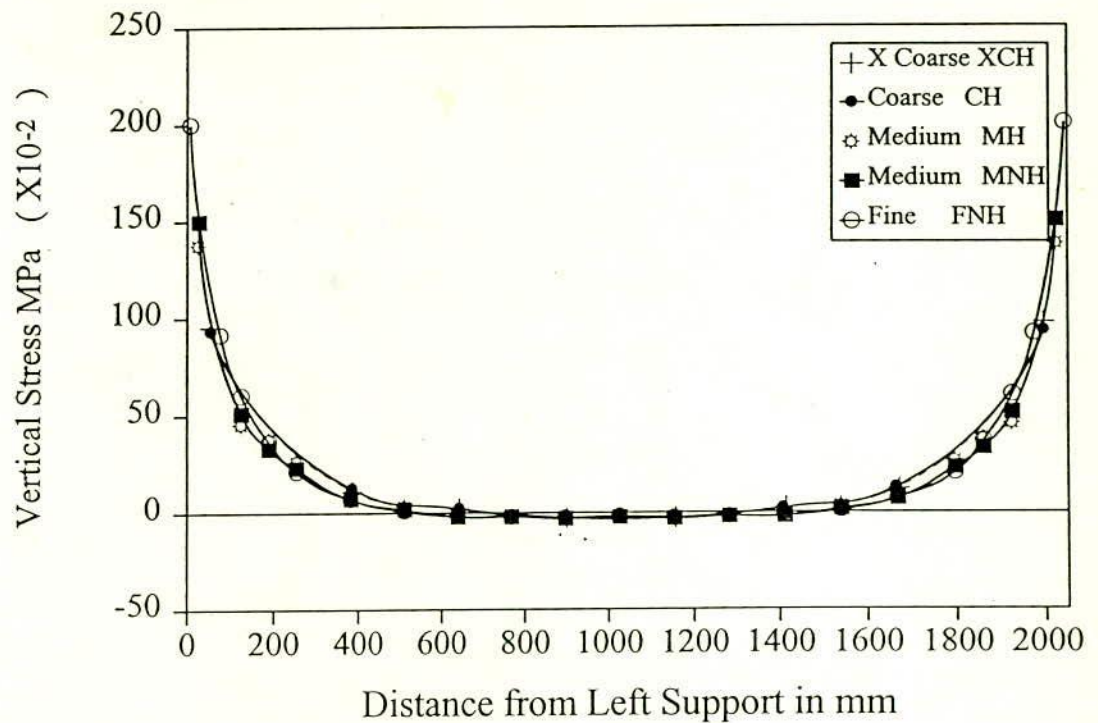


Fig. 3.7 Vertical Stress at Wall-beam interface for Different Sizes of Finite Element Mesh

3.3.2 Reinforcement of the Supporting Beam

In developing a finite element model for a reinforced concrete member, mainly three alternative representations of the reinforcement can be used (Scordelis, 1972; Al-Mahaidi and Nilson, 1979) : (a) Distributed, (b) Embedded, (c) Discrete.

For a distributed representation, as shown in Fig. 3.8(a) the steel is assumed to be distributed over the concrete element, with a particular orientation angle θ . A composite concrete-reinforcement constitutive relation is used in this case. To derive such a relation, perfect bond must be assumed between the concrete and steel.

An embedded representation, as shown in Fig. 3.8(b) may be used in connection with higher order isoparametric concrete elements. The reinforcing bar is considered to be an axial member built into the isoparametric element such that

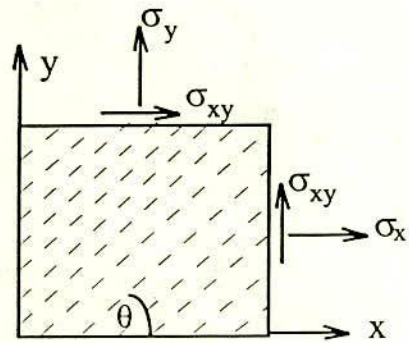
its displacements are consistent with those of the element. Again perfect bond must be assumed in this case.

A discrete representation of the reinforcement using one dimensional element, as shown in Fig. 3.8(c) has been widely used. Axial force members or bar links may be used and assumed to be pin connected with two degrees of freedom at the nodal points. Alternatively, beam element may also be used. In either case, the one-dimensional reinforcement elements are easily superimposed on a two-dimensional finite element mesh such as might be used to represent the concrete. A significant advantage of the discrete representation, in addition to its simplicity, is that it can account for possible displacement of the reinforcement with respect to surrounding concrete.

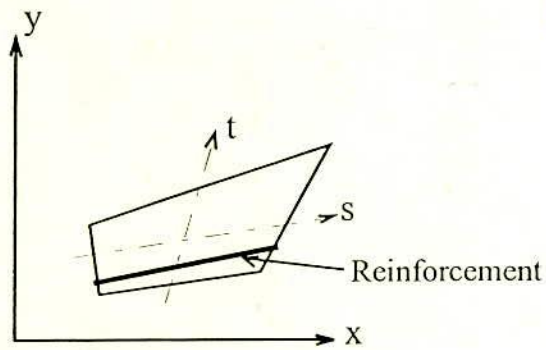
The stress-strain curves for steel are assumed to be identical in tension and compression. And for simplicity it is often necessary to idealise the steel stress-strain curve. Three different idealisations shown in Fig. 3.9 are in use depending on the accuracy required. For each idealisation it is necessary to determine experimentally the values of the stress and strains at the onset of yielding, strain hardening, and the ultimate tensile strength.

The basis on which the reinforcement is incorporated into the finite element model depends upon whether a discrete, embedded, or distributed representation of the steel is adopted. The discrete representation of the steel is adopted in this study. The idealisation of discrete representation is described below.

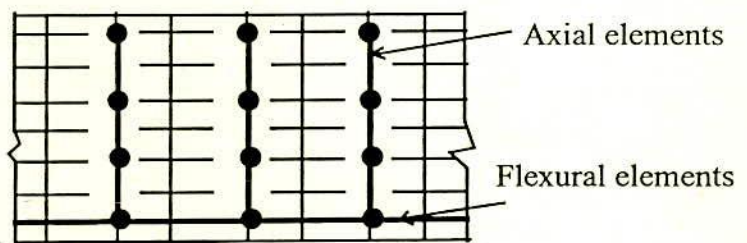
The cross section of beam is shown in Fig. 3.10(a). This includes three main tensile reinforcing bars with its width b , each bar having diameter d_b . For convenience in lying out the finite element mesh, each round bar is replaced by a rectangular bar having the same area as suggested by Fig. 3.10(b). A plane stress idealisation is adopted for the analysis, and the actual beam is reduced to a beam of unit width as shown in Fig. 3.10(c). The bar area tributary to a unit width of concrete is established as in Fig. 3.10(d), based on the number of bars included in the original beam of width b . The reduction of concrete volume resulting from the presence of the bars can be accounted for by using a reduced thickness for the concrete at the level of the reinforcement. In the analysis this effect is achieved by reducing the stiffness of the concrete elements at that level, in proportion to the reduction in concrete thickness.



(a) Distributed



(b) Embedded



(c) Discrete

Fig. 3.8 Alternate Representation of Steel

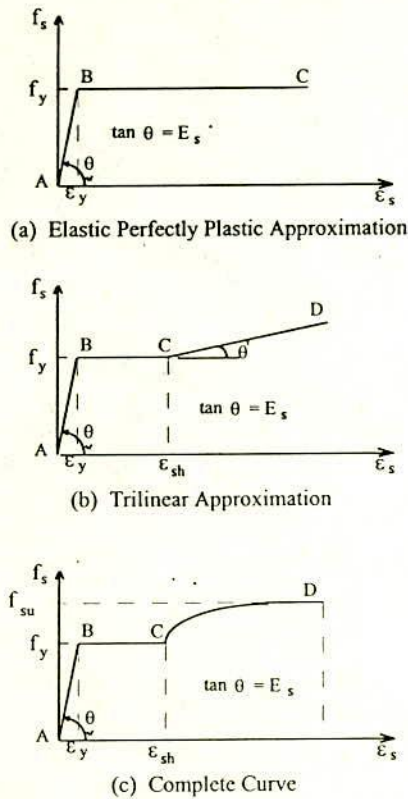


Fig. 3.9 Idealisation for the Stress Strain Curve for Steel in Tension

Thus a three-dimensional concrete beam is replaced for purposes of analysis by an approximate two-dimensional plane stress model. With this approach, the stress-strain laws for constituent materials of reinforced concrete are uncoupled permitting efficient and convenient implementation in a finite element program. In

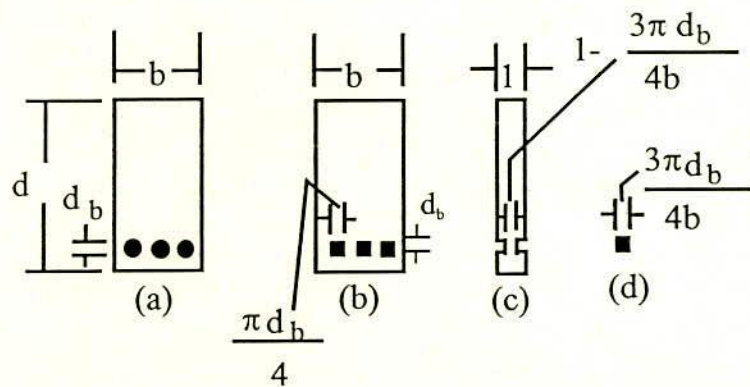


Fig. 3.10 Basis of Finite Element Model for Reinforced Concrete Beam. (a) Beam cross section. (b) Round bar has been replaced by equivalent rectangular bar. (c) Unit width of beam for plane stress idealisation. (d) Bar area tributary to a unit width of concrete

addition, the method proves convenient to investigate the relative contributions of the concrete and steel components in resisting loads. Similar method of discretizing the reinforcement in reinforced concrete structure was successfully applied by Buyukozturk (1977) using the doubly-curved isoparametric thin shell elements. In the present work the application of the method is demonstrated by the use of plane stress elements with two translational degrees of freedom defined at each node. Thus the actual reinforcing bars are represented by equivalent anisotropic steel layers by making appropriate adjustments to the thickness of the reinforcing bar (rebar) elements and having no adjustments of the $[D]$ matrix for the rebar element. The steels in layers carry uniaxial stress in the same direction as the actual bars along with the consideration of its dowel action. Strain compatibility between steel and concrete is maintained assuming that there is a sufficient strong bond between the two materials so that no relative movement of the steel and the surrounding concrete can occur. The stiffness of the reinforcement is included to the member stiffness by direct superposition. Reinforcement has been considered to be connected directly to the concrete at the nodal points in this study.

The presence of secondary reinforcement (stirrup) has not been considered in finite element model.

It should be mentioned that the flexural cracking of concrete will reduce the stiffness of the beam. Although no allowance has been made in the elastic model, the effect has been taken care by modifying the model in the subsequent chapters. This has been particularly addressed in chapter 5 where the behaviour of materials after failure has been discussed.

3.3.3 Finite Element Discretization and Boundary Condition

The basic wall-beam structure considered in this theoretical study is simply supported at its ends (see Fig. 3.6(a)). In practice this situation rarely exists. Usually the beam has some rotational restraint at its supports, due to either being built in to a wall or being connected, with some degree of rigidity, to supporting columns. In other cases, the wall is continuous over the supports. The numbers of factors affecting the rotational restraint and thereby controlling the behaviour of the structures under these conditions are therefore large. When the beam is built in, these factors include the extent of inbuilding and the height, physical properties and horizontal restraint of the wall below the support. When the beam is connected

to the columns the influencing factors include the rigidity of the fixing and the properties and the length of the columns. Other parameters affecting the structural behaviour include the length and height of the wall beyond the support. Comprehensive studies of these parameters is carried out at the end of this chapter. However, the basic wall-beam idealised for analysis in the elastic finite element study is shown in Fig. 3.6(b). The brickwork has been considered as an assemblage of bricks set in mortar matrix (homogeneous). The beam has been considered to be simply supported. The height of the wall is approximately equal to the 0.6 times the length of the wall.

Since the overall system is symmetric with respect to loading and geometry, only half of the structure has been discretized for the present study Fig. 3.6(a). The appropriate boundary conditions have been provided for nodes at the centre line of symmetry.

3.4 VERIFICATION OF THE COMPUTER MODEL

To verify the accuracy of the present finite element model developed to analyse the wall-beam structure, the results of linear elastic solutions obtained by the present model are compared with the results obtained from theory and empirical equation and with those obtained from test results. For this purpose the deflection of a simply supported beam, the split tensile strength of masonry prism and the results of a wall-beam panel tested by Rosenhaupt (1962) are compared. The comparison reveals satisfactory performance of the model.

3.4.1 Deflection of a Simply Supported Concrete Beam

To check the adequacy of the finite element program in bending the deflection of a simply supported beam has been modelled. The data used for the beam is given below.

Dimensions:

Length of the beam = 1297.5 mm
 Width of the beam = 100 mm
 Height of the beam = 75 mm

Loads:

Dead Load = Not considered
 Superimposed Load = 9.612 Newton/mm

Material properties:

Modulus of Elasticity of Concrete = 28672 MPa

Poisson's Ratio of Concrete = 0.16

Maximum Deflection at Midspan : $\Delta = \frac{5wL^4}{384EI} = 3.51 \text{ mm}$

The linear elastic finite element analysis has been carried out by using the proposed model for the above beam. Using normal rectangular element maximum deflection at midspan is 3.37 mm. using QM-6 element the value obtained is 3.49 mm. The finite element discretization and boundary condition adopted for the analysis of the beam is shown in Fig. 3.11.

3.4.2 Splitting Test of Brickwork Triplet

In masonry structures vertical joints are very critical. Under vertical load most of the vertical joints undergo tensile stress which initiates bond failure at the interface of brick and mortar joint. In the laboratory tensile bond strength of brickwork is normally determined by splitting test of brick prism (discussed in article 4.4.5). The stress state (transverse stresses) in the prism is nonuniform due to the presence of bed joint. In this study the splitting test of brickwork prism has been investigated to check the adequacy of the present finite element program in modelling nonuniform stress field.

Tensile bond strength is obtained indirectly by splitting tensile test on brickwork prism, using the following equation.

$$\text{Tensile stress, } \sigma_T = \frac{CP}{Dl}$$

where

P = applied load

l = specimen thickness

D = equivalent diameter

$$= \sqrt{\frac{h.a}{\pi/4}}$$

h, a = specimen height and width

C = constant = 0.648 (for homogeneous material)

Finite element study made by Ali (1987), revealed that the value of C varies from 0.648 to 0.71 as E_b / E_m varies from 1 to 4 and suggested the value of C to be 0.67 for average practical condition.

Two specimens were considered for the comparison, one modelling bricks and mortar joints as separate materials and the other treats brickwork as homogeneous material. The finite element discretization of the specimen is shown in Fig. 3.12.

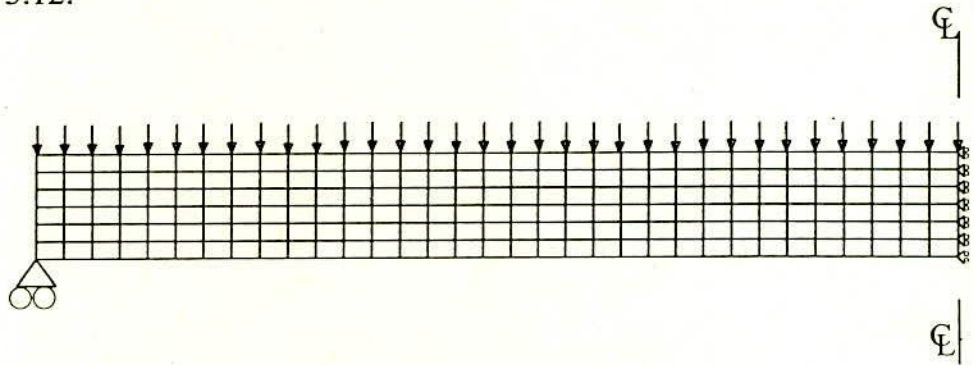


Fig. 3.11 Finite Element Discretization and Boundary Condition of a Simply Supported Beam

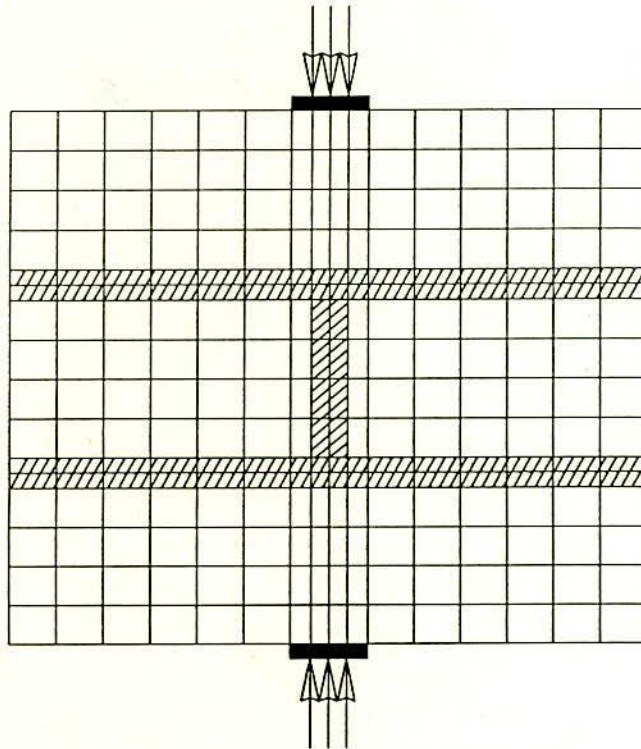
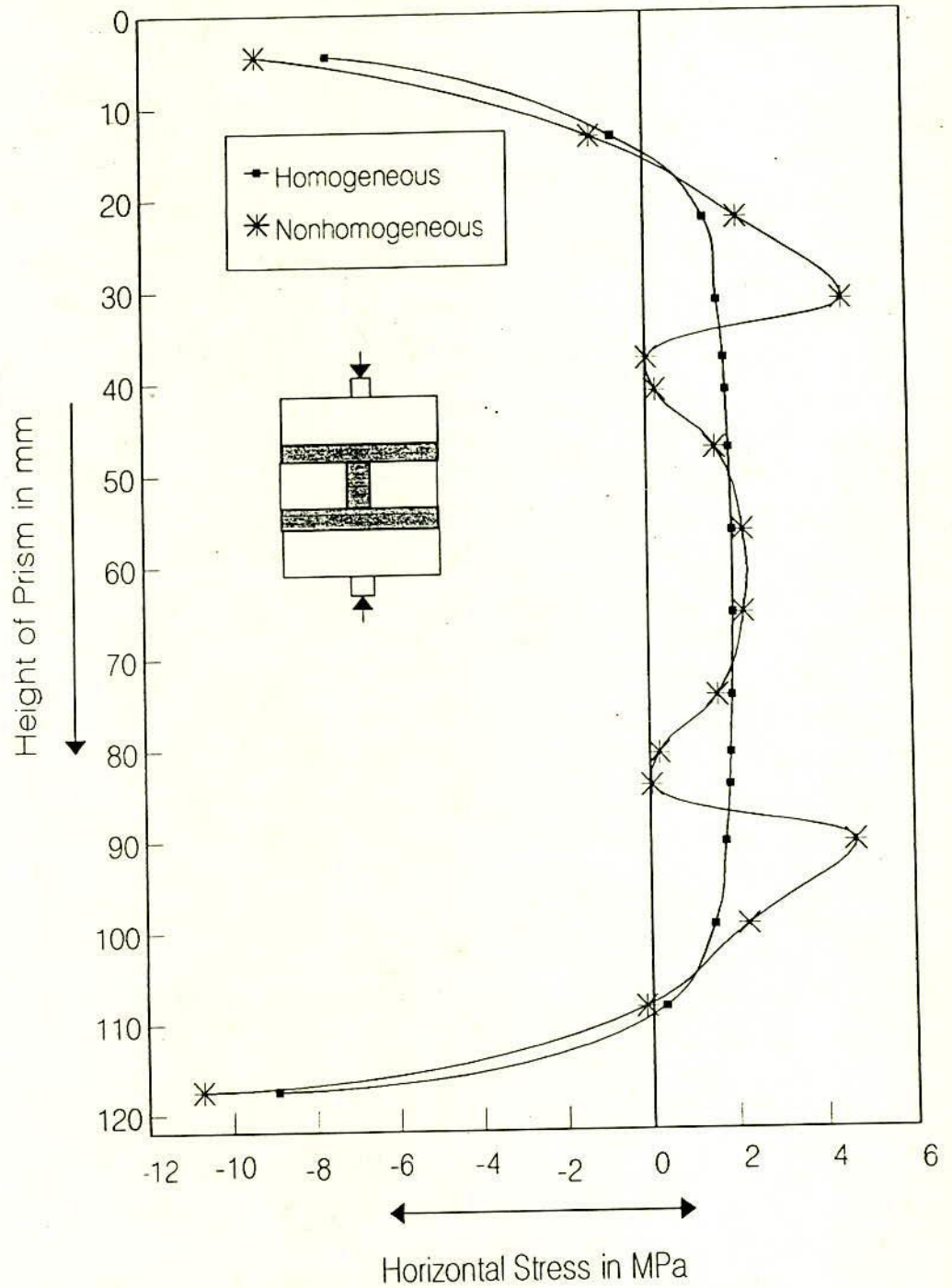


Fig. 3.12 Finite Element Discretization and Boundary Condition for Splitting Test of a Brickwork Triplet

The results obtained from the present finite element analysis are in agreement with those calculated from the above equation. The tensile stress pattern across the vertical section through the vertical mortar of the prism (both for homogeneous and nonhomogeneous conditions) is shown in Fig. 3.13. The model predicts the stress pattern with reasonable agreement.



(central vertical section through masonry prism)

Fig. 3.13 Split Tensile Test of Masonry Prism

3.4.3 Comparison with Experimental Results

In the previous articles the accuracy of the finite element program has been verified with bending characteristics of simply supported concrete beam and splitting test of masonry prism. In this article the program will be used to model the experiment performed by Rosenhaupt (1962) on wall-beam structure. Experiments carried out on wall-beam structures by other researchers like Wood (1952), Burhouse (1969) and Stafford Smith et al., (1978) are also widely known. It is mentioned earlier that the series of tests performed by Rosenhaupt (1962) provides the related material properties suitable to incorporate in the finite element models. Fig. 3.6(b) shows physical properties of a wall-beam (light weight concrete block on reinforced concrete beam) tested by Rosenhaupt (1962). This beam was later analysed by other authors. The results of the present finite element analysis of the same beam of Fig. 3.6(b) are compared with the experimental results and the analytical results obtained by Rosenhaupt (1964), Coull (1965-66), and finite element analyses of Male and Arbon (1971) and Saw (1975).

Rosenhaupt recorded vertical strain at the first course of brickwork from the bottom and horizontal strain at the mid vertical section of the panel at about half of the failure load. At this load the wall and the beam are assumed to remain in the elastic range. The comparison of these strains with those predicted by the present finite element analyses and by the finite element analysis made by Male and Arbon are shown in Fig. 3.14(a) and Fig. 3.14(b). It is to be mentioned that the finite element analysis performed by Saw (1975) has not been included in his comparison since the wall stresses obtained by him are nearly identical to Male and Arbon (1971). From the comparison it is seen that the agreement of horizontal strain at mid vertical section is quite satisfactory for both homogeneous and nonhomogeneous models, while the agreement between the test results and the finite element analysis regarding vertical strain at first brick course near the support is poor when the brickwork is considered as a homogeneous material. This may be due to the fact that, the panel section close to the support experiences high stress gradient in comparison to the middle third as can be seen from Fig. 3.7. At the lightly stressed zone of the middle of the panel the horizontal strain is very small in comparison to the vertical strain at the ends of the span. This low stress or strain at the middle is likely to be insensitive to the type of finite element model or size of mesh used. However, at the zone of high stress gradient near the support the prediction of stress by various models may vary due to different material representation and mesh size. It is also seen from Fig. 3.14(a) that the results of

nonhomogeneous solution using fine mesh agrees favourably with the test results. In addition, Fig. 3.14(b) shows that the vertical mortar joints experience much more horizontal strain in comparison to that of the brick elements located just at the top and bottom. It is generally very difficult to measure this local variation of deformation in these thin vertical mortar joints in the laboratory. This variation can not also be predicted by the homogeneous finite element model. Therefore, nonhomogeneous representation of the materials is required in the finite element analysis of wall-beam structure.

3.4.4 Comparison with Analytical results

Most of the previous authors considered brickwork in wall-beam structure as homogeneous material. In this article the comparison therefore has been made with the result of the analysis considering brickwork as a homogeneous material with those of previous investigators (Male and Arbon, 1971; Saw, 1974, 1975). The element discretization adopted in the present article and by other authors are shown in Fig. 3.15.

Vertical stress in Masonry wall

The concentration of vertical stress is given by, σ_y / w , where w is average stress applied on the top of the wall and σ_y is the vertical stress induced at the interface level of wall and the supporting beam. The comparison of concentration of vertical stress in the wall, obtained by previous authors (Rosenhaupt, 1964; Coull, 1965-66; Male and Arbon, 1971; Saw, 1975) and the present analysis can be seen from Fig. 3.16(a) that confirms reasonable agreement between the results. But the distribution of vertical stress in the zone close to the support as obtained by the present analysis differs appreciably from those of Rosenhaupt (1964). This is due to the assumption of Rosenhaupt (1964), that vertical forces at wall-beam interface are concentrated at the ends of the beam. It is clear in Fig. 3.16(a) that this assumption is not correct.

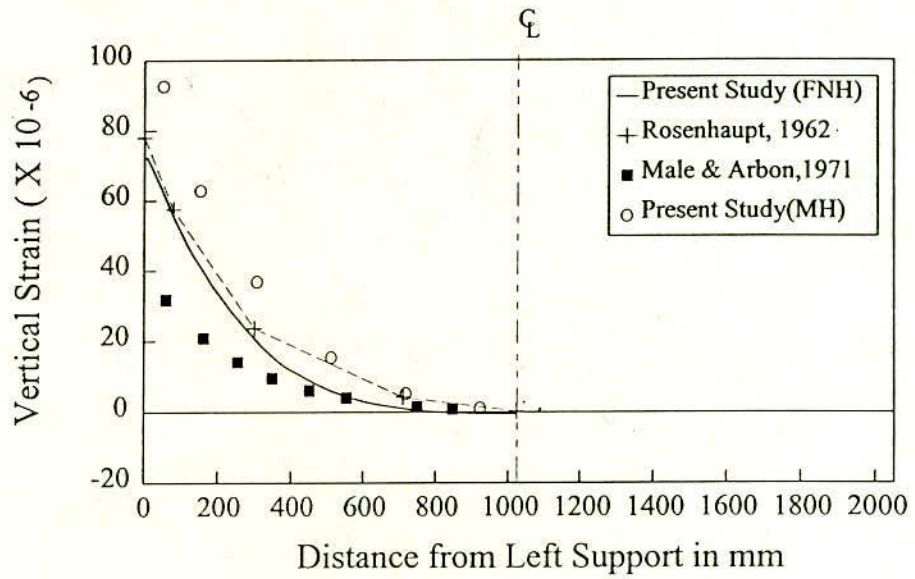


Fig. 3.14 (a) Comparison of Vertical Strain (Rosenhaupt, 1962)

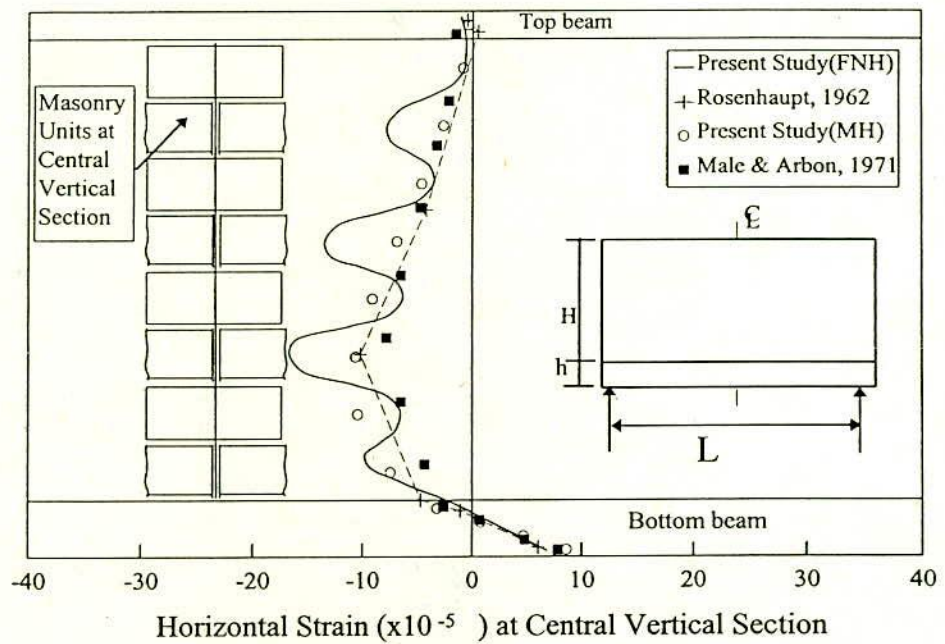
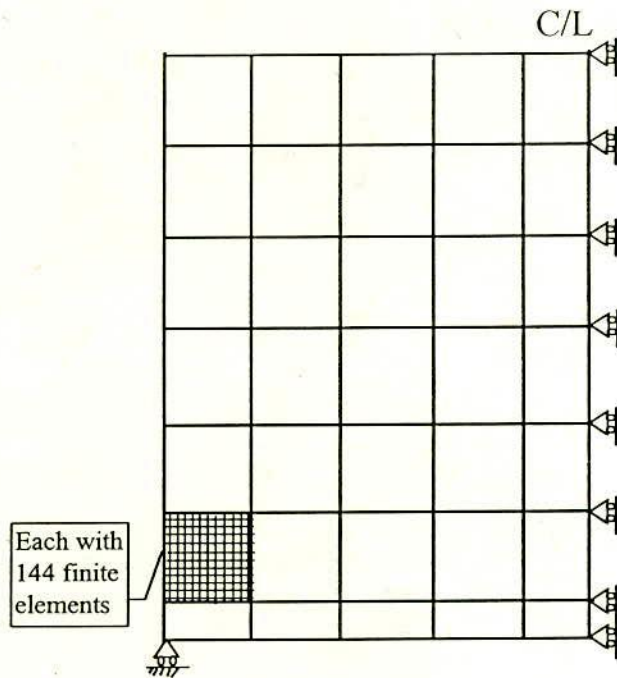
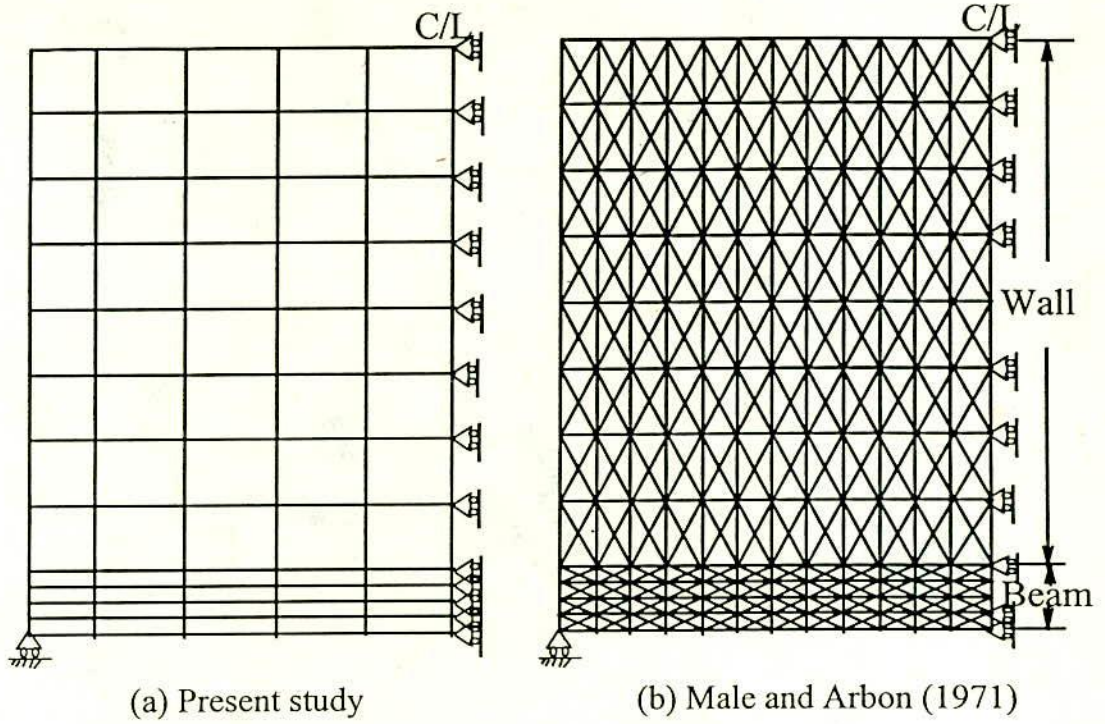


Fig. 3.14(b) Comparison of Horizontal Strain (Rosenhaupt, 1962)



(c) Saw (1974)

Fig. 3.15 Finite Element Discretization of Beam Tested by Rosenhaupt (1962)

Horizontal Stress in Masonry wall

The concentration of horizontal stress is given by σ_x / w , where, w is average stress applied on the top of the wall and σ_x is the horizontal stress induced at the interface level of the wall and the supporting beam. Fig. 3.16(b) shows the distribution of concentration of horizontal stress in the panel and confirms reasonable agreement between the present finite element analysis and that of Male and Arbon (1971). While the agreement is poor between the present finite element solution and those of Coull and Rosenhaupt in predicting the horizontal stresses of the panel. This fact however seems to present doubt regarding acceptance of the assumption made by Coull that the stresses can be expressed as a power series with coefficients being function of height only.

Shear Stress in Masonry wall

The concentration of shear stress is given by τ_{xy} / w where, w is average stress applied on the top of the wall and τ_{xy} is the shear stress induced at the interface level of wall and the supporting beam. From Fig. 3.16(c) it can be seen that the distribution of concentration of shear stress in the wall agrees favourably with the results of other authors (Rosenhaupt, 1964; Coull, 1965-66 and Male and Arbon, 1971) and indicates that the shear stress at wall-beam interface concentrates near the end.

It should be mentioned here that the stresses obtained by Male and Arbon in the masonry part of the panel are nearly identical to those of Saw as it was reported by the latter. For this reason the stress obtained by Saw (1975) has not been shown in the above comparisons.

Vertical Stress in Supporting Beam

The stress distribution in the supporting beam from the present finite element analysis and the analysis made by Male and Arbon is shown in Fig. 3.16(a). The vertical stress in the supporting beam agrees favourably with that of Male and Arbon except at section close to the support.

Horizontal Stress in Supporting Beam

The horizontal stress (see Fig. 3.16b) obtained by the present analysis agrees favourably with those of Male and Arbon (1971) at the bottom part of the beam, while at the top of the supporting beam a minor deviation has been noticed. In the analysis of Male and Arbon, the fibre at the top of the supporting beam has been found to be in tension with a non-linear variation along the depth of the supporting beam. This of course is a deviation from results of the test carried out by Rosenhaupt (1962). The panel being the same in both cases. The horizontal strains measured by Rosenhaupt (1962) at different vertical sections intersecting the supporting beam confirms that the top of the beam is under compression. Saw (1975) has used line elements to simulate the supporting beam in his finite element model. From the analysis he found that the horizontal stresses vary linearly across the beam depth, which again does not comply with the findings of Male and Arbon (1971). This difference as he concluded, may be due to the fact that although a large number of triangular finite elements have been used by Male and Arbon to discretize the beam, but the size may not be fine enough for the region near the support where the stress gradient is very high. A simple photo elastic test was made by Saw to illustrate this point. The evenly spaced isochromatics in the supporting beam confirmed that horizontal stress varies linearly across the beam depth. The phenomenon of having tension throughout the depth is likely to occur for cases where the supporting beams are relatively shallow. It is also seen from Fig. 3.16(b) that the maximum stress in the beam does not occur at the middle of the span but close to the support. By the above discussion it is concluded that the supporting beam which is assumed as a tension tie by Rosenhaupt (1964) is not equally applicable to all cases, rather should depend on relative stiffness of the wall and the supporting beam.

Shear stress in Supporting Beam

Shear stresses obtained by Male and Arbon (1971) at sections close to the support of the beam are seen not to agree with the present finite element analysis (see Fig. 3.16(c)). Saw did not show any shear stress variation in the supporting beam. The disagreement of the shear stress at section close to the support casts doubts on the suitability of triangular elements used by Male and Arbon (1971) to simulate the stress in this highly stressed region. It is important to note that for the linear displacement triangular elements used by them the strain and stress are

constant over the elements and makes the element relatively inefficient. This fact is also confirmed by Brebbia and Ferrante (1978).

It is noteworthy that the present finite element analysis for homogeneous solution uses a total of 78 nodes with 60 elements to achieve results which are comparable with the finite element analyses of Male and Arbon who employed total of 313 nodes with 576 triangular elements and Saw who employed 42 nodes with 30 macro elements (each having 144 finite elements) in conjunction with 5 line elements.

3.4.5 Comparison of Bending Moment in the Supporting Beam

The economy in the adoption of a wall-beam structure is mainly due to the saving of reinforcement and concrete of the supporting beam. From the discussion made so far, it is clear that due to wall-beam composite action the maximum portion of vertical load acting on the panel is directed towards the support thus relieving the middle portion of the beam. As a result bending moment reduces considerably compared to $wL^2/8$. Many investigators tried to quantify this reduced moment — both experimentally and analytically. But the variation of moment as obtained by different authors are noteworthy.

Since the neutral axis of the wall-beam considered happens to be within the concrete beam section, the moment at different section is calculated on the basis of actual fibre stress at the top and bottom of the section. These fibre stresses were obtained by extrapolating the values of horizontal stresses from computer output at different depths of a section. From these fibre stresses the moment at a section is obtained from following equations:

$$\sigma_{\text{bottom}} = \frac{P}{A} + \frac{MC}{I} \quad (3.2a)$$

$$\sigma_{\text{top}} = \frac{P}{A} - \frac{MC}{I} \quad (3.2b)$$

where $C \neq d/2$ is the position of neutral axis at the section considered. By putting the values of fibre stress and eliminating the term $\frac{P}{A}$ the moment at different sections can be found.

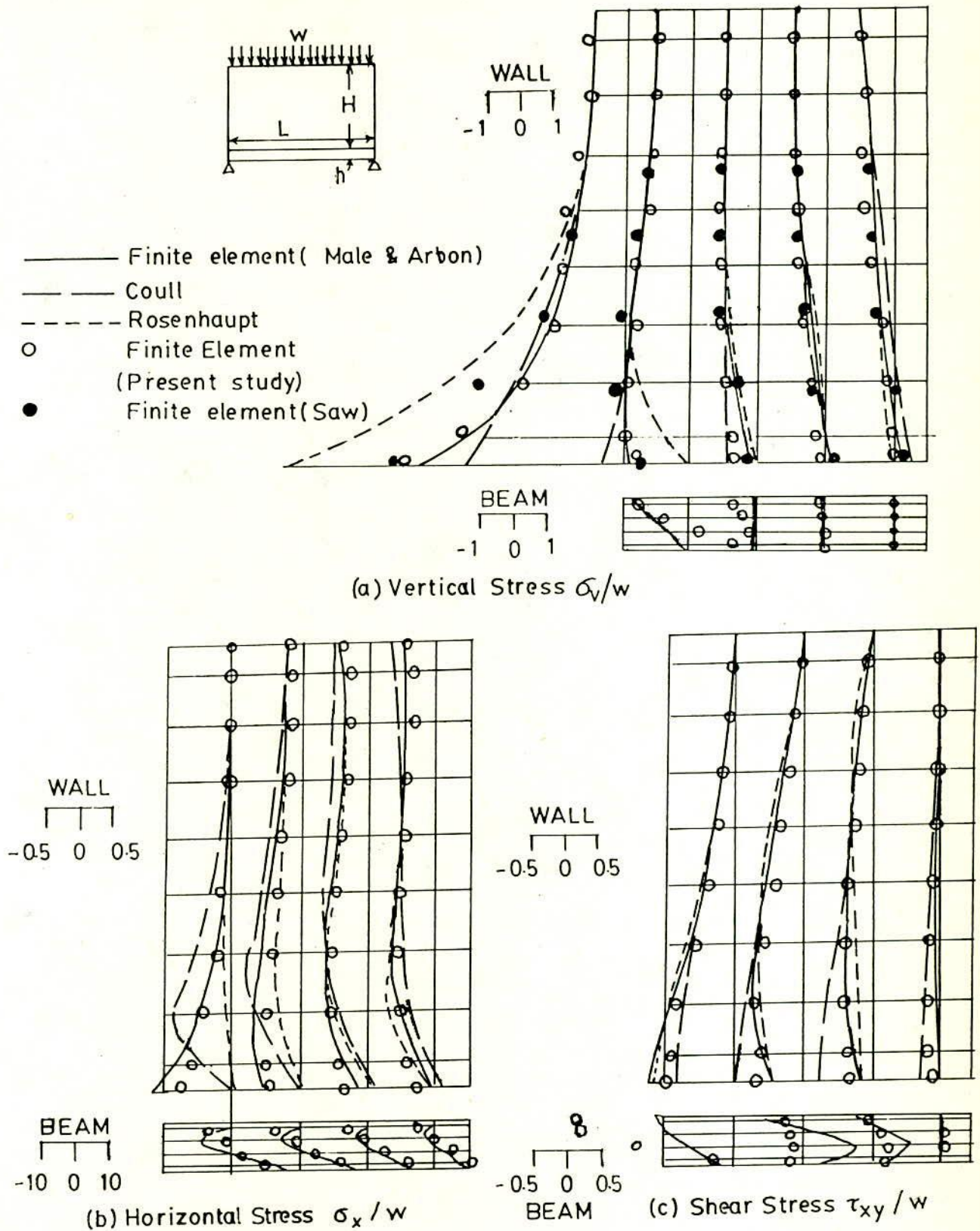


Fig. 3.16 Comparison of Stresses with other Authors

Fig. 3.17 shows the variation of moment along the span for the beam of Fig. 3.6(b) as obtained by different authors. Bending moment in the beam as proposed by Wood(1952) is based on experimental results having a constant value throughout the span. However, the moment at the mid span, as he derived from the horizontal strains measured at mid vertical section, can be assumed to represent the actual moment of the beam. Like others, the variation of moment along the span as obtained from the present finite element analysis follow the same trend with higher values nearer to support than at the middle . Nevertheless the anticipated moment is much lower in comparison to $wL^2/8$. The present analysis however agrees favourably with the results of Saw(1974, 1975), Colbourne(1969), Yettram and Hirst(1971) at the location nearer to the support and at the middle of the span. The moment coefficient obtained by the present analysis at mid-span agrees reasonably with that of Wood (1952) which was based on experimental study.

3.4.6 Comparison with the Empirical Equations

For this comparison equation for maximum vertical stress concentration derived by finite element analyses by Stafford Smith and Riddington (1973) and Davies and Ahmed (1978) are considered. The maximum vertical stress concentration within the brickwork is found to occur at the interface level near the supports. The comparison is shown on the basis of slenderness of the supporting beam which is a common and dominating parameter (discussed later). Fig. 3.18 shows the vertical stress concentration for a wide range of wall height (brick wall height to span ratio varying from 0.23 to 0.84) and supporting beam depth (varying from 50 mm to 200 mm). Vertical stress concentration predicted by the present finite element model gives results which lie within the limits bounded by both Stafford Smith and Riddington (1973) and Davies and Ahmed (1978) for the case when non homogeneity is considered. For homogeneous solution the result agrees with the equation given by Davies and Ahmed.

Comparison of results obtained by present analysis on the wall made of light concrete block on concrete beam (tested by Rosenhaupt) as discussed in the foregoing paragraphs indicate that the results of the present model agree favourably with other investigators. The following article describes the arching action in the aforementioned panel.

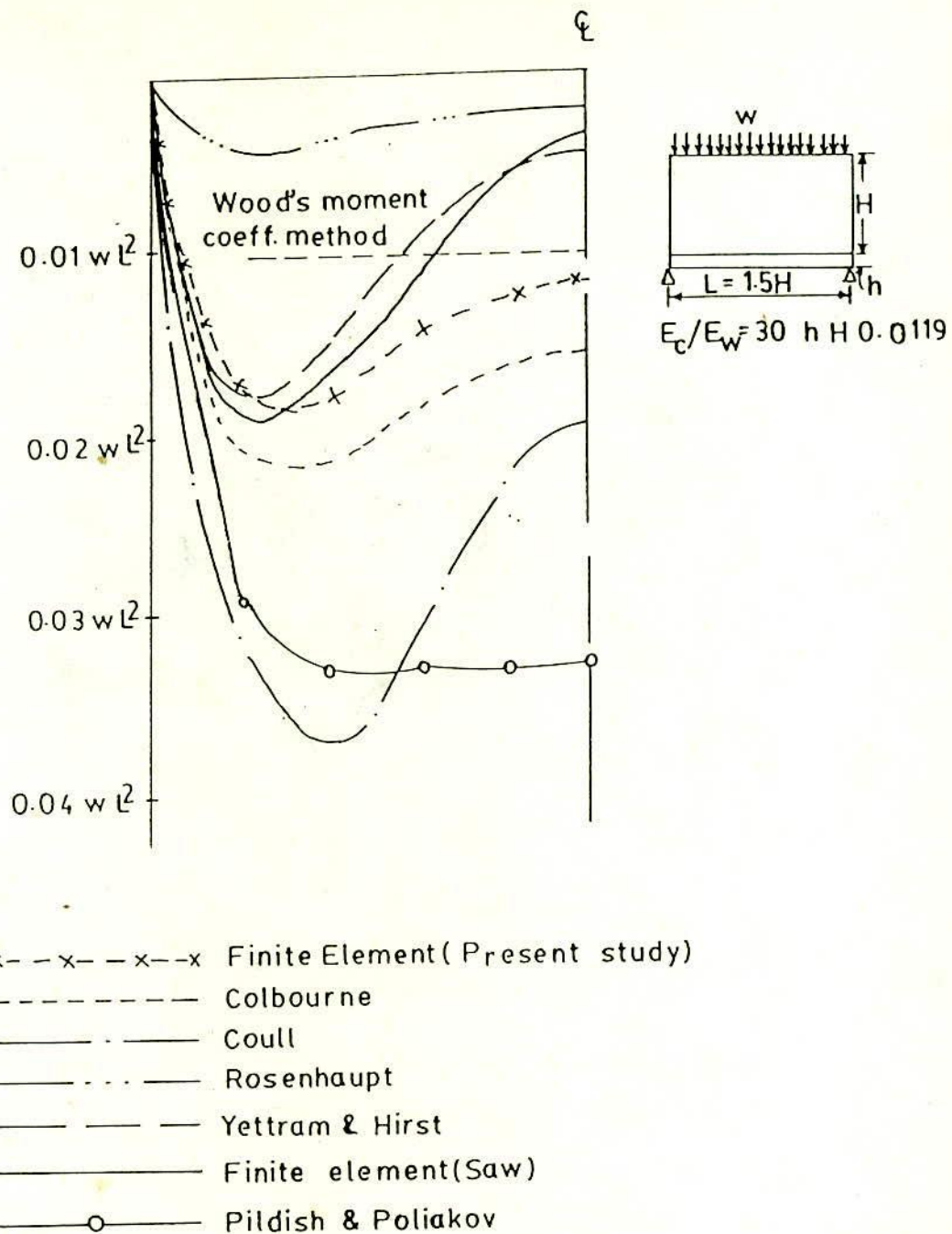


Fig. 3.17 Comparison of Moments with other Authors

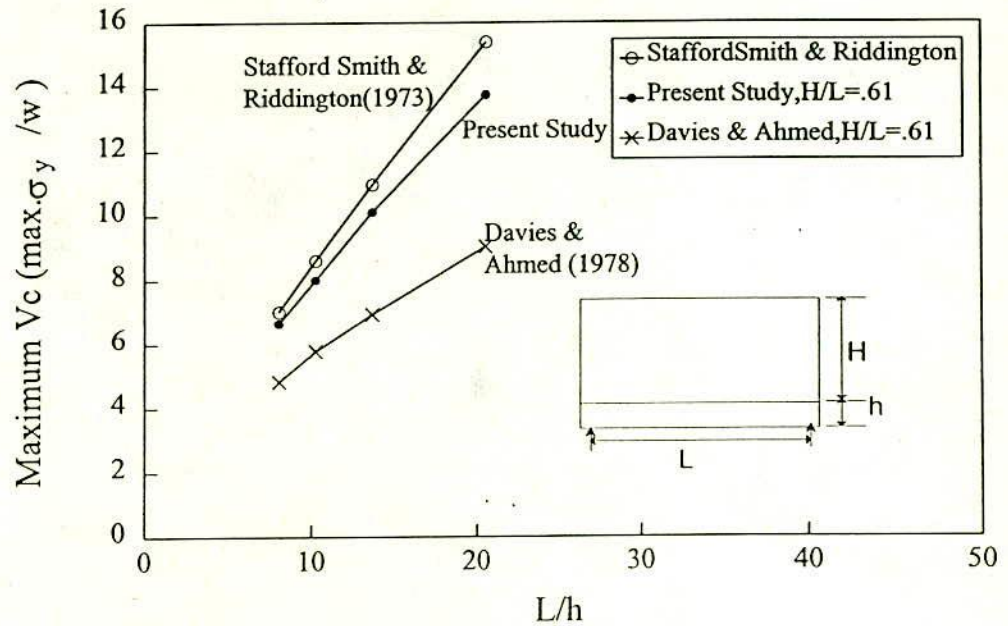


Fig. 3.18 Comparison of V_c (Non-homogeneous Case)

3.5 ARCHING ACTION

The composite action of the wall with the supporting beam produces arching action in the wall. The compression of the arch is mostly contained in the masonry wall, and the supporting beam being acted upon mostly by tension. Due to this arching action a major portion of the superimposed load concentrates towards the support providing a great relief of load on the beam at the middle of the span. This results in a considerable reduction of bending moment in the supporting beam. Reduction of moment in the supporting beam has been shown before. The arching action can be illustrated with the help of principal stress trajectories within the panel. Fig. 3.19(a) shows a typical plot of principal stresses obtained from the finite element analysis discussed earlier. Lines in the plot show the magnitude of major and minor principal stresses in terms of the average stress applied on top of the wall. The direction of the line represents the direction of the corresponding principal stress. Compressive stress is indicated by black colour and the tensile stress is indicated by red colour. From the figure it is clear that all the stresses concentrate towards the support while at the centre of the panel the magnitude of the stress is very small. It is also seen that the stress in the wall is mainly compressive and those in the beam are mainly tensile, constituting an arch action in the wall-beam panel. Some of the analyses in this section show the presence of

tensile stresses. These tensile stresses depending on the load applied may be high enough to allow the formation of tensile cracking.

Many authors recommended the presence of central opening in the wall-beam structures. Principal stress trajectories for wall-beam with central opening as obtained in the present study (Fig. 3.19(b)) reveals that due to the presence of central opening of normal size the composite behaviour of wall-beam structure is not hampered.

From non-homogeneous analyses the stresses in the brick unit, vertical joint and bed joint can be identified separately. Typical cases are shown in Fig. 3.19(b) to Fig. 3.19(d). On the basis of these analyses a zoning map can be developed for the principal stresses that will give feelings about the distribution of stresses within a wall-beam panel. In Fig. 3.19(e) principal stress zoning for different types of wall-beam structures that are normally encountered are shown.

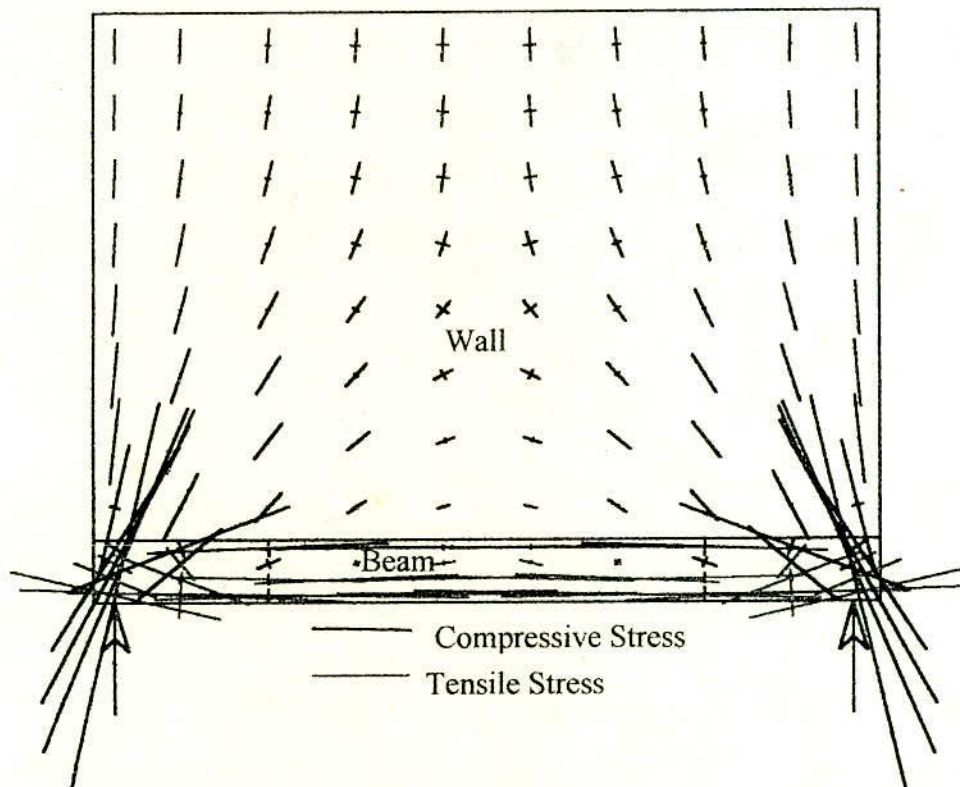
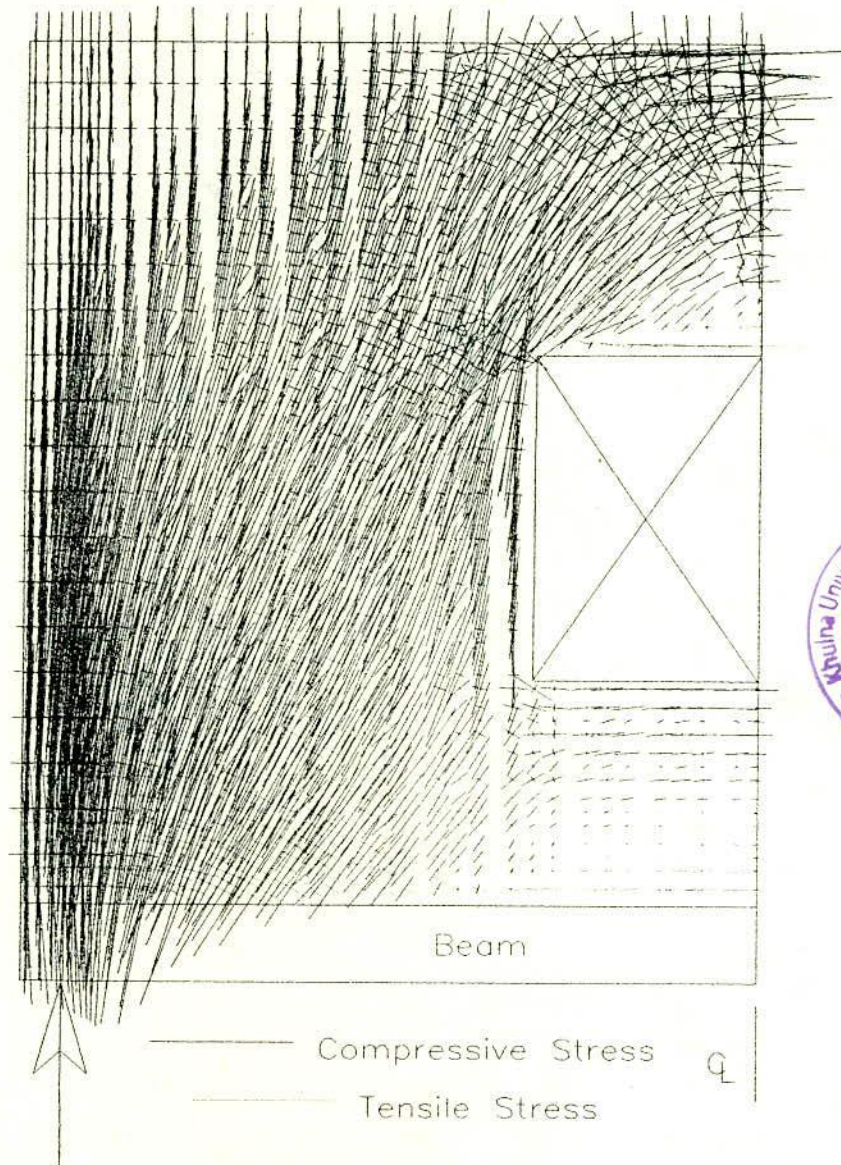
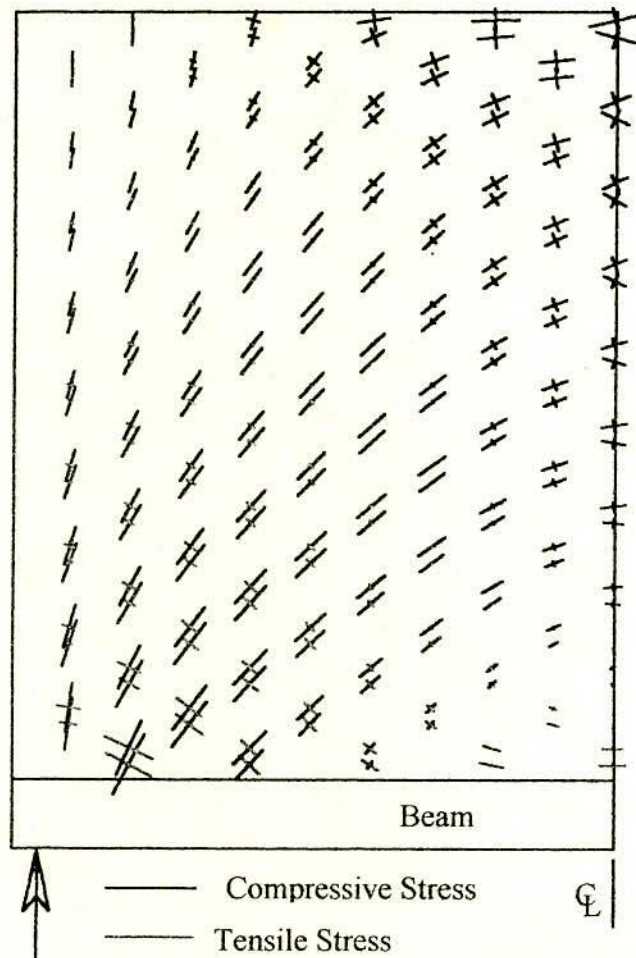


Fig. 3.19(a) Principal Stress Trajectories by Coarse Mesh Discretization
(Beam Tested by Rosenhaupt, 1962)



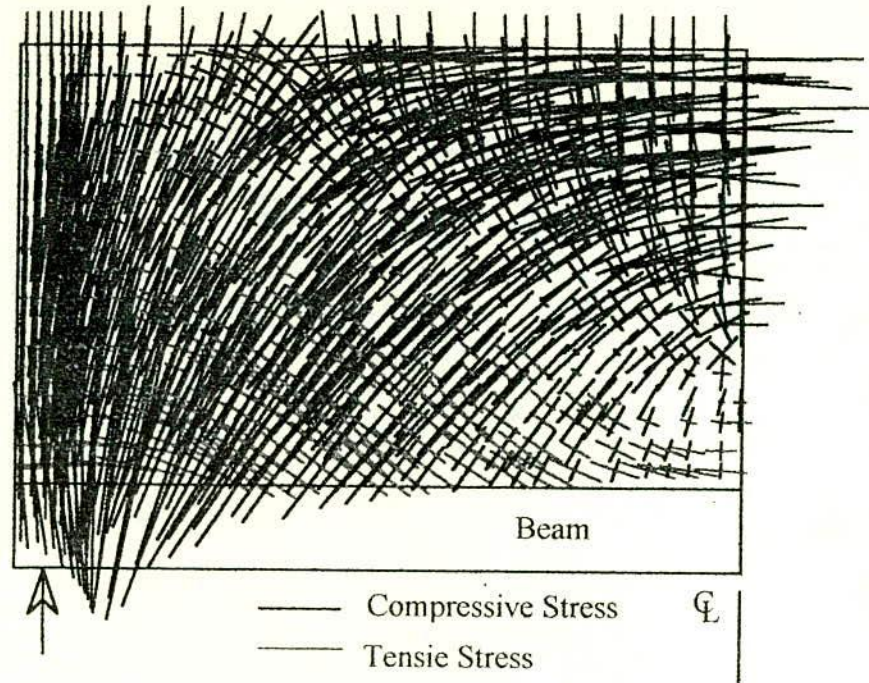
Note:- Principal Stress Trajectories for Beam are similar to Fig. 3.19(a).

Fig. 3.19(b) Typical Principal Stress Trajectories for Wall-beam with Central Opening by Fine Mesh Discretization (Elements of Brick, Vertical Mortar and Horizontal Mortar)



Note:- Principal Stress Trajectories for Beam are similar to Fig. 3.19(a).

Fig. 3.19(c) Principal Stress Trajectories for Plane Wall-beam by Fine Mesh Discretization (Elements of Vertical Mortar).



Note:- Principal Stress Trajectories for Beam are similar to Fig. 3.19(a).

Fig. 3.19(d) Principal Stress Trajectories for Shallow Wall-beam by Fine Mesh Discretization (Elements of Brick)

3.6 PARAMETRIC STUDY OF WALL-BEAM STRUCTURE

The wall-beam structure is a highly complex type of composite structure comprising about half a dozen of different materials, each having different material properties. The composite action of masonry wall with the supporting beam depends on many parameters. The main influencing parameters are outlined as follows:

1. The wall height to span ratio.
2. The depth of the supporting beam to span ratio.
3. Relative stiffness of masonry wall and its supporting beam.
4. Vertical edge column and top beam.
5. The size and position of opening in the wall.
6. Reinforcement in the supporting beam.
7. Width of the support for Beam.

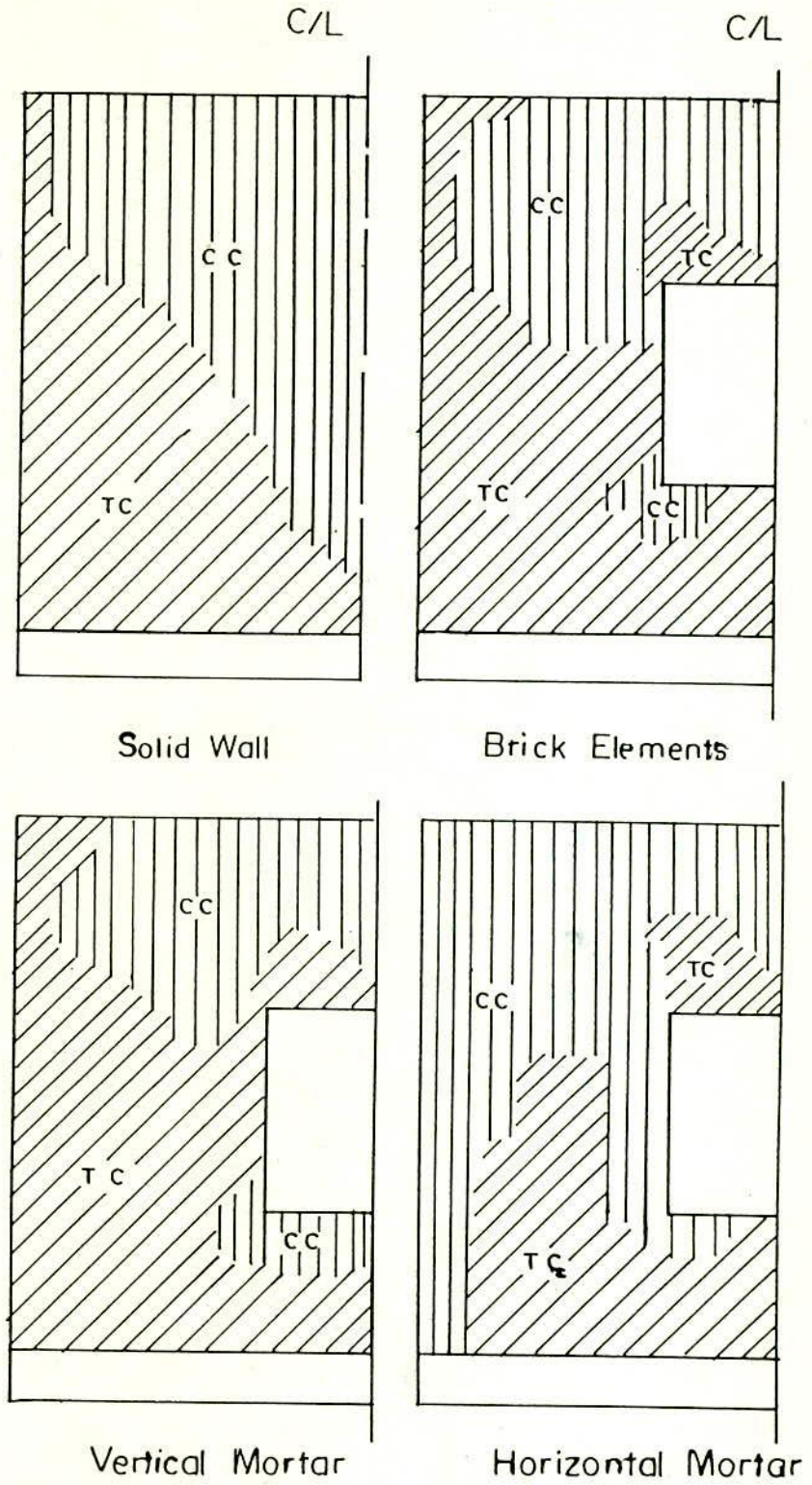


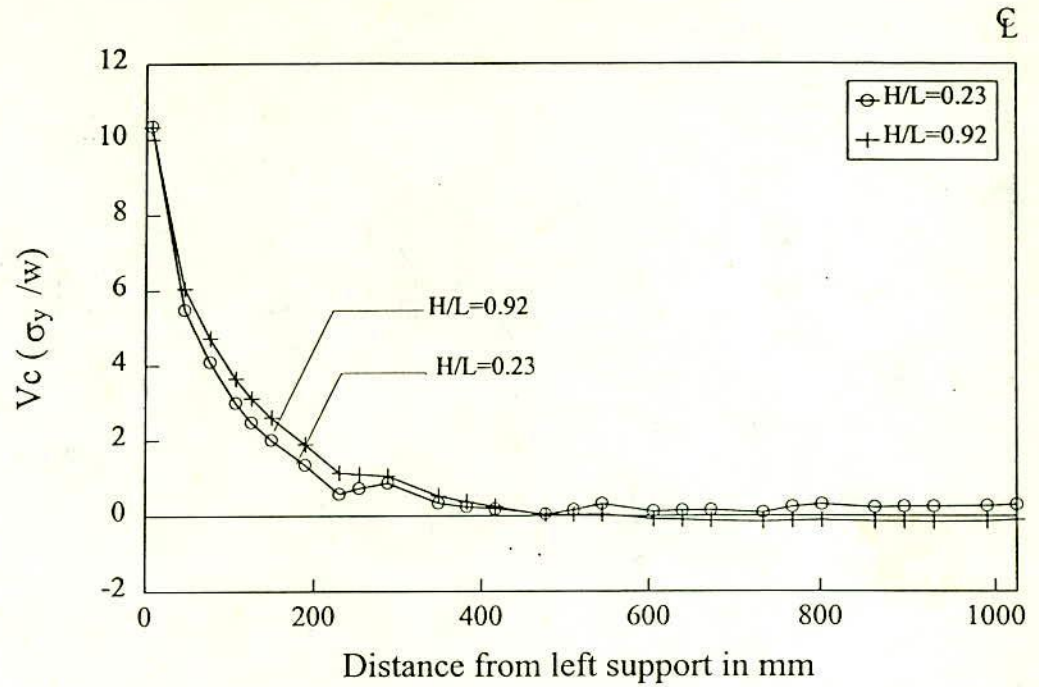
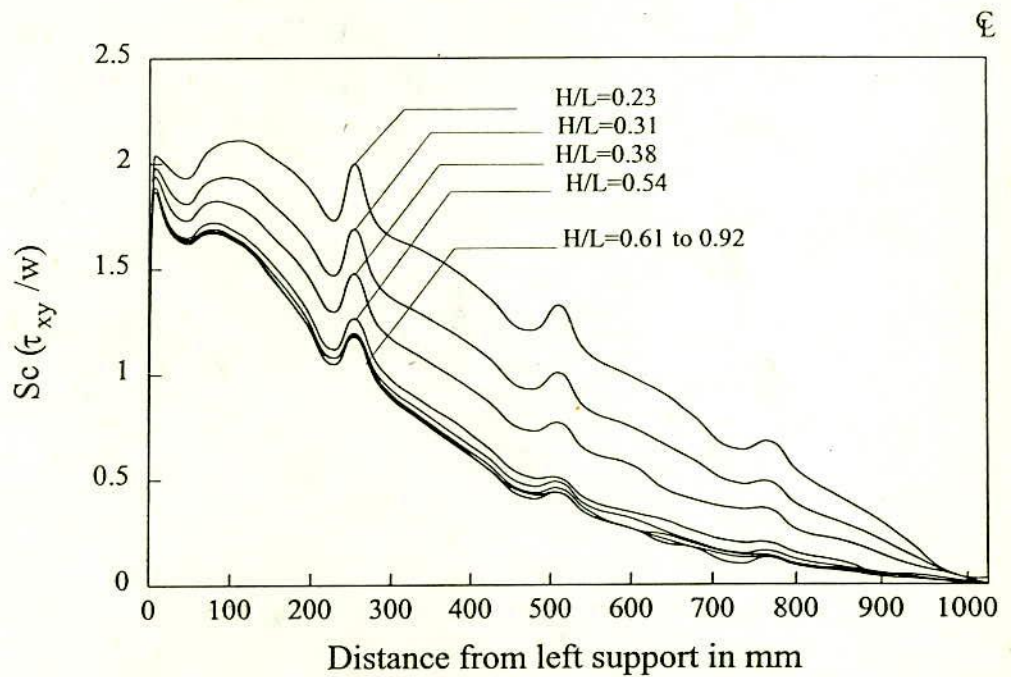
Fig. 3.19(e) Principal Stress Zoning for Wall-beams with and without Opening (Present Study).

The other parameters may include wall thickness, size of brick unit, thickness of mortar, modulus of elasticity and Poisson's ratio of constituent materials, support bearing and end conditions, anchorage of tension reinforcement and bond characteristics of mortar. The influences of the important parameters are presented below.

3.6.1 Effect of Height of Brick wall

Variation of maximum vertical stress concentration (σ_y / w) and shear stress concentration (τ_{xy} / w) and their distribution along the span for different height : length ratio of the wall is shown in Fig. 3.20(a) and Fig. 3.20(b) respectively. Shear stress concentration, Sc is obtained by dividing the shear stress, τ_{xy} by the intensity of the vertical load, w applied on the top of the wall, i.e., $Sc = \tau_{xy}/w$. The maximum shear stress concentration within the wall is found to occur at the interface level near the supports. The ratio of wall height to span length, (H/L) was varied from 0.23 to 0.92 keeping the span length constant. It is seen that the maximum vertical stress concentration and the nature of distribution of the vertical stress along the span do not differ appreciably, due to the variation of height of the brick wall. Similarly it is also clear from Fig. 3.20(b) that shear stress concentration, (Sc) and its distribution along the span is approximately the same irrespective of the height of the wall when H/L is greater than 0.54.

Most of the previous investigators observed that for composite action to occur in wall-beam structure the height of the wall should not be less than 0.6 times the length of the wall. Similar finding is also observed in the present investigation. When H/L ratio is less than 0.54 it is revealed from Fig. 3.20(b) that shear stress increases with the decrease of H/L ratio. This increase in shear stress is vulnerable to wall-beam structures. It is seen from Fig. 3.20(b) that when the height of wall-beam structure is equal to 0.25 times its span the shear stress in the panel increases to the tune of two times the intensity of the load applied on the wall. Such high shear stress may cause sliding at the interface and/or shear failure of the panel. From this comparison it can be concluded that the composite action between wall and supporting beam should not be considered for the design purpose when H/L ratio is less than 0.54.

Fig. 3.20(a) Influence of H/L Ratio on V_c .Fig. 3.20(b) Influence of H/L Ratio on S_c .

3.6.2 Effect of Modulus of Elasticity

The effect of modulus of elasticity and hence the relative stiffness of the wall-beam was studied by changing the modulus of elasticity of the component materials while keeping all other parameters constant. The results of the investigations are furnished below.

3.6.2.1 Mortar

The natures of variation of vertical and shear stress, expressed in terms of V_c and S_c , due to the variation of modulus of elasticity of mortar are shown in Fig. 3.21(a) and Fig. 3.21(b) respectively. These figures indicate that the maximum stress concentrations, V_c and S_c increase slightly with the increase of modulus of elasticity of mortar.

3.6.2.2 Brick

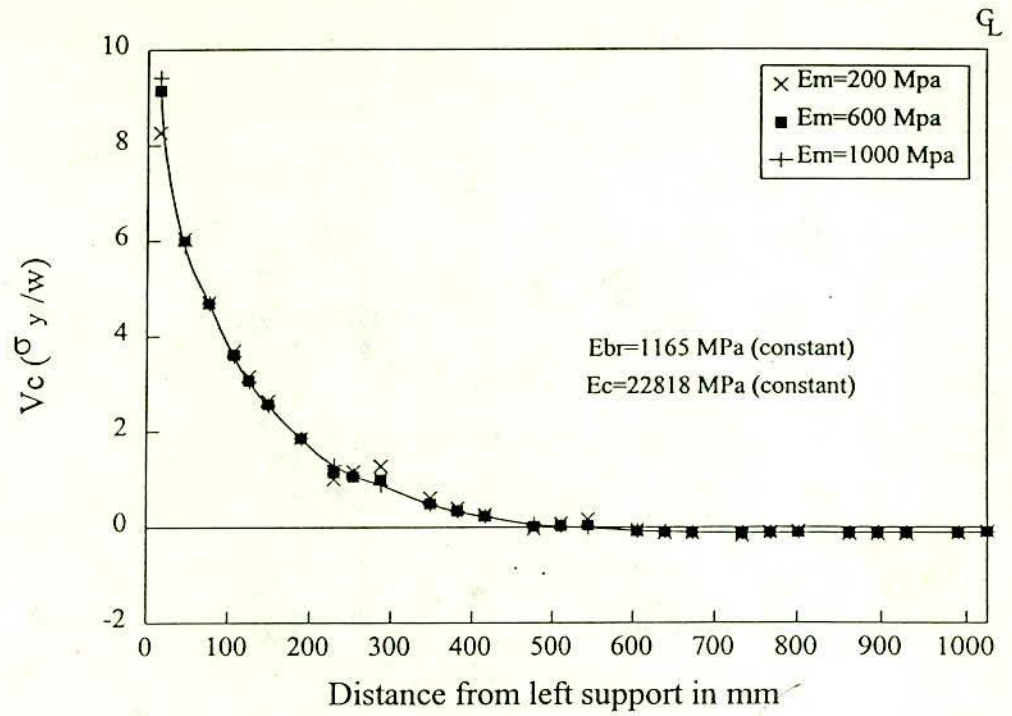
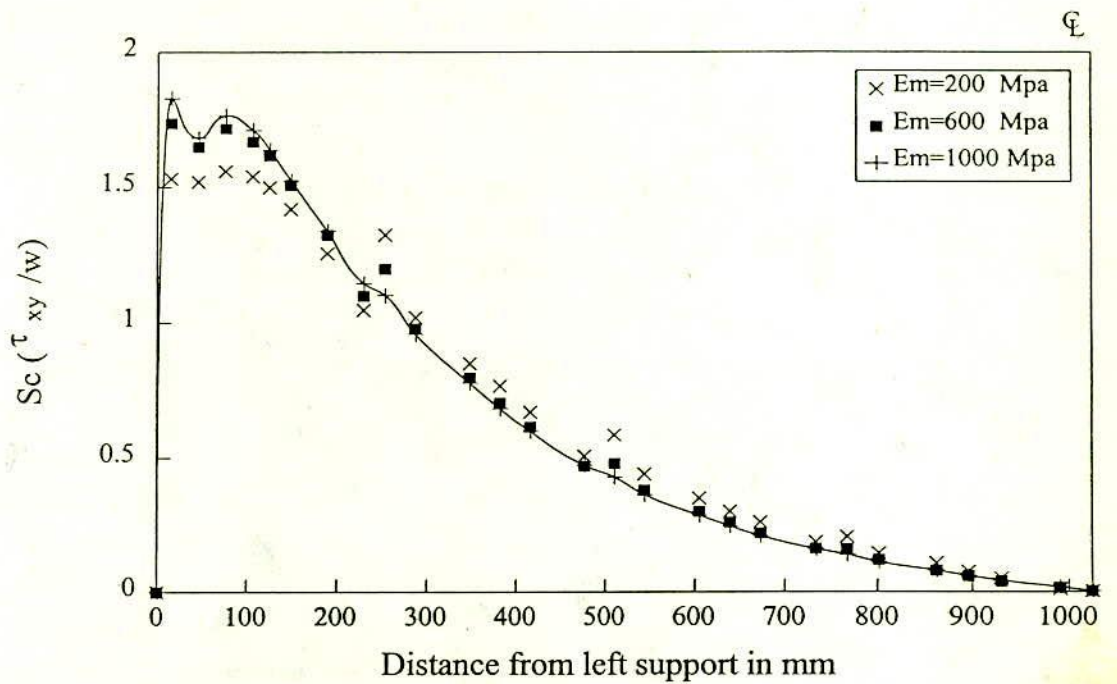
The variation of vertical and shear stress concentration along the span due to the variation of modulus of elasticity of brick is shown in Fig. 3.22(a), and Fig. 3.22(b) respectively. The vertical and shear stress concentrations are found to increase with the increase of modulus of elasticity of brick. It can be seen from the figure the variation of modulus of elasticity of brick has a greater influence than that of modulus of elasticity of mortar as is evident from the steeper curves at higher modulus of elasticity of brick.

3.6.2.3 Concrete

The variation of vertical and shear stress concentration along the span with the variation of modulus of elasticity of concrete is shown in Fig. 3.23(a) and Fig. 3.23(b) respectively. Unlike mortar and brick the vertical and shear stress concentrations are found to decrease slightly with the increase of modulus of elasticity of concrete. No noticeable variation of vertical stress distribution was observed along the panel due to the variation of modulus of elasticity of concrete.

3.6.3 Effect of Depth of Supporting Beam

The variation of vertical and shear stress concentration along the span with the variation of depth of supporting beam is shown in Fig. 3.24(a) and Fig. 3.24(b)

Fig. 3.21(a) Influence of E_m on V_c Fig. 3.21(b) Influence of E_m on S_c

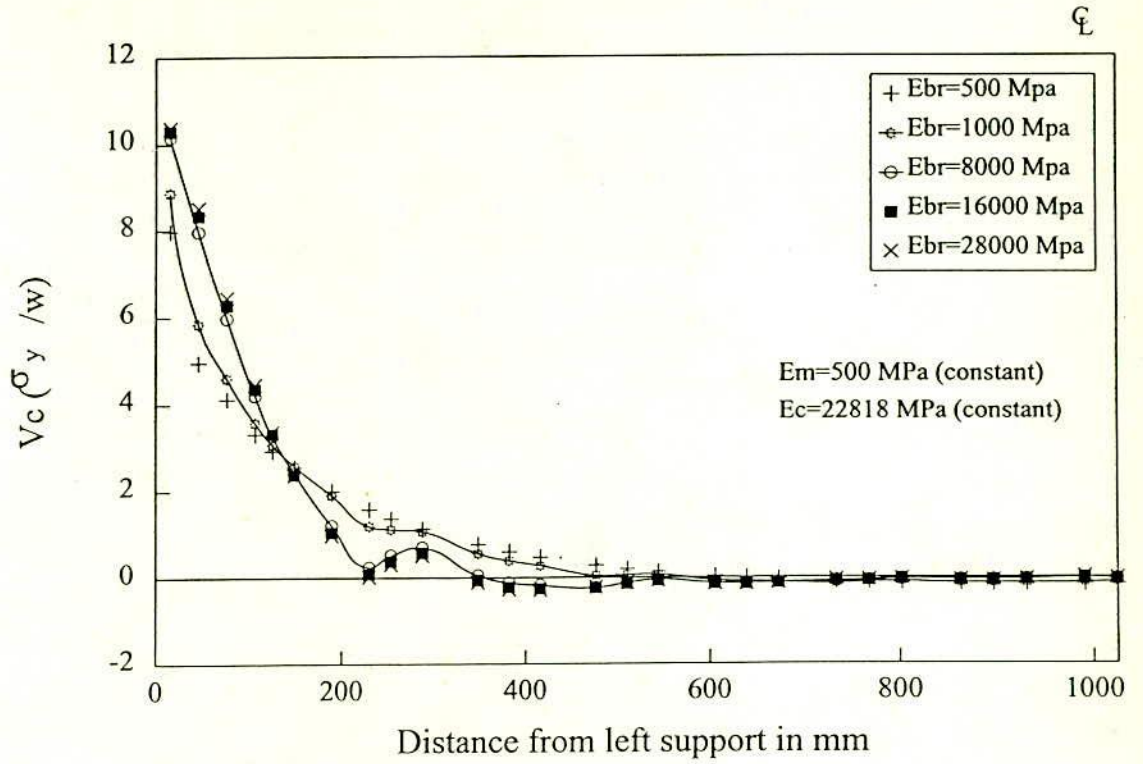


Fig. 3.22(a) Influence of E_{br} on V_c

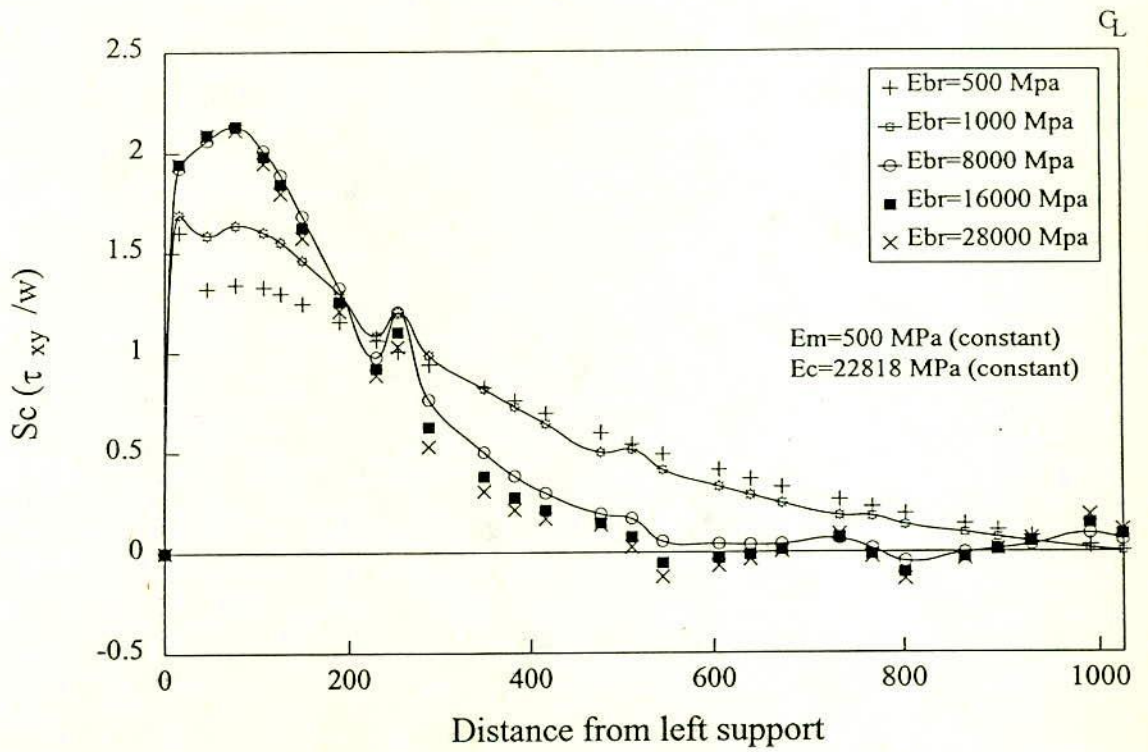
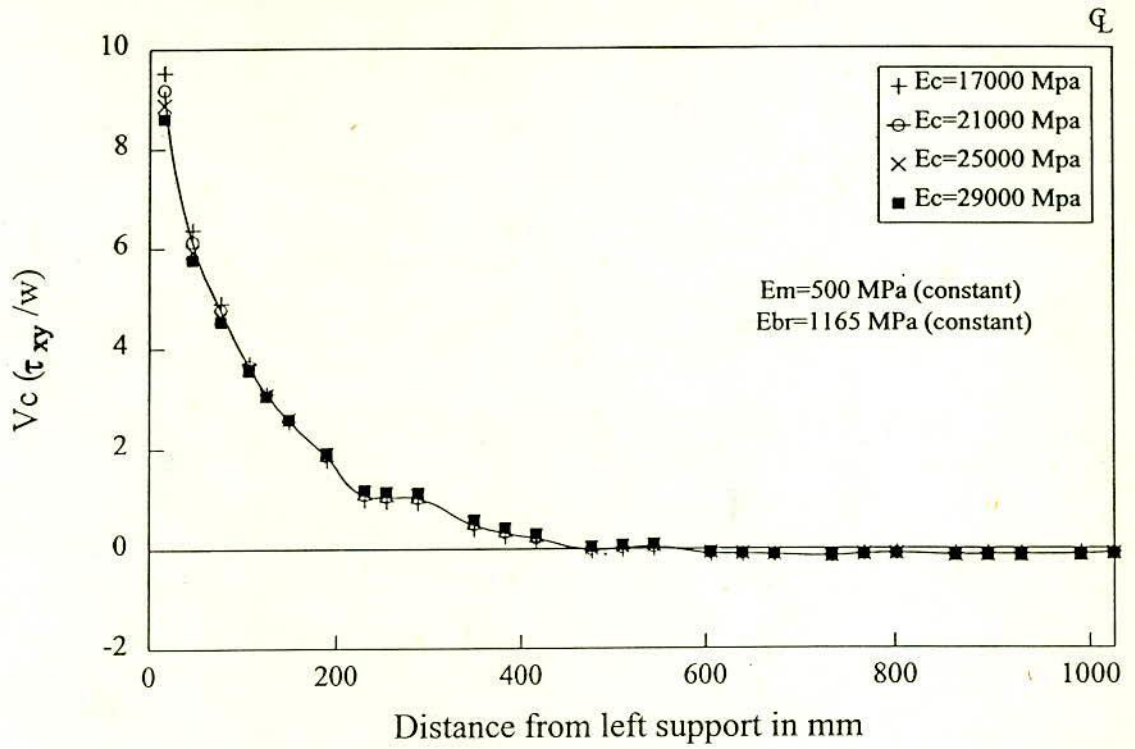
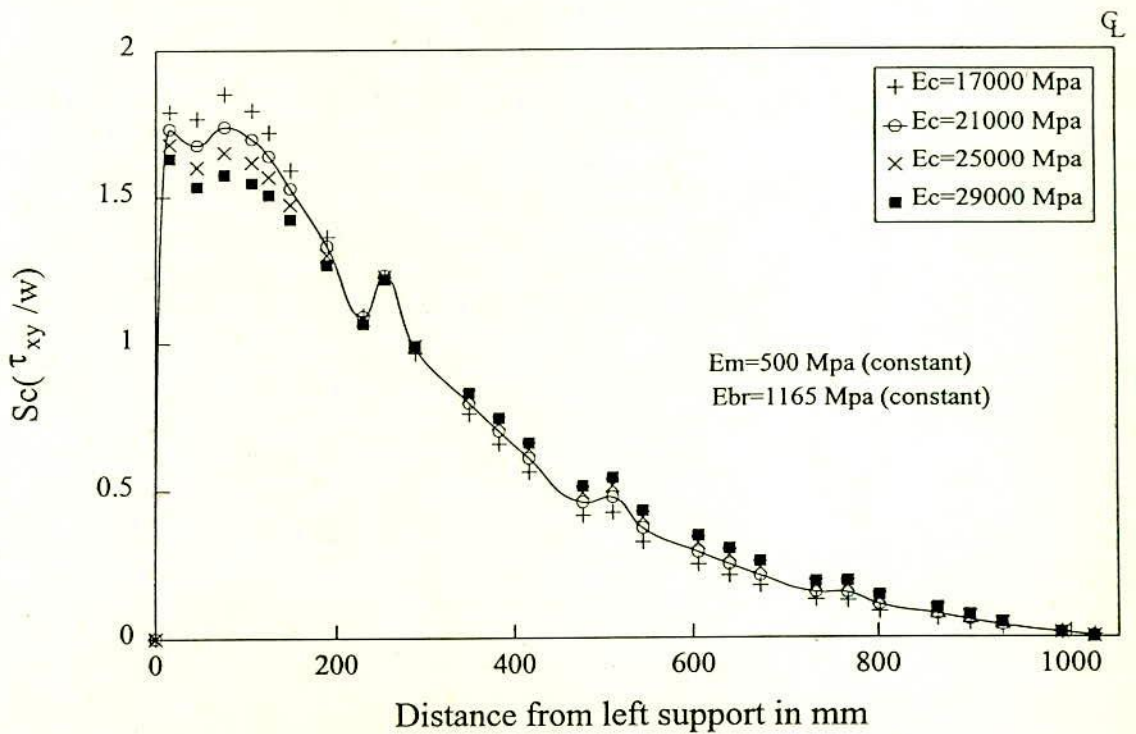


Fig. 3.22(b) Influence of E_{br} on S_c

Fig. 3.23(a) Influence of E_c on V_c Fig. 3.23(b) Influence of E_c on S_c

respectively. The vertical and shear stress concentrations, V_c and S_c are found to decrease considerably with the increase of depth of supporting beam. The distributions of stresses are also found to vary from steep gradient to flat with the increase of depth of beam. It is also seen that the stress concentration near the support increases with the decrease of beam depth. The increase of vertical stress and shear stress concentration, V_c and S_c , and their steeper distributions along the span were also observed by other investigators (Stafford Smith and Riddington (1977); Davies and Ahmed (1978) and Kamal (1990)) due to the increase of relative stiffness of the wall to that of the supporting beam.

3.6.4 Effect of Reinforcement in Supporting Beam

The relative stiffness of wall and the beam influences the behaviour of wall-beam structure considerably. Although this fact was agreed in general by previous researchers, the contribution of steel towards the stiffness of reinforced concrete supporting beam was not considered in modelling the wall-beam structure. The structural purpose of supporting beam in a wall-beam structure is to resist tension and bending, both being produced due to arching effect of the wall-beam structure. The increase of axial stiffness and bending stiffness due to the contribution of embedded reinforcement should therefore be considered. The variation of vertical stress concentration, $V_c (= \sigma_y/w)$ and shear stress concentration, $S_c (= \tau_{xy}/w)$ along the span and both calculated at the level of wall-beam interface is shown in Fig. 3.25(a) and Fig. 3.25(b) for both the cases of with steel and without steel. The figures show that when the effect of reinforcement is considered in the model, maximum V_c and S_c are decreased. It is concluded that modelling of reinforcement in supporting beam of wall-beam structure is required to simulate a real wall-beam structure.

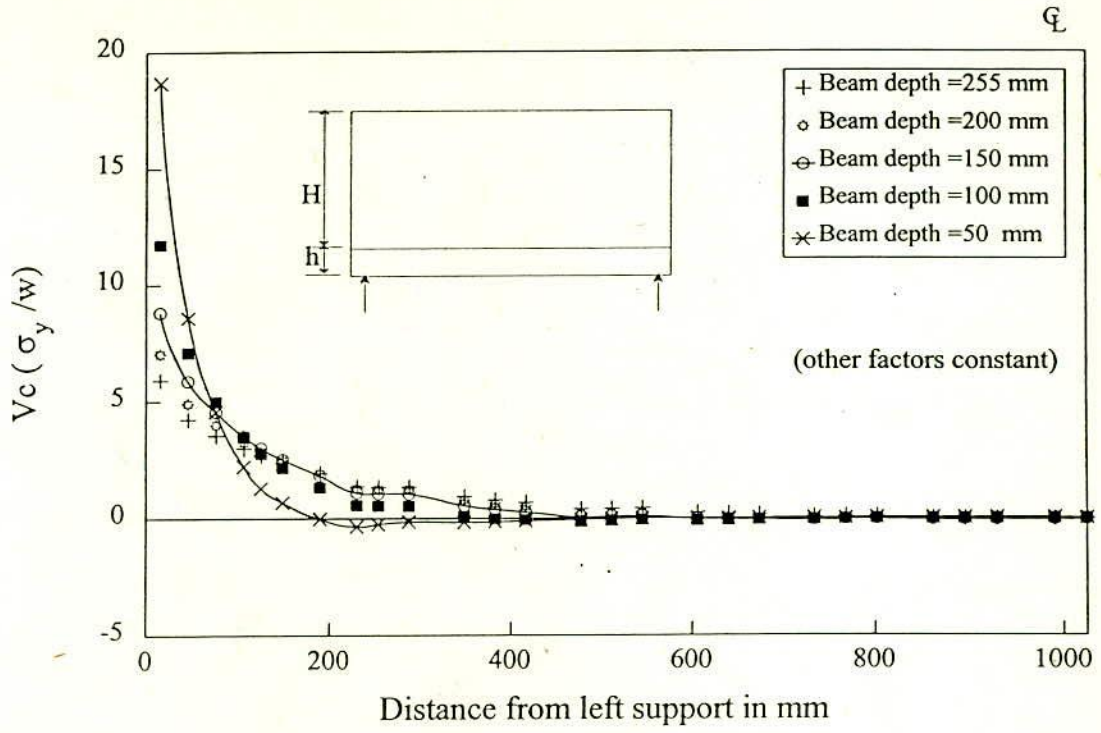


Fig. 3.24(a) Influence of Depth of Supporting Beam on V_c

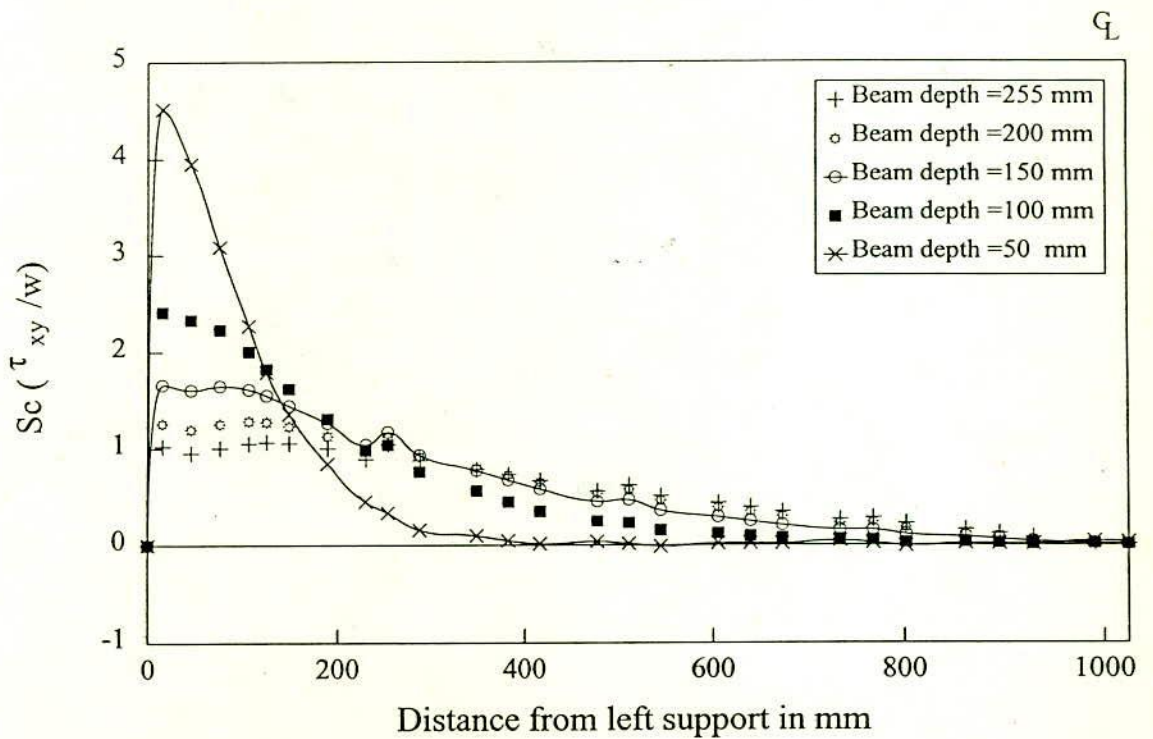
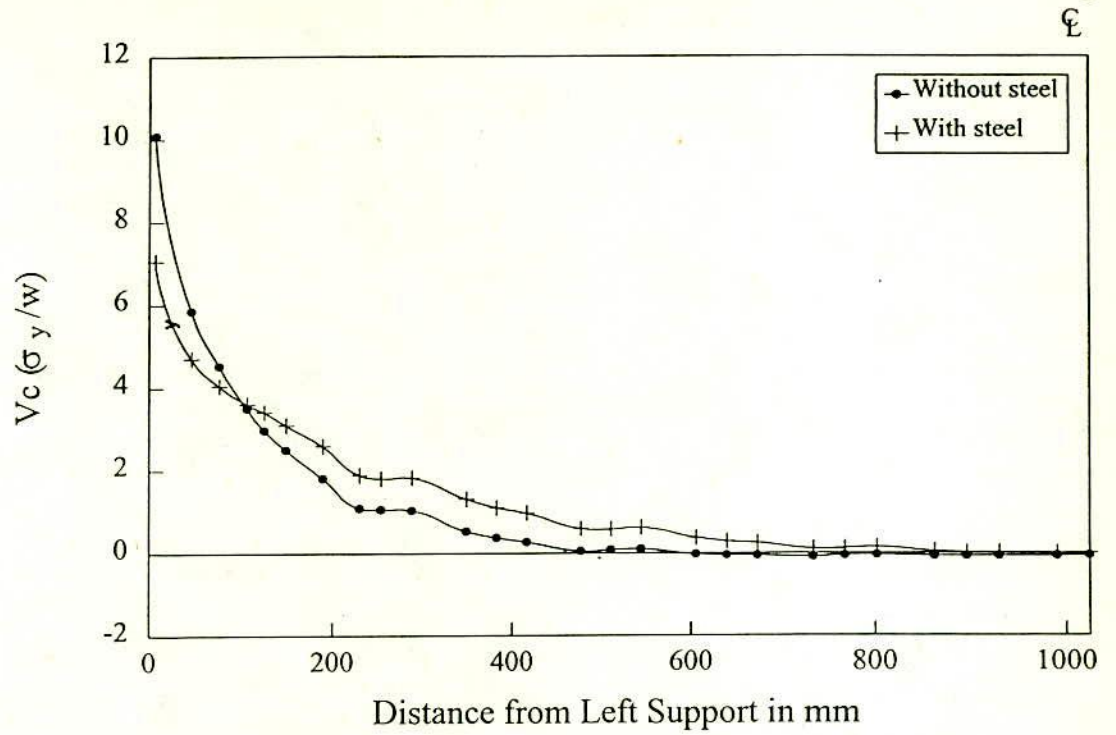
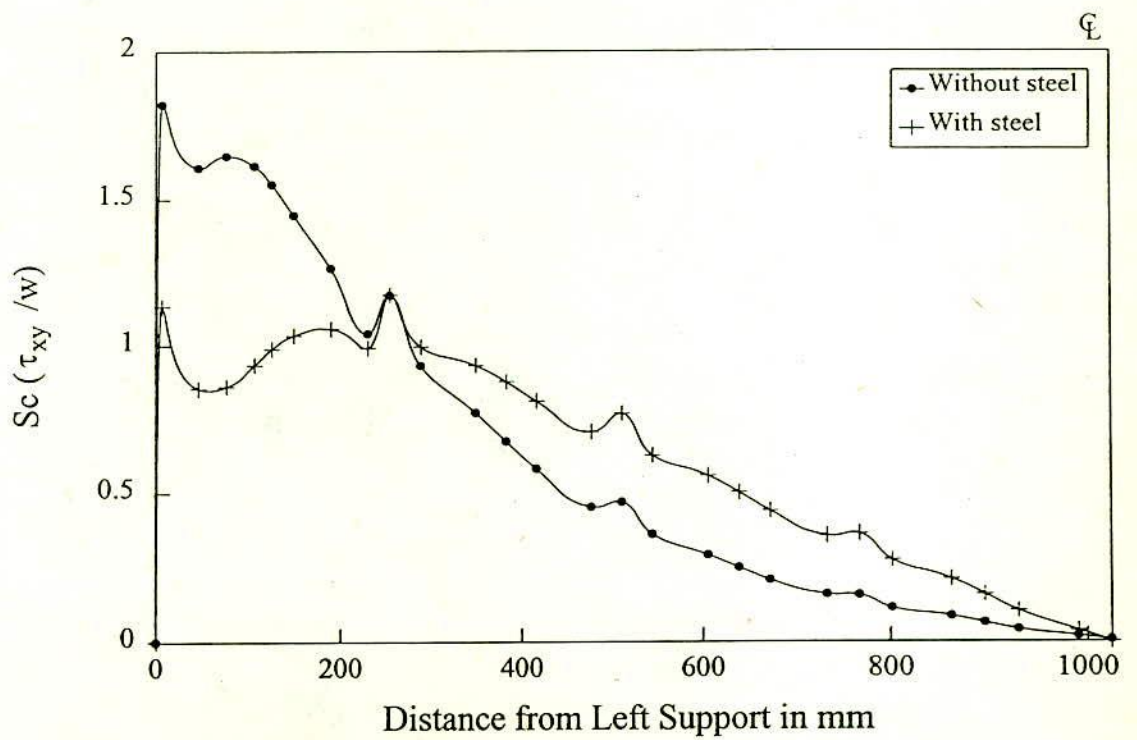


Fig. 3.24(b) Influence of Depth of Supporting Beam on S_c

Fig. 3.25(a) The Influence of Beam Reinforcement on V_c Fig. 3.25(b) The Influence of Beam Reinforcement on S_c

3.6.5 Effect of Vertical Edge Columns

The wall-beam interaction can also exist in brick infilled beam-column frame system. The possible practical arrangements may be (1) the masonry wall supported by beam at the bottom and having columns at vertical edges, (abbreviated as 'BCOL'), (2) the masonry wall supported by beam at the bottom, having columns at vertical edges and slab or beam at the top (abbreviated as 'FRM') and (3) the plane wall-beam structure i.e., the wall supported by beam at the bottom (abbreviated as 'WBM'). These arrangements are shown in Fig. 3.26(a). The above three systems were analysed to compare the stress. The distribution of vertical stress and shear stress along the span expressed as V_c and S_c are plotted in Fig. 3.26(a) and Fig. 3.26(b) respectively. The comparison shows that the 'BCOL' and 'FRM' systems behave almost in identical manner. And in both of these systems the maximum vertical stress concentration and maximum shear stress concentration are found to reduce considerably within the masonry at bottom corner of the wall-beam. Therefore 'FRM' and 'BCOL' type of wall-beam structure will enable the panel to resist against crushing of bottom corner of wall-beam more effectively, than if it is a 'WBM' type of simple wall-beam structure. For bricks having lower compressive strength such technique will be more effective. To investigate the effect of above three systems on the reinforcement of the supporting beam, the variation of tension (σ_x) at bottom reinforcement, expressed as tensile stress concentration, $T_c (= \sigma_x/w)$ is shown in Fig. 3.26(c). It is seen that for all the three type of wall-beam structures ('WBM', 'FRM' and 'BCOL') tension in the bottom reinforcement is practically unaltered.

3.6.6 Effect of Opening in Wall-beam

Masonry wall is often found to have door and window openings. When these occur in a wall-beam structure where composite action is considered, the stress state becomes complicated. A comparison of vertical and shear stresses at interface level of wall-beam and the tensile stress at the bottom rod of supporting beam have been studied for different size and position of openings. A window at the central position is abbreviated as 'WMID' and a door at the end of the span is abbreviated as 'DEND'. It is seen from Fig. 3.27(a) that the door opening at the end of the span produces very high compressive stress at the support and also high tensile stress at the bottom corner of the opening near the end of the span. Vertical tensile stress of lower intensity is also produced at the mid span. Opening at the end also produce

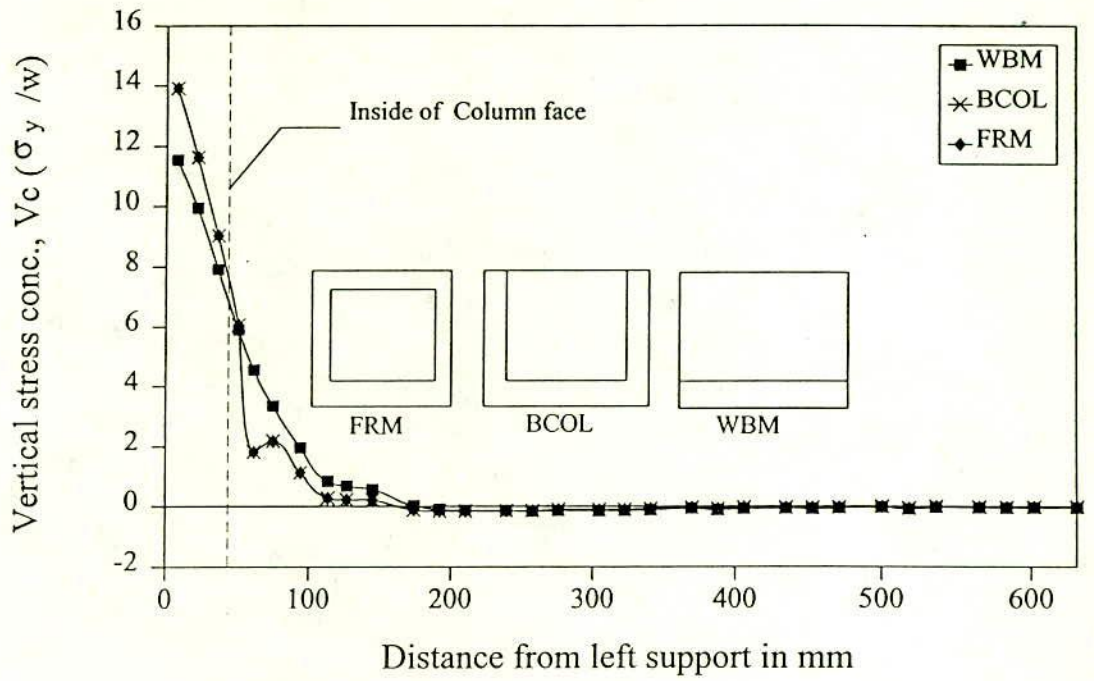


Fig. 3.26(a) Influence of Lateral Confinements on V_c

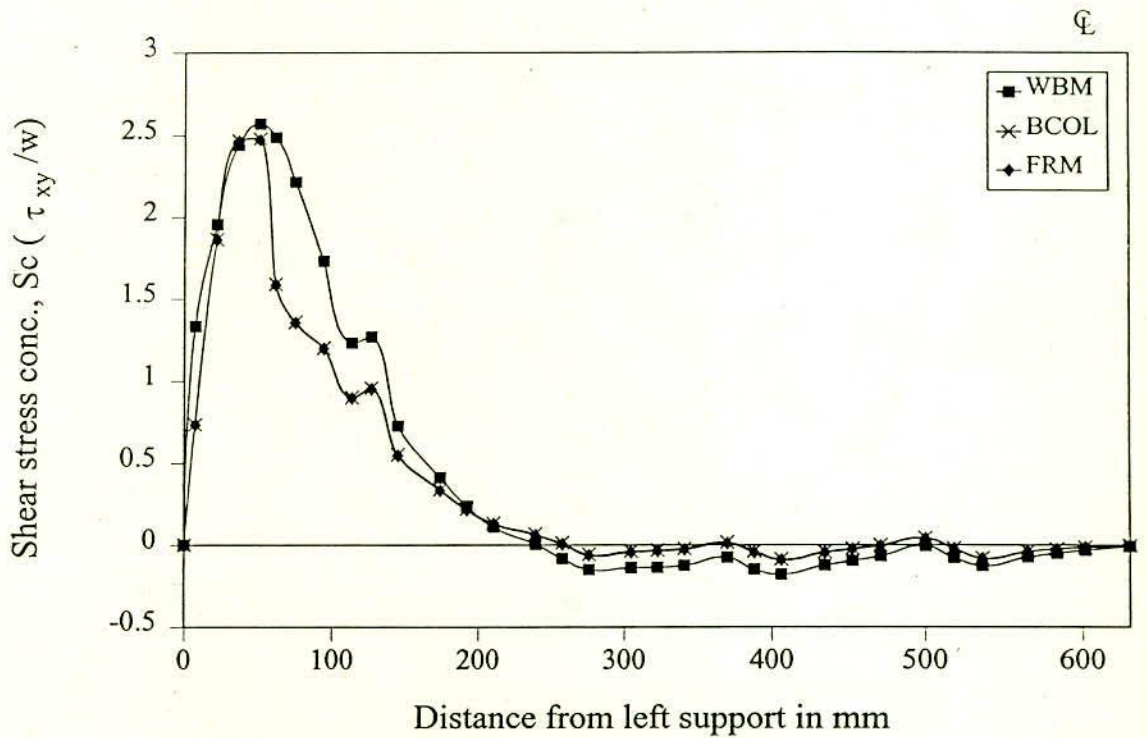


Fig. 3.26(b) Influence of Lateral Confinements on S_c

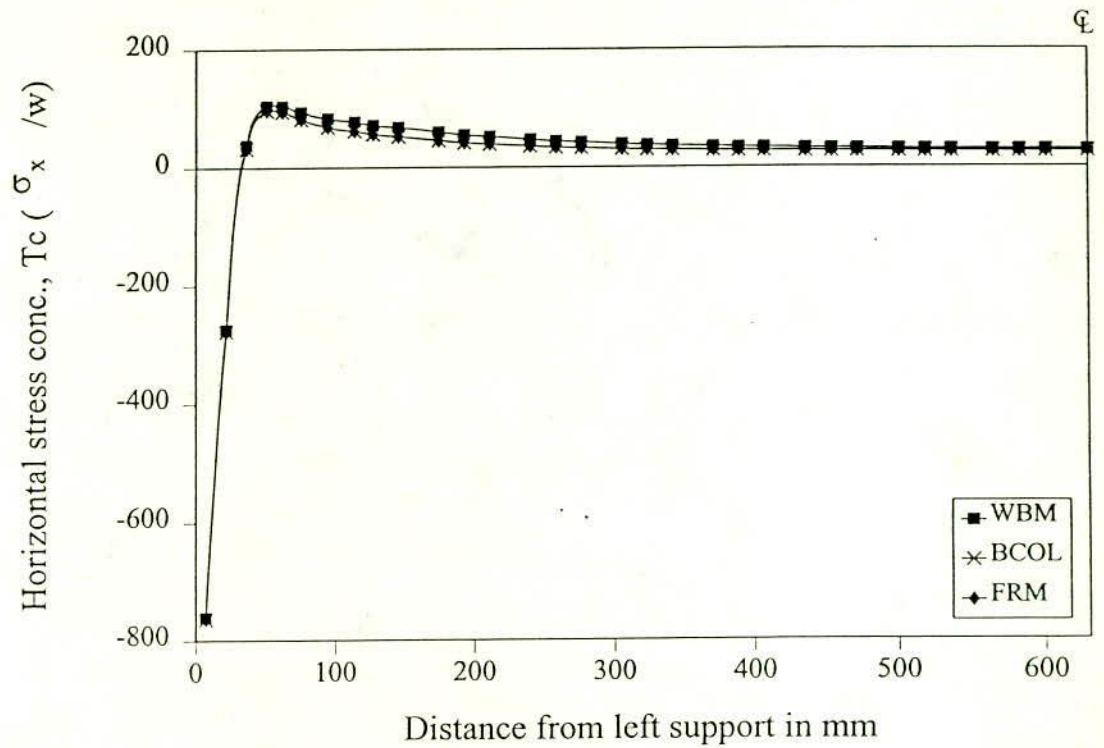


Fig. 3.26(c) Influence of Lateral Confinements on Stress in Beam Steel

maximum shear stress at mid span (see Fig. 3.27(b)) which is more than maximum S_c of a wall-beam without opening. Comparatively large tensile stress in reinforcement is also produced due to offset opening (see Fig. 3.27(c)). It is observed from Fig. 3.27(a-c) that the position of safest opening in the wall-beam structure is at the middle ('WMID'), while the door at the end ('DEND') is observed to be the most dangerous opening. Since the normal opening at the central position does not materially change the interaction behaviour it can be designed like a solid wall-beam structure. For the design of wall-beam structure with offset opening, elaborate analytical and experimental study should be carried out.

3.6.7 Effect of Support Width

In practical cases supports always occupy some place. This parameter is studied to know the extent and nature of the effect of bearing area of support on the behaviour of wall-beam structure. For this purpose supports of contact length $0.05L$, $0.025L$ and end bearing support were considered at each end of the span.

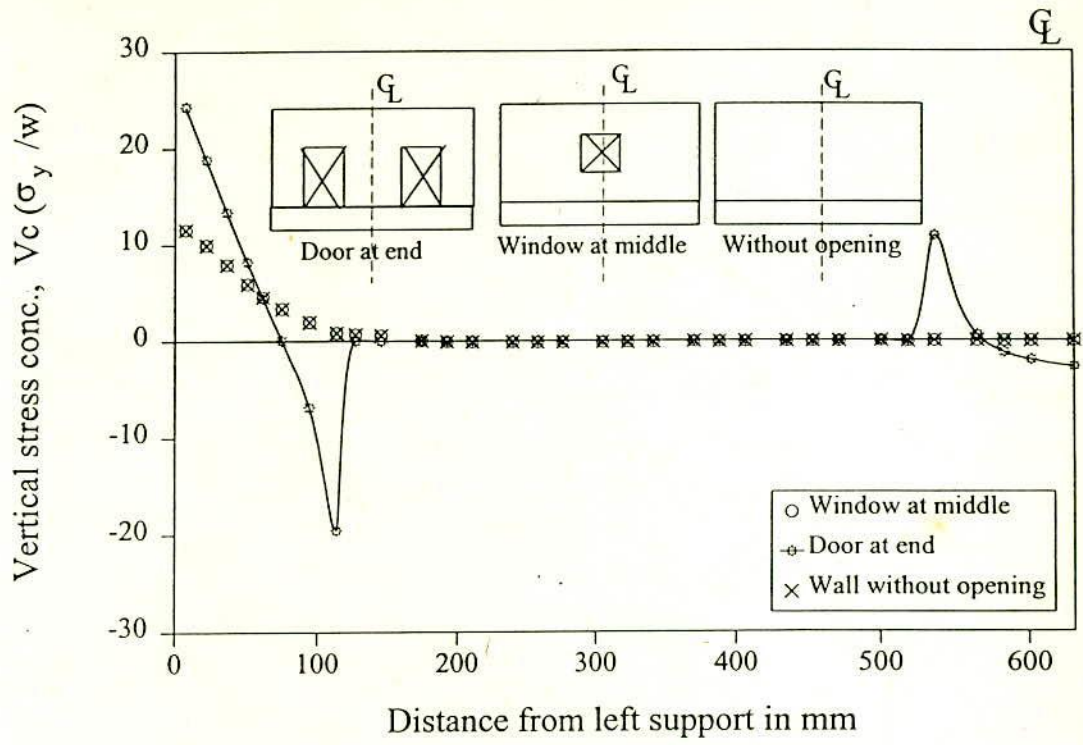


Fig. 3.27(a) Influence of Openings on V_c

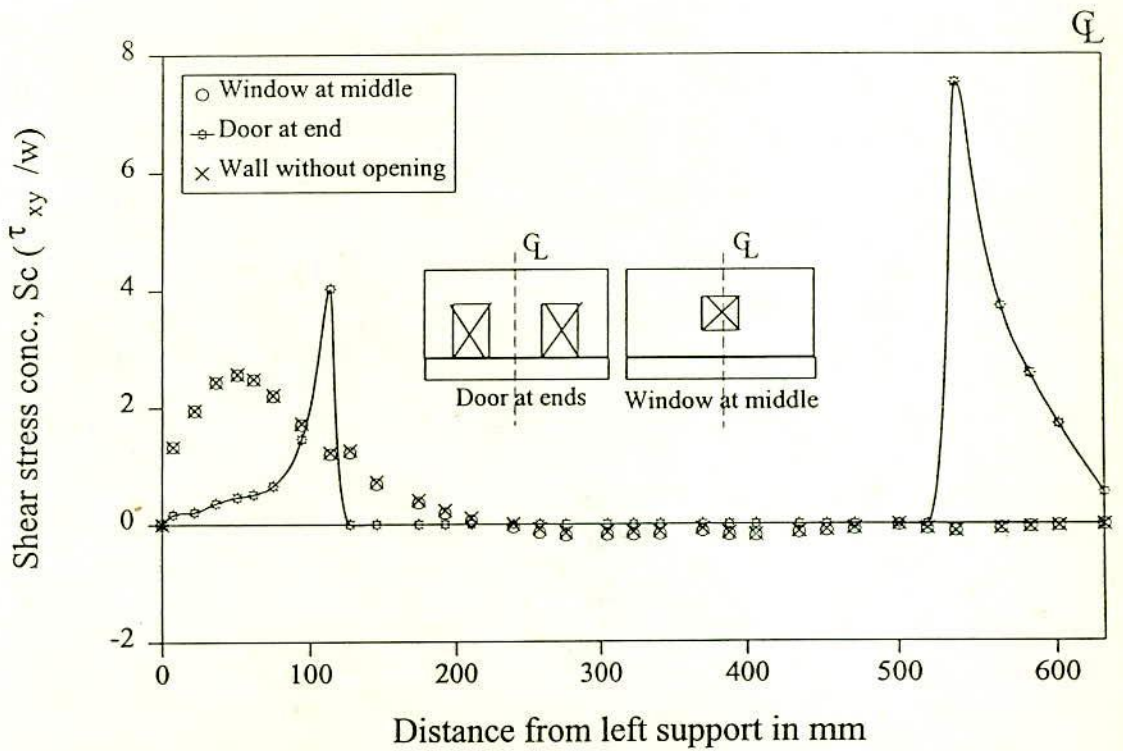


Fig. 3.27(b) Influence of Openings on S_c

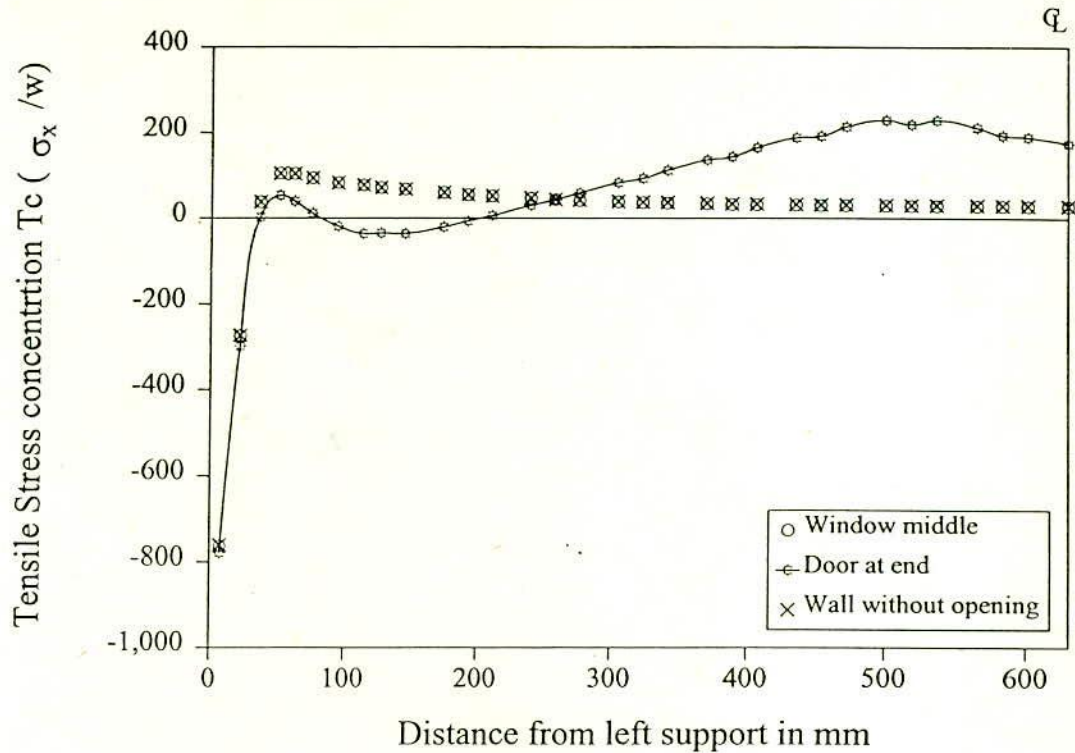


Fig. 3.27(c) Influence of Openings on Steel in Beam

The variations of vertical stress concentration, shear stress concentration at wall-beam interface level and the tensile stress concentration in the bottom reinforcement of the supporting beam are shown in Fig. 3.28(a), Fig. 3.28(b) and Fig. 3.28(c) respectively. It is clear from these figures that the support contact length has great influence on distribution of stress near the bottom corner of wall. With the increase of contact length of support, vertical and shear stress concentration are found to decrease considerably. Due to the increase of contact length of support tensile stress in the reinforcement also decreases along with shifting of location of maximum stress. It is therefore concluded that, if support width in the direction of span is duly considered stress concentration can be reduced quite significantly.

3.6.8 Effect of Column Height

When supporting beam of a single span wall-beam is connected at its ends with columns, the height of the column will influence on interaction behaviour of wall-beam structure. Unlike other researchers, this height of the column was taken

as a parameter in this study. For this purpose wall-beam with varying height of columns (0 mm, 100 mm, 300 mm, 600 mm, 900 mm, 1200 mm) were analysed. The column cross-section was kept constant which provided a constant bearing length of $0.077L$. The nodes at the interface of beam and column are assumed to have perfect bond. Simply supported condition at the ends of the column was assumed as before (i.e. the nodes at the support are restrained only in vertical direction). The variation of vertical stress concentration and shear stress concentration at wall-beam interface and the tensile stress of the bottom reinforcement of the supporting beam in terms of 'w' are shown in Fig. 3.29(a), Fig. 3.29(b) and in Fig. 3.29(c) respectively. It is seen from Fig. 3.29(a) that the maximum vertical stress concentration increases with the increase of column height up to a certain limit. These figures also show that with columns having greater length there is no appreciable change in this increase. Fig. 3.29(b) shows that effect of column height on the shear stress concentration is not significant. From Fig. 3.29(c) it is seen that with the change of column height the tensile stress concentration, T_c in the bottom reinforcement changes. This change is very sharp for column with small height (in comparison to wall-beam without column). While this change is very negligible for column with greater height (300 mm to 1200 mm for a span of 1300 mm).

It seems from above discussion that when the ends of supporting beam of wall-beam structure are monolithic with column the degree of framing action occurring between wall-beam system and the column reduces with the increase of column length from zero to normal height. The length of the column reduces the stiffness of the column and the wall-beam system. It is observed that wall-beam with column of normal length produces high vertical stress concentration at the ends.

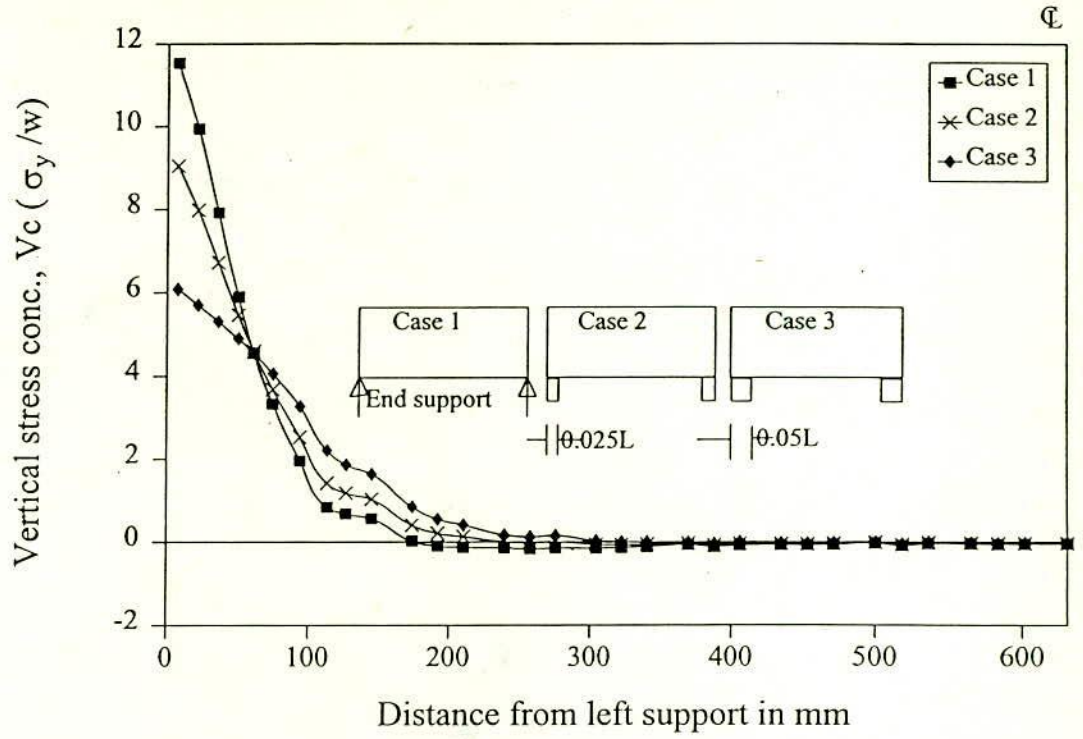


Fig. 3.28(a) Influence of Width of Support on V_c

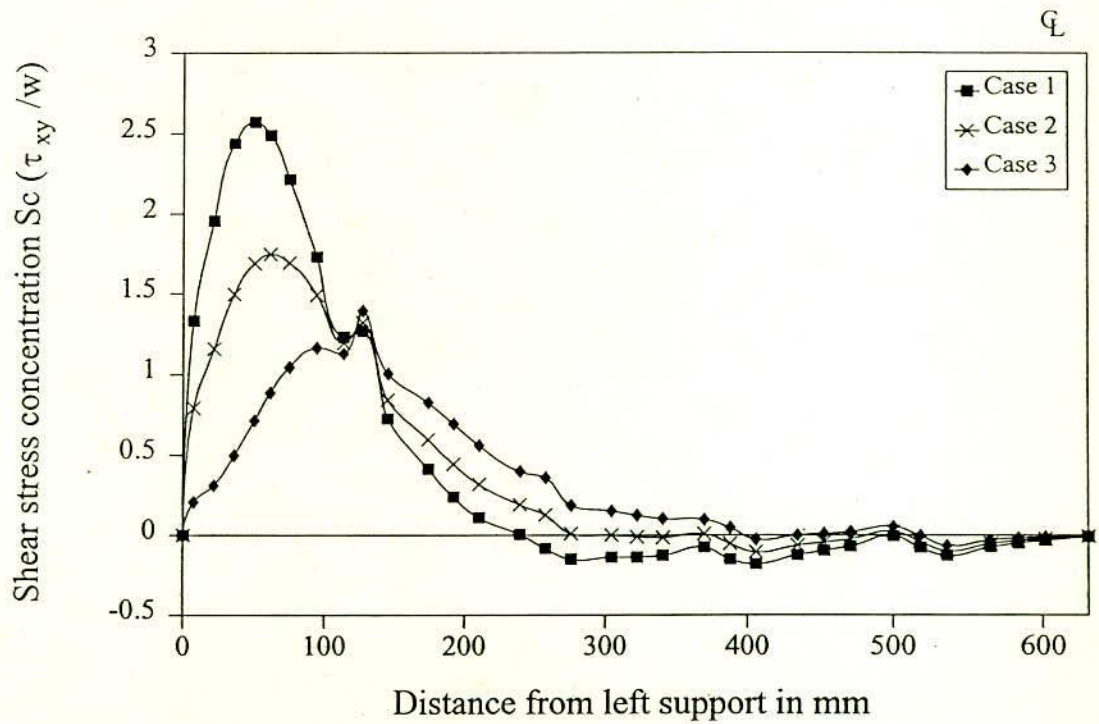


Fig. 3.28(b) Influence of Width of Support on S_c

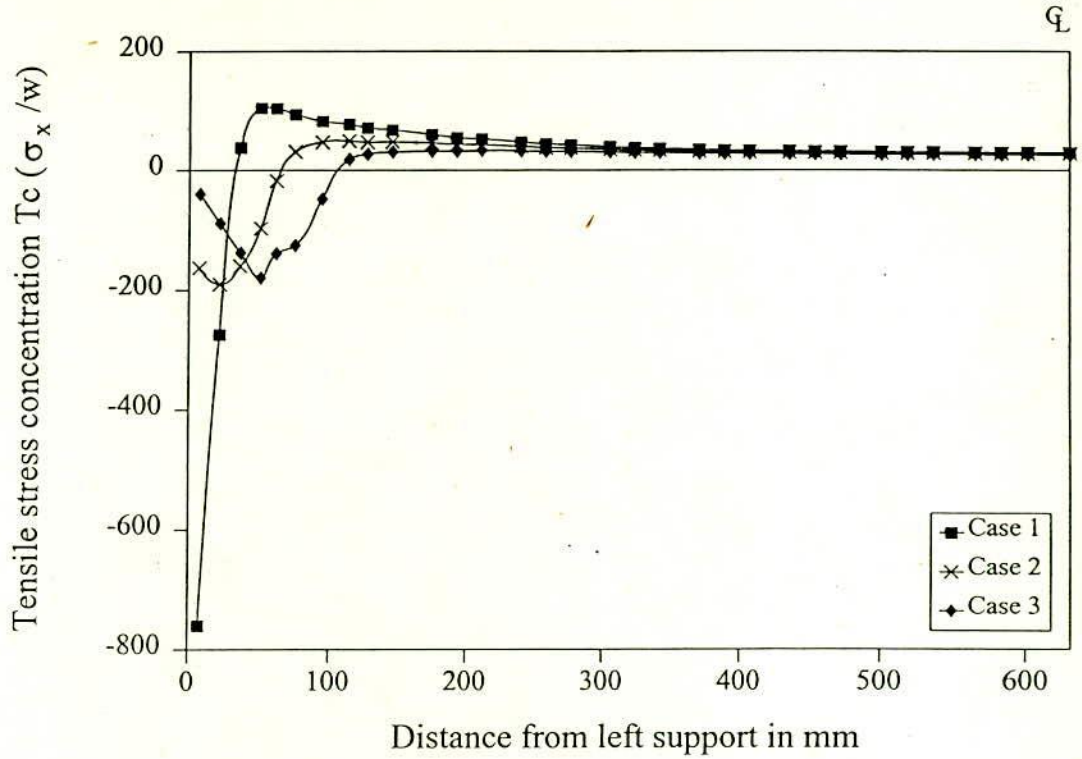


Fig. 3.28(c) Influence of Width of Support on Steel in Beam

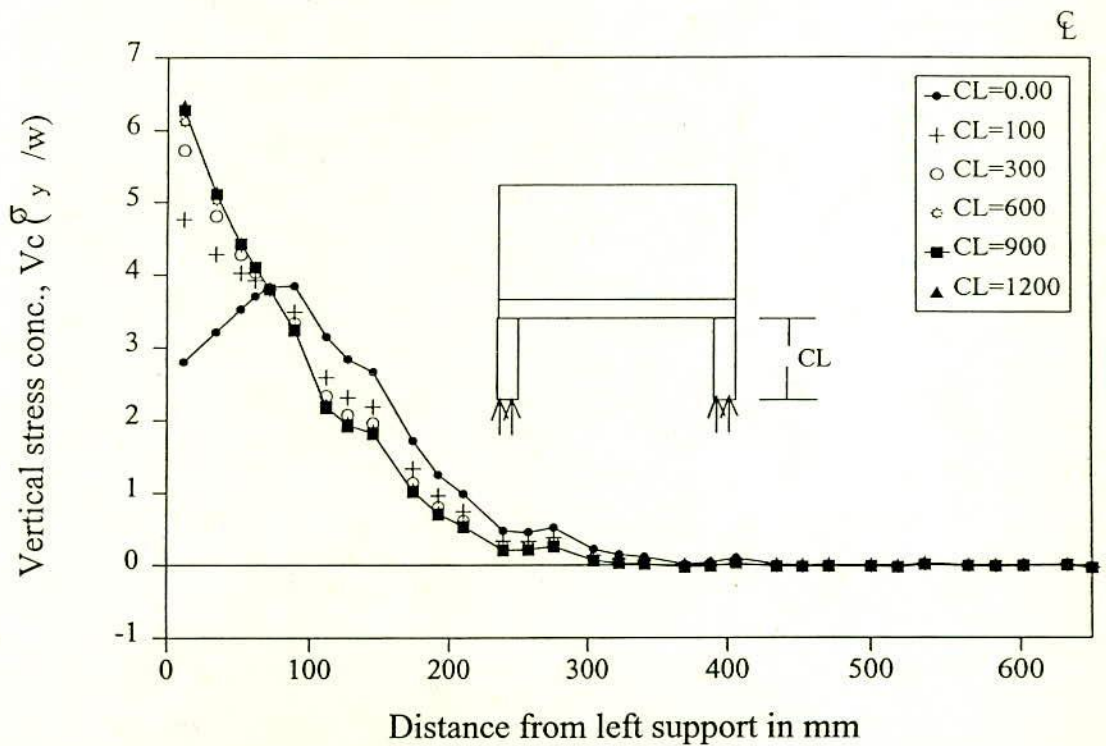


Fig. 3.29a The Influence of Column Height on V_c

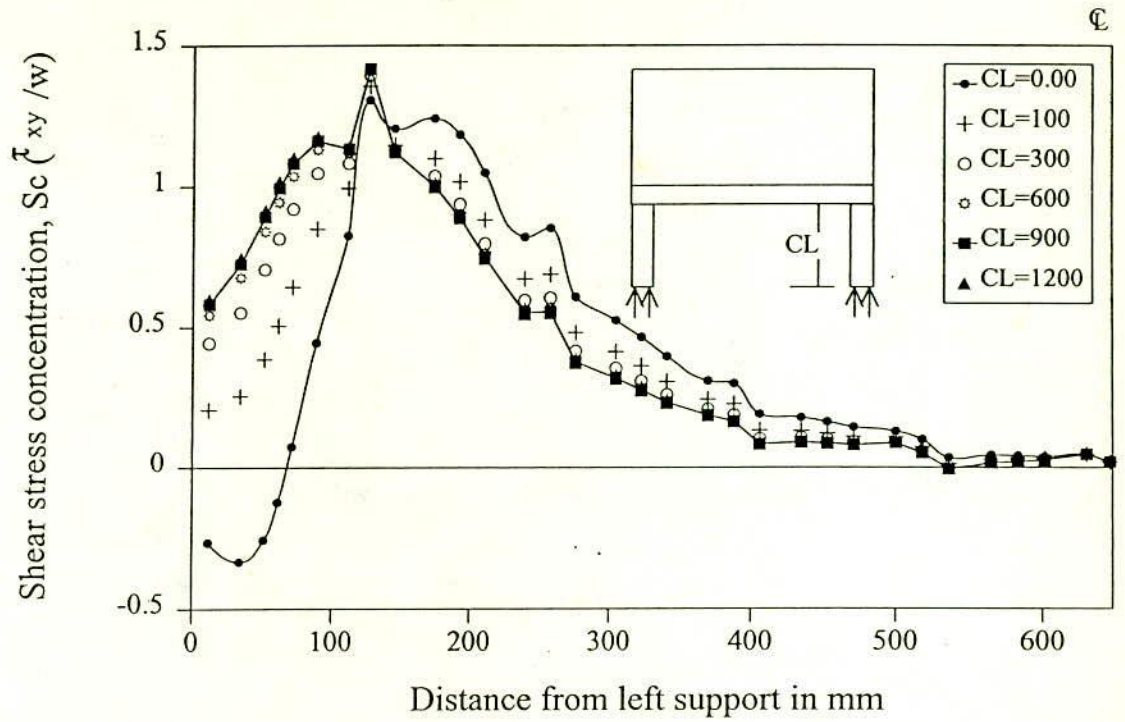


Fig. 3.29b The Influence of Column Height on τ_c

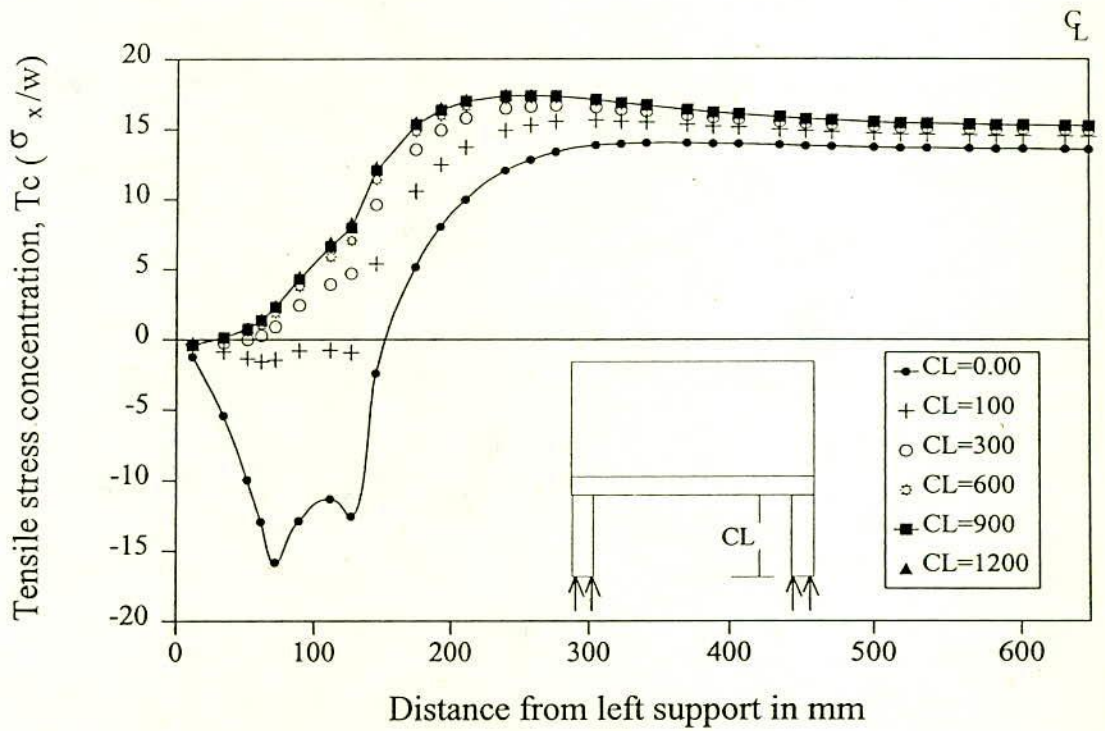


Fig. 3.29c The Influence of Column Height on Steel in Beam

3.7 SUMMARY

In this chapter a comprehensive parametric study has been made on wall-beam structure by using linear elastic finite element model. From this parametric study the following conclusions can be drawn.

1. The mesh refinement is an efficient technique which permits the use of finer element mesh in the region of high stress gradients.
2. A finite element model which treats bricks and joints separately is more effective, since it reflects the influence of the varying stiffness of its constituents.
3. Due to the arching action in the composite wall-beam system, there occurs the concentration of vertical and shear stress in the masonry above the support. These forces may cause failure to the brickwork before the yielding of the supporting beam.
4. The composite action can occur in a wall-beam structure with height/length ratio less than 0.6 provided the transfer of shear at wall-beam interface is ensured.
5. The stress distribution at interface level of wall-beam having H/L ratio greater than 0.6 is independent of the height of the wall for a particular depth of the supporting beam.
6. The concentration of stresses at the support is found to increase with the increase of modulus of elasticity of brick, while the concentration decreases with the increase of modulus of elasticity of concrete.
7. The stress near the support increases rapidly as the stiffness of the beam is decreased.
8. Keeping all other factors constant the decrease of the depth of the supporting beam results in a higher and rapid rise of stress concentration towards the supports.
9. The reinforcement in supporting beam increases its stiffness and reduces stress concentration near the bottom corner of the wall-beam. Therefore the reinforcement in the supporting beam should be incorporated in analytical models for appropriate simulation of real structure.
10. Composite action of the wall-beam structure reduces the bending moment in the supporting beam quite significantly.
11. The vertical columns of brick in-filled wall-beam panel receive maximum stresses and thus relieve the stresses in the masonry at bottom corner of the

panel. This effect may enable the wall-beam to carry higher load in the case when the failure is mainly due to crushing of the brick unit near the support.

12. The door openings at the ends of the panel produce maximum vertical compressive stress at the bottom corner of the wall to maximum vertical tensile stress at the bottom corner of the opening near the end. There is also a sharp change from high vertical compressive stress at the bottom corner near the mid span of an offset opening to high vertical tensile stress at the centre of the span. This rise in compressive or tensile stress concentration is noteworthy in comparison to a wall-beam structure with a central opening or without any opening.
13. Due to the openings at the ends, the shear stress concentration is maximum at the bottom corner of the opening near the mid span.
14. The openings at the ends of the wall-beam panel will produce higher bending moment with the shifting of its location from near the support towards the mid span.
15. The stress concentrations in the masonry wall and in the reinforcement of supporting beam of a wall-beam structure decrease with the increase of width of support. Greater width of support will increase the load carrying capacity of the wall-beam panel.
16. The vertical stress at wall-beam interface and the tensile stress in the reinforcement of the supporting beam increases with the increase of height of the supporting column .
17. A significant number of parameters have been identified in this chapter which have influence on the stress distributions in wall-beam structures. From this preliminary study important parameters which influence the composite behaviour of wall-beam structures are identified.
18. The linear elastic finite element analysis performed in this chapter has got limitations. It can be used to study the nature of stress distributions only and cannot be used to predict the failure and crack propagation. Non-linear behaviour due to crack propagation and material deformation characteristics cannot be modelled fruitfully by elastic analysis. For this purpose suitable material model should be incorporated in the finite element analysis to simulate the behaviour of wall-beam from first crack to failure. These will be discussed in the ensuing chapters.

CHAPTER 4

BRICK, MORTAR AND BRICK MASONRY PROPERTIES

4.1 INTRODUCTION

Brick masonry is one of the man's oldest building material comparatively superior to other alternatives in terms of appearance, durability and cost. The bricks are manufactured locally by burning the surface clay. The manufacturing method is labour extensive and easily adopted one, resulting a huge employment in Bangladesh. Thus brick masonry plays a key role in construction trade particularly in Bangladesh where natural stones are normally not available.

The finite element model which is developed later in this study applies to solid clay brick masonry. To allow its verification with actual load test a particular brick-mortar combination was chosen and used throughout the investigation. Brick masonry constructed from solid clay bricks and mortar consisting of 1 part cement and 4 part sand by volume was used. Ordinary building bricks prepared from surface clay, hand moulded and kiln burnt, were supplied by local manufacturer. Same brick was used throughout the study. For easy handling the dimension of brick was selected as half of the standard size with an average of 123 X 60 X 36 mm. Frog mark was not indented during the moulding, however the interlocking benefit from the frog mark on the brick will add to the factor of safety of the real structure.

To develop a finite element model which considers brick masonry as an assemblage of bricks set in a mortar matrix, the properties of the bricks, the mortar and the bond between the brick and the mortar must be determined. These were derived from various types of tests performed on representative samples of the brick, mortar and brick masonry used in the investigation. These include standard tests, and other non conventional tests. Both types of tests are important to define the individual characteristics of clay brick and cement sand mortar. In this chapter the laboratory investigations of uniaxial compression tests on bricks and mortar cylinders and split tensile tests on bricks and mortar prisms were carried out along with the determination of deformation characteristics of the materials. The principal cause of composite behaviour of masonry is the bond between the brick and the mortar. This chapter also describes tests on prisms and triplets of masonry from which bond characteristics are derived. These include compression test on

masonry prism, masonry triplet and on masonry couplets with sloping joints (to induce shear stress in the joint), and splitting tensile test on masonry prisms .

4.2 BRICK PROPERTIES

Like other masonry structures brick constitute the major part of the volume of the wall-beam structures. Therefore, maintenance of uniformity of material properties of bricks in the panel is important. All bricks were purchased from the same manufacturing company at a time and were stored in the laboratory throughout the study.

4.2.1 Compressive Strength of Brick

Brick compressive strength is an important property which has been traditionally used for quality control. Routine tests like compressive strength and absorption tests were done according to Bangladesh Standard Specification BDS 208(1980). The important results are given in Table 4.1 and the detail results are provided in Appendix II.

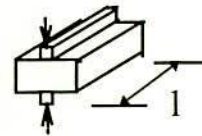
In addition to standard test, compressive strength was also determined from uniaxial compression test on brick applying load in the direction parallel to bed joint orientation. The difference between compressive strength thus obtained from that of the standard test (load applied normal to bed joint) is due to the platen effect of the testing machine. Platen effect apparently increases the actual compressive strength. Study made by Page and Marshal, (1985) with brush platen reveals that for brick and prism having aspect ratio (Height/Least width) varying from 3 to 0.4, the actual compressive strength varies from 0.85 to 0.5 times the apparent strength obtained from a so called standard test. The compressive strength test of brick loaded on end and in the direction parallel to normal bed joint ensures minimum platen restraining effect at the middle of the specimen. Strength obtained from such tests on brick units used in this study is found to be close to the actual strength obtained by applying aspect ratio correction factor (proposed by Page and Marshal) to the apparent strength from standard test. The compressive strength of brick tested on end and applying vertical load along the length of the brick may roughly be considered as the actual compressive strength. Therefore, there may be two types of compressive strength tests. One the so called standard test the value being corrected by aspect ratio correction factor (proposed by Page and Marshal) and the other with the brick tested on end and applying vertical load along the length

(requiring no modification in test apparatus or the test value). The validity of the assumption that the bricks have comparable compressive strength in both the test mentioned above should be checked by further investigation which is beyond the scope of this study.

4.2.2 Tensile Strength

In most masonry structures final failure takes place in some form of tensile splitting in the brick. This property therefore carries importance in defining the behaviour of masonry structures. It is very difficult to perform direct tensile strength test on bricks. Splitting tensile strength test as suggested by Thomas and O' Leary (1970) for homogeneous prism was followed in this study and is given by Eqn. 4.1. ASTM C1006(1984) test method for splitting tensile strength of masonry unit, uses similar equation.

$$\text{Tensile stress, } \sigma_T = \frac{CP}{DI} \quad (4.1)$$



where

P = applied load

l = specimen thickness

D = equivalent diameter

$$= \sqrt{\frac{ha}{\pi/4}}$$

h, a = specimen height and width

C = constant = 0.648 (for homogeneous material)

The value of $C=0.648$ used in Eqn. 4.1 is proposed by O'Leary and also confirmed by a finite element analysis done by Ali (1987).

A total of 10 bricks were tested. All bricks were tested dry and randomly selected from the batch. The load was applied through a steel bar of 6 mm square which is within 10 % of the width of the brick. The load was applied using a universal testing machine, with a loading rate of 25 kN/min. Failure occurred by vertical split directly beneath the loading plate. The mean tensile strength of the brick is shown in Table 4.1. Detailed experimental results are contained in Appendix II .

4.2.3 Deformation Characteristics of Bricks

Destructive uniaxial compression test was done on bricks to study its deformation characteristics. The load was applied both parallel and normal to bed joint. The load was applied at the rate of 100 kN /min until failure. The strains were measured by electric strain gauges (30 mm gauges along the length of the brick and 10 mm gauges in the transverse direction) attached to opposite faces of the bricks at mid height level. The strain readings were recorded on a data-logger giving simultaneous printout. The strain readings from opposite faces were averaged to eliminate the bending effect. The rate of loading and subsequent steps were common for both cases of loading.

4.2.3.1 Load parallel to bed Joint

For this test individual brick was loaded on end as shown in Fig. 4.1. Brick tested on end renders the central portion of the specimen relatively free from platen effect. The average stress-strain plot for bricks shown in Fig. 4.2 exhibits linear load deformation characteristics under uniaxial compression.

Fig. 4.1 Uniaxial Compression Test on Brick (Load Parallel to Bed Joint)

The individual stress-strain plot of the bricks also exhibits linear load deformation characteristics under uniaxial compression. The individual stress-strain plot of the bricks is shown in Appendix II. Average modulus of elasticity of bricks, when the load is parallel to bed joint (E_{bp}), is given in Table 4.1. The values of the parameters for uniaxial stress-strain curve (loaded parallel to bed) of brick are given in Table 4.2 and detailed results are contained in Appendix II. The variations in elastic modulus of individual brick and other parameters are inherent due to their material variability and manufacturing process.

4.2.3.2 Load normal to bed Joint

As discussed in compression test, due to significant effect of aspect ratio this deformation characteristics was studied in conjunction with that of the brick prism test as shown in Fig. 4.3. The elastic modulus is derived from the strain measured on the central brick of 5 brick-high prisms loaded in axial compression. Average modulus of elasticity, when the load is normal to bed joint (E_{bn}), is given in Table 4.1. and the detail experimental results are contained in Appendix II. The

Table 4.1 Summary of Brick Properties

Type of test	\bar{X}	S	C. of V. %	No of Specimen
Size (mm)	122.7x59.6 x 35.8	3.4, 1.2, .81	3, 2, 2	10
Weight of brick (gm)	448.7	11	2	10
Absorption (%)	13.6	4	29	10
Compressive Strength Parallel to bed Joint (MPa)	40.2	5.44	13.5	10
Compressive Strength (Standard Method) (MPa)	66.2	6.94	10.5	10
Indirect Tensile Strength (MPa)	3.2	0.44	13.6	10
E_{bn} (MPa)	12,930	3,280	25	10
E_{bp} (MPa)	17,900	2,634	14.7	10
Poisson's Ratio	0.141	av. Plot of Fig. 4.4		10

coefficient of variation of absorption and E_{bn} reflect poor quality of brick specimens. However, these did not influence the present study as saturated surface dry bricks were used and the E_{bn} value was not required in the analyses. The comparison of the deformation characteristics of brick for both the cases (load parallel and normal to bed joint) is shown in Fig. 4.2. The individual stress-strain plot of the bricks is shown in Appendix II. From prism tests, in-situ behaviour of mortar will be discussed later.

Table 4.2 Values of Material Parameters from Uniaxial Stress-Strain Curve of Brick

	\bar{X}	S	C. of V. (%)
Initial Tangent Modulus (E_0) (MPa)	17,900	2,630	14.7
Secant Modulus at Ultimate strength (E_{CS}) Mpa	17,510 11503*	2,680	15.3
Ultimate compressive strain (ϵ_{cu}) $\times 10^{-5}$	227.5	20.56	9.0

* From Prism Test

Stress-Strain Curve

The instantaneous axial deformation of specimen under load can be described conveniently by stress-strain diagram. The average stress-strain curve shown in Fig. 4.2 is approximately linear and can be represented by

$$\begin{aligned}\sigma &= 17900 \epsilon \text{ MPa when the load is parallel to bed joint} \\ \sigma &= 12930 \epsilon \text{ MPa when the load is normal to bed joint}\end{aligned}$$

The fired clay bricks used by Page(1978), was also found to exhibit elastic brittle behaviour, while the concrete solid bricks used in masonry unit by Ali(1987), exhibited non-linear stress-strain characteristics near the failure.

As was mentioned earlier most of the masonry structure the final failure takes place in some form of tensile splitting of brick. The stress strain characteristics of the brick in tension are therefore required for the finite element

models dealing with micro studies. Since the burnt clay bricks exhibit brittle behaviour both in compression and tension the stress-strain curve was assumed to be the same as the compression curve and can be expressed by the same formula.

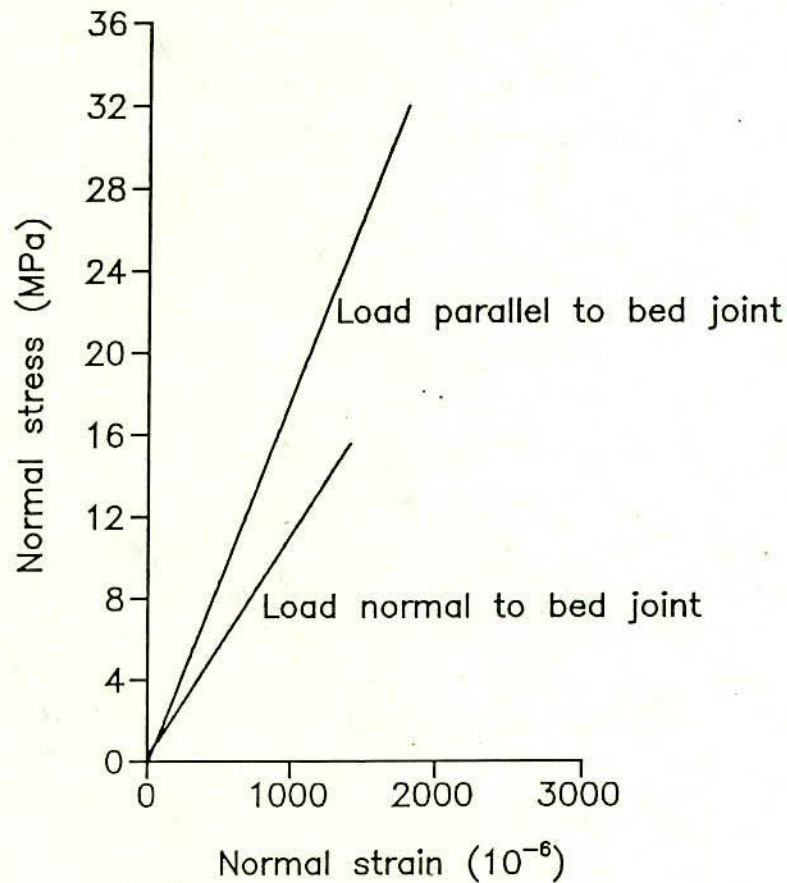


Fig. 4.2 Average Stress-Strain Curve for Brick

4.2.4 Poisson's Ratio of Brick

Poisson's ratio of the brick was calculated as the lateral strain/longitudinal strain from the values obtained from compression tests of bricks on end. A typical plot of average longitudinal strain against average lateral strain, measured from the compression test of brick unit is given in Fig. 4.4. The detail experimental results are contained in Appendix II. Poisson's ratio was found to remain approximately constant up to 82% of the ultimate load, having average value of 0.141. However, this value varies when the load is applied in the other direction as determined from prism test. It should be mentioned that in the latter case the result is influenced by the brick mortar interaction. Since the Poisson's ratio is not a sensitive parameter in

the finite element model for masonry structures, the consideration of Poisson's ratio in the orthotropic direction can be disregarded.

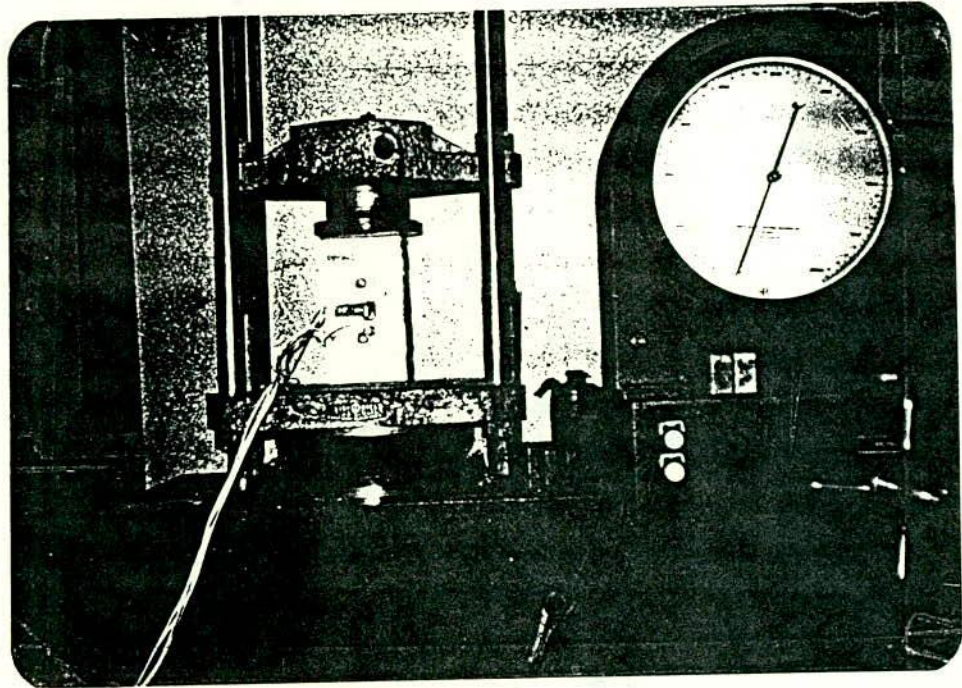


Fig. 4.3 Compression Test of Stack Bonded Prism

4.3 MORTAR PROPERTIES

Like brick unit the estimate of compressive strength, tensile strength, and deformation characteristics of mortar are required to define the material model.

Mortar was prepared from normal Portland cement and local sand (FM=1.5), mixed in ratio of 1:4 by volume. For preparation of workable paste, the amount of water required was determined from flow test of mortar as proposed by ASTM (1980), C109. The w/c ratio of 1.0 (by weight) was determined to prepare the mortar for use throughout the study. All the specimens were moist cured for 14 days and tested at 28 days.

4.3.1 Compressive Strength of Mortar

The compressive strength of mortar was obtained from test on 2 inch cubes, according to test method specified in ASTM C109(1980). The strength of mortar obtained from above mix satisfied the specification of Bangladesh National Building Code (BNBC), 1993 and corresponded to grade M2. The compressive

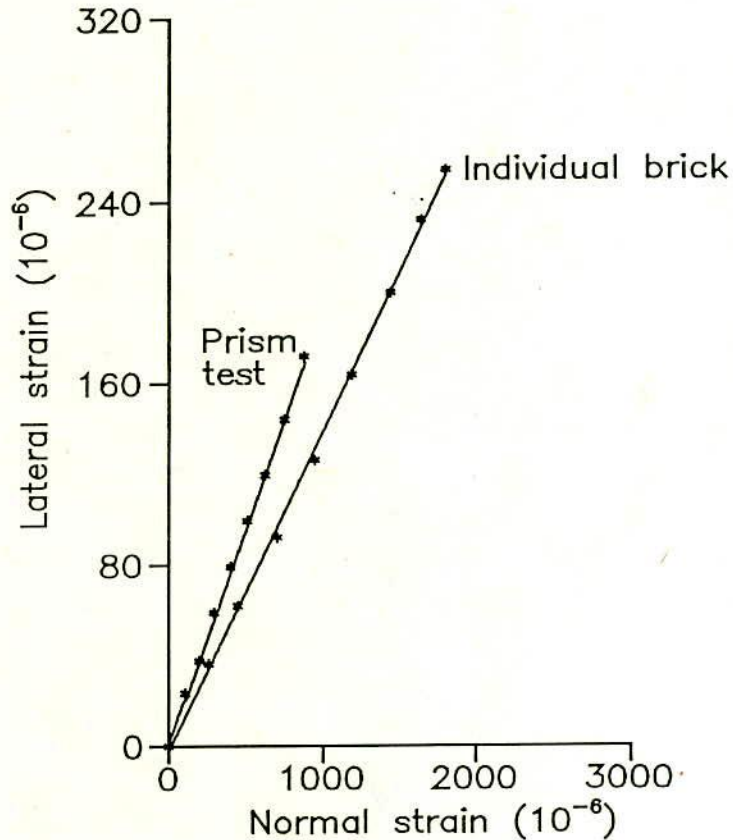


Fig. 4.4 Poisson's Ratio of Brick

strength of mortar was also determined from uniaxial compression tests on 75 mm x 150 mm mortar cylinders. Average compressive strength determined from cubes and cylinders are given in Table 4.3. Detailed results are contained in Appendix II.

4.3.2 Tensile Strength of Mortar

Tensile strength of mortar was determined from splitting test on 100 mm x 50 mm x 40 mm mortar prism. The same method as mentioned earlier for determination of tensile strength of brick has been used to determine the mortar

tensile strength. The average tensile strength is 0.97 MPa, (See Table 4.3). The detail experimental results are contained in Appendix II.

It should be mentioned that the prisms for tensile test are made in steel mould. But during laying the bricks may absorb water from mortar thus reducing the water-cement ratio which may change the tensile strength of the mortar. The development of test which in fact can estimate the true in-situ tensile strength of mortar is required in this case. However, the incorporation of the nominal tensile strength of mortar in the present model may underestimate the failure load of the panel.

In addition to tensile failure in the mortar itself, tensile failure in masonry can take place due to tensile bond failure at the brick-mortar interface. This will be discussed later. A representative material model for mortar will also require this latter parameter to be considered.

4.3.3 Deformation Characteristics of Mortar

The study of load deformation characteristics was aided by attaching 30 mm and 10 mm electric strain gauges in longitudinal and transverse direction respectively at mid height on the cylinders. Average stress-strain curves obtained from cylinders are shown in Fig. 4.5 along with the average insitu stress-strain curve for mortar obtained from prism tests (see article 4.4.3). Although, the deformation characteristics of mortar obtained from cylinder tests as depicted in Fig. 4.5 shows non-linearity, there is a marked difference between the deformation characteristics obtained from both the cases. It is therefore, clear that deformation characteristics obtained from mortar cylinder tests do not reflect the true behaviour of the mortar joints in the masonry. The average modulus of elasticity of mortar thus obtained is given in Table 4.3 and the detail results are contained in Appendix II.

4.3.4 Poisson's Ratio of Mortar

The Poisson's ratio of mortar was determined from the strains measured during uniaxial compression test on mortar cylinders. Simultaneous readings of longitudinal and lateral strain at mid height of the cylinder were recorded by previously attached electric strain gauges. A plot of average longitudinal strain vs. lateral strain of mortar obtained from cylinder tests is shown in Fig. 4.6. The figure

shows that Poisson's ratio is fairly constant up to approximately 65 % of the ultimate strength of the mortar. Beyond this limit the value increases slowly. The average value of Poisson's ratio of mortar within this elastic range is 0.182 and is given in Table 4.3. The details of experimental results are contained in Appendix II.

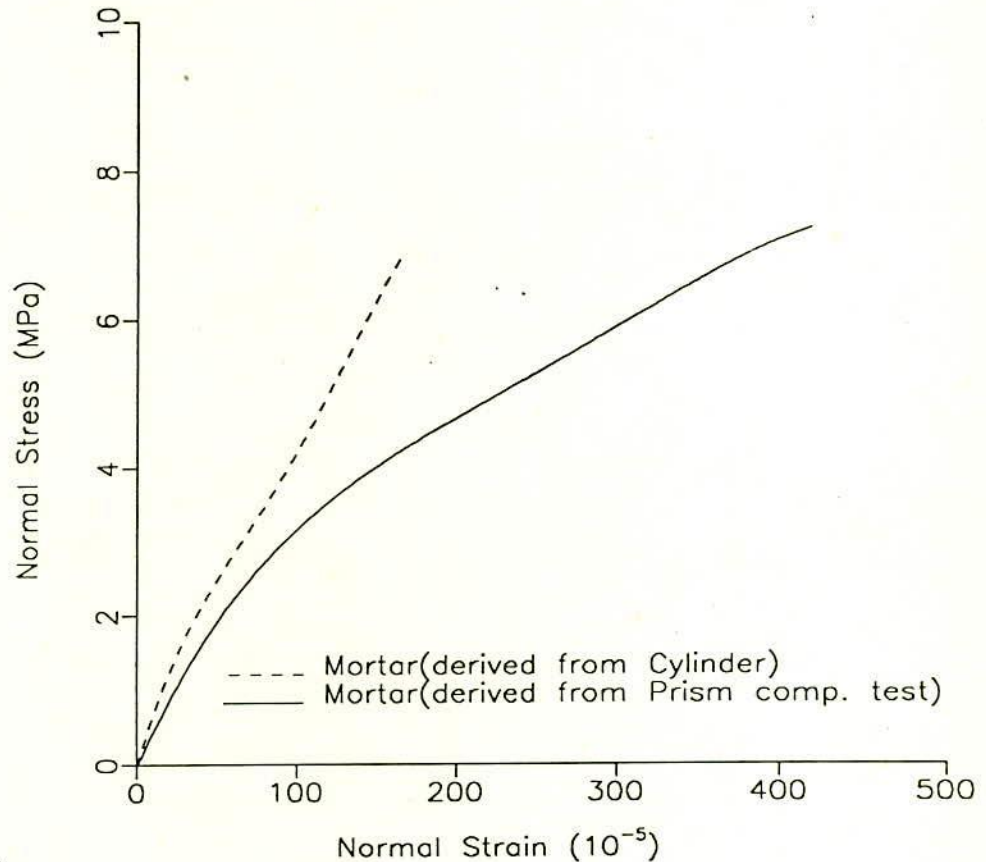


Fig. 4.5 Average Stress-Strain Curve for Mortar

4.4 BRICK MASONRY TESTS

4.4.1 General

Generally the compression tests on brick masonry prism are carried out to establish relationship of masonry strength with the compressive strength of brick and mortar. In addition to this, the elastic modulus of brickwork obtained from prism test is required to determine deformation of important brickwork structures. This is also required in the cases where composite action between brickwork and steel or concrete member is a basis of design.

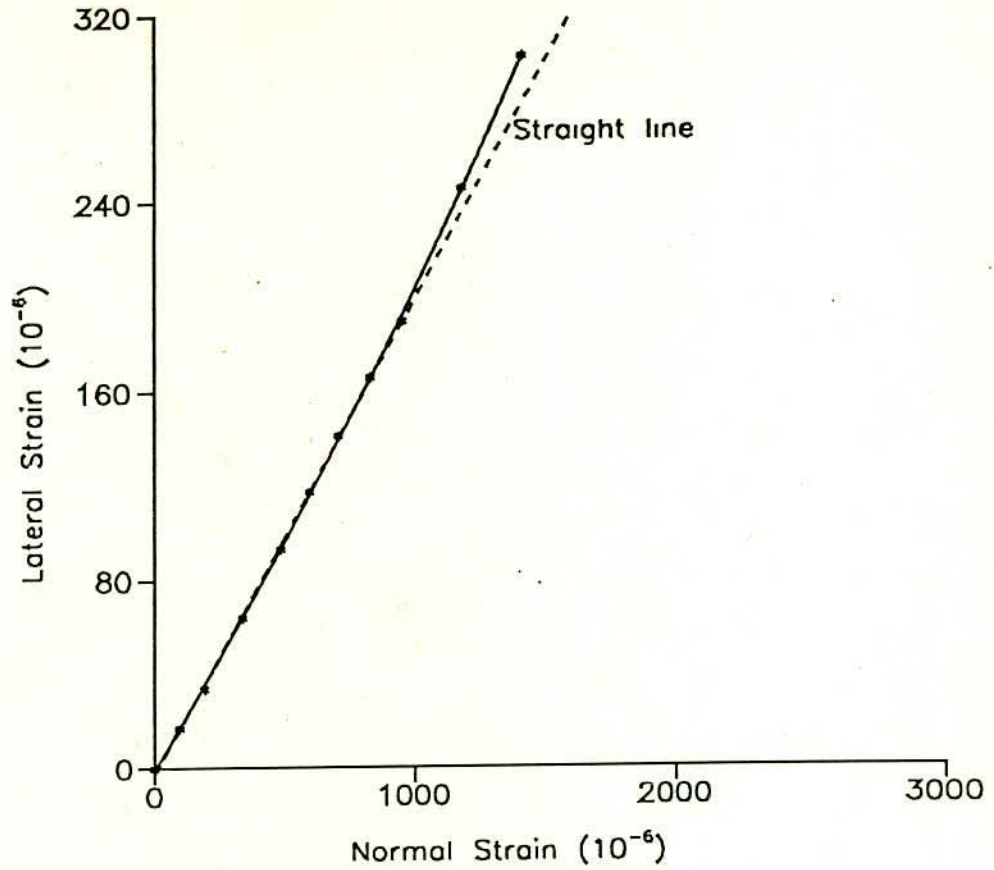


Fig. 4.6 Poisson's Ratio of Mortar (Cylinder Test)

Table 4.3 Summary of Mortar Properties

Type of Test	\bar{X}	S	C. of V. %	No of Specimens
Compressive Strength 2 in. Cube (M Pa)	12.5	0.66	5	10
Compressive Strength 3 in. X 6 in. Cylinder (M Pa)	12.0	0.43	4	5
Indirect Tensile Strength (M Pa)	0.97	0.04	4	10
Initial Modulus of Elasticity (M Pa) (from cylinder test)	9590	1587	16	3
Initial Modulus of Elasticity (M Pa) (from prism test)	3270	703.4	21	9
Poisson's Ratio	0.202	from Fig. 4.6		3

Since the finite element model developed in this study consider the bricks and mortar joints separately, the bulk of the masonry tests were aimed at obtaining brick and mortar properties indirectly and at establishing the basic bond parameters between bricks and joints. These involved compression tests on stack bonded prisms, compression tests on prisms with sloping bed joints, splitting tests on stretcher bonded prisms and compression tests on masonry triplets.

4.4.2 Uniaxial Compression Tests of Stack Bonded Prism (Load Normal to Bed Joint)

Five bricks high stack bonded prisms (208 mm height x 123 mm width x 60 mm thick) with plywood capping at top and bottom were loaded in uniaxial compression to failure. Longitudinal strains were measured on a central 86 mm gauge length on both sides of the prisms using Demec gauges. The gauge length encompassed 2 mortar joints, one full brick and two half bricks. Local strains were measured on the middle brick using electric strain gauges. The testing arrangement is shown in Fig. 4.3. Failure occurred by tensile splitting induced by the differing strain characteristics of the weaker mortar and stronger brick. A typical failure pattern is shown in Fig. 4.7. The average prism strength was 18.16 MPa with coefficient of variation 11% which agrees favourably with the empirical results of Hendry (1981). The average modulus of elasticity of the brick prisms tested was 8070 MPa with coefficient of variation 15%. The modulus of elasticity of the brickwork thus obtained from the prism tests can be expressed as $E_{BW} = 2.02 \sigma' / \epsilon'$ where σ' is the average crushing strength of the prisms and ϵ' is the corresponding strain obtained by extrapolating the average stress-strain curve of brickwork (See Fig. 4.8 below). This relation resembles with that proposed by Powell and Hodgkinson (1976). Details of the results of the prism tests are contained in Appendix II.

4.4.3 Deformation Characteristics of Mortar Joint (from Prism Test)

This section has described the derivation of deformation characteristics of mortar joints from stack bonded prisms. It is assumed that all the bricks encompassed by the demec gauge are in a uniform state of vertical stress and the difference between the total measured deformation and the brick deformation is attributed to the mortar. The mortar strain corresponding to the

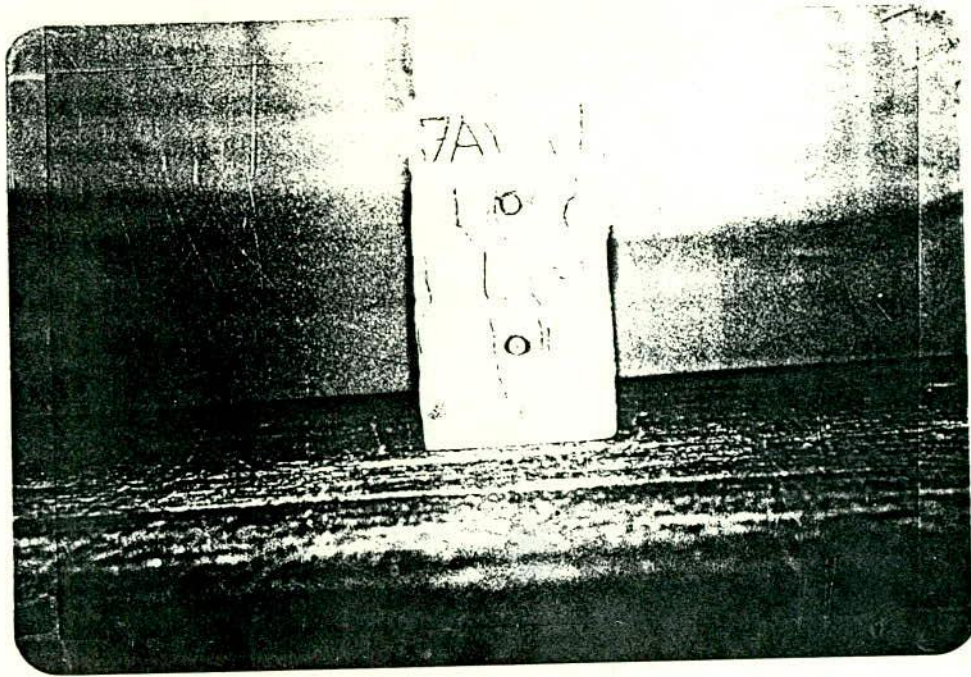


Fig. 4.7 Typical Failure of Stack Bonded Prism

stress level can be determined from Eqn. 4.2 below.

$$\varepsilon_m = \frac{\varepsilon_t L_t - \varepsilon_b L_b}{L_m} \quad (4.2)$$

in which ε_t = total measured strain; ε_b = strain in the brick; L_m = total mortar thickness; L_b = total brick thickness; and L_t = total gauge length. Using Eqn. 4.2 the net stress-strain curve for the mortar can be derived from the average measured masonry strain and brick strains for each prism. Detailed results of the tests for normal stress-strain reading of mortar joint in prisms are contained in Appendix II. The average initial tangent modulus of elasticity for the mortar thus obtained was 3270 MPa with coefficient of variation 21 %. Complete results for all the curves are contained in Appendix II. The average stress-strain characteristics for mortar and brickwork as derived from the prism tests and for brick derived from uniaxial compression tests (load parallel to bed joint) are shown in Fig. 4.9. The stress-strain curve for mortar is non-linear in nature.

The shape of the stress-strain curves for the in-situ mortar could be approximated by the relation used by Dhanasekar (1985). The relation predicts plastic strains throughout the stress range which is the sum of elastic strain $\epsilon^e = \sigma/E_0$ and the plastic strain (ϵ^p) and is given by

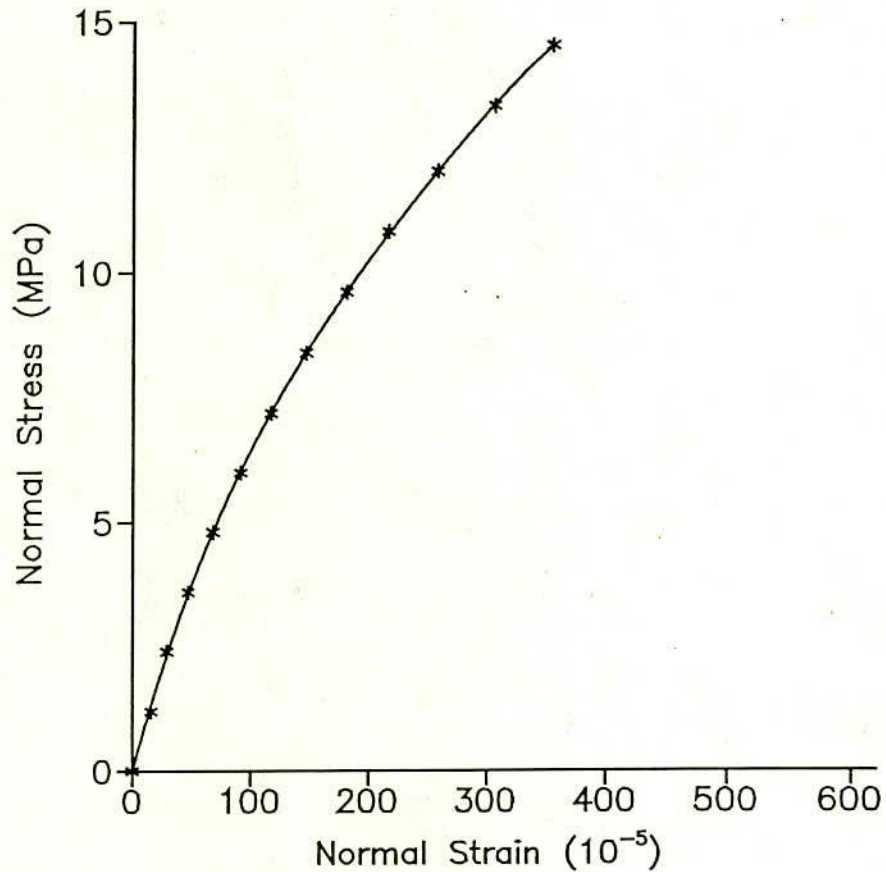


Fig. 4.8 Average Stress-Strain Curve for Brickwork

$$\epsilon^t = \sigma_n / E_0 + e^{a_n} (e^{b_n \sigma_n} - 1) \quad (4.3)$$

where ϵ^t = total strain; σ_n = normal stress; E_0 = initial tangent modulus and a_n and b_n are constants of stress-plastic strain equation determined from semilogarithmic plots of plastic normal strain against normal stress. The mean values of stress plastic strain constants with coefficients of variation are given in Table 4.4 and the detail results are contained in Appendix II. When the mean values of these constants are substituted in Eqn. 4.3 it can be simplified to

$$\epsilon_n^p = 2.64 \times 10^{-4} (e^{b_n \sigma_n} - 1) \quad (4.4)$$

4.4.4 Shear Tests on Brick Masonry with Sloping Bed Joint

This section has described the derivation of deformation characteristics of mortar joints from couplets with sloping bed joints.

These can be obtained from a uniaxial test by loading a prism with a joint inclined to the direction of loading, thus inducing shear and normal stresses on the joint as shown in Fig. 4.10.

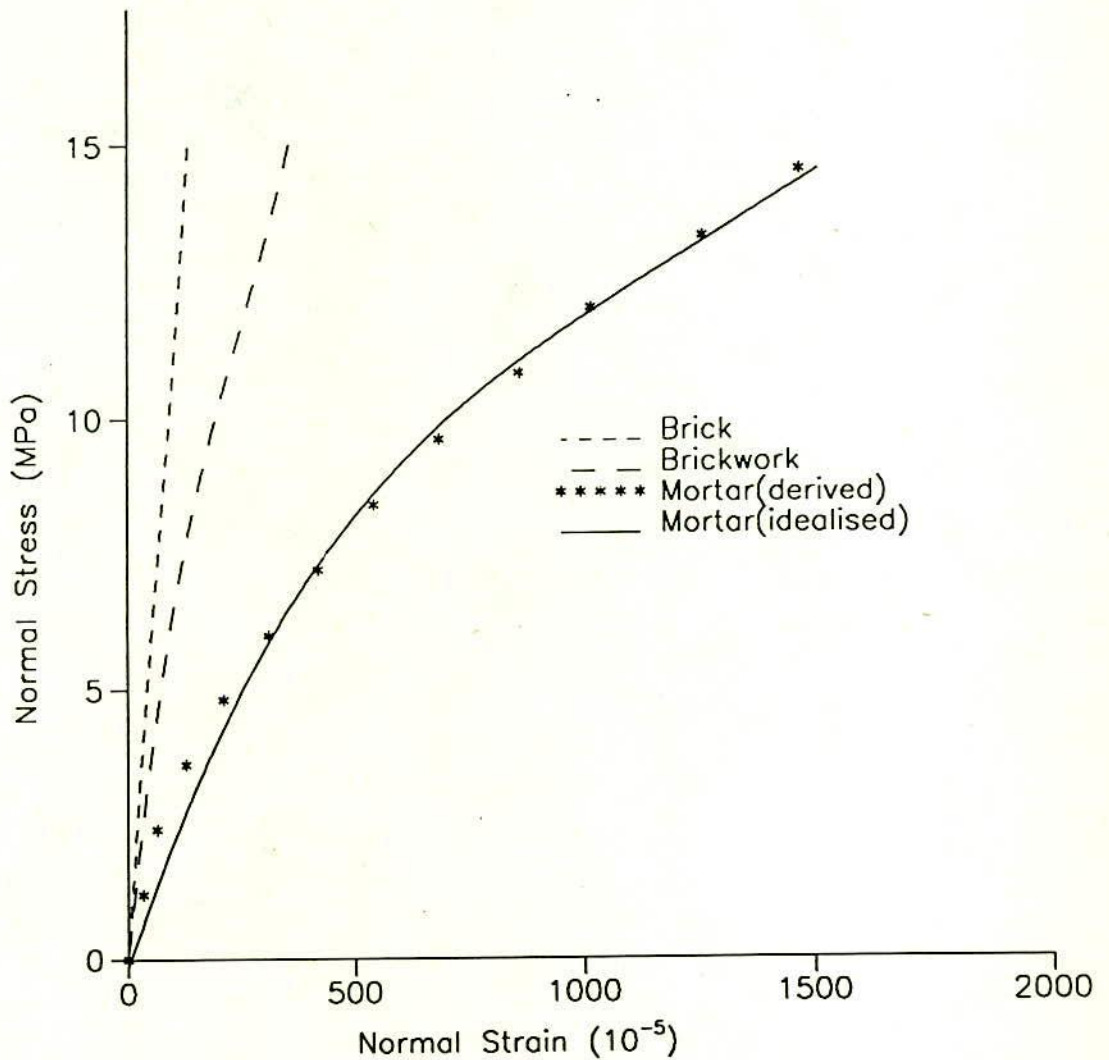


Fig. 4.9 Stress-Strain Curve of Brick, Brickwork and Mortar

The influence of normal stress was ignored and only one bed joint of orientation of 40° has been considered in this study. This steep angle ensured

significant shear deformations. For all the specimens failure was confined within the joint. Strains were measured in two diagonal directions on each side of the specimen using a Demec gauge with a 50 mm gauge length. Using the average value of strains on both faces the shear strains were determined from the strain transformation equation, Eqn. 4.4 below.

$$\gamma_{xy} = \frac{\epsilon_A - \epsilon_B}{\sin 2\theta} \quad (4.4)$$

where ϵ_A and ϵ_B are the strains in the diagonal directions. The joint shear strain was then determined at a particular shear stress level by subtracting the brick shear deformation from the total shear deformation. Thus the mortar shear strain (ϵ_m) at shear stress level (τ) is given by the equation

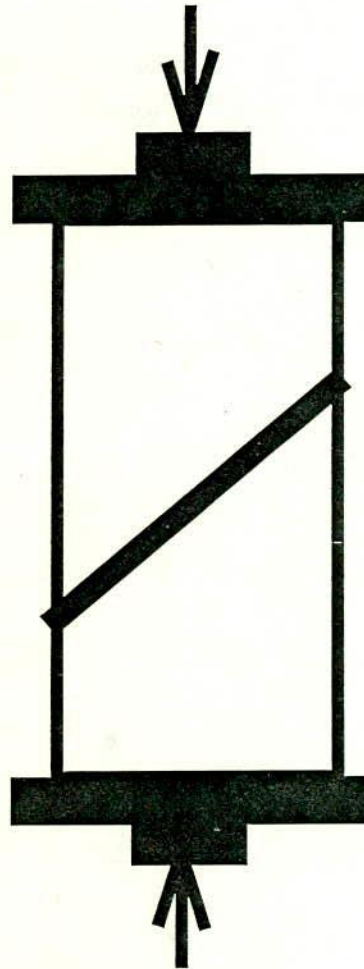


Fig. 4.10 Uniaxial Compression Test on Shear Couplets

$$\gamma_m = \frac{\gamma_t L_t - \tau \cdot \frac{L_b}{G_b}}{L_m} \quad (4.5)$$

in which γ_t = total measured shear strain and G_b = shear modulus of brick. Substituting the appropriate value of $L_t=37$ mm, $L_b=30$ mm, $L_m=7$ mm and $G_b = 9126$ MPa, the mortar shear strain can be expressed as

$$\gamma_m = 5.286\gamma_t - 0.0004696\tau \quad (4.6)$$

From the Eqn. (4.6) shear strains are calculated and the average experimental shear stress-strain curve obtained for the joint and the idealised curve are shown below in Fig. 4.11 together with the average curves for brick and brick masonry.

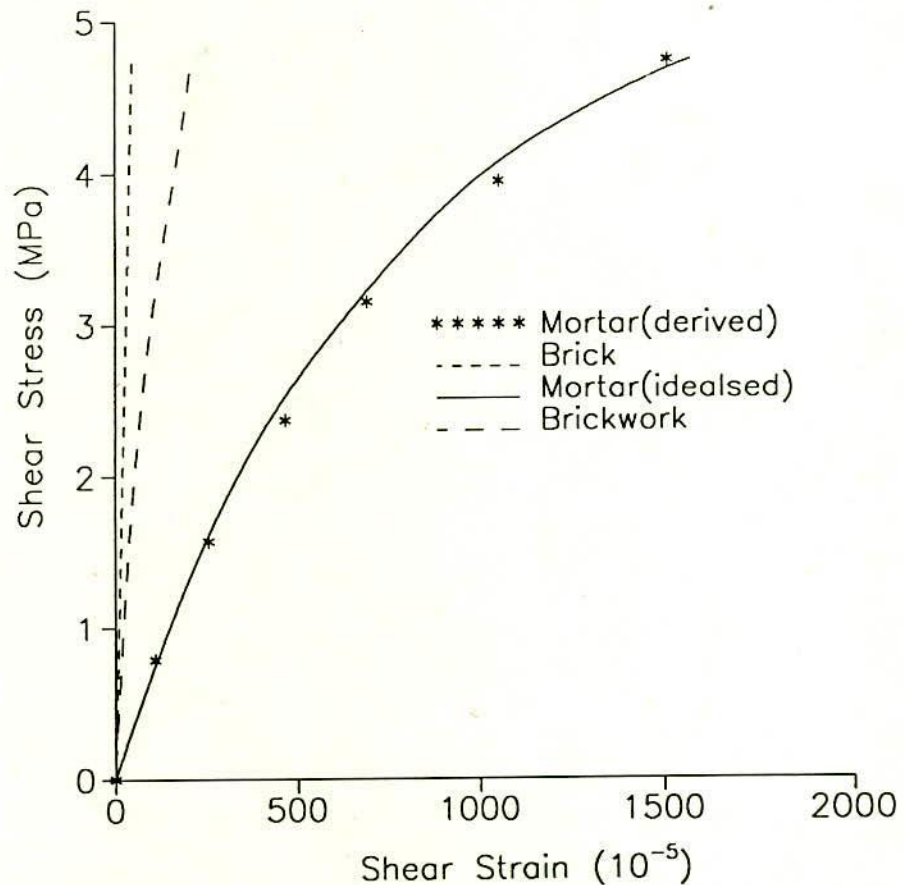


Fig. 4.11 Shear Stress-Strain Curve of Brick, Brickwork and Mortar

The shear stress-strain curve of mortar is non-linear in nature, with a linear region at low stress levels. The average initial shear modulus (G) for mortar was 1817 MPa with coefficient of variation of 40%. The details of the experimental results are contained in Appendix II. The shape of the average shear stress-strain curve for the joint can be defined by similar relation for normal stress-strain curve for the mortar and is given

$$\gamma^t = \tau / G + e^{a_s} (e^{b_s \tau} - 1) \quad (4.7)$$

Where, γ^t = Total shear strain for mortar, τ = Shear stress and a_s and b_s are constants to be determined from semi-logarithmic plots of plastic shear strain against shear stress. The mean values of stress plastic strain constants with coefficients of variation are given in Table 4.4. When the mean values are substituted in Eqn. (4.7) the plastic shear strain is given by :

$$\gamma^p = 8.11 \times 10^{-5} (e^{b_s \tau} - 1) \quad (4.8)$$

Table 4.4 Constants of Stress Plastic-Strain Equations
(Normal Stress and Shear Stress)

Constants	Mean	Standard Deviation	Coefficient of Variation (%)
a_n	-8.24	-0.67	8
b_n	0.27	0.05	18
a_s	-9.42	-0.95	10
b_s	.845	0.04	5

4.4.5 Simplified Approximation of the Bond Failure Surface

A method for the derivation of an approximate two-dimensional bond failure surface in terms of σ_n and τ obtained from splitting and shear tests respectively on brick masonry specimen have been described in this section. The surface is conservative in most cases. The approximate surface is therefore derived by obtaining the shear bond and tensile bond strength for the joint and assuming a linear relationship between these two limits. The following sections describe the relevant tests.

4.4.5.1 Tensile Bond Strength

An estimate of the tensile bond strength can be obtained from a splitting test on a small masonry prism built in running bond. The method proposed by Ali (1987) was adopted in this study. The general arrangement of the test is shown in Fig. 4.12. A compressive load is applied through narrow steel plates of width 10% to 12% of the total width of the specimen inducing an indirect tensile stress on the vertical mortar joint. The prism is 3 bricks high providing the ratio of height to width of the specimen less than 1.25. The load is applied until failure and the corresponding tensile bond strength is calculated from the Eqn. 4.1, with modified value for the constant C . The coefficient of homogeneity C has been taken from previous author (Ali (1987)). Finite element study made by Ali (1987), revealed that the value of C varies from 0.648 to 0.71 as E_b/E_m varies from 1 to 4 and suggested the value of C to be 0.67 for average practical condition. The mean

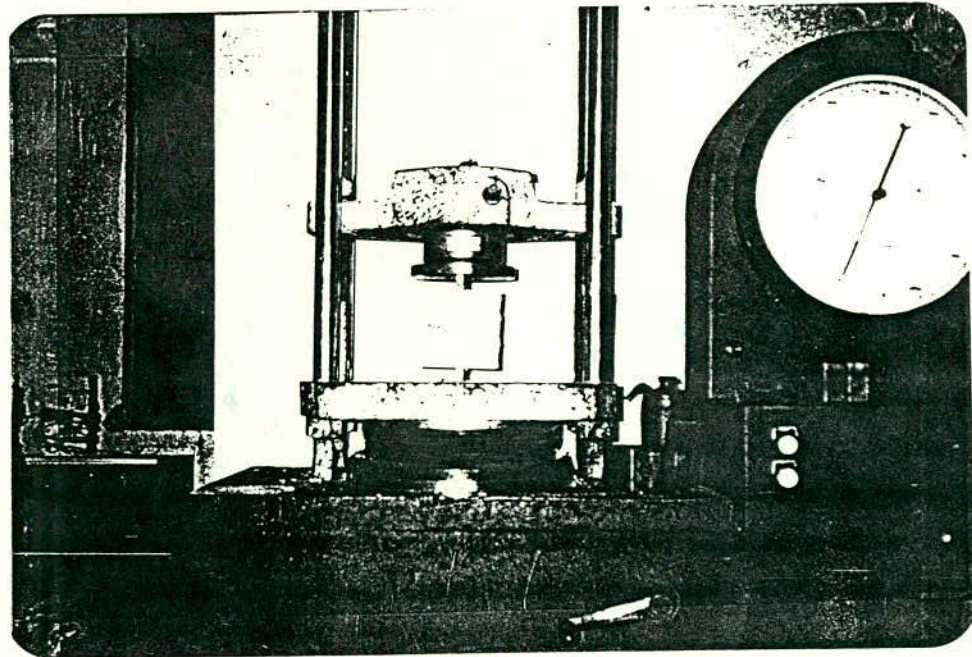


Fig. 4.12 Splitting Test on Brick Masonry Prism

tensile bond strength calculated in this manner for 10 specimens was found to be 1.443 MPa with coefficient of variation is 10%. Detailed experimental results are contained in Appendix II.

Due to lack of facilities and because the small masonry prisms were made of burnt clay bricks resulting brittle nature of failure the load corresponding to de-bonding of the vertical mortar from the brick face could not be observed. However, it has been found from the investigations made by Ali (1987) with masonry prisms made of concrete block, that the load corresponding to de-bonding of the vertical mortar from the face of the masonry unit (initial cracking load) is on average 87% of the failure load of the specimen. Therefore, as a rough guide the failure load thus obtained was taken for calculating the tensile bond strength.

For many applications this type of test is more representative than direct tensile tests on masonry joints, since it reflects the restraining influence of the surrounding bricks and joints.

4.4.5.2 Shear Bond Strength

It is difficult to devise a simple test which will produce uniform shear stress on a mortar joint. However triplet test as suggested by many investigators was adopted for this study. A total of 10 triplets were tested. The general arrangement of the test is shown in Fig. 4.13 below. The average shear stress (τ_{ab}) is obtained by dividing the ultimate load by the total sheared area. The mean shear bond stress was found to be 0.594 MPa with coefficient of variation 15% in this study. Detailed results are contained in Appendix II.

The important brick masonry tests along with the tests on bricks which are used to establish the basic material parameters are summarised in Table 4.5. All samples of brick masonry tests were moist cured for 14 days and tested at 28 days. The joint thickness for all specimen was 7 mm.

4.5 PROPERTIES OF CONCRETE

The concrete of all concrete members (supporting beams, ties and stanchions) were prepared using mix proportion of 1:1:2 (cement : sand : stone chips) and maximum aggregate size of 12 mm. The average cylinder strength was 36.5 MPa. The average modulus of rupture was 4.88 MPa. ASTM methods were

followed for these tests. The cylinders and prisms were tested simultaneously with the walls. The modulus of elasticity of concrete (28600 MPa) was obtained from standard equation and the Poisson's ratio was assumed to be 0.16.

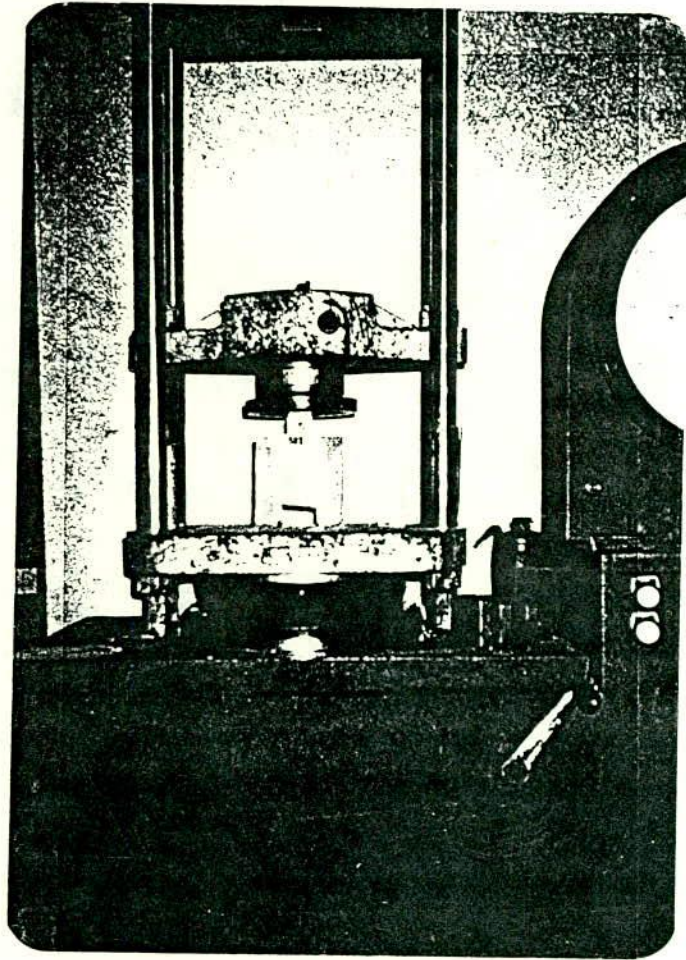

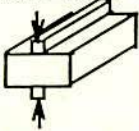
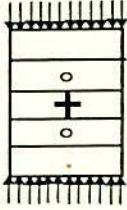
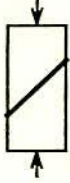
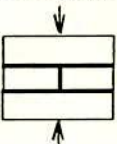



Fig. 4.13 Uniaxial Compression Test on Brick Masonry Triplet .

Table 4.5 Summary of Brick and Brick-Masonry Tests

Type of Tests	Material Property Evaluated	Section
Compression test on brick (load parallel to bed joint) 	Compressive Strength of Brick Parallel to Bed Joint. Deformation Characteristics of Brick. Initial Tangent Modulus of brick. Ultimate Strain and Secant Modulus of Brick at Ultimate Strength. Poisson's Ratio of Brick.	4.2.1 4.2.3 4.2.3 4.2.3 4.2.4
Split Tensile Test of Brick 	Tensile Strength of Brick from Indirect Test	4.2.2
Compression Test on Stack bonded brick Prism 	Deformation Characteristics and Compressive Strength of Masonry. In-situ Deformation Characteristics of Mortar Joint. In-situ Initial Modulus of Elasticity of Mortar Joint. Deformation Characteristics of Brick (Load normal to bed joint).	4.4.2 4.4.2 4.4.3 4.4.3 Appendix III
Shear Test on Brickwork Couplet 	Shear Deformation Characteristics of Mortar Joint	4.4.4
Splitting Test of Masonry Prism 	Tensile Bond Strength of Mortar Joint.	4.4.5
Compression Test on Triplet 	Shear Bond Strength of Mortar Joint	4.4.5

4.6 SUMMARY

Finite element model for masonry in which bricks and mortars are considered separately requires brick and mortar properties individually and preferably in in-situ condition along with the bond parameters between bricks and joints. Material properties for both materials have been described in this chapter. The masonry was constructed from solid fired clay bricks and a 1:4 mortar. The same quality bricks and mortar were used throughout the investigation. The following is a brief summary of the important characteristics of the materials.

Bricks:

1. The average compressive strength of bricks was 66.15 MPa, using the standard testing method. When the load was applied parallel to the bed joint, the mean compressive strength was found to be 40.2 MPa.
2. The compressive strength of brick determined by standard test overestimates the actual strength by approximately 1.65 times .
3. The burnt clay bricks under investigation exhibited linear behaviour approximately upto 80% of ultimate strength after which the non-linear behaviour was observed.
4. Some scatter was observed in all brick properties, with coefficients of variation up to 15%. This variability is predominantly caused by the manufacturing process, particularly due to forming and due to presence of local flaws.
5. The elastic moduli of the bricks varied with loading direction, although the degree of orthotropy was not excessive.
6. The Poisson's ratio of brick was fairly constant up to approximately 80% of the ultimate strength after which it gradually increased.
7. The tensile strength of brick was found to be 5% of the compressive strength determined by standard test.

Mortar:

1. Mortar exhibited non-linear stress-strain characteristics with a relatively large deformation capacity.
2. The Poisson's ratio of mortar was fairly constant up to approximately 65% of the ultimate strength after which it gradually increased.
3. The mean value of elastic modulus of mortar obtained from uniaxial test on mortar cylinder is 9590 MPa and from prism test 3270 MPa.

Masonry:

Since the finite element model developed in later chapters considers the bricks and mortar joints separately, the bulk of the masonry tests was aimed at either obtaining brick and mortar properties indirectly, or at establishing the basic bond parameters between bricks and joints. These involved compression tests on stack bonded prism, compression test on prisms with sloping bed joints, splitting tests on stretcher bonded prisms and compression tests on masonry triplets.

This chapter has described the derivation of deformation characteristics of mortar joints from stack bonded prisms and couplets with sloping bed joints. A method for the derivation of an approximate two-dimensional failure surface in terms of τ and σ_n from splitting and shear tests on brick masonry specimen has been described.

The use of these deformations and strength characteristics in the constitutive model of the finite element analysis will be described in the subsequent chapters.

CHAPTER 5

MATERIAL MODEL FOR NON-LINEAR FINITE ELEMENT ANALYSIS

5.1 INTRODUCTION

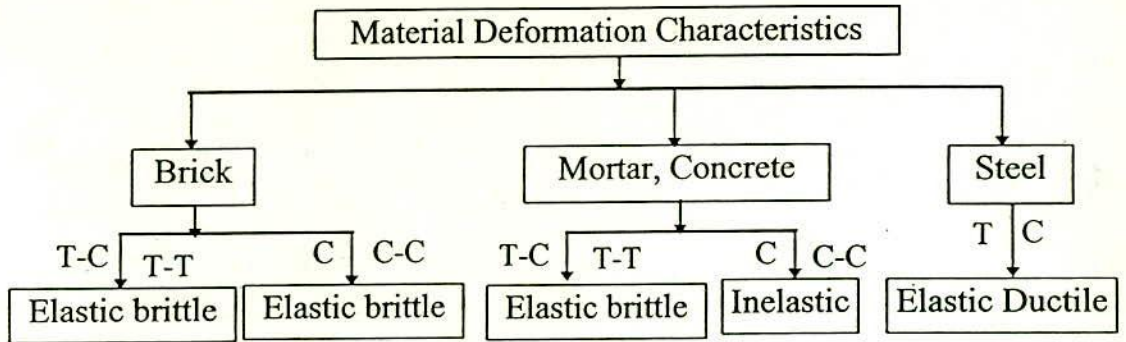
The non-linear behaviour of brick masonry is caused mainly by two major effects, cracking of the masonry and non-linear deformation characteristics of the masonry constituents, particularly in compression. For a finite element model to be representative of masonry behaviour, both of the effects must be included.

In this chapter, the material model for the masonry constituents is described. The constitutive relations adopted depend upon the stress state and any previous local failures of either brick or joint. A schematic summary of the range of possibilities shown in Fig. 5.1 is used to develop a suitable material model which allows both non-linear deformation characteristics and progressive cracking. Because of the complex nature of the behaviour of the two materials, bricks and joints are being considered separately, some simplifying assumptions are made. The finite element model incorporating these material characteristics is then described in chapter 6.

5.2 MATERIAL DEFORMATION CHARACTERISTICS

The brick, concrete, mortar and steel exhibit different deformation characteristics depending upon the stresses to which they are subjected. It is assumed that the materials exhibit elastic-brittle behaviour when a biaxial tension-tension or tension-compression stress state is present. When either of the materials are subjected to biaxial or uniaxial compression, non-linear characteristics are assumed in general.

Unlike concrete and mortar the fired clay bricks exhibit almost linear deformation characteristics as it is seen in chapter 4. Such elastic brittle behaviour of fired clay bricks are not necessarily homogeneous or isotropic. This is also observed by Page (1978) who for the first time considered brick masonry as a two phase material which typically consists of elastic brittle bricks set in inelastic mortar joints. The reinforcing steel is assumed as elastic



Note : T - T = Tension- Tension; C = Uniaxial Compression;
 T - C = Tension-Compression , C - C = Compression -
 Compression

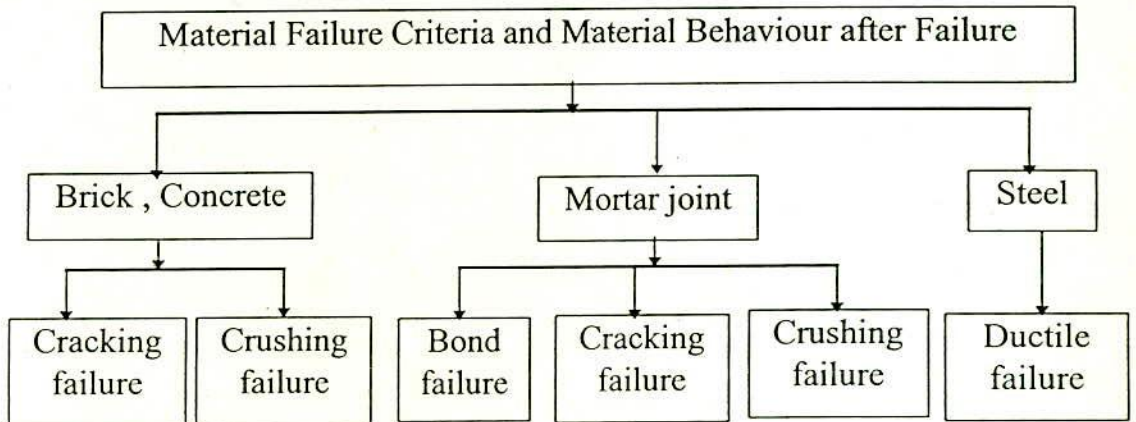


Fig. 5.1 Schematic Subdivision of Material Model

up to yield strength beyond which it is assumed as perfectly ductile material which corresponds to the elastic perfectly plastic idealisation of stress strain curve for steel, discussed in chapter 3 (see Fig. 3.9). The stress-strain curves for steel in tension and compression are assumed to be identical.

5.2.1 Constitutive Relations for Brick and Concrete Before Failure

Elastic-Brittle Behaviour

The concrete and fired clay brick subjected to biaxial tension-tension or tension-compression stress state is assumed to behave elastically up to failure. In this case, in the finite element model, the constitutive matrix $[D]$ is therefore kept

constant until the state of stress violates the failure criterion. Elastic modulus (E) of 28600 MPa and Poisson's ratio (ν) of 0.16 were adopted for the constitutive matrix for concrete, while the elastic modulus (E) of 17900 MPa and Poisson's ratio (ν) of 0.141 were adopted for the constitutive matrix for brick. The elastic properties of brick and concrete are determined experimentally in the laboratory and are explained in chapter 4. The behaviour of the materials after failure is described in section 5.5. It should be noted that the modulus of elasticity of brick in a direction normal to the bed joint was obtained indirectly from prism test (Table AII.3). Since the parameter cannot be obtained easily from conventional test it was decided not to use in the present model. However, it can be seen from chapter 3 that the variation of modulus of elasticity of brick does not affect significantly the vertical stress and shear stress at the interface of wall and beam.

Inelastic Behaviour

It is mentioned earlier that the brick is assumed to be an elastic brittle material for the entire range of loading. For concrete it is known that when a stress state of biaxial or uniaxial compression is present, the concrete exhibits non-linear deformation characteristics at higher stress levels. It has been shown in chapter 3 that the nature of stress experienced by the brickwork in the wall-beam when it is subjected to uniformly distributed vertical load on the top of the wall, is mainly one of the two forms: biaxial tension-compression and biaxial compression. Biaxial tension compression is encountered in the zone near the support while biaxial compression is experienced in a zone located at middle third of the panel at a level near the top of the wall. While the concrete in the supporting beam is mainly subjected to tension or biaxial tension-compression with only a small portion of the beam near the support being in a state of biaxial compression. In this case progressive cracking rather than inelastic material behaviour will be the main source of non linearity. The adoption of a simple non-linear stress-strain relationship for concrete, rather than an elaborate model using a conventional plasticity approach therefore seems justified. A simplified approach allows considerable saving of computer time with negligible loss of accuracy of the solution.

Such simple formulation of inelastic behaviour has been used by several previous investigators (Bathe and Ramaswamy, 1979 and Chen and Saleeb, 1982) in a number of finite element studies of reinforced concrete structures. In this approach the incremental constitutive model is formulated directly assuming

isotropic linear elastic behaviour using the instantaneous tangent modulus E_t in place of the elastic modulus E . Thus for the case of plane stress, the incremental stress-strain relations can be written as:

$$\begin{Bmatrix} d\sigma_x \\ d\sigma_y \\ d\tau_{xy} \end{Bmatrix} = \frac{E_t}{1-\nu^2} \begin{bmatrix} 1 & \nu & 0 \\ \nu & 1 & 0 \\ 0 & 0 & (1-\nu)/2 \end{bmatrix} \begin{Bmatrix} d\epsilon_x \\ d\epsilon_y \\ d\gamma_{xy} \end{Bmatrix} \quad (5.1)$$

In this equation, Poisson's ratio, ν is assumed constant and the non-linear stress-strain curve in compression is used to determine an appropriate value of E_t . The results of the compression tests on the concrete bricks made by Ali (1987) show that this approach is also appropriate for concrete.

The stiffness increase due to the contribution of the lateral compressive stress is not included with this simplified model. However, the error is known to be not great for this type of stress state (Chen and Saleeb, 1982). This error can be reduced by using biaxial or triaxial tests to determine the appropriate values of elastic moduli. However, the additional complexity of testing was not considered warranted in this case since inelastic behaviour in compression is only considered to be of secondary importance (this is confirmed in subsequent sensitivity analyses using the finite element model in chapter 8).

5.2.2 Constitutive Relations for Mortar Joint Before Failure

Elastic-Brittle Behaviour

Mortar joints, subjected to biaxial tension or tension-compression are also assumed to behave elastically up to failure. As before, the constitutive matrix is kept constant until the state of stress violates the failure criterion. An elastic modulus (E) of 3270 MPa and a Poisson's ratio (ν) of 0.202 was adopted for the constitutive matrix. These are the experimental values described in chapter 4. The behaviour after failure is described in section 5.5.

Inelastic Behaviour

When a stress state of biaxial or uniaxial compression is present, mortar exhibits non-linear deformation characteristics at higher stress levels. For simplicity a relatively simple non-linear stress-strain relationship has been adopted

similar to that used by Dhanasekar et al. (1985), allowing significant reductions in computing time. The simplified approach developed by Dhanasekar et al. (1985) was derived from a series of biaxial tests on brick masonry panels, and the relationships found to be sufficiently representative. In this approach the plastic strain components in each direction are assumed to be independent, and are treated separately. Thus the incremental strain-stress relations in the case of plane stress has been written (Dhanasekar et al. (1985)) as :

$$\begin{Bmatrix} d\varepsilon_p \\ d\varepsilon_n \\ d\gamma \end{Bmatrix} = \begin{bmatrix} 1/E + 1/H_p \cdot & -\nu/E & 0 \\ -\nu/E & 1/E + 1/H_n \cdot & 0 \\ 0 & 0 & 1/G + 1/H_s \cdot \end{bmatrix} \begin{Bmatrix} d\sigma_p \\ d\sigma_n \\ d\tau \end{Bmatrix} \quad (5.2)$$

in which $G = E/(2(1+\nu))$ is the shear modulus and $H_p \cdot$, $H_n \cdot$ and $H_s \cdot$ are the instantaneous slopes of the stress-plastic strain curves. The slopes may either be expressed as a function of the stresses or of the plastic strains. In the study by Dhanasekar, it was found that this technique more effectively reproduced inelastic behaviour than conventional plasticity theory (using yield criteria and a flow rule). This latter approach underestimated the actual shear strains and overestimated the normal and parallel strains. The stress-plastic strain relations for this investigation have been determined from the mortar stress-strain curves derived from the uniaxial compression tests on brick masonry prisms described in chapter 4 (see Fig. 4.9 and Fig. 4.11). The deformation characteristics in the normal and parallel directions have been assumed to be similar. Poisson's ratio is assumed to be constant and equal to 0.202. The values of the slopes of the curves expressed in terms of stresses are:

$$\begin{aligned} H_p \cdot &= \frac{d\sigma_p}{d\varepsilon_p^p} = 14029 e^{-0.27\sigma_p} \text{ MPa} \\ H_n \cdot &= \frac{d\sigma_n}{d\varepsilon_n^p} = 14029 e^{-0.27\sigma_n} \text{ MPa} \\ H_s \cdot &= \frac{d\tau}{d\gamma^p} = 14592 e^{-0.845\tau} \text{ MPa} \end{aligned} \quad (5.3)$$

The simplified method used to model the inelastic mortar deformation in compression is considered justified not only because of the savings in computer time, but also because the bulk of the non-linear behaviour of the wall is caused by progressive local failure rather than material nonlinearity. This latter assumption has

been confirmed by sensitivity analyses performed on the finite element model and are described in detail in chapter 8.

In the finite element model stress-strain relations instead of the strain-stress relations given in equation (5.2) are used. The stress-strain matrix in the non-linear range is given below. Note that terms in order of $(\nu/E)^2$ have been neglected.

$$\begin{Bmatrix} d\sigma_p \\ d\sigma_n \\ d\tau \end{Bmatrix} = \begin{bmatrix} \frac{EH_p \cdot}{(E + H_p \cdot)} & \frac{EH_p \cdot H_n \cdot \nu}{(E + H_p \cdot)(E + H_n \cdot)} & 0 \\ 0 & \frac{EH_n \cdot}{(E + H_n \cdot)} & 0 \\ 0 & 0 & \frac{GH_s \cdot}{(G + H_s \cdot)} \end{bmatrix} \begin{Bmatrix} d\epsilon_p \\ d\epsilon_n \\ d\gamma \end{Bmatrix} \quad (5.4)$$

This inelastic constitutive matrix is used to calculate the element stiffness matrix before failure.

5.3 NON-LINEARITY DUE TO PROGRESSIVE CRACKING

The tensile weakness of masonry and the cracking that results therefrom, is the most significant factor contributing to the non-linear behaviour of masonry structures. The failure of wall-beam subjected to in-plane vertical uniformly distributed load is characterised by the development of vertical cracks that start from vertical joints in the region near the support and then propagates through the bed joints and the bricks. In most of the cases these cracks in vertical joints are followed by flexural cracks in the supporting beam near the support which occur at higher loads.

5.3.1 Crack Modelling

In recent years a number of different models have been developed in conjunction with finite element analyses to represent cracking of reinforced concrete members. In this section the model, particularly suitable for use in the finite element analysis of the in-plane behaviour of wall-beam structures, will be discussed.

The particular cracking model to be selected from the various alternatives depends upon the purpose of the finite element study, the nature of the output desired from the study and available computing facilities. A cracking model must have three components: a definition of crack initiation, a method of crack representation and a criterion for crack propagation.

Crack Initiation

Two criteria for crack initiation are commonly used, one based on the state of stress (stress criteria), the other on the state of strain (strain criteria). Most of the existing fracture (or failure) criteria for concrete and similar materials are expressed in terms of stresses, which may not be adequate for many cases especially if the compressive stress is very high. Owing to lack of sufficient available test data, the strain criteria required for the fracture of concrete under compression are usually developed by simply converting the failure criteria in terms of stresses directly into strains. A general strain criterion for the fracture of concrete and similar materials has still not been completely developed. Therefore, for this study the failure criteria for cracking type of failure are expressed in terms of stresses.

Crack Representation

Once cracking has occurred, it can be simulated using one of two techniques, either 'smearing' the effects of the crack over all or part of the relevant element (smeared crack modelling), or by making appropriate adjustments to the element topology by separation of the appropriate nodes (discrete crack modelling). The smeared crack model used in this study has been discussed in more detail later in this section.

Crack Propagation

After modelling the crack, its propagation will depend upon the state of stress in the region ahead of the crack. Two methods can be used to predict potential crack growth. The first uses a criterion based on the inherent strength of the material and the local state of stress. The second uses a criterion based on the fracture toughness of the material.

Any combination of the above criteria for crack initiation, crack representation and crack propagation can be used. The use of a strain criterion for crack propagation was not possible for this investigation due to the lack of experimental data. Two different models can be developed using combinations of the other criteria. These models are summarised in Fig. 5.2. Model # 1 uses stress criteria for crack initiation in conjunction with smeared crack modelling and material strength criteria for crack propagation. Model # 2 is similar except the discrete crack modelling technique is used to simulate progressive cracking. The effectiveness of the two models is discussed and compared by Ali (1987). It is seen in his study that both Model #1 and Model #2 predicted approximately similar types of failure patterns in masonry wall. In this study smeared crack modelling (Model #1) has been adopted due to its simplicity, flexibility and less computational time required for implementation. Therefore, in the following sections only this particular crack modelling will be described.

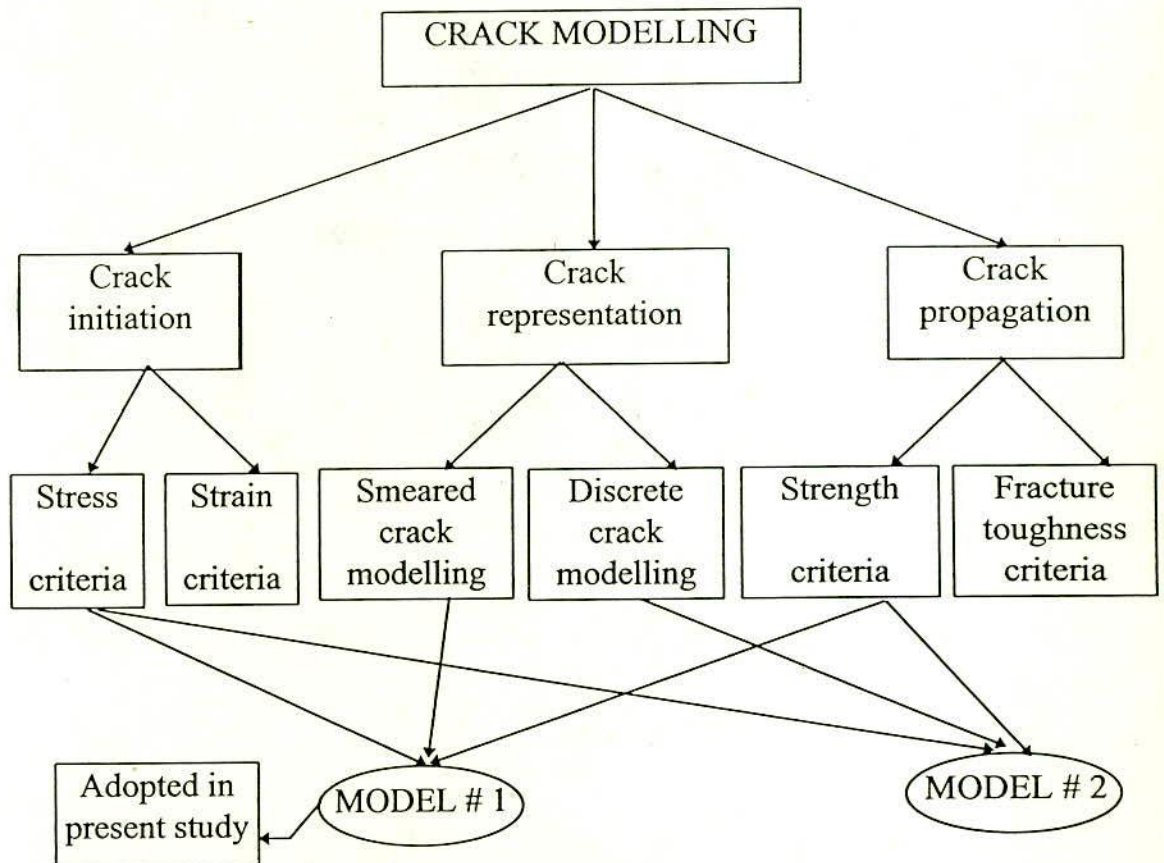


Fig. 5.2 Combination of the Criteria for Crack Initiation, Representation and Propagation

Smeared Crack Modelling

The need for a cracking model which allows for the automatic generation of cracks without the need for a redefinition of the finite element topology, as well as the ability to model cracking in any direction, has led to a vast majority of investigators adopting the 'smeared' crack modelling approach. This approach can also allow for strain softening of the material after cracking. In the smeared cracking approach, the cracked material is assumed to remain as a continuum. Rather than representing a single discrete crack, the crack is represented as an infinite number of parallel fissures across the cracked element (see Fig. 5.3). Once cracking has occurred, the cracked material is assumed to be orthotropic with one of the principal directions being along the direction of cracking.

For use of this technique in the finite element model, the appropriate modifications must be made to the material characteristics. Before cracking, the material is either linear elastic isotropic or non-linear elastic-plastic with the corresponding constitutive relations described in section 5.2.1 and 5.2.2. However, the onset of cracking induces orthotropic material properties and a new incremental constitutive relationship must be derived. This is accomplished by modifying the material constitutive matrix $[D]$. For the case of plane stress the incremental stress-strain relations become:

$$\begin{Bmatrix} d\sigma_x \\ d\sigma_y \\ d\tau_{xy} \end{Bmatrix} = [D_f] \begin{Bmatrix} d\varepsilon_x \\ d\varepsilon_y \\ d\gamma_{xy} \end{Bmatrix} \quad (5.5)$$

Where $[D_f]$ is the modified material constitutive matrix after failure.

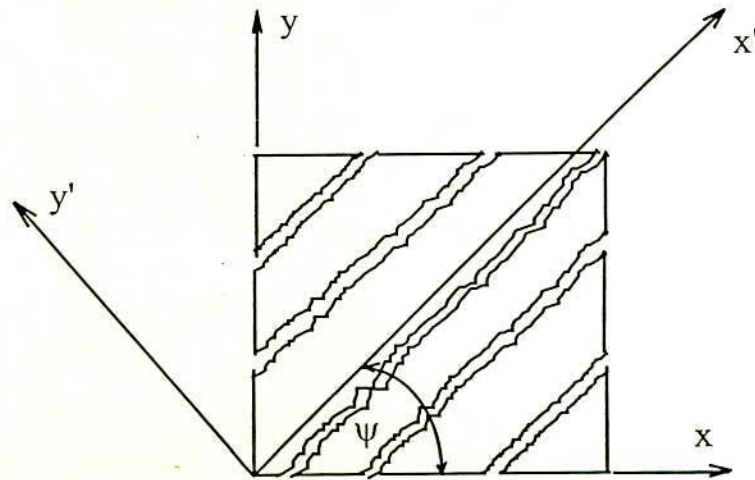


Fig. 5.3 Idealisation of a Single Crack in Smeared Crack Modelling

For stiffness calculations, it is necessary to transform the material stiffness matrix $[D_r]$ into the global co-ordinate system (X-Y).

That is:

$$[D] = [T]^T [D_r] [T] \quad (5.6)$$

where $[T]$ is a transformation matrix relating global directions to crack directions and is given by

$$[T] = \begin{bmatrix} \cos^2 \psi & \sin^2 \psi & \cos \psi \sin \psi \\ \sin^2 \psi & \cos^2 \psi & -\cos \psi \sin \psi \\ -\sin 2\psi & \sin 2\psi & \cos^2 \psi - \sin^2 \psi \end{bmatrix} \quad (5.7)$$

where ψ is the angle of cracking.

5.4 FAILURE CRITERIA

Predictions of wall-beam behaviour subjected to in-plane loading must include consideration of the state of stress in the constituent materials as well as the orientation of the jointing planes to the stresses. In general, local failures can be separated into three types:

1. Bond failure at the interface of the brick and mortar. This can occur when the stress normal to the joint is tensile. The value of the normal stress (σ_n) therefore becomes the critical parameter.
2. Tensile cracking of constituent materials (brick, mortar and concrete): This occurs when the stress state within the material is one of biaxial tension or tension-compression. For this type of failure, the principal tensile stress (σ_1) is assumed to be the critical parameter.
3. Crushing of constituent materials (brick, mortar and concrete): This type of failure occurs under compressive stresses (either uniaxial or biaxial compression). Crushing failures of the beam end may occur in wall-beams subjected to uniformly distributed loads, since the bulk of the material near the support is in highly compressive-stress state in vertical direction. The concrete of the beam at the support may also experience crushing failure due to lower bearing area.
4. In this study the reinforcement in the supporting beam is idealised as an elastic perfectly plastic material. The principal tensile stress is assumed to be the critical parameter when it exceeds the yield stress of the reinforcement.

The different types of failures for the constituent materials of the wall-beams and the corresponding controlling stresses assumed for this study are shown in the Fig. 5.4 .

Since the bricks and joints are being modelled separately series of failure criteria are required. These criteria, which cover possible joint bond failure and cracking or crushing of constituent materials are discussed in the ensuing sections.

5.4.1 Joint Bond Failure

The possibility of bond failure for each joint is checked when the jointing plane is subjected to shear stress and normal tensile stress. This is the case for most of the vertical joints in the masonry in the region near the support (as revealed by the elastic analyses described in chapter 3).

The possibility of a shear bond failure in the presence of normal compressive stress has not been included. For the problems being considered, this type of stress rarely arises in the vertical joints, so that the simplification was considered justified. When the normal stress is compressive, the joint is checked for possible cracking or crushing of the mortar itself (see Fig 5.4).

Failure surface used in checking for bond failure in presence of shear stress and normal tensile stresses was derived from the tests described in chapter 4 (section 4.4.5). The surface is a function of the shear stress (τ) and normal stress (σ_n) on the joint, and ignores the contribution of the parallel stress (σ_p). This surface has been incorporated into the finite element model. However, for the model is to be general and capable of modelling stepped failure (involving tensile failure in the vertical joint and sliding in the bed joints) the failure mode of joint shear/sliding should be included in the model.

5.4.2 Cracking and Crushing of Brick, Mortar and Concrete

Since both bricks and mortar joints when subjected to tensile or tension-compression stress state behave as brittle materials, similar in properties to concrete, conventional concrete failure criteria have been adapted to model the failure of the masonry materials .

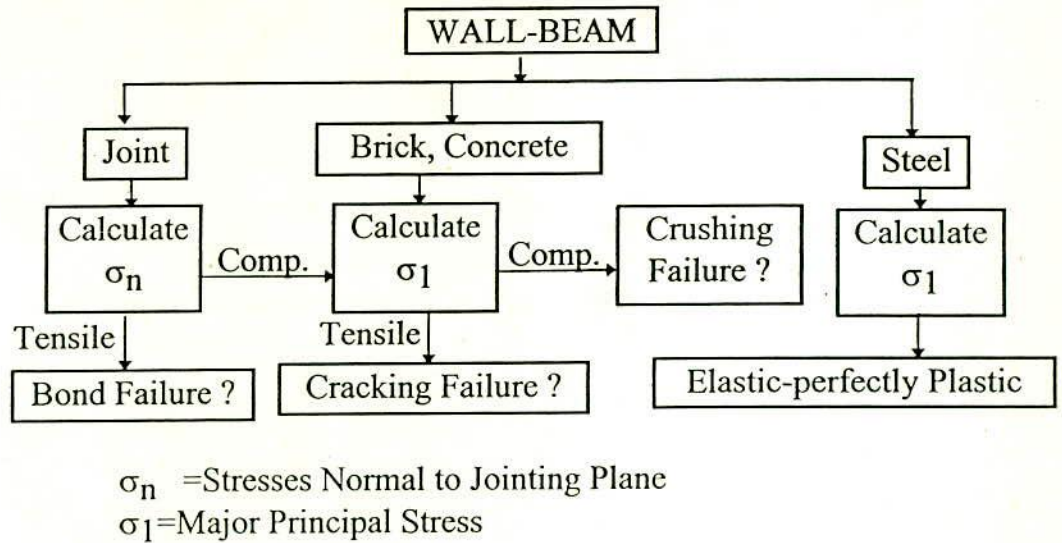


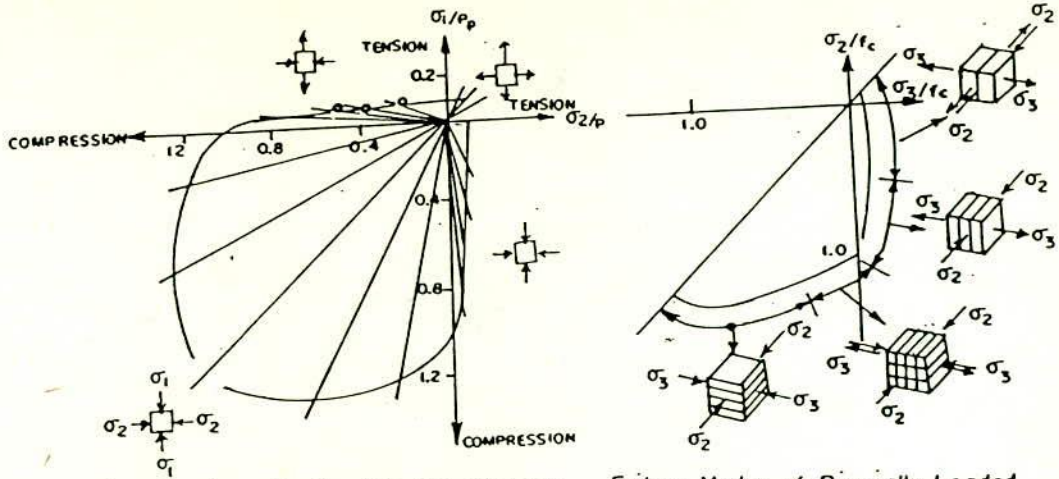
Fig. 5.4 Selection of Failure Criteria from the Corresponding Controlling Stress

In the past, extensive research has been carried out on the failure of concrete under multiaxial stress states. The most commonly used failure criteria are defined in stress space by a series of material constants, with the number of constants depending upon the sophistication of the model. Some of the failure criteria used for concrete subjected to biaxial stress in recent years (Kupfer et al. 1969; Nelissen, 1972; Argyris et al, 1976; Buyukozturk, 1977; Duncan and Johnarry, 1979 and Chen and Saleeb, 1982) are summarised in Fig. 5.5.

To predict failure of brick or mortar under a state of biaxial tension-tension or tension-compression, the failure surface shown in Fig. 5.6(a) has been adopted. For comparative purposes a typical surface for concrete (Chen and Saleeb, 1982) is also shown. The parameters for the Strength characteristics (f'_c and f'_t) were obtained from the uniaxial compression and splitting tests on brick and mortar specimens described in sections 4.2 and 4.3.

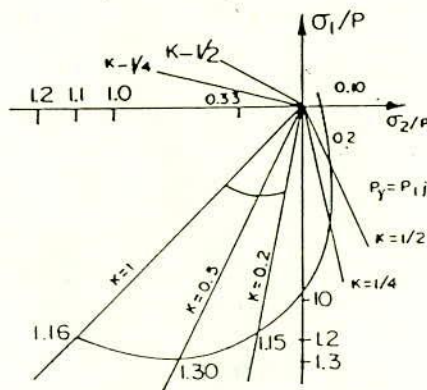
To predict a crushing type of failure for brick or mortar under a state of biaxial compression the Von Mises failure surface has been used (expressed in terms of strain). The crushing surface is shown in Fig. 5.6(b) and can be defined as follows:

$$C(\varepsilon) = \sqrt{\varepsilon_1^2 - \varepsilon_1\varepsilon_2 + \varepsilon_2^2} - \varepsilon_{cu} = 0 \quad (5.8)$$

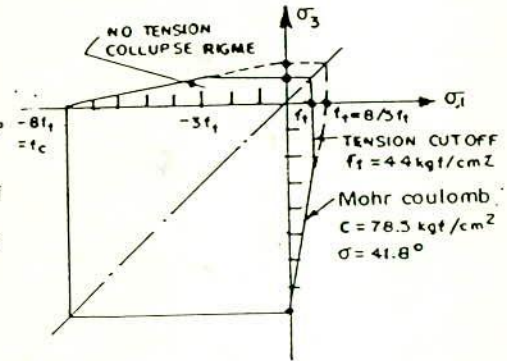


Typical Envelope for the Biaxial Strength of Concrete (Kupfer et al, 1969)

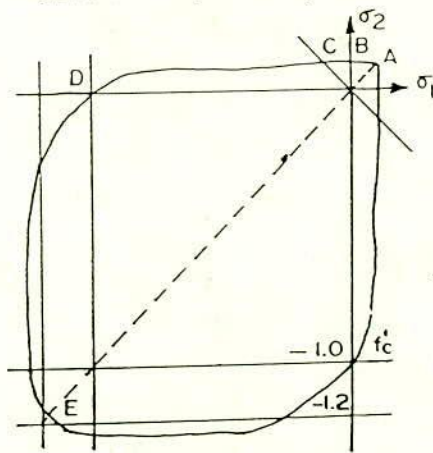
Failure Modes of Biaxially Loaded Concrete (Nellisen, 1972)



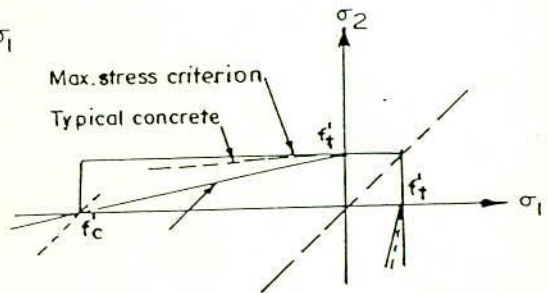
Analytical Failure Envelopes for Concrete (Buyukozturk, 1977)



Biaxial Failure Model of Concrete (Mohr-Coulomb Condition with Tension cutoff) (Argyris et al, 1976)



Biaxial Strength of Concrete (Duncan and Johnarry, 1979)



Biaxial Failure Criteria in Tensile Zones (Chen and Saleeb, 1982)

Fig. 5.5 Biaxial Failure Surface for Concrete

in which ϵ_1 and ϵ_2 are the principal strains and ϵ_{cu} is the ultimate strain determined from the uniaxial compression tests described in chapter 4. (sections 4.2.3 and 4.3.1).

Although the use of this surface may be conservative in many cases its use was considered justified, since a local crushing type of failure in wall-beam subjected to uniformly distributed vertical loads is confined in very small area. When local crushing does occur, its influence on the overall behaviour of the panel is small compared to the effects of tensile cracking.

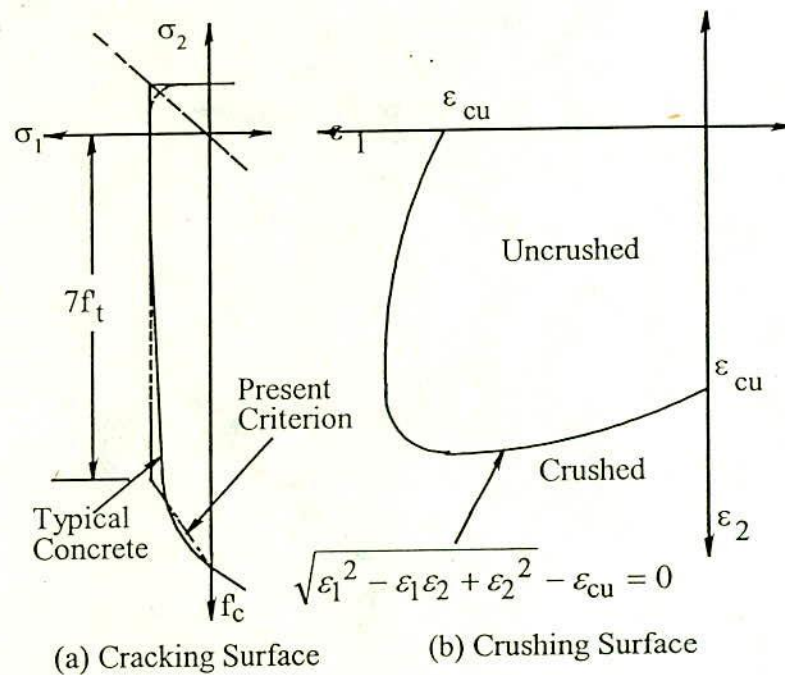


Fig. 5.6 Typical Biaxial Failure Surface for Concrete, Brick and Mortar

5.5 BEHAVIOUR OF THE MATERIALS AFTER FAILURE

Once local failure has occurred in one of the modes previously described, appropriate modifications must be made to the assumed stress-strain characteristics. In addition, consideration must be given to the manner in which the local stresses in the failure regions are redistributed.

5.5.1 Stress-Strain Relations After Failure

The schematic fracture model shown in Fig. 5.7 can be used to derive the incremental stress-strain relationships for the materials after failure. The slope of line 0-1 represents the material stiffness before failure. The slope of line 2-3 represents the material stiffness after failure upon the application of a further increment of loading. The stresses to be released are denoted by the stress vector (σ_0) (line 1-2 in Fig. 5.7). The stresses can be released suddenly or gradually depending on the type of collapse model used. This is discussed in detail in section 5.5.2. The incremental stress-strain relationship after failure can be represented by the relationship:

$$\{d\sigma\} = [D_f] \{d\varepsilon\} \quad (5.9)$$

where, $[D_f]$ = material constitutive matrix after failure.

The form of this matrix will depend on the mode of failure as discussed in the ensuing sections. The net stress change $\{\Delta\sigma\}$ in the material after failure during the fracturing process can be written as:

$$\{\Delta\sigma\} = \{d\sigma\} - \{\sigma_0\} = [D_f] \{d\varepsilon\} - \{\sigma_0\} \quad (5.10)$$

where $\{\sigma_0\}$ = the released stress vector

Joint Bond Failure

Bond failure occurs at the interface of the brick and the mortar. In this study it is assumed that this type of failure only occurs when the normal stress (σ_n) in the joint is tensile. When bond failure occurs, the normal stress perpendicular to the crack and the shear stress along the cracked plane are released. The stiffness of the mortar joint is also modified to simulate cracking

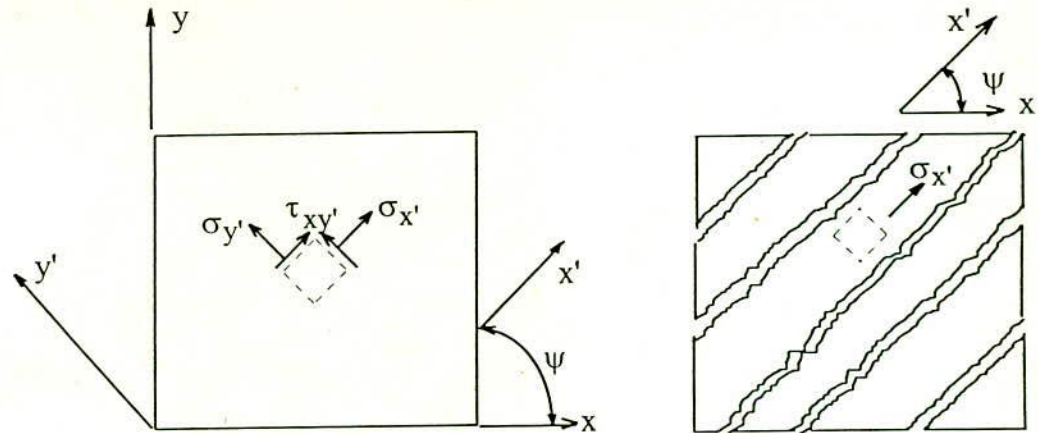


Fig. 5.8 Pattern of Cracks and Stress Distribution in a Cracked Material

Crushing of Brick, Mortar and Concrete

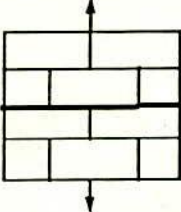
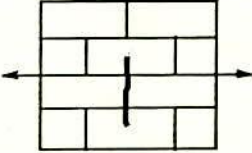
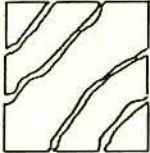
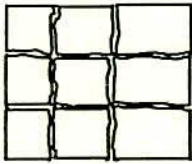
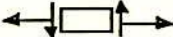
As has been previously described, a crushing type of failure can occur in regions where the stress state is one of uniaxial or biaxial compression. In this case all local stresses are released completely and the material is assumed to lose all its capacity to transmit further loads. To simulate this behaviour all the terms of the material constitutive matrix $[D]$ are reduced to approximately zero (see Table 5.1).

5.5.2 Redistribution of Stresses in the failure Regions.

When local failure occurs by cracking, the rate of crack propagation depends upon the manner in which the stresses in the cracked region are allowed to redistribute. The assumptions on the rate of stress redistribution can vary between immediate dissipation of stresses (a brittle collapse model), to no dissipation of stresses (a ductile model). There is a range of other possibilities between these two limits (intermediate or 'softening' models). These assumptions are shown schematically in Fig. 5.9.

Previous work (Argyris et al., 1976) has shown that an intermediate type of collapse model is appropriate for concrete structures. It seems logical therefore to adopt a similar model for cracking in masonry part of wall-beam structure. The use of these different models in conjunction with the finite element analysis is described in detail in section 7.5.

Table 5.1
 [D_f] Matrices for Different Modes of Failure of Wall-beam Components

No	Mode of Failure	[D _f]	Failure Code
1	Tension Bond Failure Normal to Bed Joint 	$\begin{bmatrix} E & 0 & 0 \\ 0 & \phi E & 0 \\ 0 & 0 & \beta' G \end{bmatrix}$	11
2	Tension Bond Failure Parallel to Bed Joint 	$\begin{bmatrix} \phi E & 0 & 0 \\ 0 & E & 0 \\ 0 & 0 & \beta' G \end{bmatrix}$	11
3	Cracking Failure 	$\begin{bmatrix} E & 0 & 0 \\ 0 & 0 & 0 \\ 0 & 0 & \beta' G \end{bmatrix}$	11 (Brick, Concrete) 33 (Mortar)
4	Crushing Failure 	$\begin{bmatrix} \phi E & 0 & 0 \\ 0 & \phi E & 0 \\ 0 & 0 & \phi G \end{bmatrix}$	22
5	Tensile Failure of Steel 	$\begin{bmatrix} \phi E & 0 & 0 \\ 0 & E & 0 \\ 0 & 0 & \beta' G \end{bmatrix}$	11

$$\phi = 10^{-3} \text{ and } \beta' = 0.10 \text{ (Aggregate interlock factor)}$$

5.5.3 Further Cracking or Crushing of the Cracked Material

After the formation of initial cracks, the structural element can often deform further without overall collapse. Thus the possibility of a crack closing and opening and the formation of further cracks can arise. Some possible cracking sequences that a material could experience during its loading history are illustrated in Fig. 5.10. There is obviously a need for a representative material model to include this type of post-failure behaviour.

Formation of Secondary Cracks

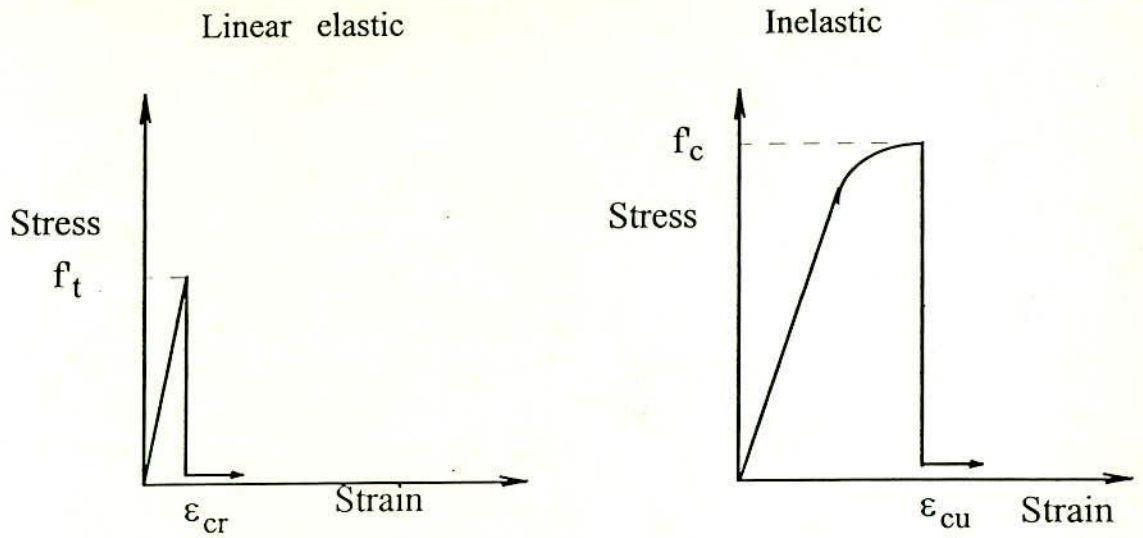
For a cracked material, the stress state reduces to a uniaxial one parallel to the direction of cracking. If upon further loading, the stresses in this direction violate the appropriate failure criterion (cracking or crushing), additional failure is assumed to occur with the appropriate modifications being made to the $[D_r]$ matrix. This means that either cracking or secondary cracks will occur perpendicular to the direction of primary cracks (see Fig. 5.10).

Opening and Closing of the Cracks

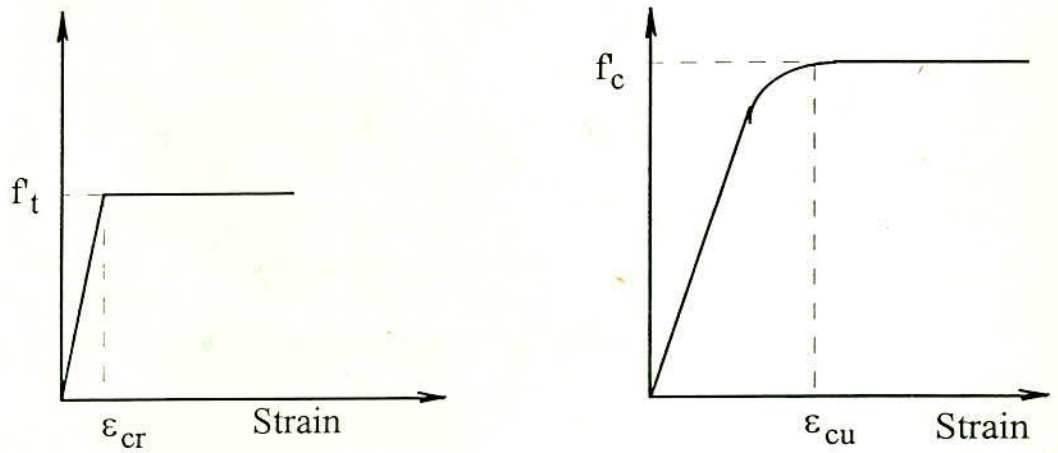
If the normal tensile strain across the existing cracks remains constant or continues to increase the crack is assumed to remain open. If the strain reduces and becomes compressive, the crack is assumed to have closed, and the appropriate terms of the $[D_r]$ matrix are modified back to their original values (see Fig. 5.10).

Formation of a New Set of Cracks:

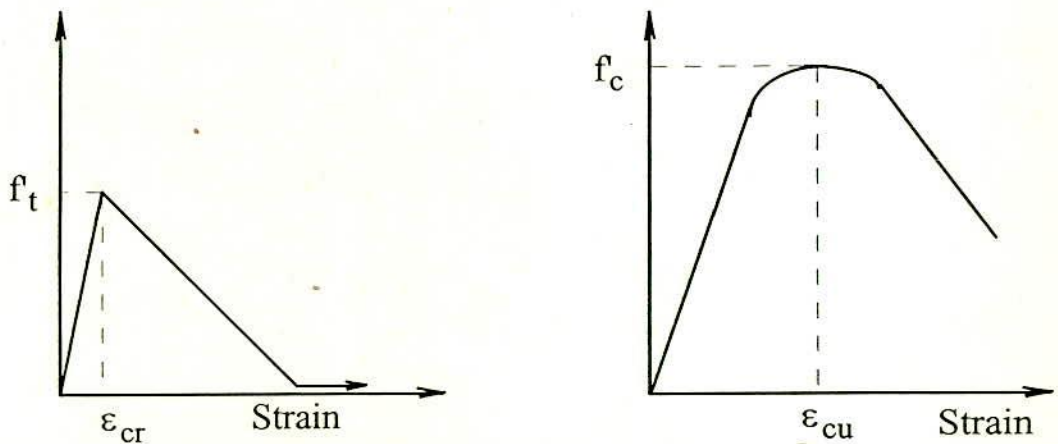
If all cracks in the cracked material become closed it is assumed that the uncracked material is linearly elastic. For such a material, the original failure criteria for crushing or cracking can again be applied in ensuing load increments.



(a) Brittle Collapse Model

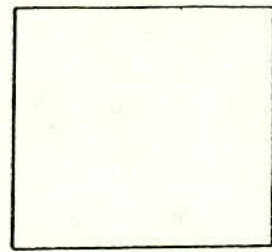


(b) Ductile Model

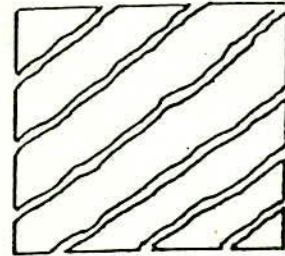
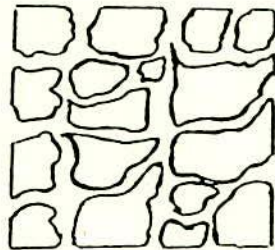


(c) Intermediate Collapse Model

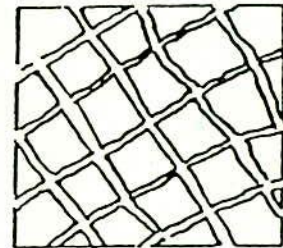
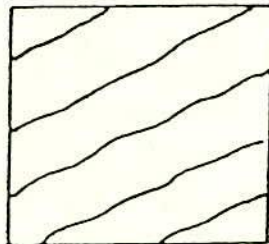
Fig. 5.9 Stress-strain Relations of wall-beam Components After Failure



Uncracked

First Primary
Cracks Formed

Crushed

Primary Cracks Open
Secondary Cracks Formed

All Cracks Closed

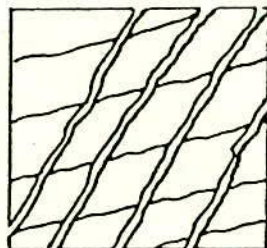
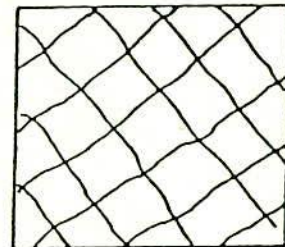
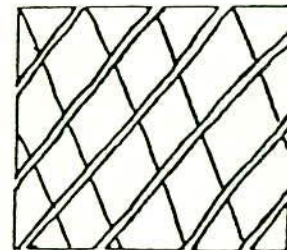
First Set of Cracks Closed
Second Primary Cracks Formed

Fig. 5.10 Opening and Closing of Existing Cracks and Formation of New Cracks in a Cracked Material

5.6 SUMMARY

The non-linear response of wall-beam structure is caused by two major effects, progressive cracking and non-linear deformation characteristics of the component materials. Of these two effects, progressive cracking is the major source of non-linearity.

This chapter has described the techniques used for the mathematical modelling of the in-plane behaviour of wall-beam structure in both of its uncracked and cracked states. The constitutive relations for brick, concrete, mortar and steel before and after failure have been described. Failure criteria for joint bond failure, tensile and compressive failure of constituent materials have been presented, as well as appropriate techniques for crack modelling. Considerations have been given to the manner in which the local stresses in the failure regions are redistributed. The possibility of crack closing and opening and the formation of secondary cracks have also been considered. The incorporation of these material characteristics into the appropriate finite element model is described in chapter 6.

CHAPTER 6

NON-LINEAR FINITE ELEMENT PROGRAMS

6.1 INTRODUCTION

Failure models, corresponding failure criteria and constitutive models for wall-beam components have been described in the previous chapters. The incorporation of the material model into appropriate finite element program is described in this chapter.

The program is incremental in nature, allowing material non linearity and progressive cracking to be simulated as the applied load is increased. Final failure is indicated by either excessive cracking or lack of convergence of the solution. The program used the smeared crack modelling technique.

6.2 FINITE ELEMENT SELECTION

The selection of the element type for this study was based on the following three criteria:

1. Efficiency in the formation of element stiffness matrix (in terms of computing time).
2. The accuracy of the assumed displacement interpolation in reproducing the true stress distribution.
3. The adaptability of the element geometry to brick masonry.

Although in recent years the trend is towards the use of higher order elements it has been shown by Ali (1987) that the use of higher order elements is not warranted for the analysis of masonry structures where the non-linearity is mainly due to the progressive cracking and not material characteristics, provided a relatively fine mesh is adopted. This agrees with the findings of Bazant and Cedolin (1980) in the fracture analysis of reinforced concrete.

In view of the above findings, linear four noded elements were used throughout this investigation to model the constituent materials. Rectangular element was chosen as it was most suited to the geometric nature of the bricks and joints which constitute the major part of the wall-beam structure. To achieve

accuracy of solution a fine mesh was used in regions of high stress gradients. The element and mesh are shown in Fig. 6.1.

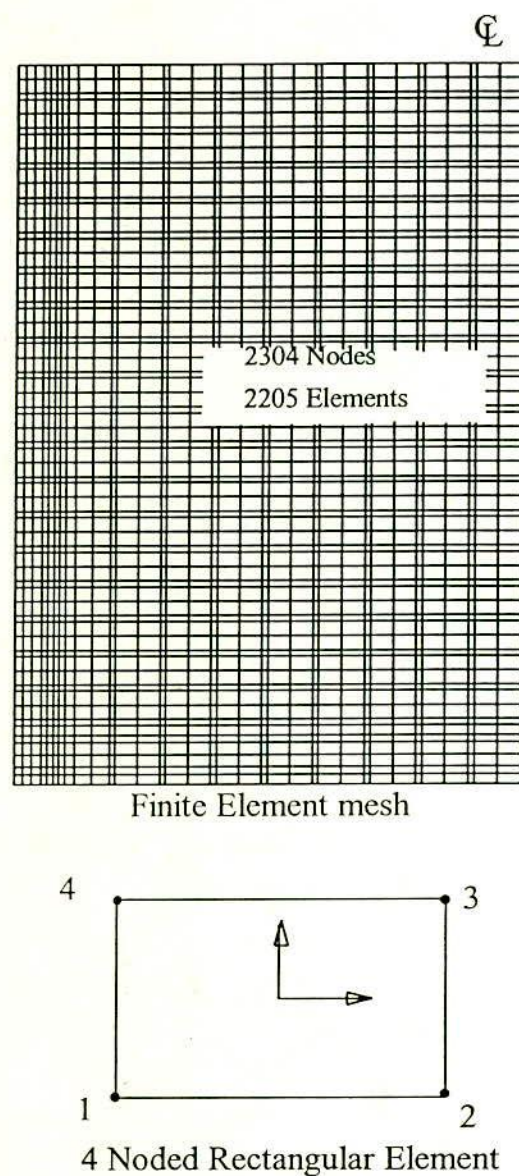


Fig. 6.1 Typical Finite Element Mesh with 4 Noded Rectangular Elements

6.3 NON-LINEAR ANALYSIS

There are two major non-linearities usually encountered in structural analysis namely material and geometric non-linearities. Since this investigation is confined to small deflection, geometric non-linearity is not considered and only procedures related to material non-linearities are described.

6.3.1 Solution Techniques

Solution procedures for non-linear problems have been discussed by several authors (Ortega and Rheinboldt, 1970; Bergan and Soreide, 1973; Gallagher, 1973; and Bergan and Holand, 1979). In contrast to linear problems it is not possible to develop a single general method of solution. Several of the existing solution procedures are either limited to certain classes of non-linear problems or particular requirements must be satisfied in order to ensure convergence to the correct solution. The computer program adapted in this study utilises several solution algorithms for the non-linear wall-beam structures. Such a scheme provides increased flexibility and offers the experienced user the possibility of obtaining improved reliability and efficiency for the solution of a particular problem.

There are three basic solution techniques to account for non-linearities, namely incremental, iterative and combined methods (incremental - iterative).

The Incremental Method

In the incremental method of solution, the external load is applied as a sequence of sufficiently small load increments so that the structure can be assumed to respond linearly within each increment. For the 'N' loading step this may be written in matrix notation as:

$$K_{N-1} \Delta d_N = \Delta P_n \quad (6.1)$$

from which incremental displacements Δd_N are found. Here,

$$\Delta P_N = P_N - P_{N-1} \quad (6.2)$$

The incremental stiffness K_{N-1} is normally based on the displacement state d_{N-1} . The displacements at the new load level are

$$d_N = d_{N-1} + \Delta d_N \quad (6.3)$$

The procedure is shown in Fig. 6.2(a)

Due to the ease with which the pure incremental method can be applied, it is still popular for problems with moderate non-linearity. However, this procedure

has a serious disadvantage in that no estimate of the drift of the solution from the equilibrium path is generally available. More efficient incremental schemes can be obtained by combining the pure incremental method with a single equilibrium correction. Formally this procedure may be written as:

$$K_{N-1} \Delta d_N = \Delta P_N + (P_{\text{ext}N-1} - P_{\text{int}N-1}) \quad (6.4)$$

where the parentheses contain the discrepancy between external loads and internal forces at the beginning of load step number N.

The iterative Method

In the iterative method, the structure is fully loaded for each iteration and an approximate constant value of stiffness is used for the solution. The iterations are continued until equilibrium is satisfied. The disadvantage of the method is that it only gives a solution for a given load level. The procedure is shown in Fig. 6.2(b).

Combined Method (Incremental Iterative Method)

To ensure that the solution satisfies equilibrium throughout the loading, the incremental method can be combined with equilibrium iterations at each level of loading. This is known as the Incremental -Iterative method and is shown in Fig. 6.2(c). For iteration cycle i at load level N the process may be written as :

$$K_{N,i-1} \Delta d_{N,i} = \Delta P_{N,i} \quad (6.5)$$

where,

$$\Delta P_{N,i} = P_{\text{ext}N} - P_{\text{int}N,i-1} \quad (6.6)$$

yielding an improved solution vector

$$d_{N,i} = d_{N,i-1} + \Delta d_{N,i} \quad (6.7)$$

The incremental -iterative procedure has been used in this investigation to account for non-linearity caused by both material deformation and progressive cracking.

6.3.2 Solution Method for the Incremental-Iterative Procedure

The incremental-iterative procedure usually uses one of three methods, namely: Newton-Raphson, Modified Newton-Raphson and the Initial stiffness method. These methods are shown in Fig. 6.3. Each of these methods has advantages and disadvantages with regard to convergence and computing time.

In the current investigation, a combination of the initial stiffness method and the modified Newton-Raphson method have been used. For the early stage of the analysis, before any local failures occur, the initial stiffness method proposed by Zienkiewicz et al. (1969) was found to be the most effective in reproducing material non-linearities (see Fig. 6.3(a)). This approach used the initial stiffness matrix for all iterations and adjusts for non-linearity by applying a series of additional corrective forces for each successive iteration.

However, once local failure occurs in the masonry constituents, convergence becomes very slow using the above method. Hence after the initiation of the first crack the solution procedure is changed to the Modified Newton-Raphson method (see Fig. 6.3(b)). Using this method the stiffness matrix $[K]$ is updated at the first iteration for each load increment.

6.3.3 Constitutive Equation for the Incremental-Iterative Solution Procedure

As the finite element program utilises an incremental loading procedure for solving the non-linear equations an incremental form of the constitutive relations is therefore needed. These incremental stress-strain relations must include the effects of non-linear material characteristics as well as the possible failure of the masonry components (Bond failure or a cracking or crushing type of failure): They can be expressed in matrix form as:

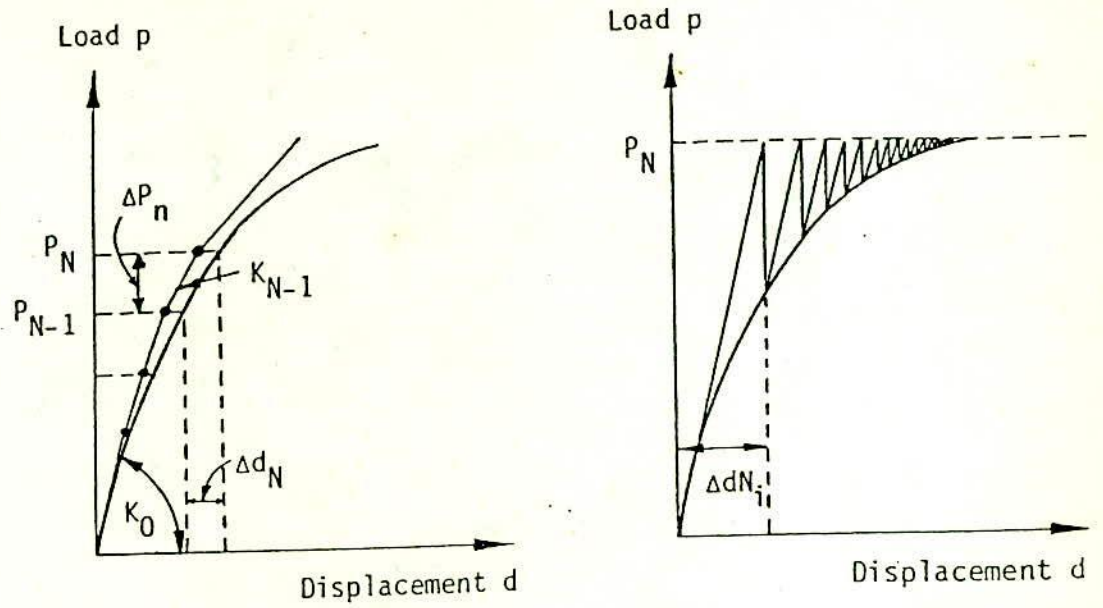
$$\{\Delta\sigma\} = [D_r] \{\Delta\varepsilon\} - \{\sigma_0\} \quad (6.8)$$

in which

$\{\Delta\sigma\}$ = Stress increment vector

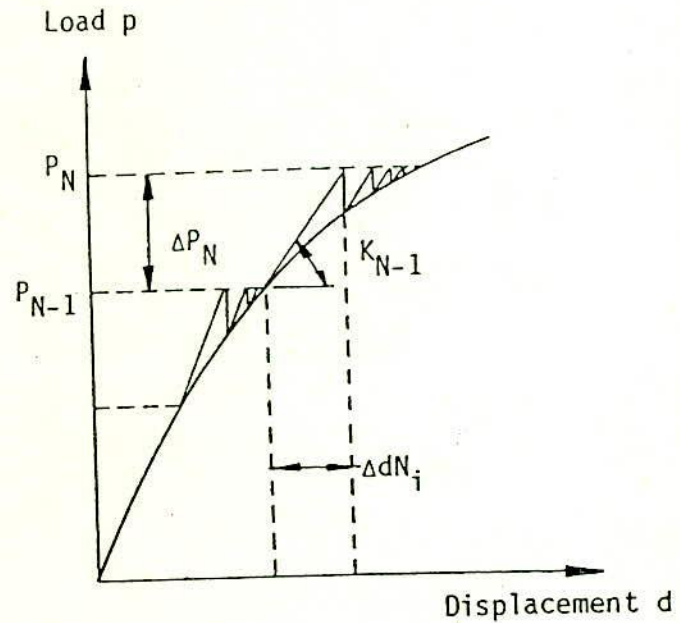
$\{\Delta\varepsilon\}$ = Strain increment vector

$[D_r]$ = Material constitutive matrix. This depends on the particular constitutive model used and is modified to



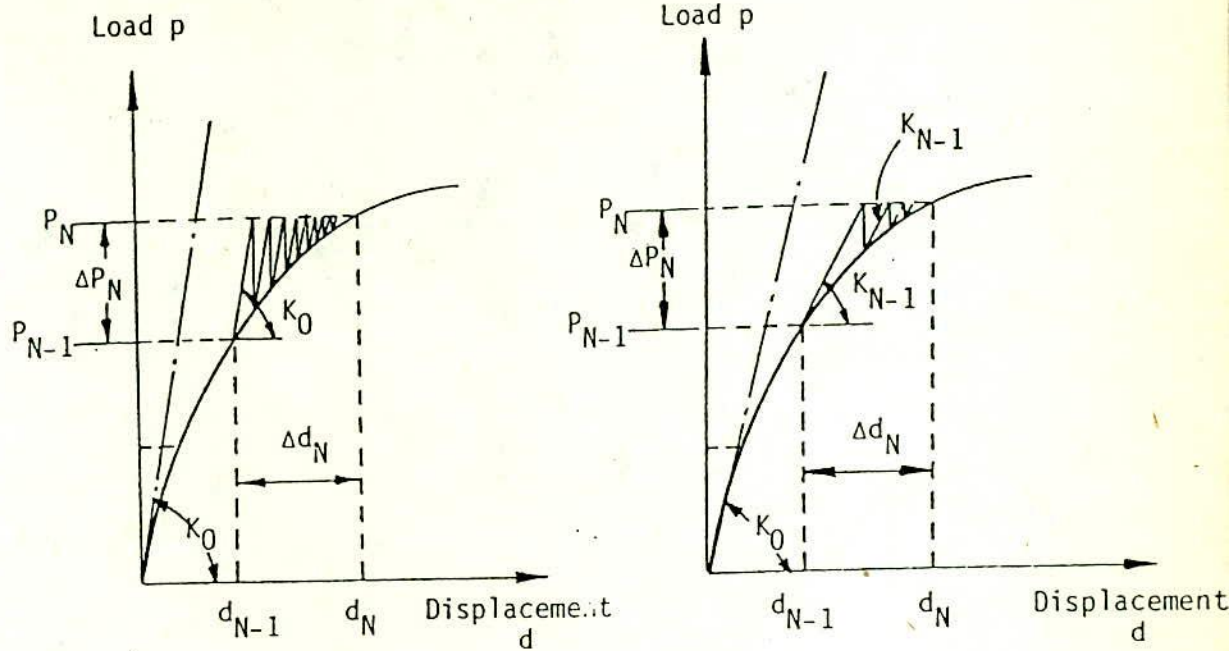
(a) Incremental Equilibrium Approach

(b) Iterative Procedure



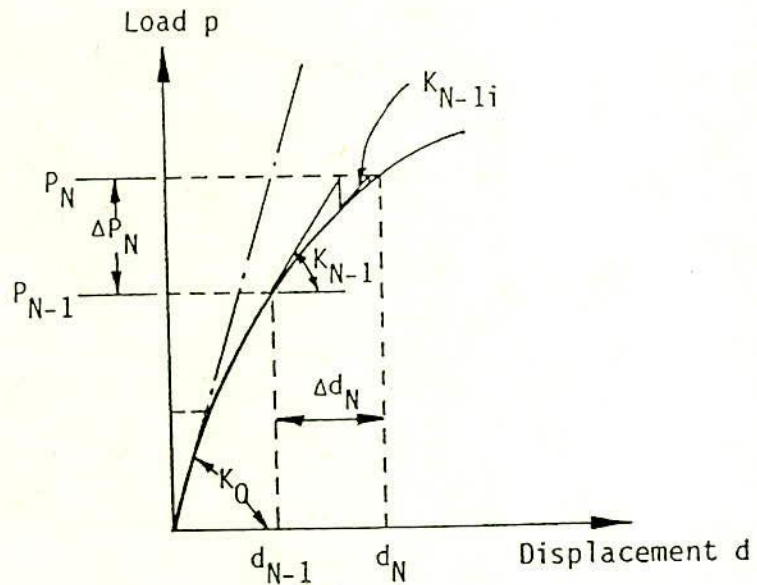
(c) Incremental-Iterative Procedure

Fig. 6.2 Different Solution Techniques



(a) Initial Stiffness Method

(b) Modified Newton-Raphson Method



(c) Newton-Raphson Method

Fig. 6.3 Different Solution Techniques for the Incremental Iterative Procedures.

reflect any changes of the martial stiffness due to the progressive failure in the brick masonry components.
 $\{\sigma_o\}$ = The 'appropriate' released stress vector during fracture

The above relationship has been shown diagrammatically in Fig. 5.7. For typical loading increment $[N, N-1]$, the equilibrium equation for the entire structure can be written as:

$$[K] \{\Delta d\} = \{\Delta P\} \quad (6.9)$$

in which

$$\begin{aligned} [K] &= \text{Tangent structural stiffness matrix} \\ \{\Delta d\} &= \text{Incremental nodal displacement vector} \\ \{\Delta P\} &= \text{Incremental nodal force vector} \\ &= \{P\}_N - \{R\}_{N-1} \end{aligned} \quad (6.10)$$

where $\{P\}_N$ is the applied external load vector at the end of the step under consideration (step N), while $\{R\}_{N-1}$ is the resisting nodal force at solution step N-1, i.e.

$$\{R\}_{N-1} = \sum \int [B]^T \{\sigma\}_{N-1} dv \quad (6.11)$$

Here, $\{\sigma\}_{N-1}$ is the vector of internal element stresses at step N-1 and $[B]$ is the element strain-displacement matrix.

6.3.4 Convergence criteria for Iterative Solution

The convergence criterion for the iterative solution of non-linear structural problems can usually be classified as a force criterion, a displacement criterion or a stress criterion.

A force criterion is normally based on a comparison of the current unbalanced or residual forces within the structure to the external loads. Making use of such a comparison is not always realistic, because the force quantities to be compared may be of a completely different order of magnitude or even in different directions (Bergan and Clough, 1972). In comparison of this nature, it is often difficult to establish what magnitude of forces is acceptable in a test for

convergence. The use of a displacement criterion involves the comparison of changes in displacements; these changes can be compared with the stiffness properties of the structure which in fact corresponds to the displacements. The stress criterion involves a check on changes in stress values during an iteration cycle; these changes can be compared with prescribed stress levels. This type of criterion is well suited for truss, cable and membrane structures during very large deformations.

For this study, a displacement criterion has been used in the solution technique. However, the program also includes the optional use of a force criterion if required. For both cases a residual norm (ψ') has been used. The residual norm (ψ') may be define as :

$$\text{Displacement criterion, } \psi' = (\{\delta\Delta d\}^T \{\delta\Delta d\} / \{d\}^T \{d\})^{1/2} \quad (6.12)$$

$$\text{Force criterion, } \psi' = (\{\delta\Delta P\}^T \{\delta\Delta P\} / \{P\}^T \{P\})^{1/2} \quad (6.13)$$

where, $\{\delta\Delta d\}$ and $\{\delta\Delta P\}$ are the deformation and force vectors for the iteration and $\{d\}$ and $\{P\}$ are the total deformation and force vectors. The iteration is terminated when the norm becomes smaller than a specified value. For practical purposes a value of this norm is ≤ 1.0 (i.e. 1 %) is generally adequate (Owen and Hinton, 1980). For this study a value of 1 % was found to be suitable.

6.4 THE NON-LINEAR FINITE ELEMENT PROGRAM

The elastic, plane stress finite element program for preliminary investigation of the problem (chapter 3) has been modified to incorporate the constitutive model described in chapter 5 and the solution algorithm described in this chapter. The variable names used in the program are similar to those used by Hinton and Owen (1977).

The program uses smeared crack modelling and 'smears' the influence of a local crack across a part or the full element width. The program is capable of analysing wall-beam structure subjected to in-plane loading through the full loading range up to and including failure.

The program has some flexibility with regard to the material model which can be used, depending upon the problem to be analysed. The user has the option

of choosing a linear-elastic fracture model, a fracture model incorporating either elasticity in brick and non-linearity in mortar, or non-linearity both in brick and in mortar. The concrete can be considered linear or non-linear as may be required. If desired, material non-linearity and failure characteristics can be omitted, thus limiting the analysis to be within the elastic range. The program is quite general and can be applied to any material if its basic material characteristics are known.

This section describes the principal features of the program. More details of the program, including descriptions of important subroutines are given in Appendix III.

6.4.1 Program "WBMGEN"

The program is incremental (to allow the progressive application of the applied load) and iterative (to allow for material non-linearity and progressive cracking at a particular load level) in nature and capable of reproducing the non-linear behaviour caused by material non-linearities and progressive local cracking. The program is thus capable of modelling the behaviour of wall-beam structures subjected to in-plane loads from first crack to final failure. As the bricks and joints are modelled separately, the finite element is suitable for any brick mortar combination if the material parameters are known. The material model used in this program was derived from tests on brickwork components (brick and mortar) and small brickwork specimens manufactured from clay bricks and mortar consisting of 1 part cement and 4 parts sand and without any water thickening additives. The model includes elastic and inelastic stress-strain relations, failure criteria and the post failure behaviour. The program uses the smeared crack modelling technique to model cracking. The program is also flexible since it has the capacity for changing the solution algorithm, convergence criteria, failure criteria, post-cracking characteristic and types of fracture analysis. The general logic of the program is shown in Fig. 6.4.

In this program elastic behaviour is assumed for the first (small) load increment. Principal stresses were calculated at the centre of each element, and if any are tensile, the local behaviour is assumed to elastic brittle. For other cases non-linear material behaviour is assigned (these characteristics have been previously described in section 5.2.2).

In the program the load is applied incrementally for which the incremental nodal displacements are calculated using the initial stiffness matrix (constant stiffness method) until the first crack forms in the panel. The stresses are then checked for violation of the failure criteria. If fracture is indicated the [D] matrix of the element is modified in accordance with its mode of failure and the stresses are released. In this model the stresses are released suddenly (Brittle collapse model, (see Fig. 5.9(a).). When cracking occurs, the sudden loss of tensile capacity creates more reduction in the element stiffness. As a result, convergence towards the tolerance is very slow if the initial stiffness method is continued. The modified Newton-Raphson method is therefore used after cracking starts in the panel (see section 6.3.2).

Convergence is indicated by the use of either the force or displacement criterion described in section 6.3.4. Two different criteria are used to define final failure. Either the solution fails to converge, or a dominant crack or cracks propagate through a substantial portion of the panel.

The program ('WBMGEN') consists of sixty-two subroutines. Important subroutines are discussed in Appendix III. Most of the subroutines were adopted (Hinton and Owen, 1977 and Owen and Hinton 1980) and were written in FORTRAN 77. The program structure for new or modified subroutines are given in Appendix III. The program was run by FORTRAN compiler FTN77/386 produced and updated by University of Salford 1990 for 80386 based Personal Computer using MS-DOS revision 3.30 and later. The program is also tested by following systems:

- 1) FORTRAN compiler of the Mainframe computer IBM 4331 with VM/Sp operating system.
- 2) FORTRAN compiler of the Mini computer RS/6000 with AIX 3.2 operating system.

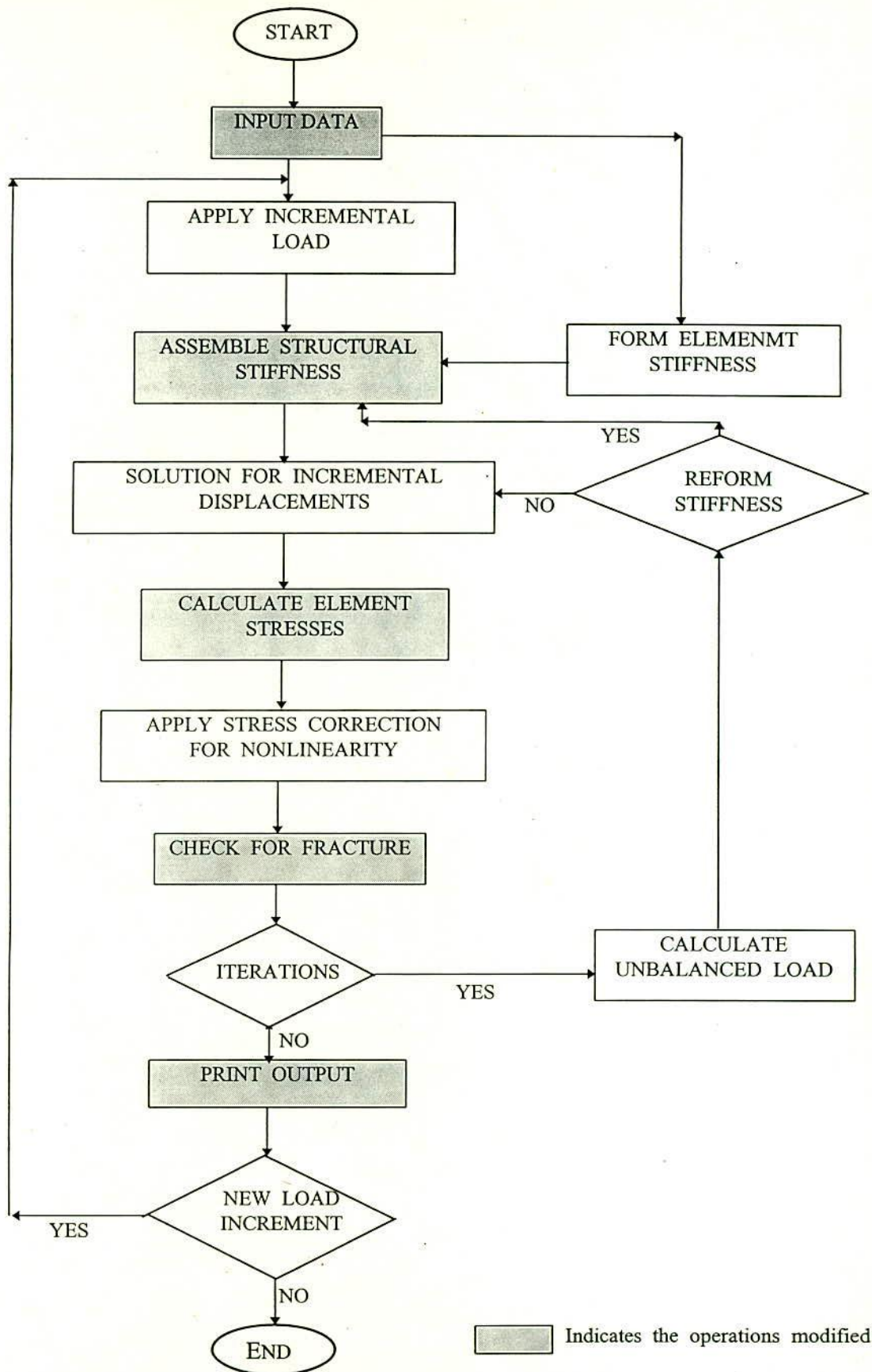


Fig. 6.4 Structure of Finite Element Model " WBMGEN"

6.5 SUMMARY

This chapter has described the finite element model for the analysis of wall-beam structure subjected to in-plane distributed load. The model treats bricks and joints separately and incorporates the failure criteria and deformation characteristics reported in chapter 5. The model used the smeared crack modelling technique to simulate progressive cracking.

The program is incremental and iterative in nature allowing material non-linearity and progressive cracking to be simulated as the load is increased.

The effectiveness of the program is assessed in chapter 7 where experimental results of the tests on wall-beam panels are compared to those predicted by the finite element model. In the light of these comparisons, program 'WBMGEN' is refined to allow for strain-softening of the mortar joint after initial failure and adopted as the final model for the investigation. The program is then used to carry out a detailed investigation of storey-height walls subjected to uniformly distributed loads in chapter 9.

CHAPTER 7

EXPERIMENTAL VERIFICATION OF THEORETICAL MODEL

7.1 INTRODUCTION

Verification of the finite element model has been carried out by comparing the results of uniformly distributed load tests on clay brick wall-beam panels with those predicted by the finite element model described in the previous chapters. The objective of the test was to verify the accuracy of the finite element models, (and hence the material models described in chapter 5), rather than to draw extensive conclusions about the general behaviour of wall-beam panels subjected to uniformly distributed load. Once the model has been verified, a comprehensive theoretical study of the uniformly distributed load on wall-beam can be carried out. Such a study forms a later stage of the investigation and is described in chapter 9.

A total of 3 panels were used in the verification tests. They were of different types of wall-beams subjected to uniformly distributed load. For each test the predicted and observed cracking load, failure load and mode of failure were compared.

Two different finite element models were used in the comparison. Both models incorporated smeared crack modelling. The first model assumes the immediate release of the stresses in the region of a crack (a brittle collapse model, Model 'A'). The second is refinement of Model 'A' which assumes gradual release of the stresses in the region of a crack (a strain softening model or intermediate collapse model, Model 'B'). The latter more realistically reflects the propagation of the crack which is inhibited to some extent by the more lightly stressed bed joints surrounding the vertical joint. The characteristics and development of strain softening model are described elsewhere (Ali, 1987). Model 'B' is shown to be the most representative, and is adopted for all subsequent load analyses.

7.2 TESTS ON WALL-BEAM PANELS

As stated previously tests on full scale masonry panels have been used to verify the theoretical models. Uniformly distributed load tests on wall-beam panels which produce high stress gradient near the support were chosen as a means of

checking the validity of the finite element model, since this type of application of load is normally encountered in masonry buildings.

7.2.1 Panel Details

To realistically compare the test results of the derived theoretical model, the properties of the masonry panels must be similar to the small brick masonry specimens used to obtain the deformation and strength characteristics of the constituents. The panels were therefore constructed from the same type of clay bricks and mortar used in chapter 4. The construction procedures and curing history are also same as in the tests described in chapter 4.

Three different wall-beam panels were used to verify the theoretical model. One with solid brick wall resting on reinforced concrete beam, one with opening in the wall and the third one solid wall confined with reinforced concrete frame. The aspect ratio (height : length) of all panels was 0.7. This aspect ratio was considered to be sufficient to be representative of real wall-beam. The panels were 19 courses high with 10 bricks in length. This provides 9 perpendicular planes of weakness (in line with vertical mortar joints), which was considered to be sufficient to be representative. Horizontal and vertical mortar joints for all panels were 7 mm. The thickness of all panels was 60 mm which is equal to the breadth of the brick unit. The details of three different panels are shown in Fig. 7.1(a) to Fig. 7.1(c). These figures illustrate the critical dimensions, reinforcement details and loading arrangement for the panels tested. The wall-beam panel confined by concrete frame (Fig. 7.1(b)) was 9 bricks in length and 18 courses high. The overall dimensions for all the panels are same.

7.2.2 Panel Construction

The dimension of wall-beam panel was determined on the basis of some practical considerations such as safe brick laying, safe handling of the panel to the testing machine and the maximum height of the panel that the machine would accommodate. With equal projection of 25 mm at both ends the length of the supporting beam was chosen as 1350 mm having width of 100 mm and depth of 75 mm. The bearing area for the support of the concrete beam was 100 mm X 100 mm in this case. The resulting effective span for the supporting beam was 1200 mm (c/c distance of supports) with depth to span ratio of 1/16. In the concrete beam nominal reinforcement of 4 numbers 10 mm ϕ bars were used as main

reinforcement and $3\text{ mm } \phi$ at the rate of 50 mm c/c near the support and 100 mm c/c at the middle were used as shear reinforcement. The beam was cast using $1:1:2$ concrete mix (using 12 mm down graded stone chips) and moist cured for 7 days until the construction of wall on it. Construction of brick wall on this beam in stretcher bond was aided by means of a vertical wooden board. The constant thickness of vertical and horizontal mortar joint was maintained by using small piece of plastic sheet of required thickness. The bricks were immersed in water and then dried in air to make them saturated surface dry (SSD) condition. Brick courses being laid using $1:4$ mortar without any admixture. To minimise workmanship effects and to be consistent with the procedure adopted for the small brick masonry samples, the panels were constructed by a professional brick layer. The panel under construction is shown below in Fig. 7.2. For quality control purposes three 25 mm mortar cubes were also made during construction of each wall. The results of these quality control tests for all panels are given in Appendix IV.

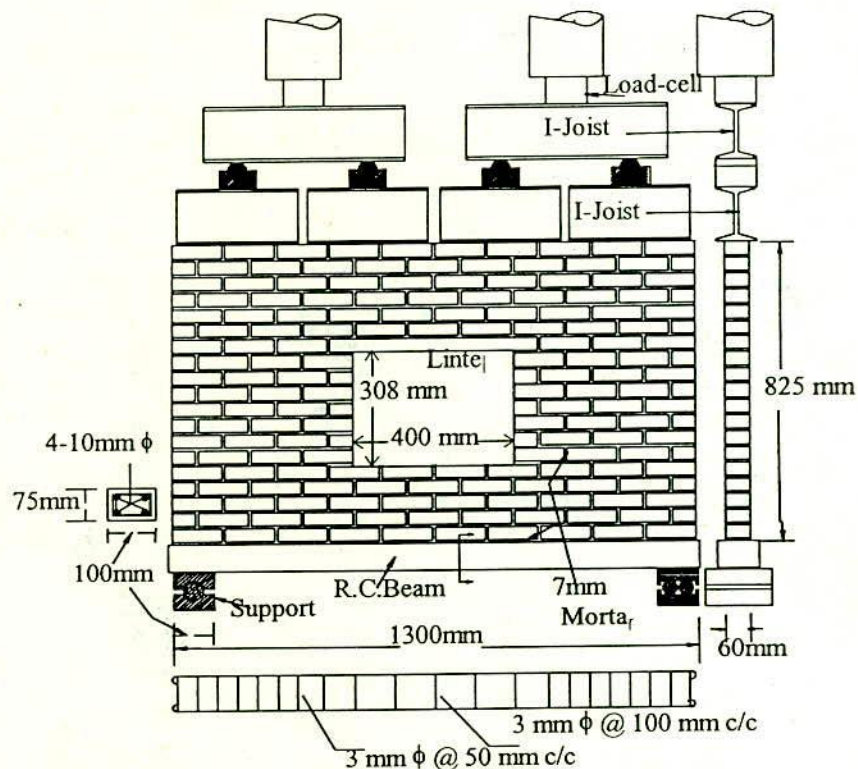


Fig. 7.1(a) Details of Panel and Testing Arrangement for Wall-beam with Central Opening

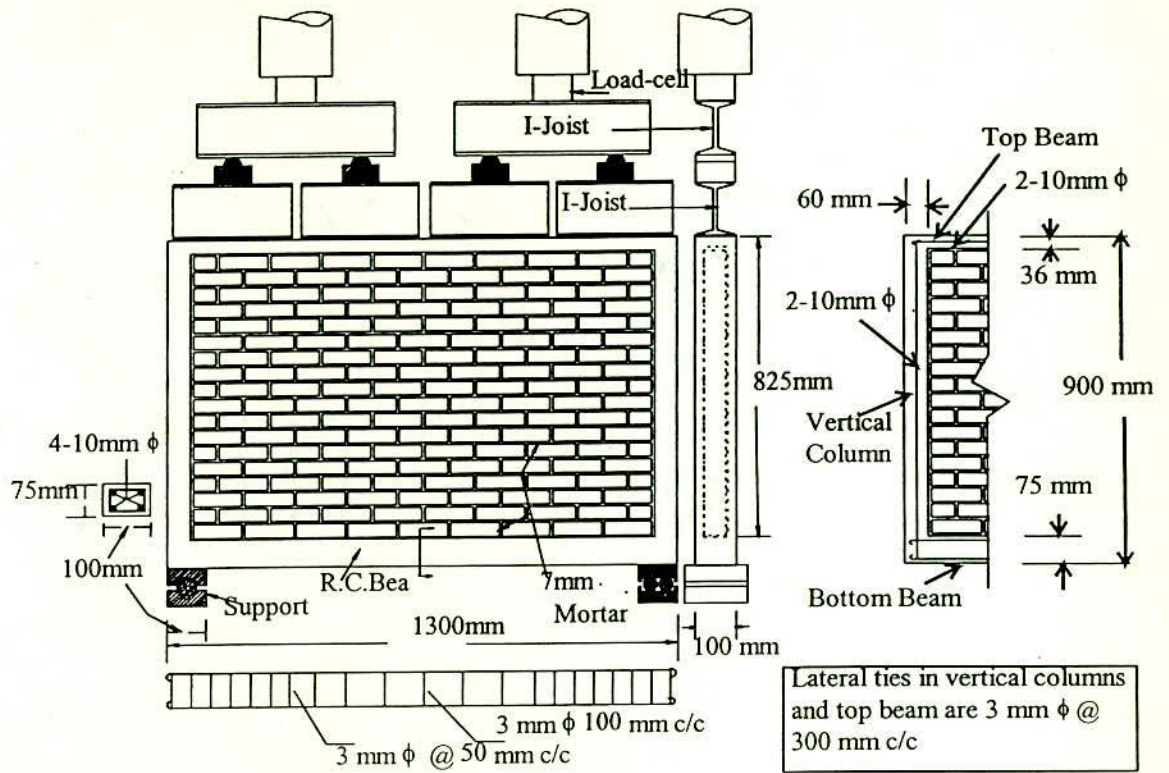


Fig. 7.1(b) Details of Panel and Testing Arrangement for Wall-beam Confined by Concrete Frame

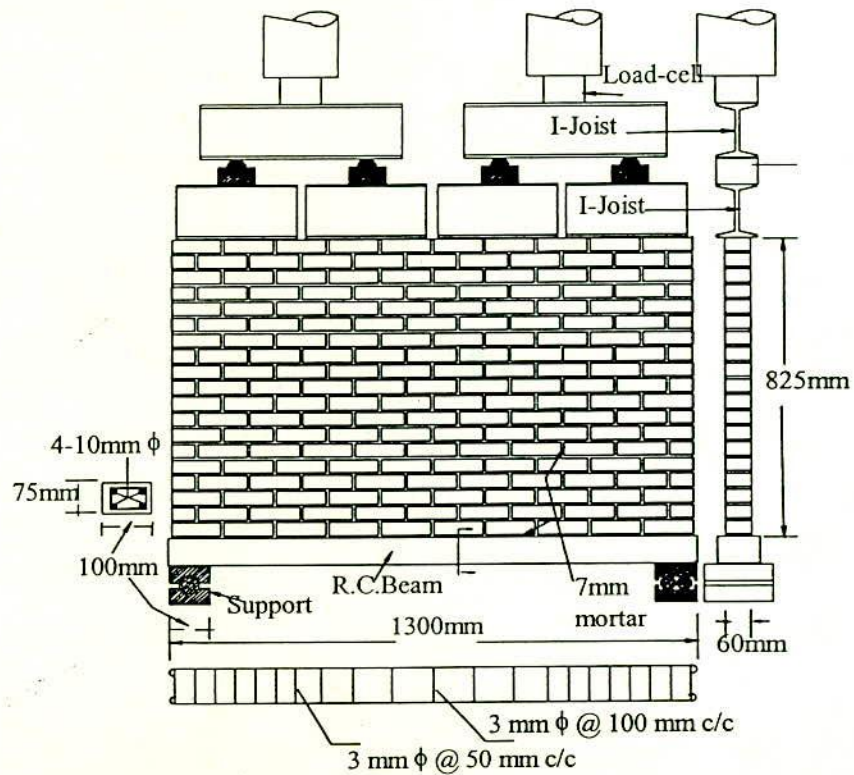


Fig. 7.1(c) Details of Panel and Testing Arrangement for Plane Wall-beam

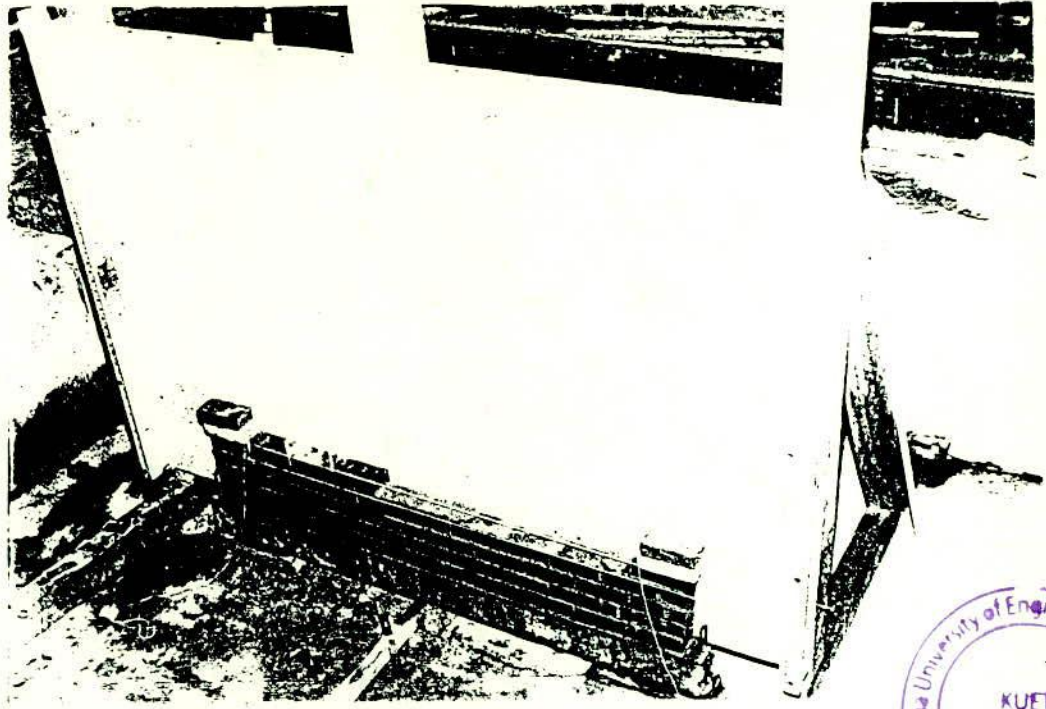


Fig. 7.2 Wall-beam Panel Under Construction



After construction, the panels were moist cured for 14 days and air cured in the laboratory for a further 14 days until the date of testing. Electrical strain gages were attached to both faces of the wall-beam to read vertical strain in alternate bricks of first layer and horizontal strain in alternate bricks at mid vertical section. Strain gages were also attached to the beam to measure the horizontal strain in concrete at mid span. The strain recorded from these gages are used to compare the results obtained from the finite element model and is discussed in later part of this chapter.

7.2.3 Testing of the Panels

The wall-beam structures were simply supported over a clear span of 1100 mm and were loaded under a monotonically increasing vertical load until failure. The vertical load was applied by means of two 500 kN capacity hydraulic jacks through a system of distributing steel beams (I-joists) arranged in steps on the top of the panel. A typical testing arrangement is shown below in Fig. 7.3. To ensure even bearing to the joists, they were seated on the top of the wall using a thin layer of mortar. Previously calibrated load cell was used to measure the applied load.

At the start of each test, a small load (20 kN) was applied and then released. The zero readings of the gages were then recorded. The load was applied in increments. The load was held constant at each increment and gage readings were taken. The procedure was repeated until failure. A summary of the cracking loads and failure loads is contained in Table 7.1 and Table 7.2 respectively.

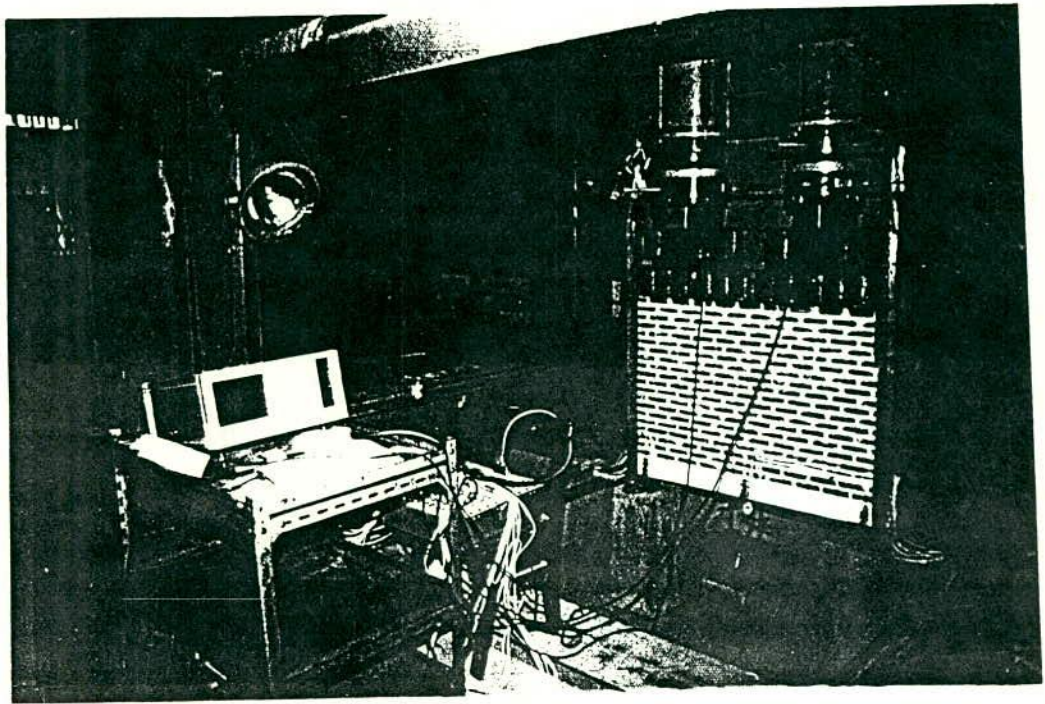


Fig. 7.3 A View of Uniformly Distributed Load Test

7.2.4 Modes of Failure

The failure modes of the wall-beam panels tested are shown in Fig. 7.4(a) to Fig. 7.4(c). As can be seen from the figures, that failure modes were usually of the same general form but depending on the type of the panels there were small variations. The distinct modes of failure exhibited by the test walls were as follows:

1. Diagonal shear failure in supporting beam and wall over the support along the entire height.
2. Vertical tensile splitting and crushing of bricks over the support. In some cases crushing of the end of the supporting reinforced concrete beam may also occur.

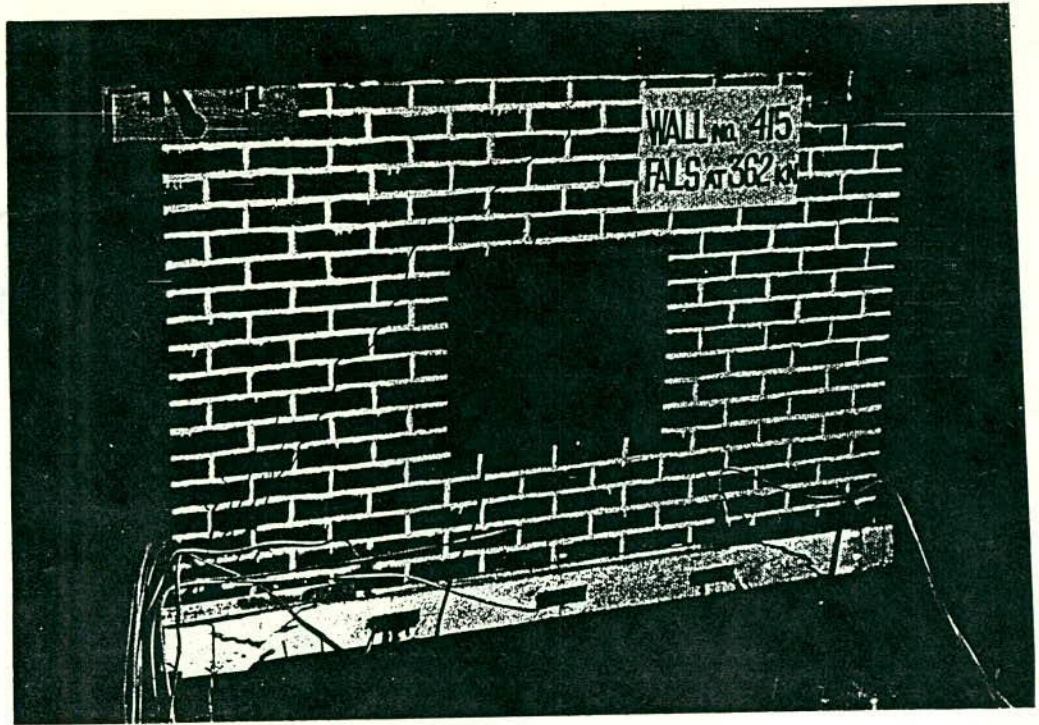


Fig. 7.4(a) Failure of Wall-beam Panel (with opening).

It is generally accepted that micro cracks initiates in the vertical joints due to inherent low tensile bond strength. These were not visible by the naked eye. The formation of flexural cracks in the supporting beam are the first visible cracks. With the progress of loading the cracks then propagate through the bed joints, vertical joints and the bricks leading to ultimate failure of the system. At loads exceeding approximately half of the ultimate load the separation of the wall from supporting beam at mid-span was observed in general. But the continuous vertical crack at interface of vertical ties and the wall (see Fig. 7.4(b)) propagated at earlier stage of loading.

7.3 FINITE ELEMENT ANALYSIS OF THE WALL-BEAM PANELS

7.3.1 Modelling of the tests

The typical finite element mesh used for this investigation is shown in Fig. 6.1. Only half of the panel was discretized because of symmetry. The effect of the element size on the non-linear fracture analysis is described in chapter 8. The applied load from the I-joists was simulated by applying loads of equal intensity at the nodes at the interface of the panel and I-joists. These nodes were unrestrained

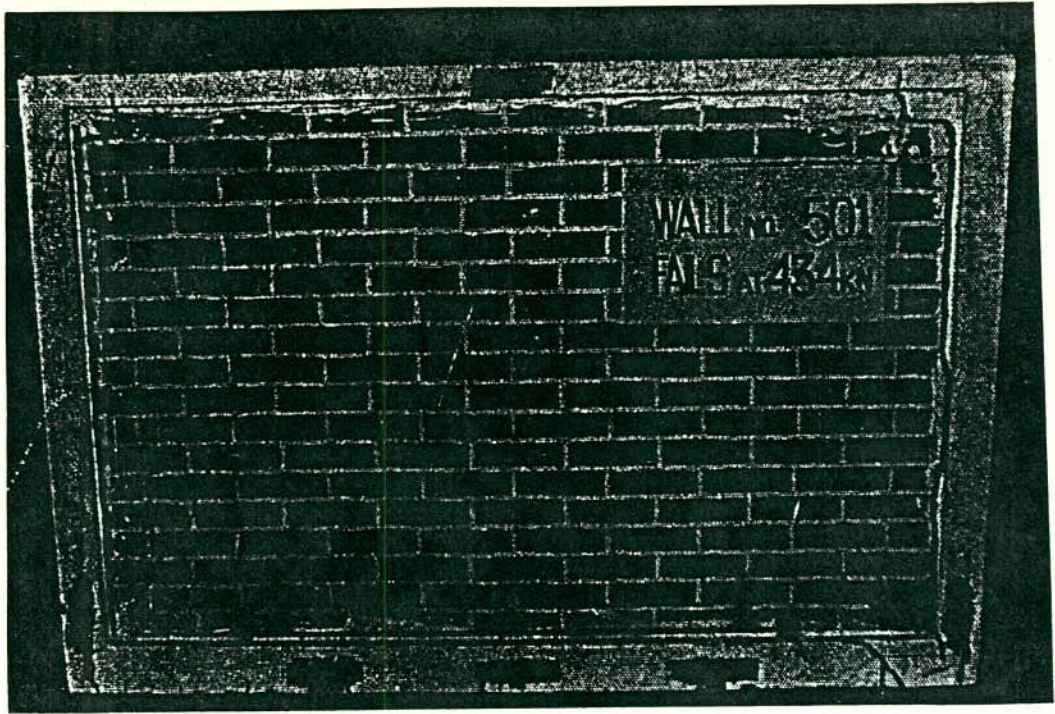


Fig. 7.4(b) Failure of Wall-beam Panel (with frame).

in all direction. The nodes at the interface of the support and the panel were restrained in Y-direction only while the nodes at the axis of symmetry were restrained in the X-direction only. The sensitivity of these assumed boundary conditions in relation to the predicted behaviour is also studied in chapter 8. The applied load when simulated by the prescribed displacements of the nodes at the interface of the loading plate and the panel are also studied and no noticeable difference was found in predicting the failure load.

7.3.2 Analysis and Results

For all the analyses used to simulate the tests, the load was applied in incremental form. This increment was maintained at constant rate until an initial crack formed after which a smaller rate of load increment was used. This procedure of varying the increment produces the faster convergence of the solution and allows accurate prediction of the crack pattern. In the analytical plots of crack propagation, it is of interest to note the varying failure modes for different portions of cracks shown below in Fig. 7.5. It can be seen that local failure mode can include tensile cracking, bond failure and crushing. A similar terminology is used for all the subsequent plots of cracking patterns reported in this chapter.

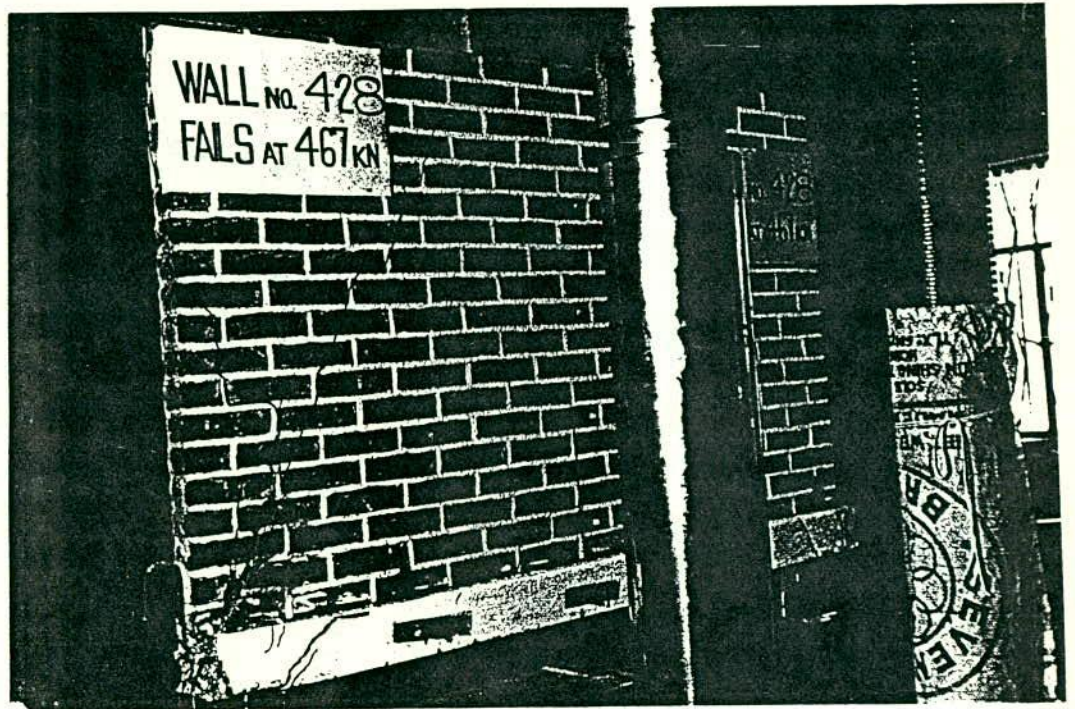


Fig. 7.4(c) Failure of Wall-beam Panel .

In analyses of all the panels the crack initiated from the vertical joints in the region near the support. This was a bond failure type of crack. The flexural cracks then initiated in a zone normally between the support and the middle of span. These can be seen from the progressive flow of cracks for different panels shown in Fig. 7.6. With the application of higher load cracking goes on through the vertical joints, bed joints and bricks responding to any of the three failure forms of localised failure (i.e., bond failure, cracking failure and crushing failure). And these elements which experience failure constitute a band in diagonal direction indicating the seat of the potential diagonal tension crack in the panel. Simultaneously the concrete elements in the supporting beam and the interface mortar elements of wall-beam experience tensile cracking. For each type of panel the loads at which failure commenced in the vertical joints are nearly equal. Similarly the load at which flexural cracks commence in the supporting beam is also nearly equal for all the panels tested. The panels continued to sustain further load much higher than the initial cracking load (discussed later) until the main diagonal crack propagated through a substantial portion of the height of the panel.

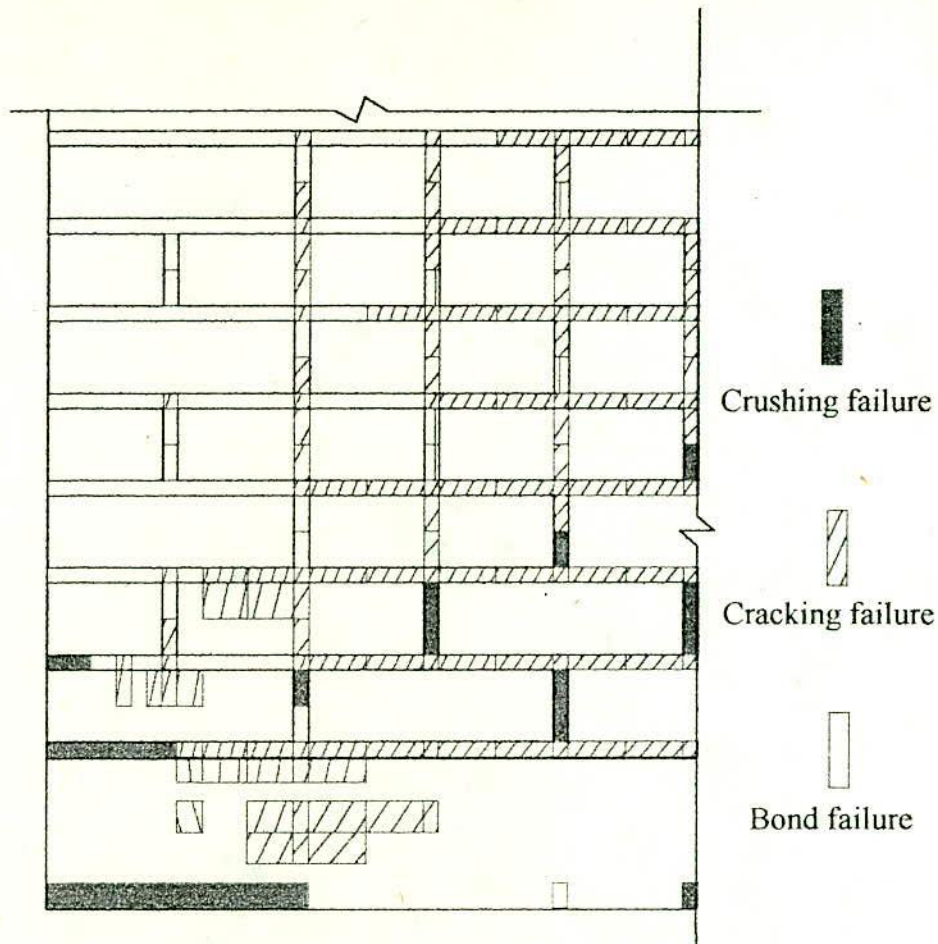


Fig. 7.5 Varying Failure Modes for Different Portion of Crack

During the progress of the application of the load in all beams tested, at about 50 % of the ultimate load new crack opened at mid span and propagates horizontally through the bed mortar at wall-beam interface and continues both sides for a total length of about half of the span. Finally, the failure was indicated by lack of convergence of the solution or the propagation of the crack through the height of the wall. In the analyses of all the panels the final failure did not occur unless the major crack travelled through brick elements and in a diagonal direction for the full height of the wall.

For all the analyses, the output is given after the full convergence of the solution is met. The output includes the nodal displacements, the reactions at the supports and the element stresses and strains. The output can be taken at any desired load increment and for the elements at any selective section. The mode of failure and stresses at failure for each element were also indicated. To facilitate the plotting of crack pattern an output file was created giving the failure mode,

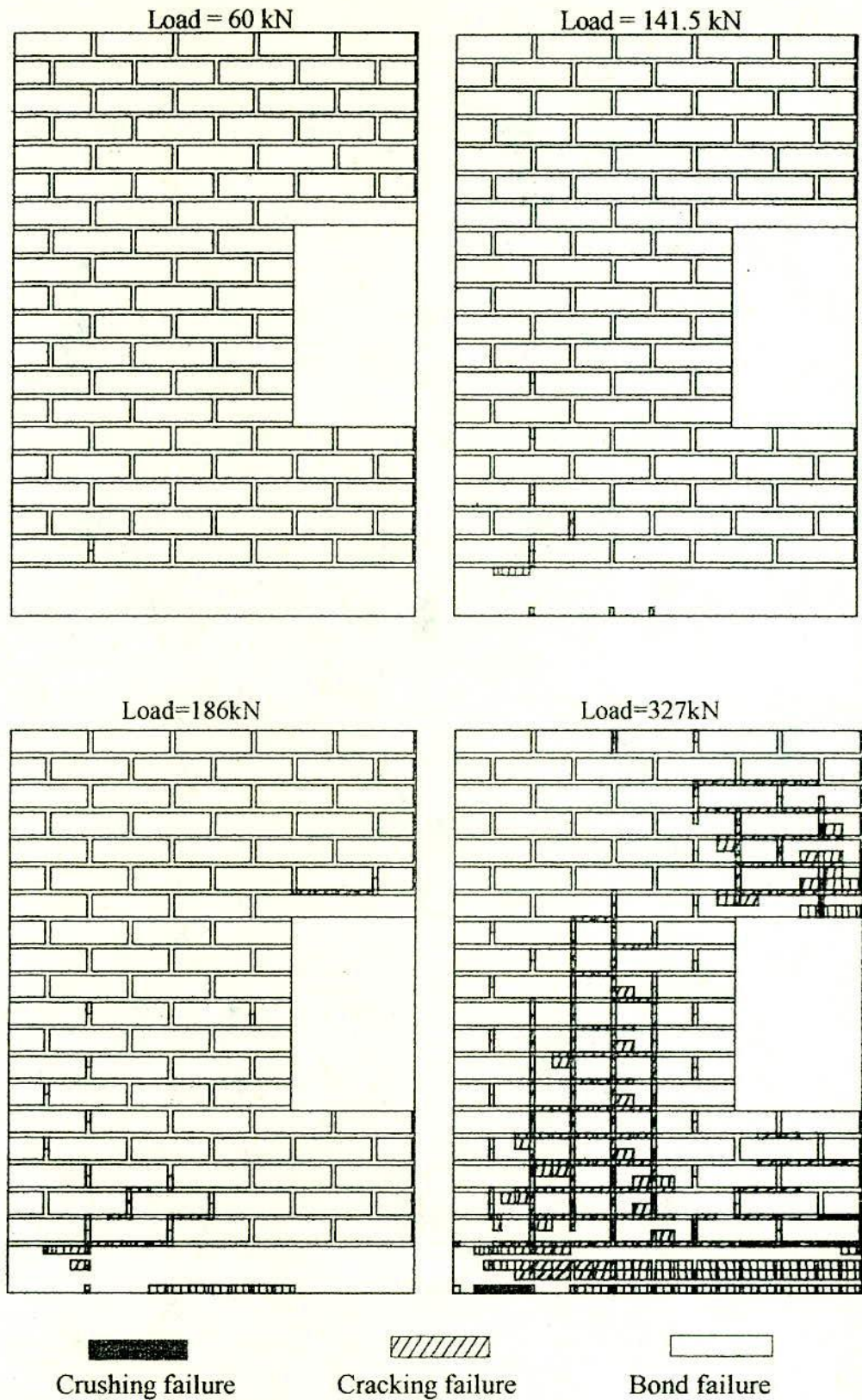


Fig. 7.6(a) Sequence of Failure of Panel (Wall-beam with Opening)

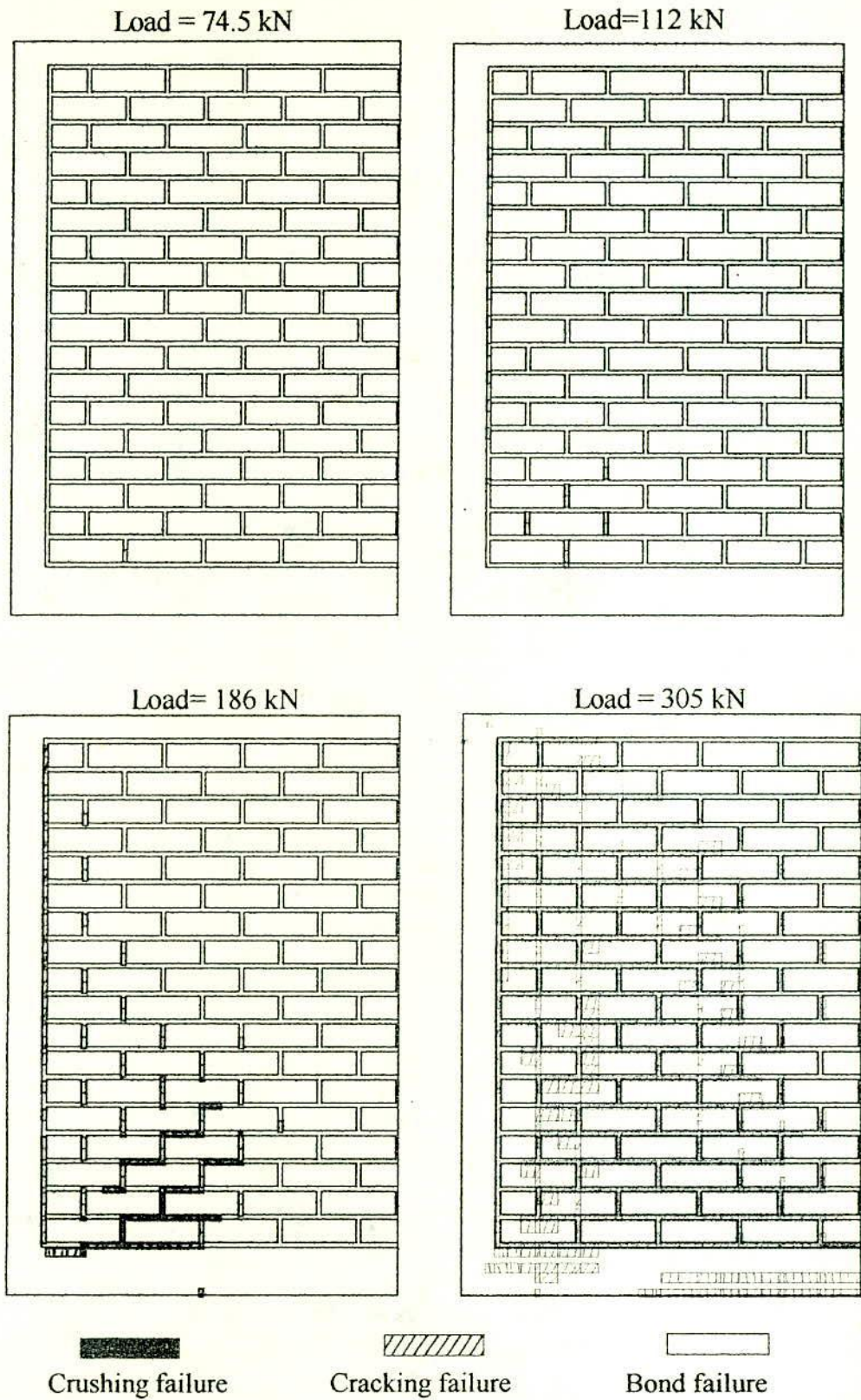


Fig. 7.6(b) Sequence of Failure of Panel (Wall-beam with Frame)

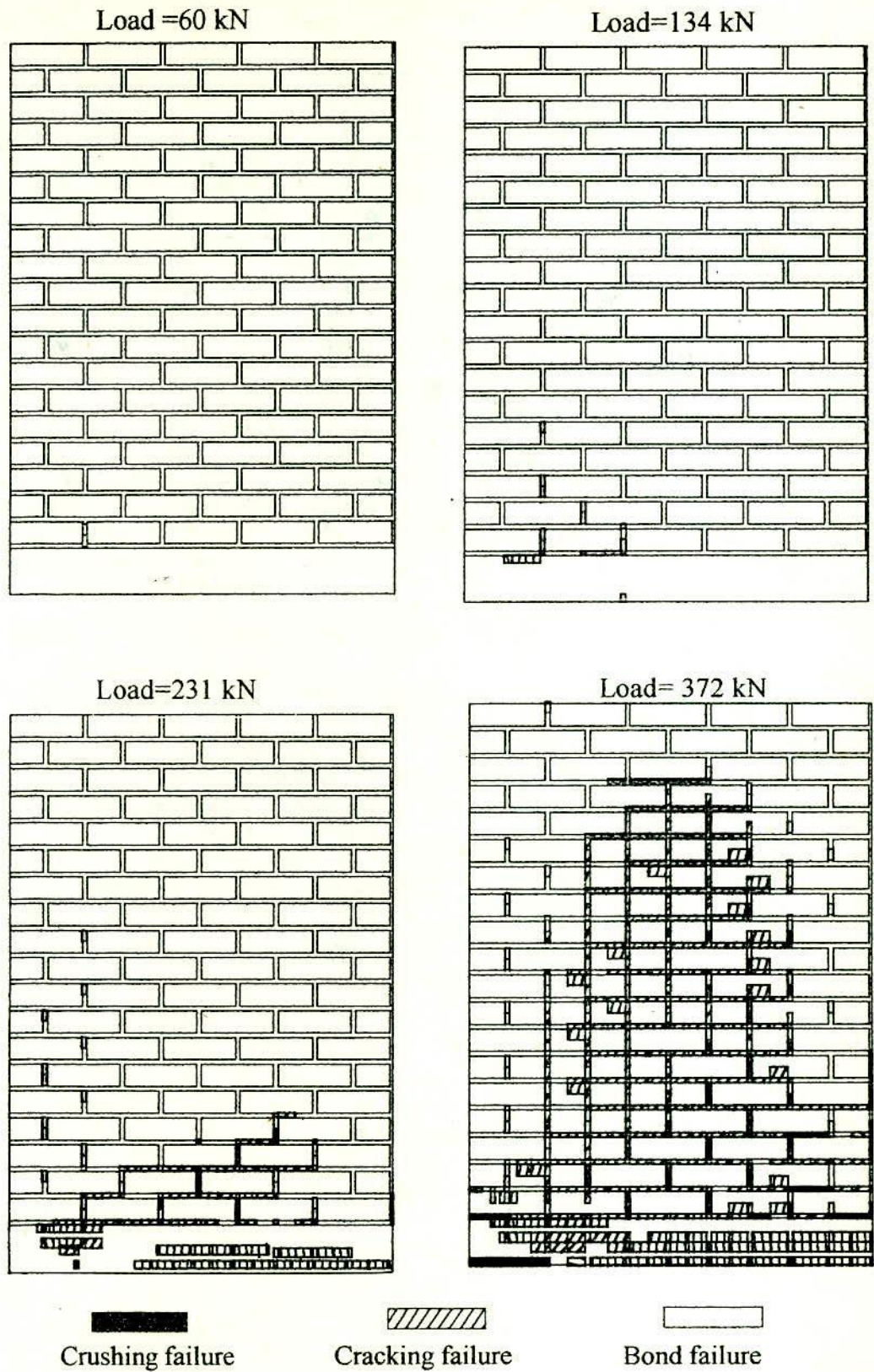


Fig. 7.6(c) Sequence of Failure of Panel (Plane Wall-beam)

geometry and locations of elements which have been failed during each load increment.

7.4 COMPARISON OF THEORY AND EXPERIMENT

A comparison of the test results with the results of the corresponding finite element analyses is given in this section. For the comparison the initial cracking load, the ultimate load and the final failure pattern were considered. The strains measured at selected levels were also compared. Agreement between the experiment and theory is good.

7.4.1 Initial Cracking Load

In all the analyses of this study the cracks initially form at the interface of brick and vertical mortar due to bond failure. These take place near the supports. Due to presence of lightly stressed bed joints and bricks or concrete over these vertical cracks, they cannot propagate or open at low loads. These cracks at low loads could not be observed with naked eye during tests. Therefore, corresponding load is not designated as initial cracking load.

In all tests of the present study the flexural cracks formed in the supporting RCC beam are visible due to the surface roughness of the crack. In the analyses the flexural cracks form at loads higher than the load causing local bond failure at the initial stage (see Fig. 7.6(a) to Fig. 7.6(c)). Since during tests these flexural cracks could be observed physically the load corresponding to these cracks are designated as initial cracking load hereafter. To check the accuracy of the model the initial cracking load as obtained from finite element prediction are compared to the experimental values in Table 7.1.

The agreement between theory and experiment can be considered reasonable although the predicted results tend to be lower than the observed values. This is possibly due to the crack initiation criterion used for crack propagation in the material model. The micro cracks (and corresponding cracking load) are predicted by the model at a stage when the crack width does not grow sufficiently to be visible. With the progress of loading when the cracks become visible, by that time the load step reaches to higher value resulting a lower trend of the predicted value.

7.4.2 Failure Pattern

Generally the wall-beam panels which were tested failed due to the formation of few dominant inclined cracks (see Fig. 7.4 and Fig. AIV.2 in Appendix IV). Vertical tensile splitting and crushing type of failure in the masonry close to the support was observed in most of the cases at a load approaching to failure. In all the cases the cracks commenced in the supporting beam as it was observed by the naked eyes. These cracks then propagated through the beam in inclined direction and finally through mortar joints and bricks. As the load approached to failure horizontal crack at wall-beam interface was observed for about half of the span length in the mid span.

In all three walls tested, the shear crack appeared first in the supporting beam and then extended upward in the wall through the vertical mortar joints and the bricks. It follows that the factors influencing the shear strength of the wall are, the shear strength of the supporting beam, the height of the wall, the strength of vertical joints and bricks. In general, the final mode of failure is accompanied by the vertical tensile splitting and crushing of corner bricks at end supports. This fact is mainly attributed to high concentration of vertical stress over the supports at loads approaching to failure. The vertical tensile splitting can also occur as a result of the differential strength and deformation characteristics of bricks and mortar. The uniaxial compressive strength and modulus of elasticity of mortar are considerably lower than the corresponding values of bricks. Therefore, if the mortar could deform freely, its lateral strain will be larger than the strain in the bricks. However, because of bond and friction between brick and mortar, the mortar is confined. Thus an internal state of stress is developed which consists of axial compression and lateral tension in brick and triaxial compression in the mortar. If the transverse tensile stress exceeds the brick flexural tensile strength vertical tensile cracking would take place in the bricks. However, the wall at this stage is not considered to be failed because it can withstand more load. With the increase of further load the tensile cracks widen and when the compressive strength of the bricks is exceeded, failure will set in by both vertical splitting and crushing of the corner bricks over the supports. It can therefore be concluded that for wall in which the primary failure criterion is vertical splitting and crushing of corner bricks, the ultimate strength can be increased by strengthening the corner bricks. This can either be achieved by introducing bricks of very high compressive strength or providing horizontal reinforcement in the bed joints in that locality.

This provision however can cause vertical splitting at the end of the reinforced concrete supporting beam in orthogonal direction before failure.

The failure of the panel due to external bending moment and due to axial tensile force in the supporting beam both being the result of the tied arch action, were not observed in this test series.

In the present test series no failure through sliding of wall from beam was observed. Such mode of failure may be anticipated if the bond of the interface mortar joint is not capable of transferring the horizontal shear force across the wall-beam interface. In wall-beam structure the high stress concentration at the ends of the span produces proportionately high frictional resistance at wall and beam interface which counteracts sliding failure along the wall and beam interface.

Since it was not possible to record the experimental cracking sequence, final cracking pattern rather than the sequence of cracking is compared. The final failure pattern of the panels as predicted by the present finite element models (brittle collapse model and intermediate collapse model) are shown in Fig. 7.7 to Fig. 7.9 together with the observed experimental failure pattern. The predicted cracking pattern constitutes a general zone of cracking which corresponds with the localised cracking as shown in the panels tested. As it is mentioned earlier, the present study uses stress criteria for crack initiation, and strength criteria for crack propagation with smearing the effect on the whole element when it is cracked. The present study reproduces the separation at brick and vertical mortar interface which initiates at a load as low as 13% of the experimental failure load. These cracks at brick mortar interface are not observed by naked eye. The present study also reproduces cracking of horizontal and vertical mortar, concrete and brick. Crushing of these materials which occur at higher loads are also reproduced in the model. As a result a number of elements undergo failure resulting in a wider band. Again in the strength criteria, the element is declared failed as soon as the limiting strength is exceeded, while at that stage of loading the panel under test may not show cracking. The properties of any material in the analytical model is same throughout the panel, but in the test panel the material variability is inherent and the crack propagates through weak locations along its path showing a discrete nature of cracking. This is more prominent because the micro cracks (constituting large zone of general cracking) which are formed in addition to main diagonal crack are not visible and/or could not be measured. Considering the above facts the agreement between the predicted cracking patterns and experimental observations can be

considered reasonable. However, the discrete crack modelling with fracture toughness criteria for crack propagation will be able to track the individual crack in a better way with an increased computing cost. It should be noted that the failure of the horizontal bed mortar at the interface of wall and supporting beam is truly reproduced in the model.

It is quite interesting to note that both model 'A' (brittle collapse model) and model 'B' (strain-softening model) predicted approximately similar types of failure patterns. In both models crack propagated in a band which was one or a few elements wide. As mentioned earlier the vertical joints typically experienced a bond type of failure and the brick and the bed joints experienced mainly cracking type of failure.

7.4.3 Failure Load

The theoretical ultimate load of the panels was predicted by both finite element models described in chapter 6 (i.e., brittle collapse model and intermediate collapse model). For both models the crack always started from the vertical joints near the support. At higher load increment, flexural cracks appeared at the bottom of the supporting beam. With the progress of loading the cracks then propagate through the bed joints, vertical joints and the bricks and finally propagate diagonally upward leading to ultimate failure.

The predicted ultimate loads determined by brittle collapse model and intermediate collapse model are compared to the observed failure load in Table 7.2. There is a reasonable agreement between theory and experiment except for the wall-beam panel confined by frame. The experimental failure load for wall-beam with frame is higher in comparison to predicted failure load. The possible reason for this difference is due to the contribution of vertical end columns. The joists on the top of the wall used to apply load are placed on the full length of the wall (see Fig. 7.1(b)). As a result some load is being applied directly on the columns from the end joists. The uninterrupted vertical mortar joint between wall and column gets cracked at earlier load and the vertical load carried by columns are directly transferred to the supports. As a result the wall-beam panel with confinement fails at higher load resulting a large difference in prediction and test value.

For Model 'A' (brittle collapse model) predicted results are consistently lower than those of observed values. This difference can be substantially attributed

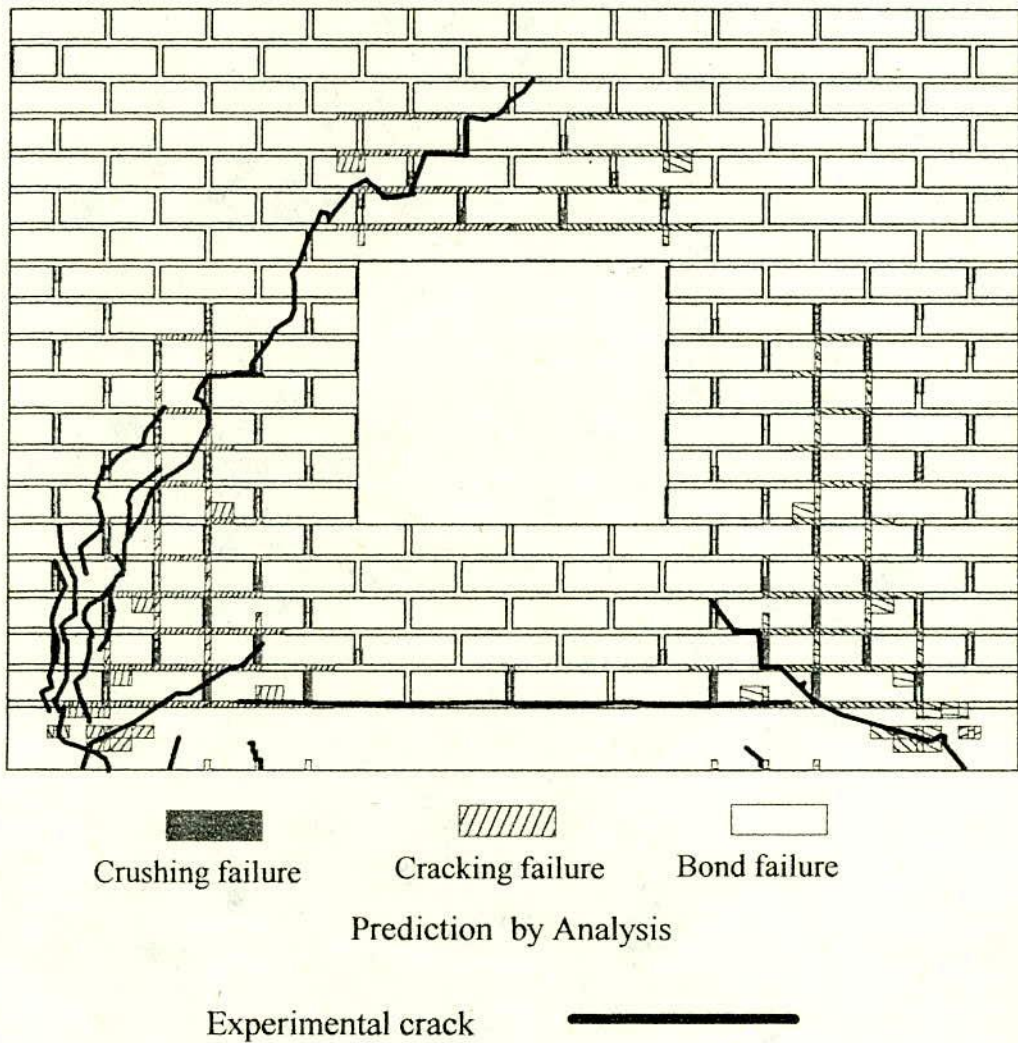


Fig. 7.7(b) Modes of Failure of Wall-beam Panel with Opening
(Prediction by Strain-softening Model)

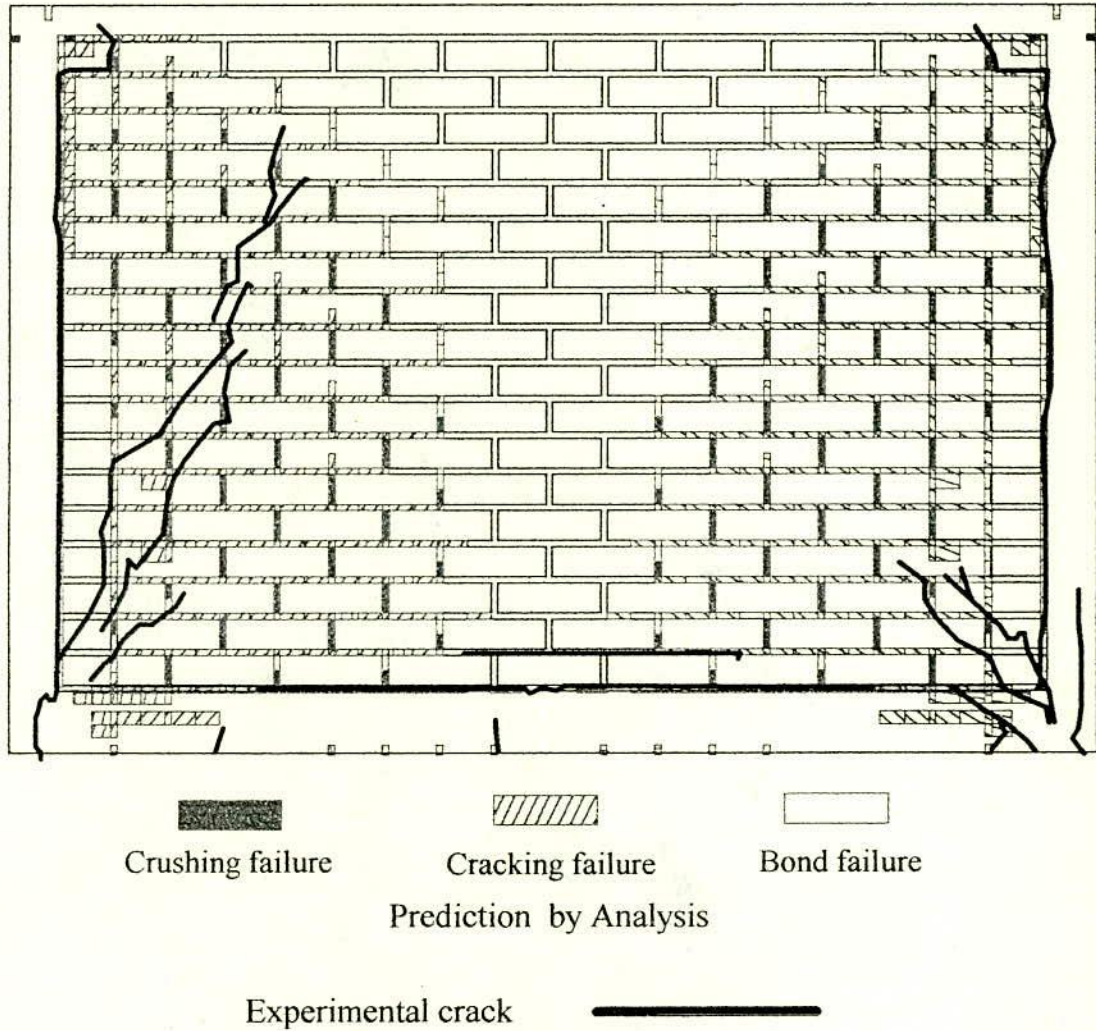


Fig. 7.8(a) Modes of Failure of Wall-beam Panel with Frame
(Prediction by Brittle Collapse Model)

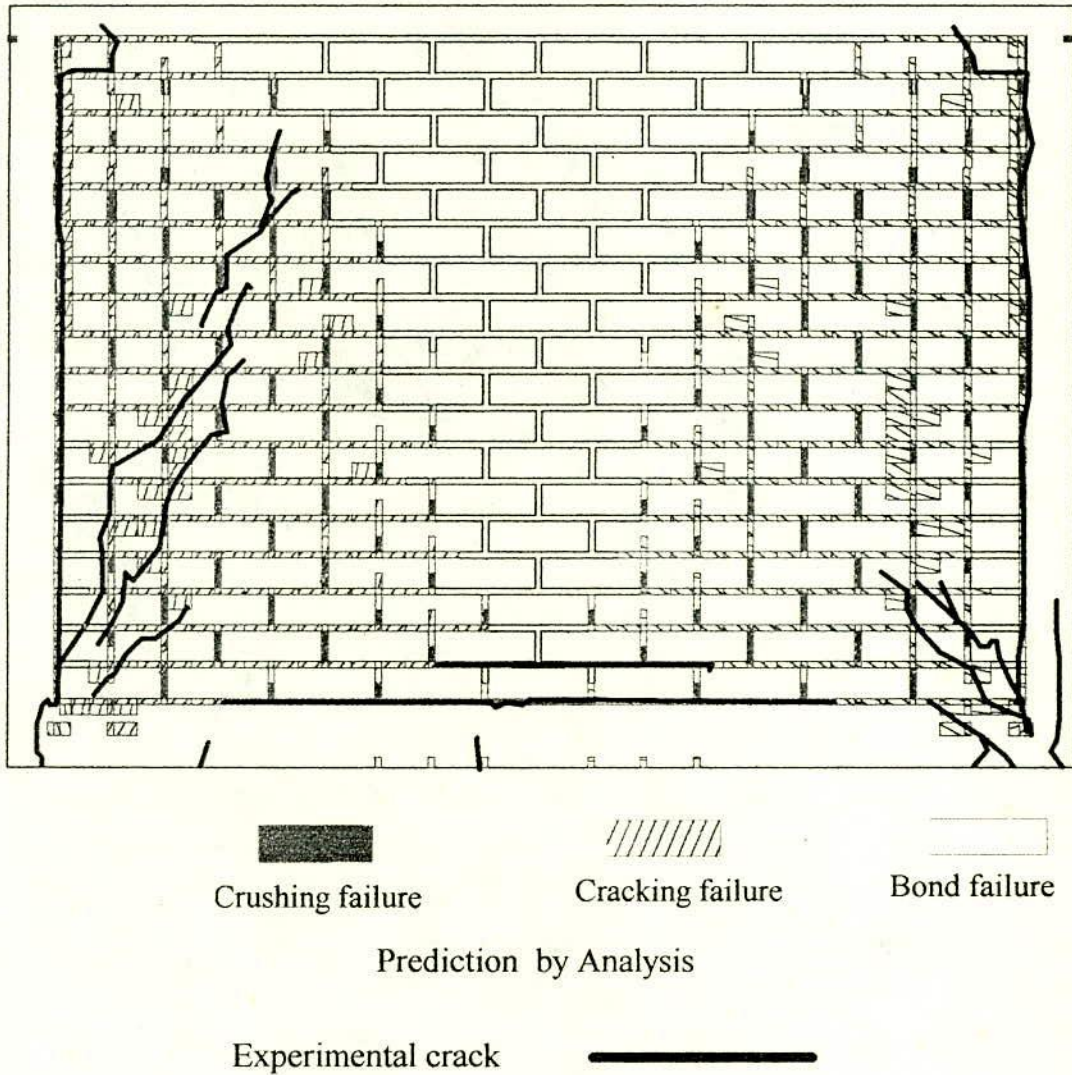


Fig. 7.8(b) Modes of Failure of Wall-beam Panel with Frame
(Prediction by Strain-softening Model)

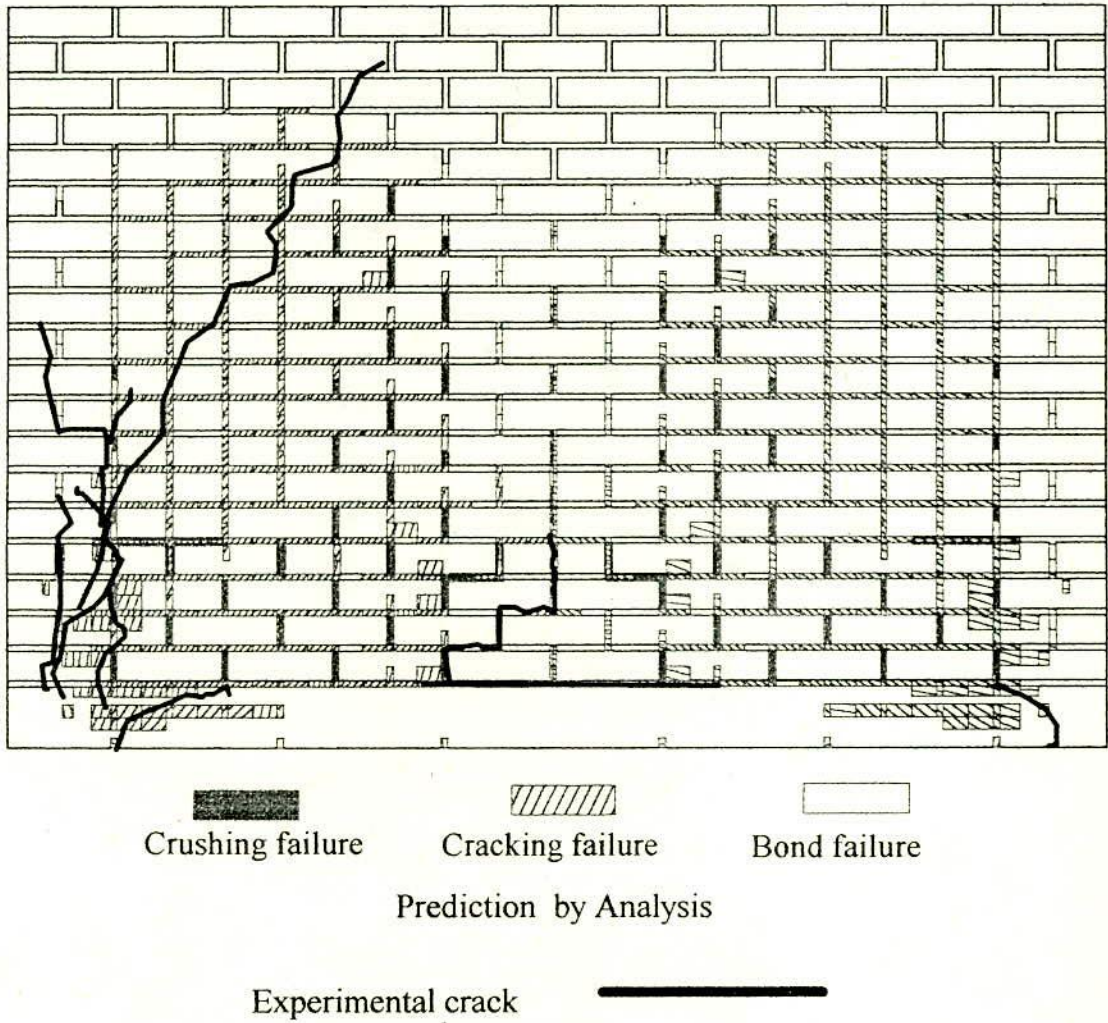


Fig. 7.9(a) Modes of Failure of Plane Wall-beam Panel
(Prediction by Brittle Collapse Model)

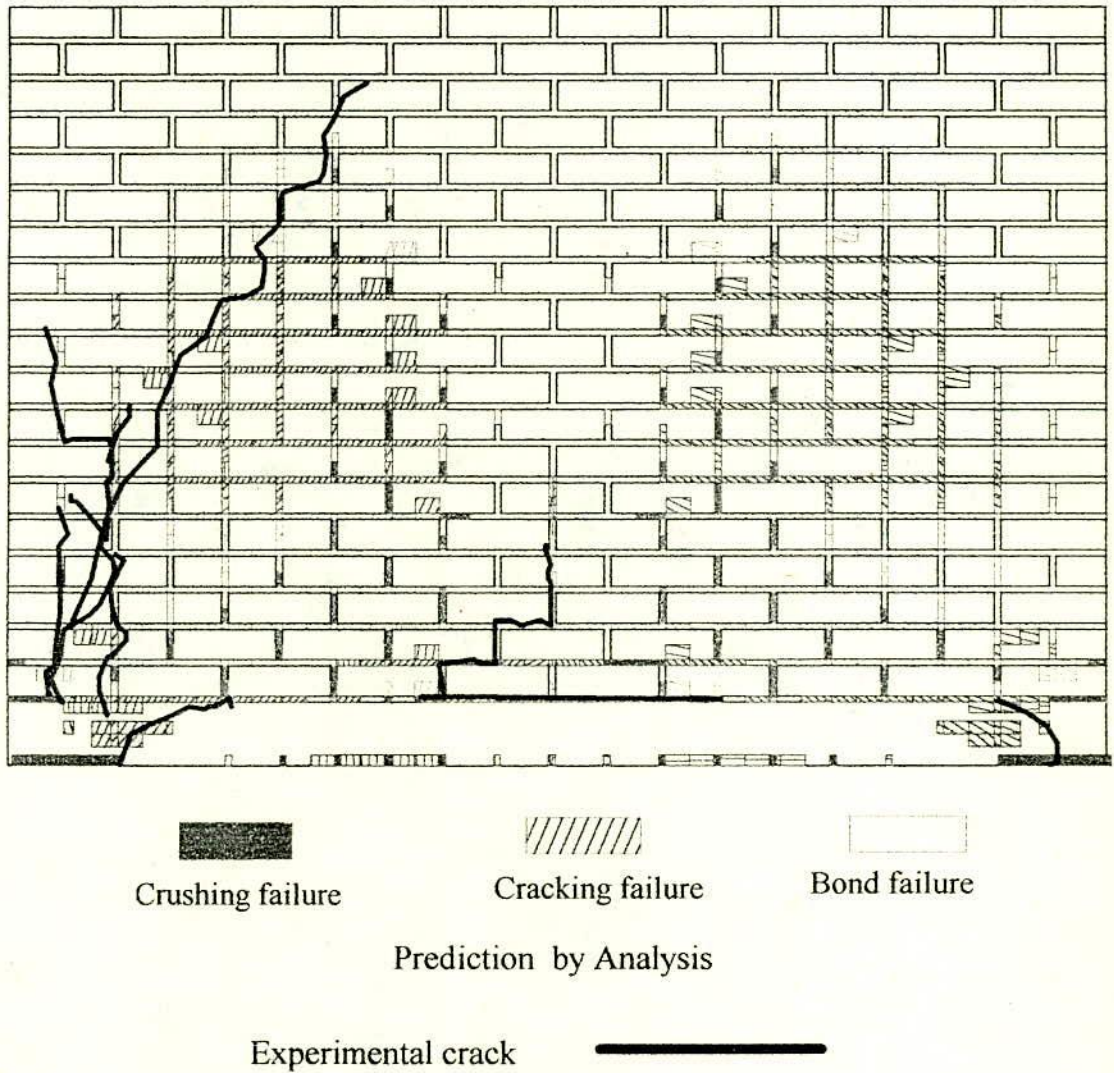


Fig. 7.9(b) Modes of Failure of Plane Wall-beam Panel
(Prediction by Strain-softening Model)

7.5 COMPARISON OF STRAINS

In this section the strain predicted by the model is compared to the strain measured at different locations in the panels during the experiments. The discrete locations of measuring the strains on a typical wall-beam can be seen from Fig. 7.10. As the zone near the end of the span experiences very high stress concentration, considerable joint cracking have occurred within comparatively low applied load. Thus for comparison between experimental and predicted results from the non-linear analysis it is justified that the comparison be made within a low range of applied load.

In the analysis the load on the beam was applied at the rate of 15 kN/increment at the beginning. After the first crack was opened the load was applied at the rate of 7.5 kN/increment until failure. This was needed for efficient convergence of the solution and for better simulation of the cracks. However, during experiment the load was applied before and after the first crack at rates different from those with the analysis. This was due to limitations of the machine and the operator. As a result the load at which the experimental strains were recorded by data logger and the load at which strains from analysis were available coincided in few cases. The comparison of strains at some of these load levels are shown in following sections.

Comparison of strains obtained from elastic analysis and those of non-linear analysis considering progressive cracking and non-linear deformation characteristics of materials are discussed in Appendix IV.

7.5.1 Horizontal strains along the centre line of the wall-beam:

Horizontal strains in the bricks along the centre line of the panel were measured by electric strain gages at four locations along the height. For wall-beam with frame one extra location was fixed at top beam and for wall-beam with central opening intermediate two locations were not needed. These measured strains (front and back face reading being averaged) and predicted strains are compared in Fig. 7.11 for all the three types of wall-beam panels. The agreement between the strains obtained by the tests and analyses are reasonable. The general pattern of increase of horizontal compressive strain in the upper regions of the panels, as predicted by the analytical model, is also confirmed by the experimental results.

Table 7.1
Predicted and Observed Initial Cracking Load in kN

Type of Wall-beam	Experiment	Theory	$\frac{\text{Theory}}{\text{Experiment}}$
With opening \perp	151	142	0.94
With frame!	200	186	0.93
Plane#	156	134	0.85

Table 7.2
Comparison of Experiment and Theoretical Prediction

Types of Wall-beams	Experiment		Theory (Model 'B')		$\frac{\text{Theory}}{\text{Experiment}}$
	Failure Load (kN)	Failure Mode	Failure Load (kN)	Failure Mode	
With opening \perp	362	Type 1	327	Type 2	0.90
With frame!	434	Type 1	305	Type 2	0.70
Plane#	467	Type 1	372	Type 2	0.80

\perp Wall-beam panel with opening designated by Wall No. 415

! Wall-beam panel with frame designated by Wall No. 501

Plane wall-beam designated by Wall No. 428

Failure mode :-

Type 1:- Diagonal tension failure accompanied by crushing at an end at ultimate load. For wall-beam with frame crushing at end was not prominent.

Type 2:- Bond failure at vertical joints accompanied by diagonal tension failure. For plane wall-beam crushing at the ends was recorded at ultimate load in addition to other failures of Type 2..

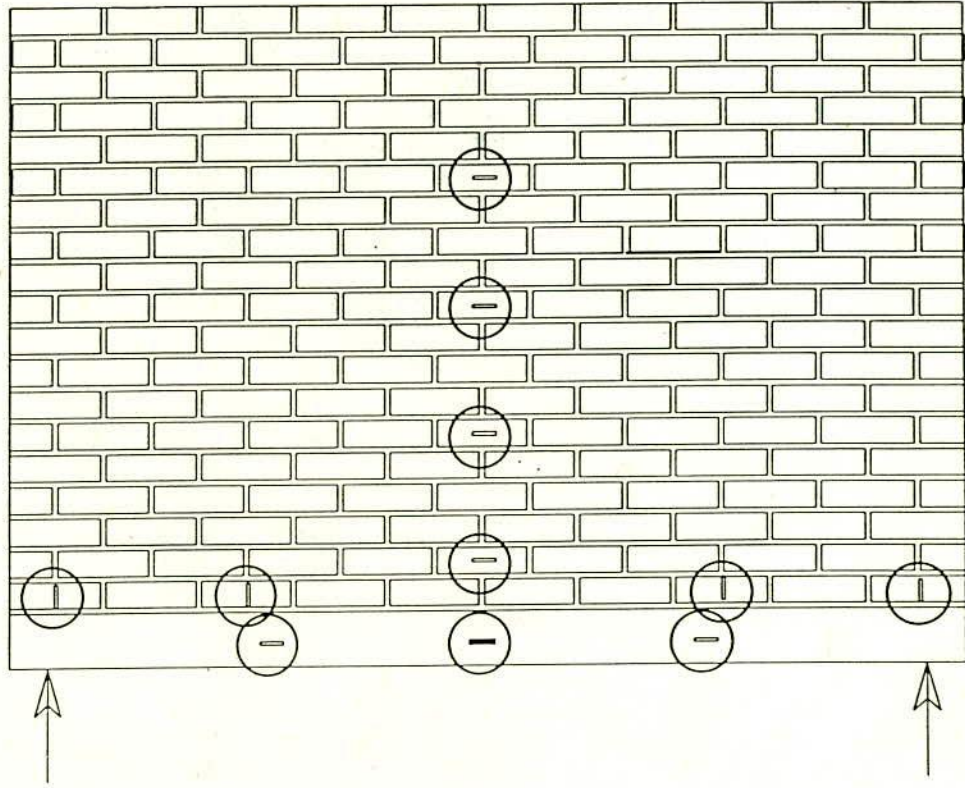


Fig. 7.10 Locations of the Electric Strain Gages in the Panel

Large horizontal strains in between the locations of gages correspond to the horizontal strains in vertical joints between the bricks. The local variations in strain in these thin vertical mortars are possible to be determined only by the non-homogeneous analysis.

7.5.2 Vertical strain along the first brick course :

Vertical strains at the first brick course were measured by electric strain gages in four locations along the span. These measured strains and predicted strains are compared in Fig. 7.12. The measured strains on opposite faces of the wall were found to show acceptable difference (see Fig.AIV.3in Appendix IV) and were, therefore, averaged. General agreement is again evident, with some scatter in the experimental results. The maximum deviation from the predicted vertical strain is observed at the ends of the plane wall-beam, Fig. 7.10c. The difference can be attributed to possible experimental error which needs more tests to justify.

However this was not attempted within the limited scope of this study as better agreement was observed in other walls.

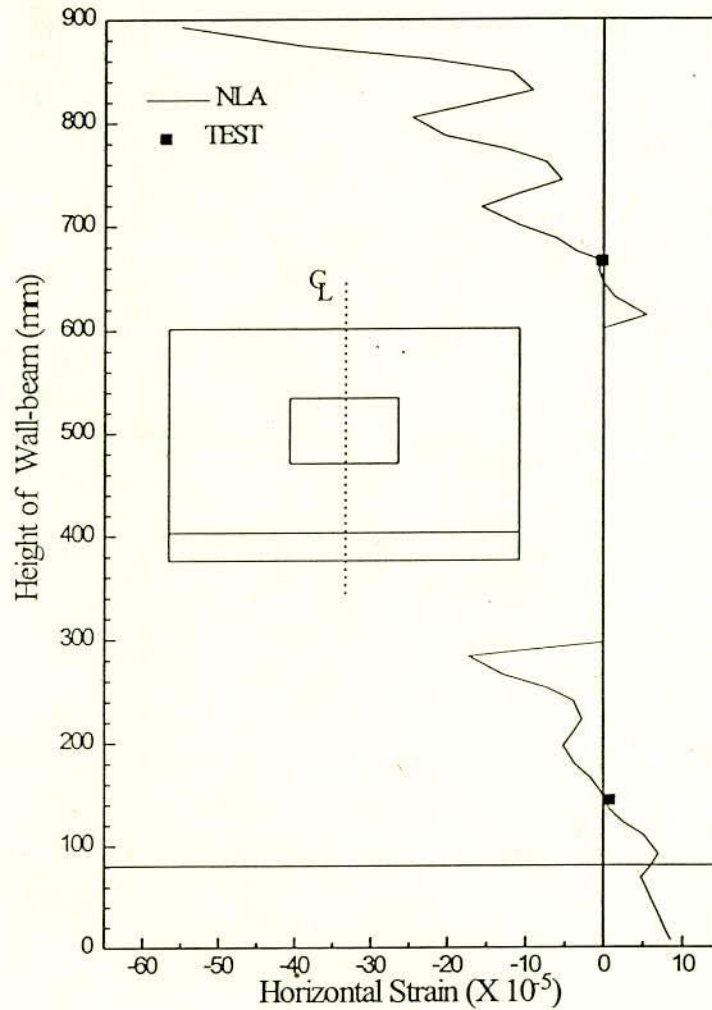


Fig. 7.11(a) Horizontal Strain at Mid Vertical Section at a Load of 112 kN.
(Wall-beam with Opening)

7.5.3 Horizontal strain in the supporting beam:

Horizontal strains at mid depth of the supporting beam are measured by electric strain gages in three locations along the span. These measured strains (front and back face reading being averaged) and predicted strains are compared in Fig. 7.13. The amount of tensile strain measured in different types of wall-beams tested in this study gives a general idea that the supporting beam remained in

tension between the supports. These measured strains are in general found to be greater than the predicted value. In few gages the lower value may be due to local crack or flaws. The fact that the measured tensile strain at the

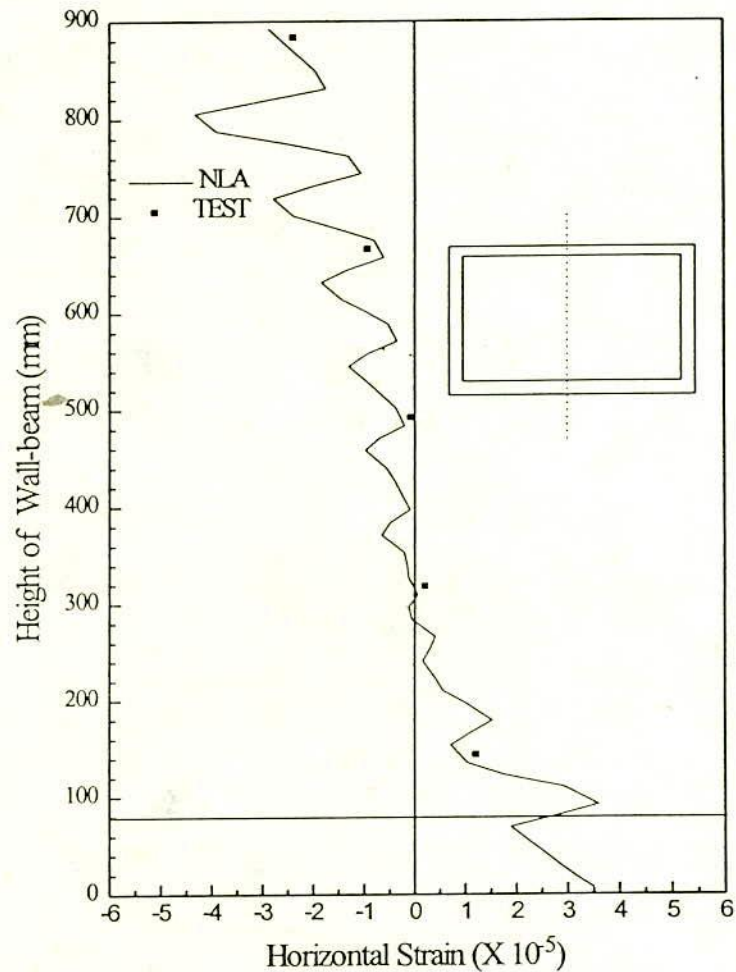


Fig. 7.11(b) Horizontal Strain at Mid Vertical Section of Wall-beam with Frame (Load = 45 kN)

middle of the supporting beams, being higher than the predicted one, indicates that a higher magnitude of deformation is being induced in the beam. This may be due to shear deformation and /or premature joint failure.

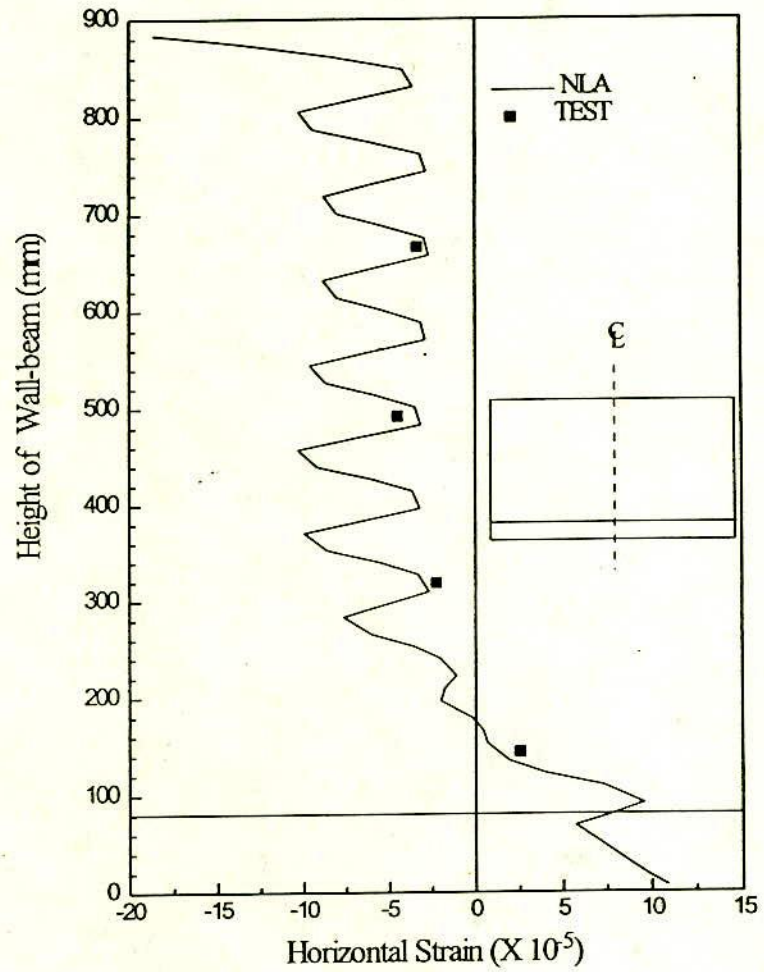
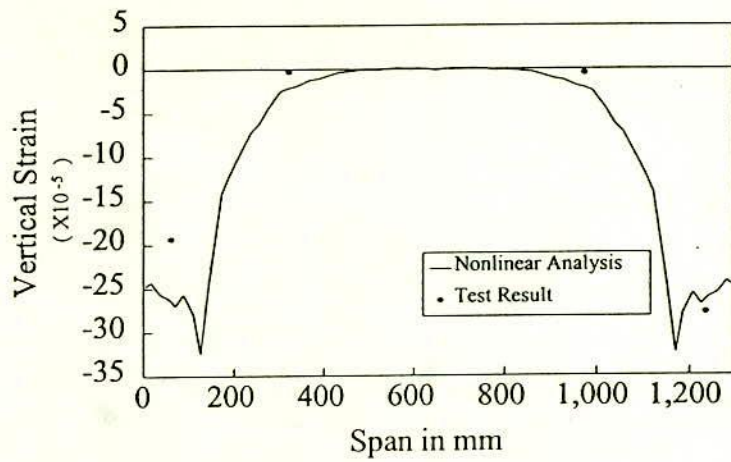
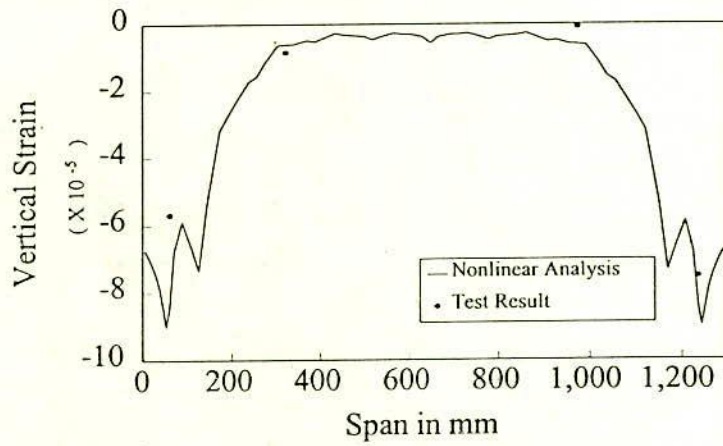


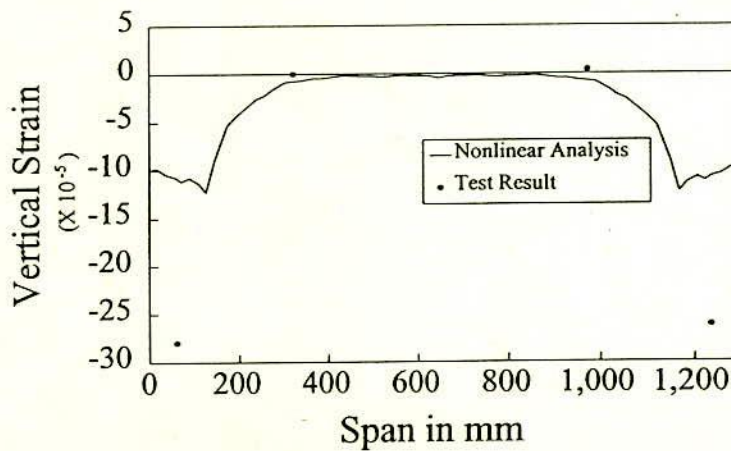
Fig. 7.11(c) Horizontal Strain at Mid Vertical Section of Plane Wall-beam..
(Load = 112 kN)



(a) Wall-beam with Opening (Load = 112 kN)

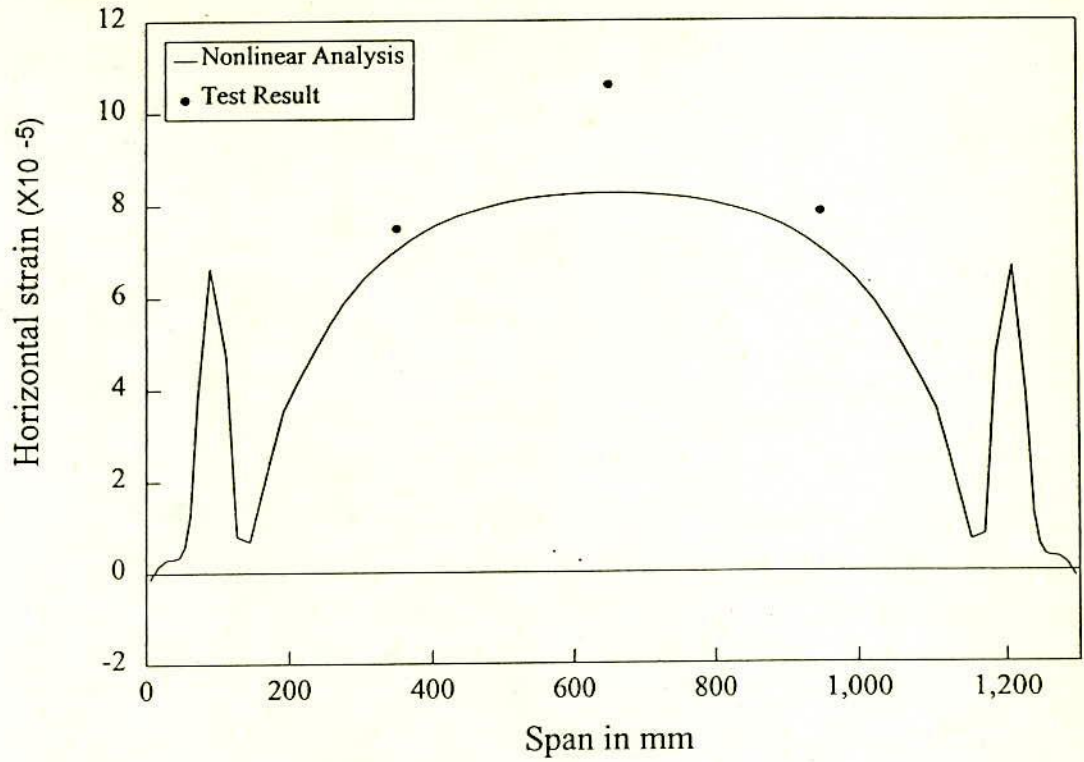


(b) Wall-beam with Frame (Load = 45 kN)

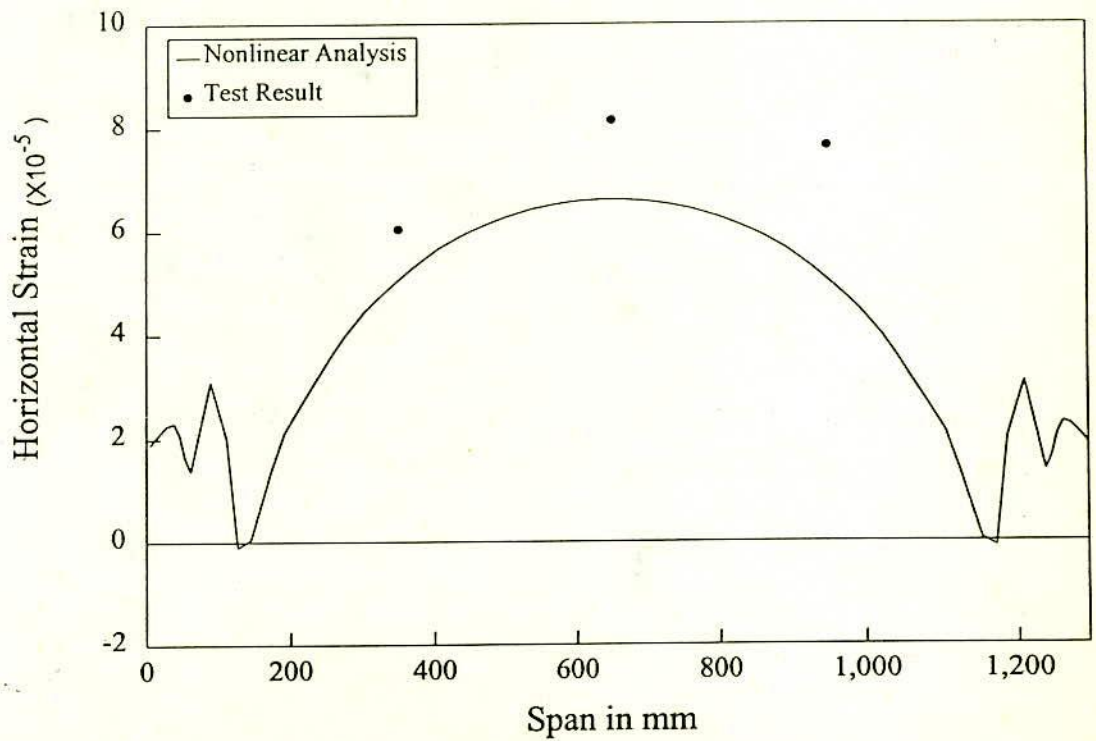


(c) Plane Wall-beam (load = 45kN)

Fig. 7.12 Vertical Strain at First Brick Course



(a) Plane Wall-beam (Load = 112 kN)



(b) Wall-beam with frame (Load = 112 kN)

Fig. 7.13 Horizontal Strain at Supporting Beam

7.6 SUMMARY.

This chapter has described the verification and refinement of a finite element model for the analysis of wall-beam structure subjected to static load. Different types of panels were tested to produce variations in behaviour and different failure modes. The tests were simulated using the proposed non-linear finite element models and the results compared. Two different finite element models were used using the smeared cracking approach. The first model (Model 'A') used a brittle collapse model in the post-failure region and the second model (Model 'B') was a refinement of the first one, which utilised tension softening in the post-failure region.

In general the agreement between theory and experiment was good, thus indicating that the proposed material model developed in chapter 4 and chapter 5 is realistic. The final finite element model (Model 'B') is capable of predicting the initial cracking load, the failure load and the failure pattern with reasonable accuracy and thus can be considered appropriate for static load analysis on wall-beam structure.

Model 'B' has been adopted for the remainder of this investigation. A parametric study of the relative importance of the various properties used to define the model is carried out in chapter 8. The model is then used in chapter 9 to analyze the behaviour of story height walls subjected to uniformly distributed load to allow design recommendations to be derived.

All panels failed by the development of few dominant inclined cracks. Hence, the capability of the finite element model to reproduce other types of failure (such as stepped type of failure for racking load) was not verified by these tests. The applicability of the model to other types of loading was considered to be outside the scope of this study.

Horizontal and vertical strains at discrete locations were compared with the predicted strains. Considerable joint cracking occurred within low range of applied load. Therefore comparison was made between experimental and predicted strains within low range of applied loads and the agreement was found to be reasonable.



CHAPTER 8

SENSITIVITY ANALYSIS OF CRITICAL PARAMETERS

8.1 INTRODUCTION

The finite element model developed in chapter 6 incorporated the material model derived from tests on individual components and small brick masonry specimens (chapter 4). The accuracy of the material model and the validity of the finite element program have been verified by carrying out experiments on wall-beam structures as described in chapter 7. Although the results of the tests compared well with the prediction of the finite element model, the relative importance of the parameters used to define the finite element model needs to be investigated to determine which parameters are particularly significant. In this chapter a study of the parameters affecting the non-linear fracture analysis of wall-beam structures subjected to uniformly distributed vertical load has been performed. Individual parameters are changed in turn and the influence of each change is investigated.

Two groups of parameters are considered for this sensitivity analysis. One which affect the material model and the other which relate directly to the finite element analysis. The main parameters which directly affect the material model are the elastic properties; the joint thickness; the tensile strength of the brick; the tensile strength of the mortar and the joint bond failure criterion.

The second group consists of the parameters which do not affect the material model directly but affect the non-linear fracture analysis. These are the type of element; the element size and the boundary conditions. In all the analyses, comparisons are made on the basis of ultimate load and the final failure patterns.

8.2 PARAMETERS AFFECTING THE MATERIAL MODEL

8.2.1 Influence of Elastic Properties of the Constituents

The properties of constituent materials used in the previous chapter were obtained from laboratory tests. These values are referred to as values of original material model. It was assumed that for practical cases properties of materials will remain within the limit bounded by 50 % lower and higher than the values of

original material model. Values thus obtained were taken for parametric study carried out in this chapter.

The influence of elastic properties was studied by varying both the Young's Modulus and Poisson's ratio of the constituents. Only one parameter was varied at a time. A summary of the values used and the corresponding failure load in each case is given in Table 8.1

The ultimate load of the panel was influenced by changes in the value of modulus of elasticity of some of the constituents. However the mode of failure was not significantly affected. The final failure pattern for different values of E_b/E_m and ν are shown in Fig. 8.1 and Fig. 8.2. Due to symmetry the ultimate failure pattern of half of the panel has been shown. For comparison, the failure pattern of original model is also shown in Fig. 8.1(d). In all the cases the crack started from the vertical joints near the support and then propagated through the bed joints and the bricks. The ultimate load for each case is given in Table 8.1

The influence of the value of the Young's modulus of mortar, and hence the modular ratio of brick and mortar (E_b/E_m) on the ultimate strength of the wall-beam panel can be seen from Table 8.1. An increase of 100 % in the value of E_b/E_m ($E_b/E_m = 11$, obtained by decreasing the value of E_m only) resulted in a decrease of 10 % of the ultimate load. When E_b/E_m is reduced by 50 % ($E_b/E_m = 2.74$) by increasing the value of E_m the ultimate load increases by 34 %. On the contrary, E_b/E_m can also be changed by changing the modulus of brick. When E_b/E_m is reduced by 50 % ($E_b/E_m = 2.73$) by decreasing the modulus of elasticity of brick the ultimate load decreases by 16 % which shows that different combination of modulus of brick and mortar will lead to different failure loads in spite of the fact that combinations may have the same value of modular ratio. Therefore, for realistic comparison of the effect of modulus of elasticity of brick and mortar on the ultimate load carrying capacity of the wall-beam structure the use of the ratio of these two parameters known as modular ratio (E_b/E_m) is likely to mislead the interpretation. Rather these parameters should directly be related to the ultimate load capacity. It is also seen from Table 8.1 that the reduction of modulus of elasticity of concrete if reduced by as much as 31% reduces the ultimate load by only 2 %. Therefore this parameter is considered not to have any major effect on ultimate capacity of wall-beam structure.

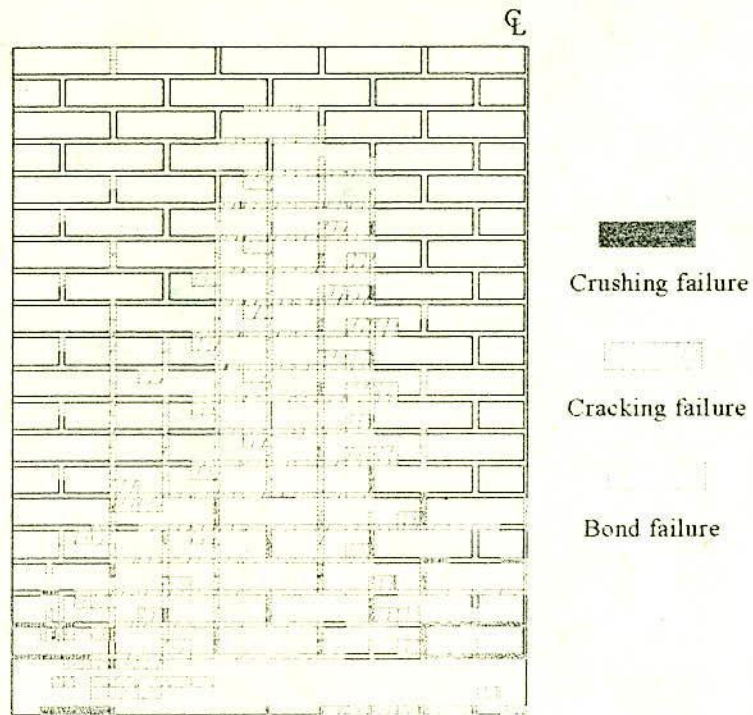
Table 8.1 Parametric Study of Elastic Properties

Material	Poisson's Ratio (ν)			E (MPa)			$\frac{E_b}{E_m}$	Pu (kN)	$\frac{P_u}{P_u^*}$
	Mortar	Brick	Concrete	Mortar	Brick	Concrete			
Concrete	*	*	0.12	*	*	*	*	364	0.98
	*	*	0.24	*	*	*	*	364	0.98
	*	*	*	*	*	23256	*	342	0.92
	*	*	*	*	*	19655	*	342	0.92
Mortar	0.273	*	*	*	*	*	*	431	1.16
	0.136	*	*	*	*	*	*	335	0.90
	*	*	*	1635	*	*	11	335	0.90
	*	*	*	6540	*	*	2.74	497	1.34
Brick	*	0.104	*	*	*	*	*	342	0.92
	*	0.208	*	*	*	*	*	356	0.96
	*	*	*	*	13425	*	4.1	371	0.99
	*	*	*	*	8950	*	2.73	312	0.84
	0.182*	0.139*	0.16*	3270*	17900*	28600*	5.47*	372*	

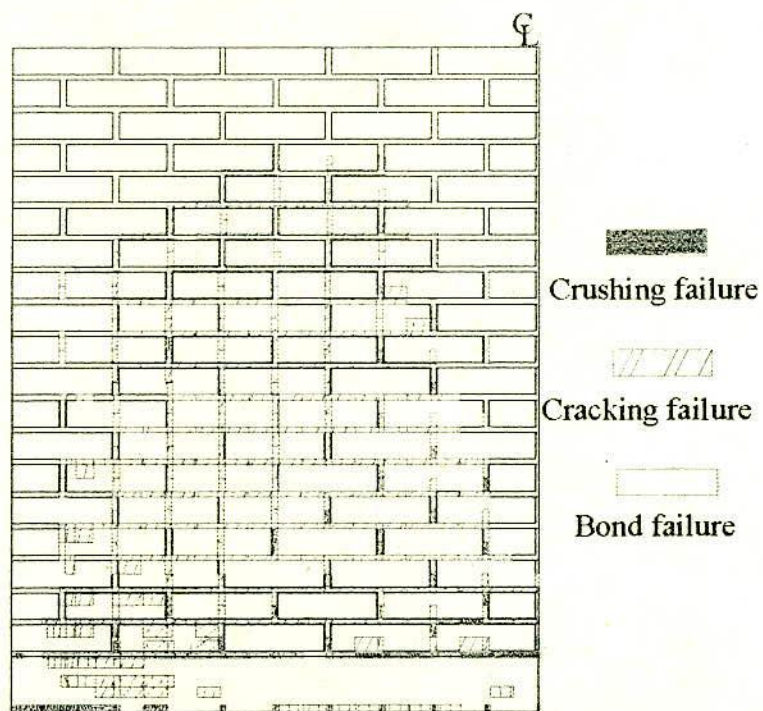
* Indicates the value of the original Material Model

The influence of Poisson's ratio is less significant in general (see Table 8.1 and Fig. 8.2). A minor influence was observed due to variation of the Poisson's ratio of mortar. When ν of mortar was reduced by 25% the ultimate load decreased by 10% and due to 50% increase of ν the ultimate load increased only by 16%.

It can be considered therefore that the analysis of wall-beam structure is not sensitive to all the elastic parameters of its constituents in general. The approximation made in the original evaluation of the elastic material properties in chapter 4 therefore seems justified. Poisson's ratio greater than 0.3 was not considered for this study because of the limitations of the element characteristics.

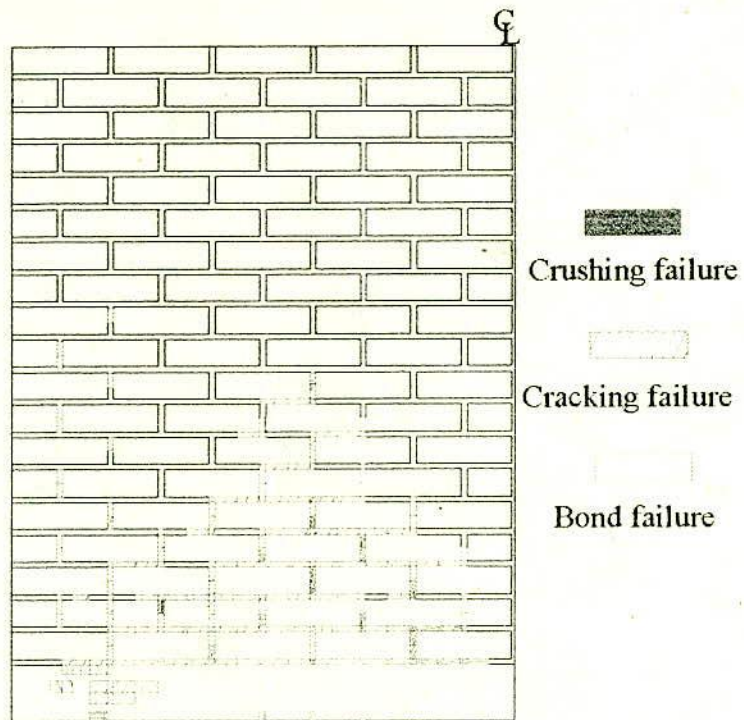


(a) $E_b/E_m = 11$ ($E_b = 17900$ MPa, $E_m = 1635$ MPa)

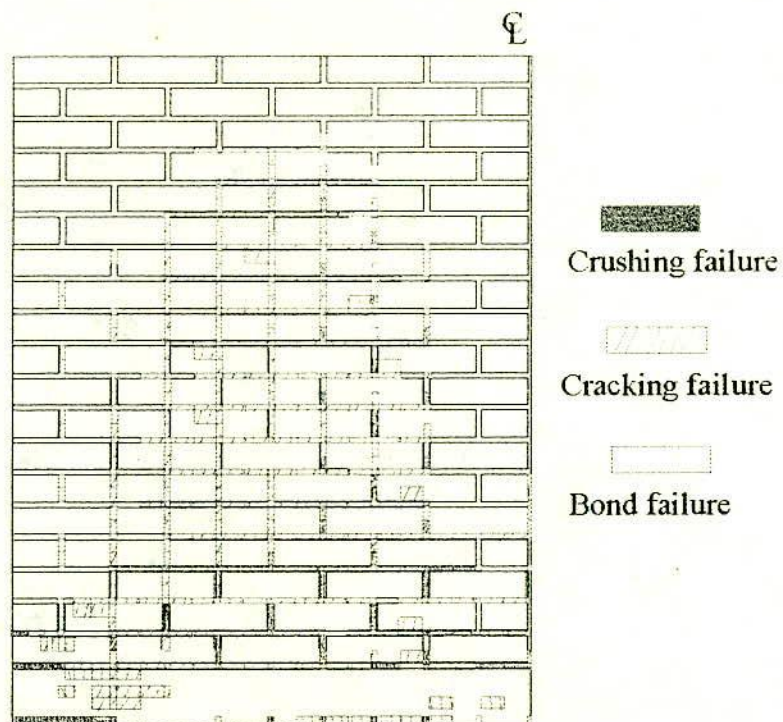


(b) $E_b/E_m = 2.74$ ($E_b = 17900$ MPa, $E_m = 6540$ MPa)

Fig. 8.1 Ultimate Failure Pattern of Wall-beam for Different Values of E_b/E_m

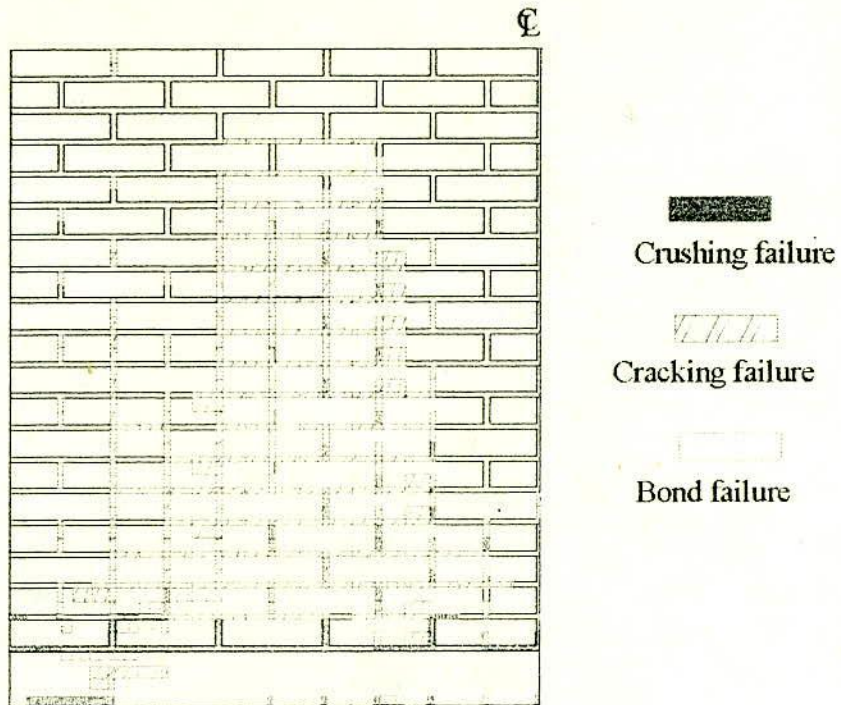


(c) $E_b/E_m = 2.74$ ($E_b = 8950$ MPa, $E_m = 3270$ MPa)

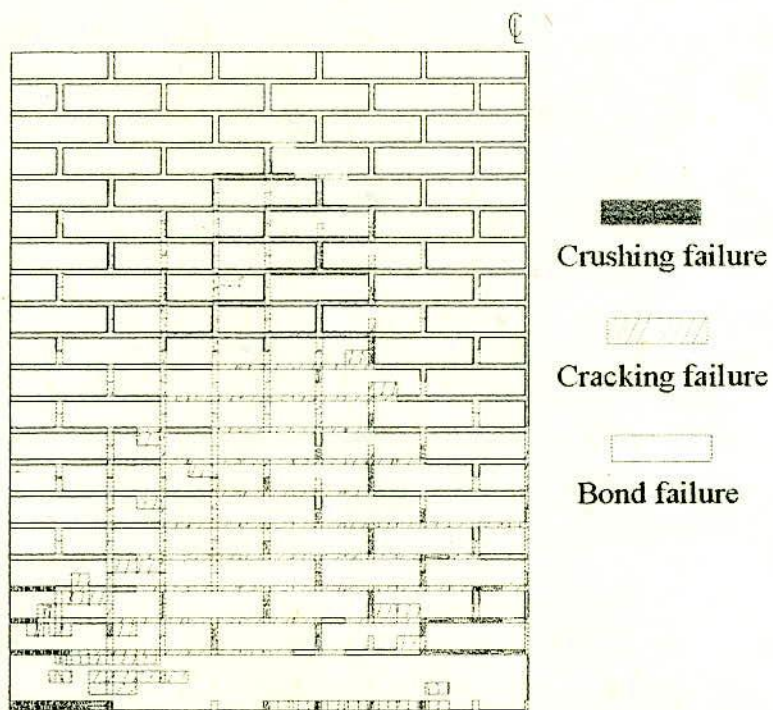


(d) $E_b/E_m = 5.47$ MPa (original model)

Fig. 8.1 Ultimate Failure Pattern of Wall-beam for Different Values of E_b/E_m



(a) Poisson's Ratio of Brick = 0.104



(b) Poisson's Ratio of Mortar = 0.273

Fig. 8.2 Ultimate Failure Pattern of Wall-beam for Different Values of Poisson's Ratios

8.2.2 Influence of Joint Thickness

Variations in joint thickness (and hence brick thickness/Joint thickness, T_b/T_m) have similar effects to the variations in the modulus of brick and mortar, since both vary the relative contribution of the two constituents. This was shown by the analysis of the panel described in section 8.2.1. The joint thicknesses considered in this case were 5 mm, 10 mm, and 12 mm resulting in a thickness ratio of the brick and the mortar (T_b/T_m) of 7.2, 3.6, 3.0 respectively. The original joint thickness was 7.5 mm ($T_b/T_m = 4.8$). The ultimate load of the panel for different joint thickness is given in Table 8.2. Final failure patterns for some of the panels are shown in Fig. 8.3.

The results of Table 8.2 show that the ultimate strength of the panel decreased with the increase of joint thickness. However, within the practical range the effect was insignificant. A 50 % increase in the T_b/T_m ratio ($T_b/T_m = 7.2$) resulted in a 7% increase of ultimate strength while 25 % decrease in the T_b/T_m ($T_b/T_m = 3.6$) resulted in a 15 % decrease of ultimate strength. From the above comparisons it seems that for higher values of T_b/T_m (i.e. with lower mortar thickness) the wall-beam panels carry higher loads. However, the excessive reduction of mortar joint thickness may not satisfy the mason's requirements. This fact will lead to an optimum ratio of T_b/T_m for a particular thickness of brick unit.

Table 8.2 Influence of Joint Thickness

Joint Thickness (mm)		T_b/T_m	P_u (kN)	P_u/P_u^*
Horizontal	Vertical			
5	5	7.2	400	1.07
7.5*	7.5*	4.8*	372*	
10	10	3.6	317	0.85
12	12	3	298	0.80
7.5	3.75	4.8	349	0.94
7.5	12	4.8	305	0.82

* Indicates the value of the panel using original material model

Again for a particular thickness of bed mortar the influence of thickness of vertical joint (dominant plane of weakness) was studied by varying the thickness of

vertical mortar joint as shown in Table 8.2. From comparison it seems that within practical range the effect was insignificant.

In all the cases the failure started from the vertical joints near the support and then propagated through the bed joints and the bricks. A mode of failure similar to that predicted for original beam ($T_m = 7.5$) was observed (see Fig. 8.1(d) and Fig. 8.3).

8.2.3 Influence of Brick Tensile Strength

The influence of tensile strength of brick was studied by increasing and decreasing the original tensile strength of brick while holding all other parameters constant. Three different strengths and the original value were studied and summarised in Table 8.3 (together with ultimate loads). Final failure patterns are shown in Fig. 8.4. For comparison, the failure pattern for the original model has also been shown. As would be expected, changes to tensile strength of the brick affected the ultimate strength of the panel. This is evident because for this type of loading on wall-beam structure, failure involves tensile failure of both brick and joint. Results of Table 8.3 show that a 100 % increase in brick tensile strength resulted in 38 % increase in panel ultimate strength, and a 50 % decrease in brick tensile strength resulted in a decrease of 20 % in the ultimate strength.

Table 8.3 Influence of Tensile Strength of Brick

Tensile Strength (MPa)	Ultimate Load, P_u (kN)	P_u/P_u^*
3.24*	372*	
1.62	297	0.8
4.86	490	1.31
6.48	513	1.38

* Indicates the value of the original Material Model

The higher tensile strength of brick did not influence the mode of failure appreciably. However, in case of a brick with a lower tensile strength several elements cracked simultaneously at the crack front in a band of several elements wide.

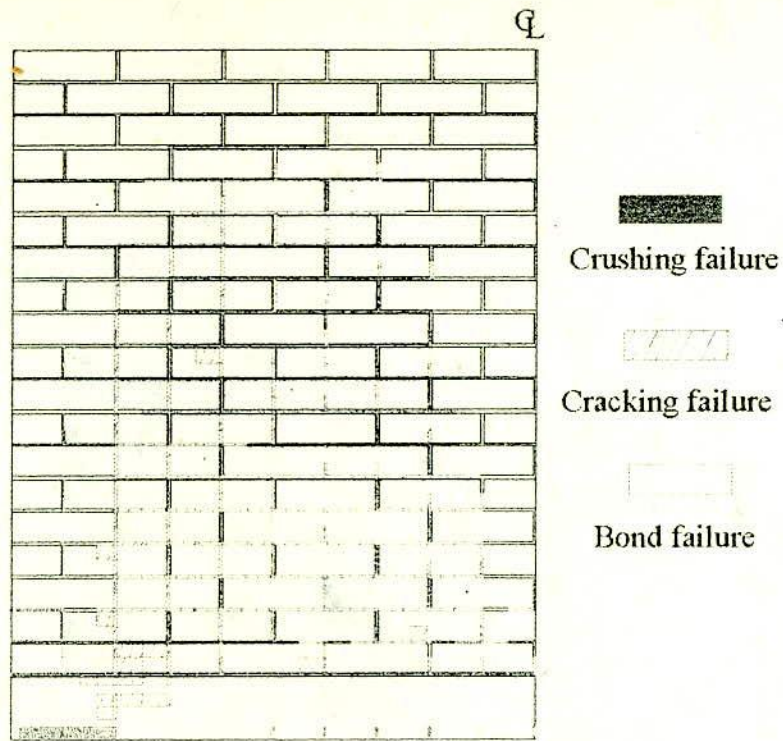
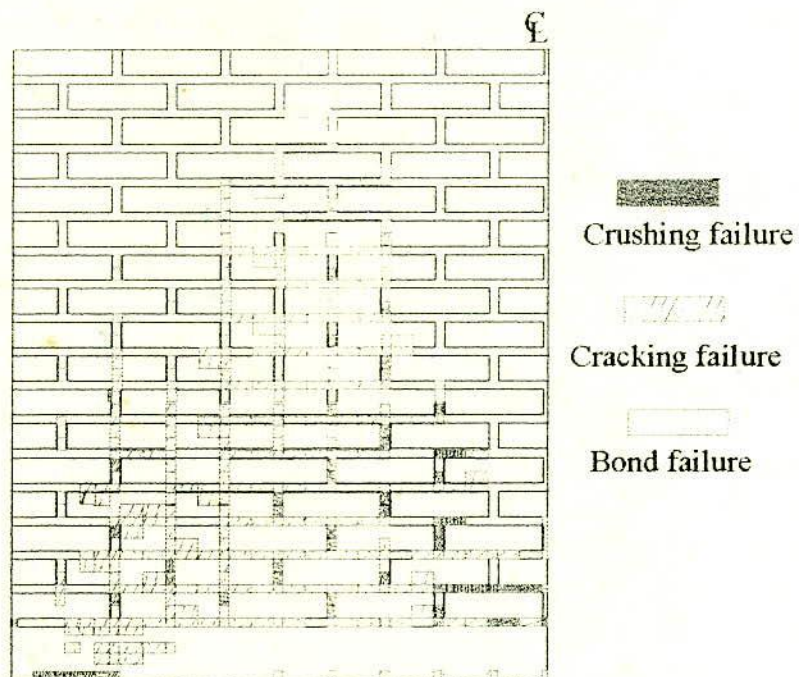
(a) $T_b/T_m = 7.2$ (b) $T_b/T_m = 3.0$

Fig. 8.3 Ultimate Failure Pattern of Wall-beam for Different Values of Joint Thickness

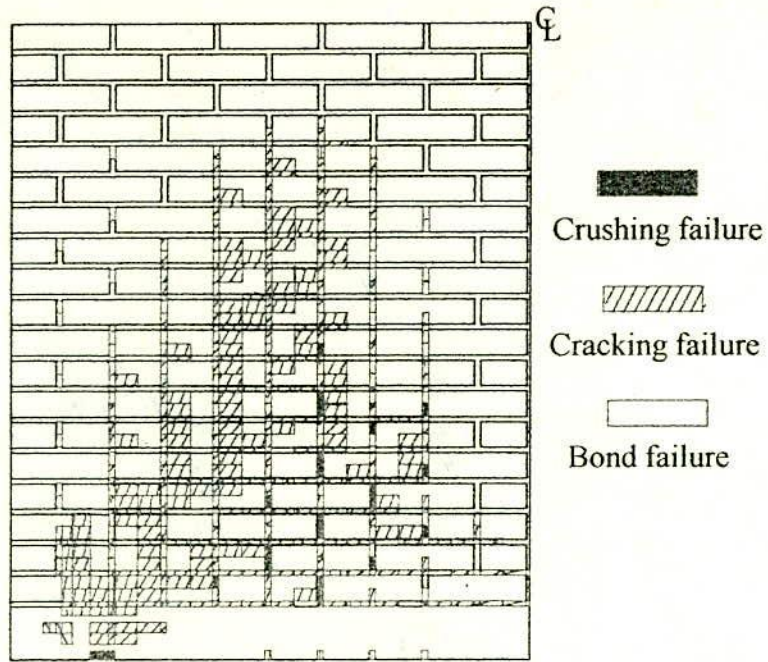
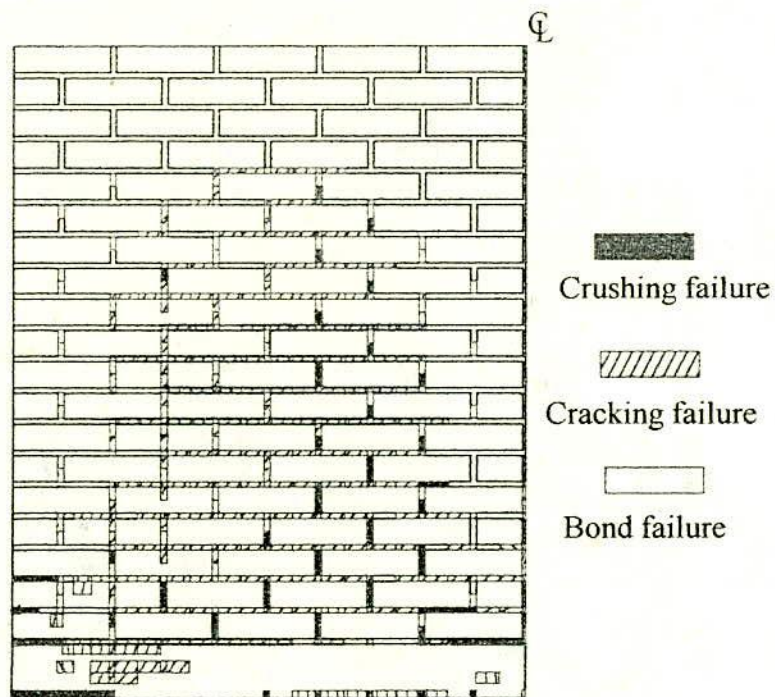
(a) $f_t(\text{brick}) = 1.62 \text{ MPa}$ (b) $f_t(\text{brick}) = 6.48 \text{ MPa}$

Fig. 8.4 Ultimate Failure Pattern of Wall-beam for Different Values of Tensile Strength of Brick

From the results, it can be concluded that the model is sensitive to this parameter. Therefore, the tensile strength of the brick should be incorporated if any design equation is deduced for ultimate load carrying capacity of wall-beam structure. Care should also be taken to evaluate this property during the experimental investigation.

8.2.4 Influence of Mortar Tensile Strength

In a vertically loaded wall-beam structure the initial failure typically occurs at the interface of vertical joints and the bricks. At higher loads tensile failure of mortar joints and bricks takes place. The tensile strength of mortar therefore is expected to exert a major influence on panel behaviour.

The influence of the tensile strength of mortar on the behaviour of the wall-beam panel was studied by increasing and decreasing the tensile strength of the mortar whilst keeping all other properties constant. The failure load of the panel for different values of tensile strength of the mortar is given in Table 8.4. Final failure patterns are shown in Fig. 8.5.

It is interesting to note that the ultimate strength of the wall-beam panel increases significantly due to increase of tensile strength of mortar joint. The results of Table 8.4 show that a 50 % increase in mortar tensile strength resulted in 42 % increase of panel strength. The failure pattern in this case is similar to the failure pattern predicted by the original model. It is also observed from Table 8.4 and from Fig. 8.5 that the ultimate behaviour of the panel changes due to decrease of tensile strength of mortar joint. The table shows that a 25 % decrease in the value of tensile strength resulted in 18 % decrease of ultimate strength. Due to significant reduction in mortar tensile strength, almost all of the bed joints and some of the vertical joints experienced a material tensile failure rather than a bond failure. Therefore, it can be concluded that mortar tensile strength is also a significant parameter. The accurate evaluation of this parameter is therefore necessary. This parameter also should be incorporated if any design equation is deduced for ultimate load carrying capacity of the wall-beam structure. It was mentioned earlier that the mortar tensile strength was obtained using splitting test on a prism. But the in-situ tensile strength of the mortar in a joint which will have lower water-cement ratio due to brick suction likely to have higher tensile strength. This could be one explanation for the model under-predicting the strength of the panel in Chapter 7.

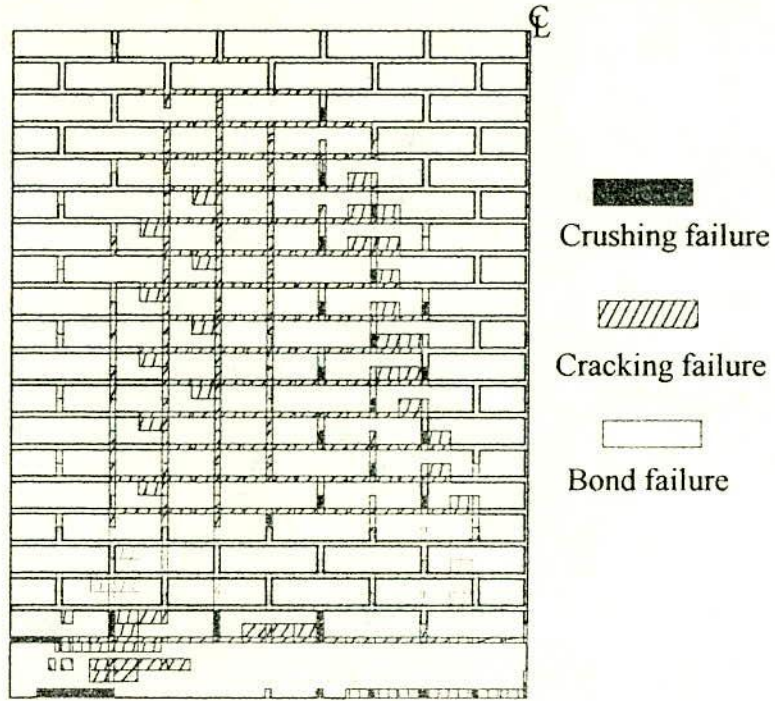
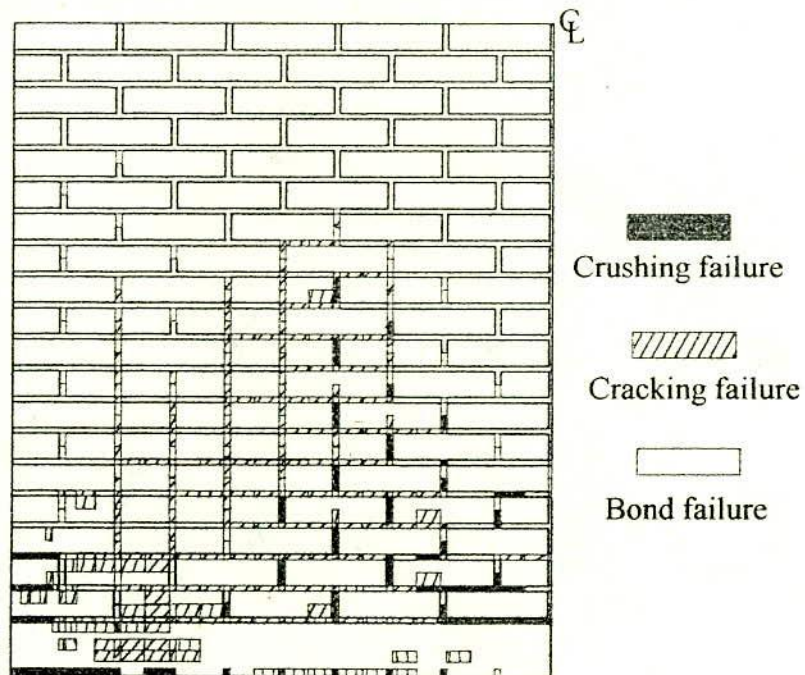
(a) $f_t(\text{mortar}) = 0.73 \text{ Mpa}$ (b) $f_t(\text{mortar}) = 1.45 \text{ Mpa}$

Fig. 8.5 Ultimate Failure Pattern of Wall-beam for Different Values of Tensile Strength of Mortar

Table 8.4 Influence of Tensile Strength of Mortar

Tensile Strength (MPa)	Ultimate Load, Pu (kN)	Pu/Pu*
0.97*	372*	
0.73	305	0.82
1.45	527	1.42

* Indicates the value of the original Material Model of panel in Chapter 7.

8.2.5 Influence of Bond Strength of Mortar Joint.

The influence of joint bond strength was studied by increasing and decreasing the bond strength while keeping all other parameters constant. The initial cracking load and ultimate load are shown in Table 8.5.

From the table it can be seen that initial cracking load is highly sensitive to this parameter. The initial cracking load of the panel is directly related to the bond strength of the mortar joint. Within practical limits of the bond strength the initial cracking load of the panel increases with the increase of bond strength and decreases with the decrease of bond strength of the mortar joints.

Table 8.5 Influence of Bond Strength

Tensile Bond Strength (MPa)	Shear Bond Strength (MPa)	Pc (kN)	Pu (kN)
1.443*	0.594*	59.6*	372*
1.082	0.446	44.68	350
1.804	0.7425	74.5	364
2.164	0.894	89.36	357

* Indicates the value of the original Material Model

From the table it is seen that although the initial cracking load is influenced by this parameter, the ultimate load carrying capacity of the wall-beam panel is found to be insensitive to this parameter. The vertical mortar joints which are the

dominant planes of weakness in the masonry part of wall-beam structure are always the prime seat for initial cracking, particularly near the support. The initial cracking is due to interface bond failure of vertical joints.

As it is seen from the table that a reduction in joint bond strength by 25 % produced a corresponding reduction of 6 % in the ultimate load carrying capacity of the panel (Failure load = 350 kN). The ultimate load of the original panel was 372 kN. The failure mode did not change appreciably in this case (see Fig. 8.6). On the other hand a 25 % increase in bond strength decreased the ultimate load of the panel by 2%. The variation is insignificant.

Ali (1987) carried out an elaborate study by biaxial test and finite element analysis on brick triplet and concluded that the approximate bond failure criterion is conservative in comparison to the exact bond failure surface which considers the effect of parallel stress on shear strength. This exact bond failure criterion could not be adopted in this study due to lack of biaxial tension-compression test values. It should be mentioned here that the bond failure criterion used in this study is linear and an approximate one which is determined from simple laboratory tests discussed in Chapter 4.

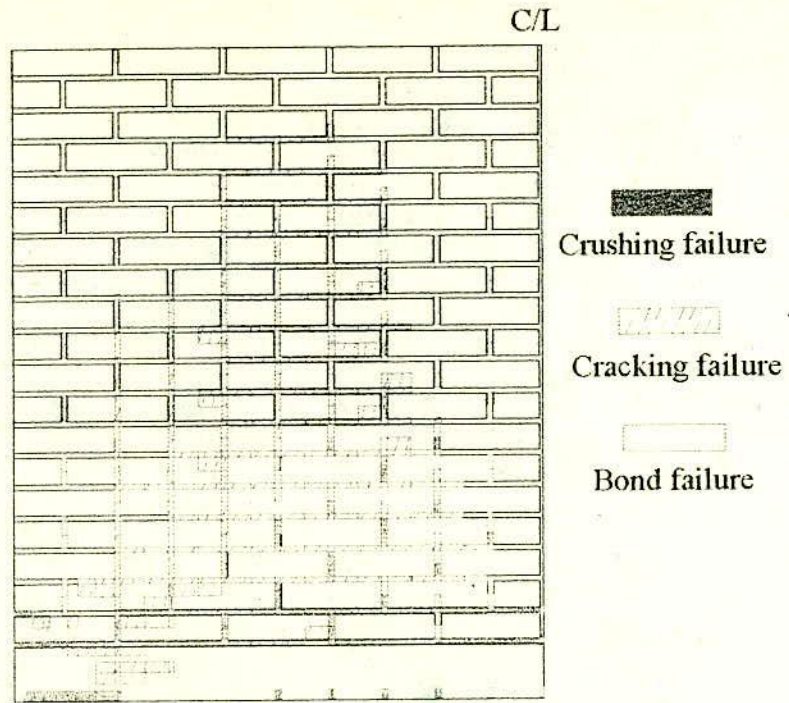
It can be concluded therefore that accurate estimation of the bond properties of the joint is required if realistic prediction of the initial cracking load of wall-beam panels subjected to uniformly distributed load are to be made. However, this parameter is less sensitive to the ultimate load of the panel.

8.3 PARAMETERS AFFECTING THE FINITE ELEMENT ANALYSIS

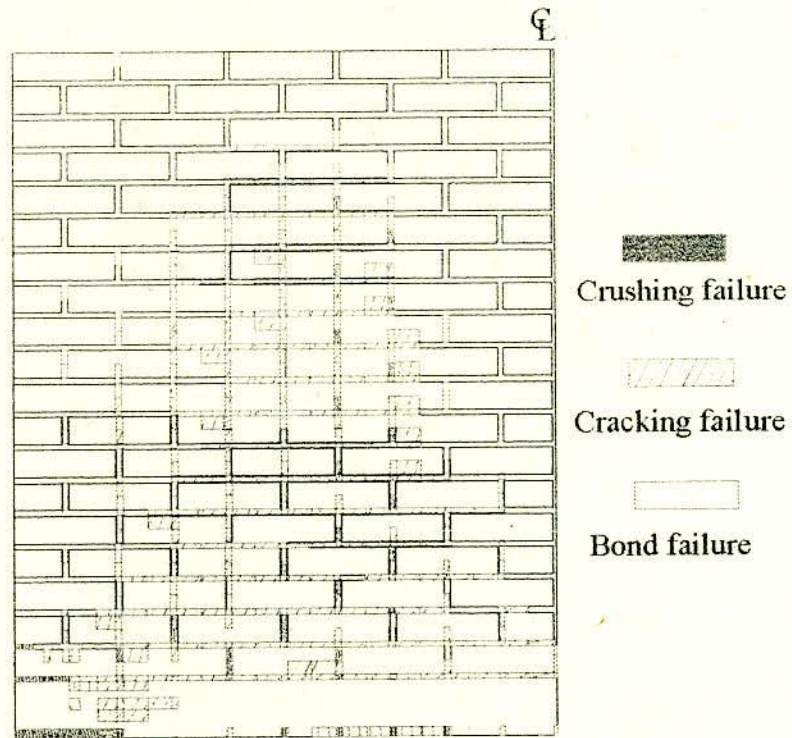
In general the result of a finite element analysis can be significantly influenced by the characteristics of the model itself. Element type and size and assumed boundary conditions, etc. can have an influence, with a subsequent distortion of the results. These aspects are investigated in this section.

8.3.1 Element type, Size and Subdivisions

In recent years the trend has been towards the use of higher order finite elements, particularly isoparametric elements. The adoption of more elaborate elements allows the use of a larger element size, but the computing time can be increased in comparison. The influence of element type on the ultimate strength of the masonry wall was investigated by Ali(1987) by comparing the performance of 8 noded isoparametric element and the 4 noded linear element. He concluded that



(a) 25% Decrease in Bond Strength ($P_u = 350$ kN)



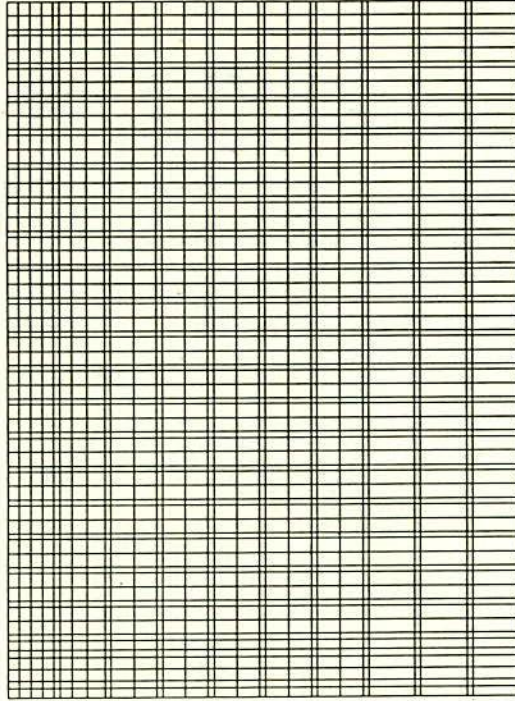
(b) 50% Increase in Bond Strength ($P_u = 357$ kN)

Fig. 8.6 Ultimate Failure Pattern of Wall-beam for Different Values of Bond Strength of Mortar Joint

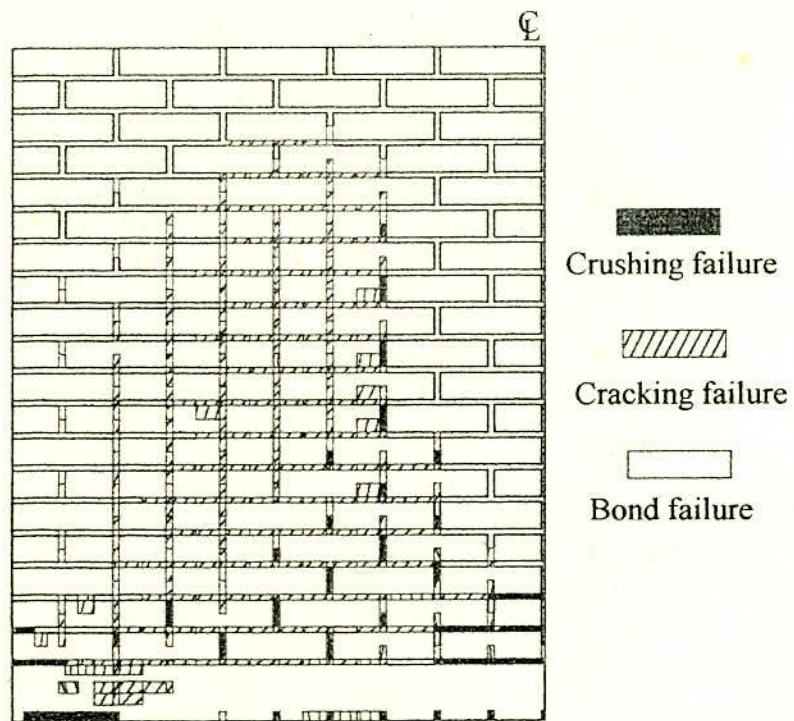
the use of more elaborate elements in this case does not appear to be warranted. Similar findings were obtained by Bazant and Cedolin (1980), when element types were compared in the fracture analysis of plain concrete. Particularly for non-homogeneous analysis of wall-beam structure comparatively small finite elements have to be chosen for discretization of joints. In addition to this the high stress gradient near the support warrants the selection of finer meshes in this zone. Considering these practical reasons higher order element has not been adopted in this study.

The influence of the element size on the non-linear fracture analysis is studied by changing the number of elements in the panel as shown in Fig. 8.7(a) and Fig. 8.7(c). Within the practical range of element numbers there was small difference in the predicted ultimate load. For example due to 14% reduction in number of elements (see Fig. 8.7(a)) the predicted failure load was 368 kN in comparison to the original analysis used in chapter 7 (Failure load 372 kN). A failure pattern similar to that predicted in the original analysis was obtained (see Fig. 8.7(b)). If bigger mesh size is used the predicted failure load increases considerably. For example due to 20% reduction in number of elements (see Fig. 8.7(c)) the predicted failure load was increased by 11% in comparison to the original analysis used in chapter 7. Further reduction of number of elements (bigger element size) will further increase the ultimate load which does not model the actual composite behaviour of wall-beam structure. However, the effect of mesh configuration and element size on the analysis of wall-beam structure made of standard size of brick unit is discussed in details in the next chapter.

When large elements are used, each element has a large influence on structure stiffness. When a single element of large size cracks, the stiffness of the entire element is reduced resulting in the softening of a relatively large portion of the structure. On the other hand large elements tend to be less sensitive to stress concentration than small elements resulting a crack which occurs at a higher load. When small element is cracked although stiffness of the entire element is reduced but being very small does not drastically affect the surrounding elements and the resulting softening is localised which ultimately carry less significant influence on the overall structural stiffness. Again small elements being sensitive to stress concentration undergoes cracking at lower loads. This balance between stress concentration and reduction of stiffness of the fractured elements is the probable cause of apparent effect of mesh size on the prediction of failure load. For analysis of wall-beam structure this fact is also valid when the variations of aspect ratio of the elements are within the usual limit.

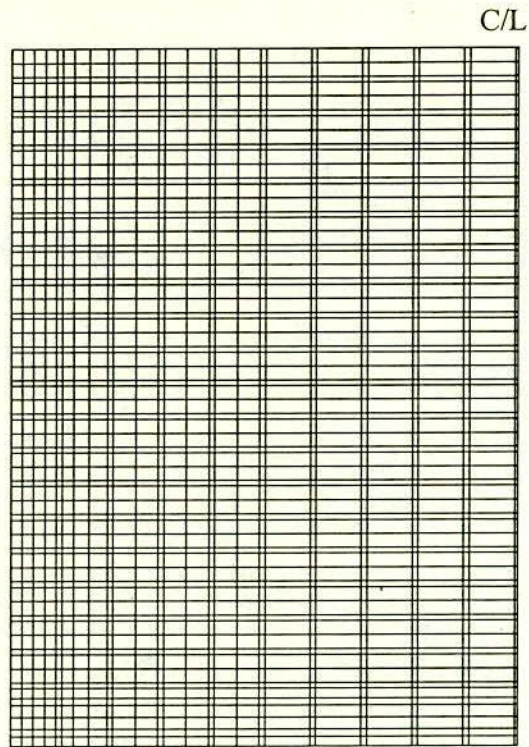


(a) Finite Element Mesh (Number of Elements = 1890)

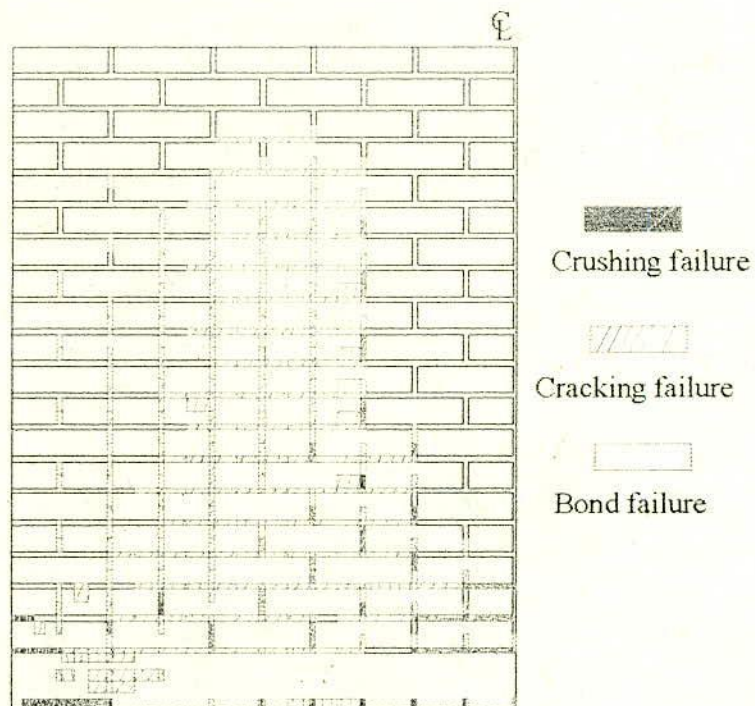


(b) Ultimate Failure Pattern

Fig. 8.7 Influence of Element Size on the Non-linear Fracture Analysis



(c) Finite Element Mesh (Number of Elements = 1764)



(d) Ultimate Failure Pattern

Fig. 8.7 Influence of Element Size on the Non-linear Fracture Analysis

8.3.2 Linear Elastic Fracture Analysis.

This study was carried out to test the possibility of assuming linear elastic properties for all the constituents of the wall-beam structure in the finite element model. This has significant advantages in computing efficiency. Bricks, mortar and the concrete were assumed to remain linearly elastic in this case. Therefore, the progressive cracking is the only source of non-linearity in this case. Accordingly, an analysis of the wall-beam panel was carried out with the elastic properties of brick, mortar and concrete. The ultimate load in this case was 335 kN which is 10% lower than that of original analysis. The failure pattern is shown in Fig. 8.8. For comparison the failure pattern predicted by the original model can be seen from Fig. 8.1(d).

This sensitivity of the parameter could be due to the nature of the test adopted in the investigation. A considerable portion of the panel for this type of loading is subjected to biaxial compression and hence deforms in-elastically (see Fig. 3.19(e)). Since the zone affected by the biaxial compression corresponds to the zone of low stress gradient this sensitivity due to inelastic deformation is not of considerable amount. Therefore, it reveals from the foregoing discussion that the effect of material non-linearity is not of great importance for the analysis of wall-beam structure. Previous investigators have shown that the effects of cracking tend to have a much greater influence on the non-linear behaviour than the material deformation characteristics (Page, 1978, 1979 and Dhanasekar, 1985).

From this study it can therefore be concluded that the stress-plastic strain equations are not seriously important to predict the behaviour of wall-beam panels subjected to uniformly distributed load and that a linear elastic fracture model may be considered useful for wall-beam analysis. It can be noted here that under service condition the brickwork is stressed only to a fraction of its ultimate load. Therefore, the deduction of empirical equations based on elastic analysis can be considered as a useful aid for design purpose. The related derivations and their comparison with other authors are discussed in the next chapter.

8.3.3 Boundary Conditions

In this section the influence of the effects from boundary conditions on the ultimate behaviour of the panel is investigated. The same panel and the material model as described in section 8.2 were adopted for this study.

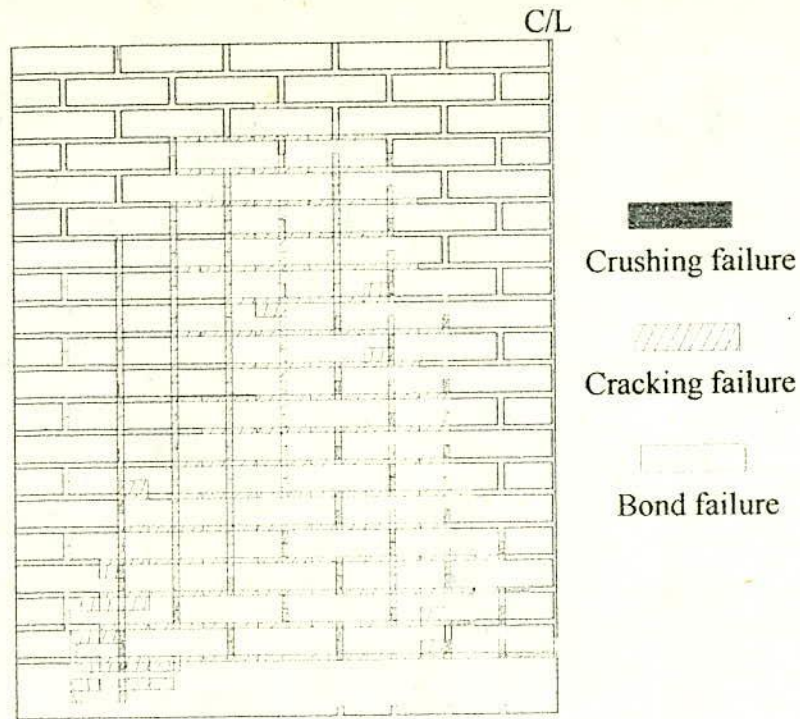
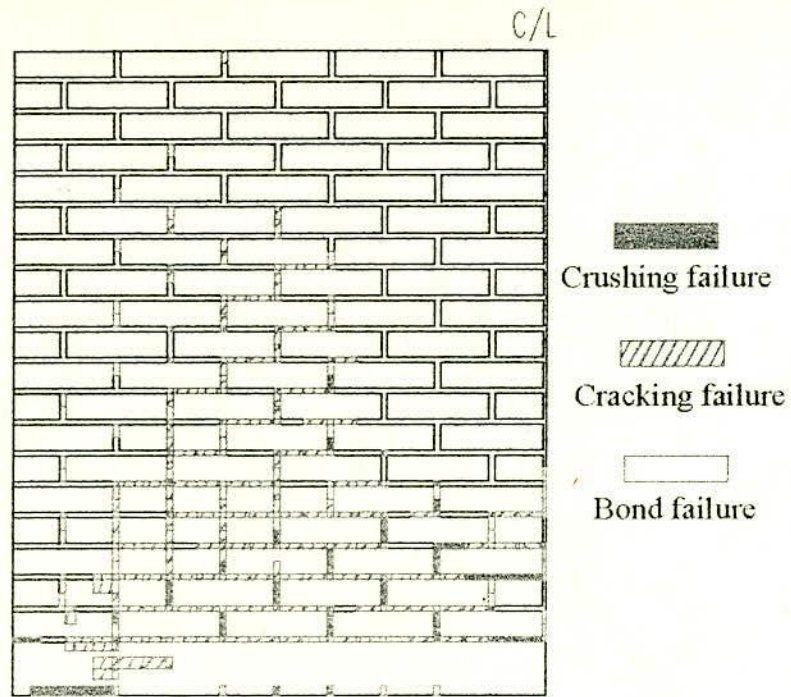


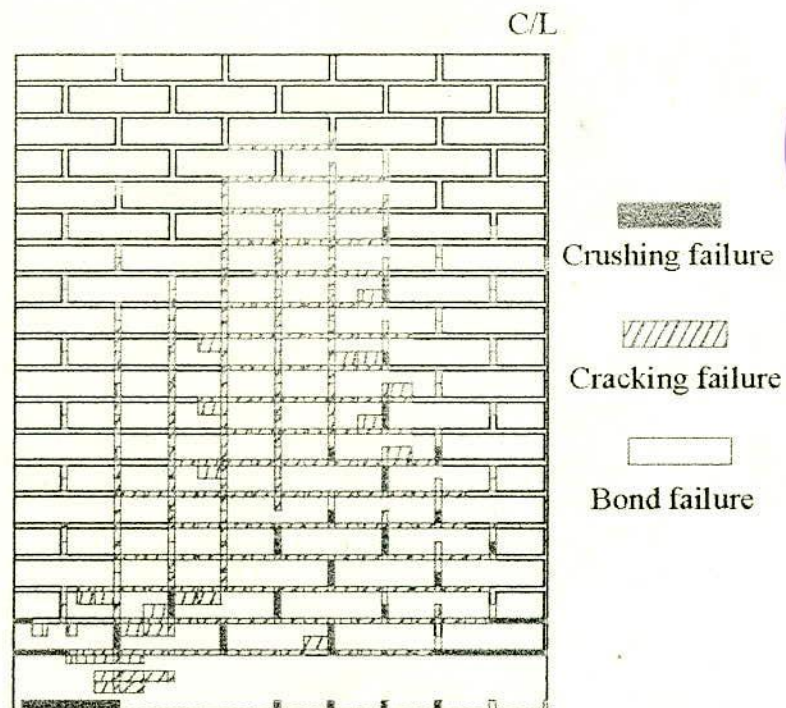
Fig. 8.8 Ultimate Failure Pattern of Wall-beam in Case of Linear Fracture Analysis

Two separate analyses were performed. In the first case nodes at the base of the support unrestrained horizontally, and with the nodes at the interface of the loading plate and the panel restrained against horizontal movement. In the second case nodes at the base of the support was restrained horizontally while the nodes at the interface of the loading plate and the panel unrestrained against horizontal movement. The ultimate load and the final failure pattern are shown in Figure 8.9. For comparison see the failure pattern predicted by the original model as shown in Fig. 8.1(d).

It is seen that for the first case there is no significant difference in the failure load or failure patterns when compared with the original model (see Fig. 8.9). The ultimate load in this case was decreased only by 6%. In the second case the crack propagation was slower at the interface of the wall and the beam since the base of the panel was restrained against horizontal movement and the failure load also increased by 30% (see Fig. 8.9). The differences between the second case and the original model appear to be quite significant and is not adopted in this study. The above discussion therefore reveals that modelling of boundary conditions of the test used to verify the original finite element model is not particularly sensitive to



(a) Loading Surface Restrained Horizontally ($P_u = 349.6$ kN)



(b) Base Restrained Horizontally ($P_u = 482.8$ kN)

Fig. 8.9 Ultimate Failure Pattern of Wall-beam Panel for Different Boundary Conditions



lateral restraint at wall top and loading plate which may have been applied by testing apparatus. The boundary conditions assumed in chapter 7 therefore appear to be reasonable.

8.4 SUMMARY

In this chapter the finite element program with intermediate collapse model was used to study the relative importance of the various parameters used to define the non-linear fracture model. Two groups of parameters were considered for this investigation. The first group were the parameters which directly affect the material model and the second group were parameters which affect the finite element analysis. Since the investigation has been confined to the behaviour of the wall-beam panels subjected to uniformly distributed vertical load, the conclusions will relate specifically to the behaviour of wall-beam structure, although some of the conclusions will apply to masonry in general. The following conclusions can be drawn:

1. The ultimate strength of the panel increases with the increase and decreases with the decrease of modulus of elasticity of brick and mortar. The final failure pattern of the panel was not influenced significantly by this parameter. The experimental evaluation of these parameters as described in Chapter 4 is therefore justified.
2. The ultimate strength of the panel increases with the decrease of joint thickness and decreases with the increase of joint thickness, but within practical range this change is not of significant extent.
3. The tensile strength of the brick influenced the load carrying capacity of the panel. The lower the tensile strength of the brick the lower is the ultimate load of the panel. This parameter is important since the crack propagates through the bricks when the wall-beam structure is subjected to uniformly distributed load. Accurate estimation of this property is important if it is to be used for the prediction of ultimate load carrying capacity of wall-beam structure.
4. The tensile strength of mortar also affected the ultimate strength and failure pattern of the wall-beam panel. The accurate experimental evaluation of this parameter is also essential.
5. The influence of material non-linearity of the constituent materials on the behaviour of masonry is not significant in general when compared to the effects of progressive cracking of the panel. Since a considerable portion of wall-beam panel is subjected to biaxial compression and hence deforms inelastically, the general assumption of elastic behaviour may not represent the actual stress

state of the panel. However, the zone affected by biaxial compression being of low stress gradient the linear elastic-fracture material model may be considered useful for analysing this type of problem if greater accuracy is not warranted.

6. The bond strength of the mortar joint did not influence the ultimate load of the wall-beam panel subjected to uniformly distributed load. However, the initial cracking load of the panel is seriously affected by this parameter. The lower the bond strength the lower the initial cracking load of the panel. Since vertical joints typically experience a bond type of failure, this characteristic is extremely important for the prediction of local failure.
7. A simple linear quadrilateral element with a reasonably fine mesh near the support in the regions of high stress gradient is suggested for the analysis of wall-beam structure. The use of higher order elements in this case is not required since the progressive fracture of the constituent materials is the main source of non-linearity in the vertically loaded wall-beam panel.
8. The influence of the secondary effects from the boundary conditions of the loading plate is negligible. Therefore, the assumptions made for boundary conditions of the original model appear to be reasonable.

CHAPTER 9

PARAMETRIC STUDY AND DESIGN RECOMMENDATIONS

9.1 INTRODUCTION

The assessment of the strength of wall-beam structure subjected to uniformly distributed load is a problem commonly encountered in design. At present the codes do not provide any straight forward equation and available empirical equations are based on limited number of experiments and/or simplified analysis of wall-beam structures. The simplifications are necessary because of the large number of variables involved.

For realistic analysis of the behaviour of story-height wall-beam structure proper constitutive relations and failure characteristics of the constituent materials are required together with efficient numerical method of modelling its behaviour. In this investigation such a material model has been derived and incorporated into a finite element model. A comprehensive parametric study is carried out on story-height wall-beam structure composed of full size brick unit. From the results of this study, design rules incorporating the influence of important parameters are developed and presented in a series of design recommendation. To place this investigation in context, a review of previous research and existing design recommendations is also carried out and compared with the proposed recommendations.

9.2 FINITE ELEMENT ANALYSIS OF STORY-HEIGHT PANEL

This section describes the use of finite element model to carry out detailed parametric study of the behaviour of story-height wall-beam subjected to uniformly distributed load. For efficient execution of the parametric study an appropriate finite element idealisation is necessary in which the important parameters may be easily varied. The typical mesh configuration (see Fig. 6.1) which was used for the analysis of wall-beam made with half sized brick in the previous chapters may not be suitable for the accurate analysis of story-height wall-beam panel made with full size (240 mm X 115 mm X 70mm) brick. For a particular size of any structure, even though the aspect ratio and type of element used being same, the result will vary significantly depending upon the number of nodes and number of elements (Brebbia and Ferrante, 1978). To select a suitable mesh configuration for the

present analyses a comparative study was made with a varying number of elements. A summary of this comparison is given in Table 9.1. It is seen that the failure loads decrease with the increase in the number of finite elements in the mesh. The pattern of convergence is shown in Fig. 9.1. Details of different mesh configuration can be seen from Fig. AV.1 of Appendix V. In the mesh type 'f' of Fig. AV.1 instead of providing finer mesh throughout the height of wall, a relatively coarse mesh was provided at top 1/3 rd height of wall. The failure load in this case was quite comparable (see Table 9.1) with that of the walls having finer meshes althrough the panel. Therefore, a reasonable fine mesh near the support and a coarse mesh layout for the rest of the wall have been adopted for the comprehensive parametric studies.

Once the mesh configuration was finalised a suitable height and span of the wall-beam representative of story-height wall-beam was selected to investigate the influence of main parameters on the moment and tie action in the supporting beam and vertical stress concentration and shear stress concentration at the wall-beam interface. From the results of this parametric study empirical formulae for moment, shear and tie force will be proposed.

Table 9.1 Influence of Number of Elements on Failure Load.

*Mesh Designation	Number of nodes	Number of elements	Failure load (kN)
a	777	720	528
b	1316	1242	482
c	1596	1512	468
d	1995	1904	430
e	2613	2508	430
f	1372	1296	468

* Mesh configurations (a to f) are shown in Fig. AV.1 of Appendix V

9.3 PARAMETRIC STUDY OF STORY-HEIGHT WALL-BEAM PANELS

The important parameters influencing the composite behaviour of walls and their supporting beams have been discussed in the previous chapters. The incorporation of all these variables in a single equation will be very complex for

practical use. Therefore, simplifications have to be made to develop simple equation. However, care has been taken to ensure that such simplifications lead to a rational and conservative estimate of the most important interaction effects.

It is shown by stress analyses in chapter 3 that the interaction between wall and supporting beam is independent of height of the wall-beam when H/L exceeds 0.54. Similar finding was also observed by Wood, (1952). It was

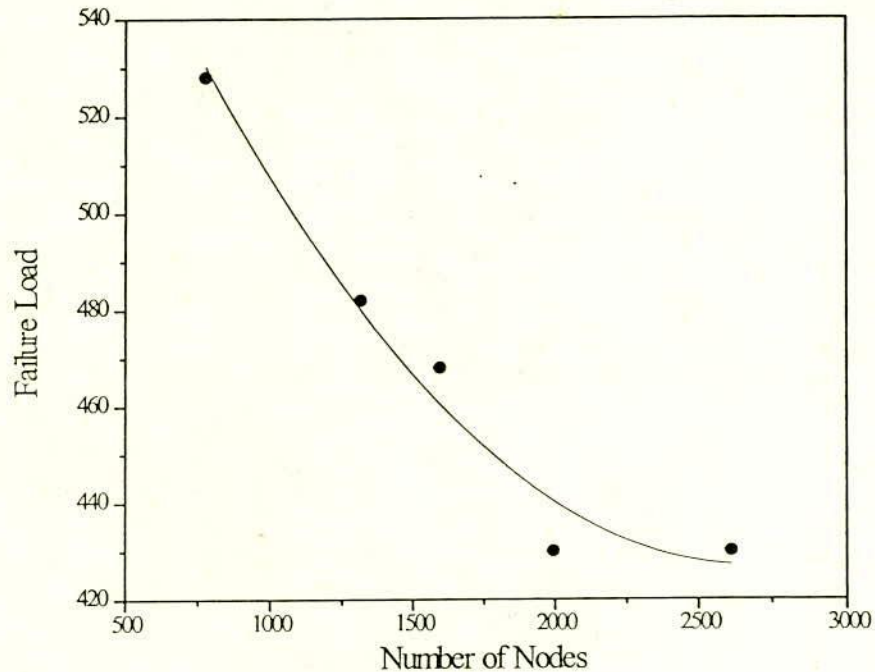


Fig. 9.1 Convergence of Failure Load with Increasing Number of Elements

therefore decided that the arching action be ensured by restricting the minimum height of the wall-beam to be 0.6 times the span. For the design of wall-beam this minimum height of 0.6L is also agreed by other researchers (Burhouse, 1969; Riddington and Stafford Smith, 1978). It was therefore decided that the 0.6L height of the wall-beam would be appropriate and convenient for the deduction of proposed design method. Height of the wall-beam greater than this value does not produce appreciable change in concentration of stresses and will eliminate the risk of sliding along the interface of beam and wall.

It is also shown by stress analyses in chapter 3 that the wall-beam having a normal size opening at the middle of the span behaves like a solid wall-beam

element. This fact is also confirmed by other researchers (Wood, 1952; Riddington and Stafford Smith, 1978).

In practice the support occupies a finite width. The support width along the span of the beam is an important parameter and has a significant effect on the wall-beam interaction which is described in chapter 3. Unlike other researchers due consideration has been given to this parameter in this study. Finally, for the parametric study of story-height panels important variables like the span of the wall, modulus of elasticity of the constituent materials, depth of the supporting beam and the width of the support were considered for a solid wall-beam structure or wall with central opening of normal size. These parameters were varied individually while keeping all other variables constant.

A total of 192 finite element analyses were performed to cover the practical ranges of important variables. A summary of the variables investigated is shown in Table 9.2 (a) to Table 9.2 (c). In all cases the height and thickness of the wall-beams are kept constant. A typical wall-beam is shown in Appendix V. The gravity load and the superimposed load are assumed at the top to act uniformly distributed over the full thickness and length of the wall-beam. From these analyses the maximum tie force, bending moment in the supporting beam and vertical stress and shear stress concentration in the wall have been obtained. These values are then plotted against non dimensional characteristic parameters c_1 and c_2 (discussed later). Thereafter, by means of regression analysis formulae were derived for maximum moment, maximum tie force in the supporting beam and maximum vertical stress concentration and maximum shear stress concentration in the masonry wall. The derivation of design curves and design constants are carried out in the following sections.

9.4 DESIGN ASPECTS OF WALL-BEAM STRUCTURE

The aim of design method is to determine the size of the wall and the beam so as to be economic whilst being adequate to withstand the actions resulting from the arching behaviour. This calls for the actions to be properly identified and then for any particular structure and system of loads, for the magnitude of actions to be estimated on a rational basis.

9.4.1 Deduction of Non Dimensional Characteristic Parameters

Characteristic Parameter c_1

It is seen from the parametric study that the stresses at the interface level of wall and beam of a solid wall-beam are dependent on many important factors. They can be represented by the expression:

$$V_c \propto E_m, E_b, \frac{1}{E_c}, \frac{L}{h}, \frac{L-2B}{L}$$

where, V_c = Maximum vertical stress concentration

E_m = Modulus of elasticity of mortar

E_b = Modulus of elasticity of brick

E_c = Modulus of elasticity of concrete

h = Depth of the supporting beam

B = Width of support at each end in the direction of span

L = Length of supporting beam including support width

The above parameters will be combined together to form a non-dimensional characteristic parameter, c_1 to incorporate the relative stiffness of wall and the supporting beam. Since brick unit and mortar are acting together, their individual modulus of elasticity must contribute toward the combined effect of the resulting material (brickwork). However, the accuracy of incorporation technique of individual stiffness and size effect of brick and mortar will have influence on the modulus of elasticity of brickwork, E_w to be a representative value. In the above expression E_m and E_b can be replaced by a combined modulus of elasticity of masonry wall, (E_w). This E_w can be related with E_m and E_b by an expression given by Kawsar (1991) as shown below:

$$E_w = \frac{E_b}{(\mu + \beta\phi)}$$

where, $\mu = \frac{\alpha}{1+\alpha}$; $\phi = \frac{1}{1+\alpha}$; $\beta = \frac{E_b}{E_m}$ and $\alpha = \frac{T_b}{T_m}$ (T_b and T_m are thickness of brick and mortar respectively). The expression for equivalent modulus of elasticity of masonry was derived from the linear portion of stress-strain deformation characteristics of brick and mortar. Since under service conditions brickwork is stressed only to a fraction of its ultimate load this assumption is quite reasonable. Non-homogeneity of mortar and brick, and their relative thickness were also

considered in the expression for equivalent modulus of elasticity of masonry. Thus E_m and E_b can be replaced by equivalent modulus of elasticity of wall E_w , and finally the non dimensional characteristic parameter, c_1 is represented by the expression as shown below in Eqn. 9.1.

$$c_1 = \frac{E_w}{E_c} \cdot \frac{L-2B}{h} \quad (9.1)$$

Deduction for SR, FR and c_2

It has been found from the analyses that the interaction between wall and the supporting beam is greatly influenced by the width of support and depth of supporting beam. These parameters are considered in the design formulae in terms of the total length of the wall-beam and is expressed by

Slenderness of the supporting beam, $SR = h/L$

Clear span ratio, $FR = (L-2B)/L$ and

$$c_2 = \sqrt{(1000.SR/FR)} \quad (9.2)$$

9.4.2 Bending Moment in Supporting Beam

The supporting beam is subjected to the action of vertical forces and horizontal shear at the wall-beam interface. The horizontal shear force at the interface is thus eccentric with respect to the centroid of the beam. This has the effect of causing a substantial reduction in the bending moment produced by the vertical forces. The moment in the supporting beam was calculated considering the vertical forces at the interface of the beam and wall due to wall-beam interaction. The moment is calculated at mid vertical section passing through each element at interface level considering all vertical forces on the left of the section. The subroutine MOMAX in the finite element program calculates the moment in the supporting beam according to the method just discussed, ignoring the shear force at wall-beam interface. Bending moment in the supporting beam due to shear force at the wall-beam interface is also calculated separately in the subroutine MOMAX. The moments calculated at different sections are stored in an array separately. From these values the maximum moment and its corresponding location is obtained. The maximum bending moment in the supporting beam of the wall-beam

structure thus obtained is expressed in terms of 'WL' traditionally in the form of $WL/K1$, where, W is the total load at the top of the wall and L is the span and $K1$ is known as coefficient for maximum moment. The contribution of shear force in calculating $K1$ is not considered in this case with an aim to remain in the conservative side. It has been mentioned in chapter 7 during discussion of modes of failure of wall-beam and progressive flow of cracking that a major portion of the mortar joints at the interface level fail before reaching the failure load of the panel. Therefore, it seems justified not to consider the reduction of moment due to shear force acting at the interface of wall and the supporting beam. The variation of maximum moment coefficient with respect to elastic properties, support width and depth of supporting beam as obtained from finite element analyses can be observed from Table 9.2(a) to Table 9.2(c). The value of $K1$ is found to vary considerably with the width of support and depth of supporting beam. Therefore $K1$ values are plotted against characteristic parameter c_1 for each value of beam depth and support width. The variation of coefficient for maximum moment with characteristic parameter c_1 for a particular case of support width ($B = 100$ mm) and depth of supporting beam ($h = 125$ mm) can be seen from Fig. 9.2. Polynomial regression analysis (in the form of $y = a + bx + cx^2$, where $y = K1$ and $x = c_1$) is performed to get a best fit curve and corresponding equation for each set of moment coefficients for a particular support width and beam depth. All these curves are then combined together in Fig. 9.3 to see their relative nature and the deviations. It is seen from Fig 9.3 that although the natures of the curves are similar their relative deviation for the same value of c_1 is noteworthy depending on the variables such as support width and beam depth which are respectively denoted by 'FR' and 'SR'. In order to determine degree of influence the important variables are now considered as width of the support, depth of the supporting beam and the characteristic parameter c_1 . The moment coefficients derived by previous researchers (Wood, 1952; Stafford Smith and Riddington, 1977; Davies and Ahmed, 1978) was not on the basis of critical examination of these critical parameters. It is interesting to note that even at a constant value of support width and beam depth, the moment capacity of a wall-beam can be increased or decreased by selecting different brick mortar combination and was not considered as a parameter in the analytical tools proposed by previous investigators (Rosenhaupt, 1964; Colbourne, 1969; Wood and Simms, 1969; Male and Arbon, 1969; Ramesh et. al., 1970; Yettram and Hirst, 1971; Green, 1972; Saw, 1974, 1975; Ahmed, 1977; Stafford Smith and Riddington, 1977; Davies and Ahmed, 1978; Riddington and Stafford Smith, 1978 and Kamal, 1990). The reason may be due to the limitation of the material model developed in the analytical tools. The

Table 9.2 (a) Comparison of K1 (FE Vs. Design Equation, Eqn. 9.3)

FR= 0.95 $c_2=6.236, 7.25, 8.1, 9.6$ $K1n = 150, 112, 86, 60$

Em	Eb	K1 from FE				K1 (Design)				K1 (Design)/K1(FE)			
		Depth of Beam (mm)				Depth of Beam (mm)				Depth of Beam (mm)			
		75	100	125	175	75	100	125	175	75	100	125	175
1635	8950	180.5	124.4	92.5	60	182.6	126.5	94.5	62.5	1.01	1.01	1.02	1.04
1635	13425	190.6	130.4	96.8	62.7	190	130.6	97.3	63.7	.99	1.00	1.00	1.01
1635	17900	197.7	134.2	99.5	64.5	195.1	133.7	99.33	64.7	.98	.99	.99	1.00
1635	22375	203.4	137.2	101.7	65.8	198.8	135.9	100.9	65.5	.98	.99	.99	.99
2453	8950	188.7	130.3	97	63	189.5	130.4	97	63.6	1.00	1.00	1.00	1.00
2453	13425	202	137.8	102.6	66.7	200.7	137.1	101.7	65.9	.99	.99	.99	.98
2453	17900	211.5	143.2	106.4	69	208.9	142.3	105.3	68.01	.98	.99	.98	.98
2453	22375	218.6	147.6	109.2	70.8	215.2	146.3	108.2	69.83	.98	.99	.99	.98
3270	8950	194	133.8	99.8	65	194.1	133.1	98.9	64.5	1.00	.99	.99	.99
3270	13425	209.3	142.7	106.3	69.2	208.4	141.9	105.1	67.8	.99	.99	.98	.98
3270	17900	219.7	149.3	110.8	71.9	219.4	149.1	110.2	71.08	.99	.99	.99	.99
3270	22375	228	154.7	114.3	74.1	228.1	155	114.6	74.08	1.00	1.00	1.00	1.00
4088	8950	197.7	136.3	101.7	66.2	197.4	135.1	100.3	65.2	.99	.99	.98	.98
4088	13425	214	146.2	109	70.9	214.1	145.6	107.7	69.5	1.00	.99	.98	.98
4088	17900	225.5	153.7	113.9	74.03	227.3	154.5	114.2	73.8	1.00	1.00	1.00	.99
4088	22375	234.2	160	117.9	76.6	238.5	162.2	120	78.0	1.01	1.01	1.02	1.02
SR						0.037	0.05	0.06	0.087				
b						0.039	.0227	.0199	.0086				
n						1.09	1.358	1.514	2.17				

Table 9.2(b) Comparison of K1 (FE Vs. Design Equation, Eqn. 9.3) (cont.)

FR= 0.9 $c_2= 6.41, 7.45, 8.32, 9.85$ $K1n= 172.2, 131.2, 101.5, 69.3$

Em	Eb	K1 from FE				K1 (Design)				K1 (Design)/ K1 (FE)			
		Depth of Beam (mm)				Depth of Beam (mm)				Depth of Beam (mm)			
		75	100	125	175	75	100	125	175	75	100	125	175
1635	8950	215.2	149.3	109.5	68.6	211	151.2	111.6	71.7	.98	1.01	1.02	1.04
1635	13425	234	159.4	116	72.23	221	157.1	115.2	73	.94	.98	.99	1.01
1635	17900	246.6	166.7	120	74.6	227.8	161.4	117.8	74.2	.92	.97	.98	.99
1635	22375	255.7	172.2	124	76.4	232.7	164.5	119.8	75.1	.91	.95	.97	.98
2453	8950	226	156.2	114.6	72	220.3	156.6	114.9	72.9	.97	1.00	1.00	1.01
2453	13425	249	169.0	123	76.5	235.2	166.1	120.8	75.6	.94	.98	.98	.99
2453	17900	264	178.3	129	79.7	246.4	173.5	125.6	78.02	.93	.97	.97	.98
2453	22375	276	185.6	134	82.3	255.1	179.3	129.5	80.2	.92	.97	.97	.97
3270	8950	233	160.6	118	73.9	226.4	160.5	117.3	73.9	.97	1.00	.99	1.00
3270	13425	258	175	127.5	79.3	245.7	173.0	125.3	77.9	.95	.99	.98	.98
3270	17900	276	185.7	135	83.3	260.8	183.2	132.2	81.8	.94	.98	.98	.98
3270	22375	290	194.5	140.6	86.4	272.4	220.5	137.9	85.6	.94	1.13	.98	.99
4088	8950	238	163.7	120	75.4	230.8	163.3	119	74.7	.97	.99	.99	.99
4088	13425	264	179.2	130.7	81.4	253.5	178.2	128.8	79.8	.97	.99	.98	.98
4088	17900	284	191.2	139	85.8	272.4	220.5	137.6	85.2	.96	1.15	.99	.99
4088	22375	300	201.2	145	89.4	287.8	236.8	145.5	90.6	.96	1.17	1.00	1.01
SR						0.037	0.05	0.06	0.087				
b						0.038	0.028	0.02	0.007				
n						1.18	1.38	1.6	2.39				

Table 9.2(c) Comparison of K1 (FE Vs. Design Equation, Eqn. 9.3) (cont.)

$$FR = 0.846 \quad c_2 = 6.41, 7.45, 8.32, 9.85 \quad K1n = 185, 142, 111.6, 76$$

Em	Eb	K1 from FE				K1 (Design)				K1 (Design)/K1(FE)			
		Depth of Beam (mm)				Depth of Beam (mm)				Depth of Beam (mm)			
		75	100	125	175	75	100	125	175	75	100	125	175
1635	8950	228	160.2	118	74	231.2	163.3	121.8	78	1.01	1.02	1.03	1.05
1635	13425	248	172.1	126	78.24	244.5	170.5	125.9	79.5	.98	.99	1.03	1.01
1635	17900	264	181	132	81.09	254	175.8	129	80.7	.96	.97	.99	.99
1635	22375	277	188.6	136	83.3	261	179.8	131.4	81.6	.94	.95	.97	.98
2453	8950	239	167.2	124	77.3	243.6	170	125.6	79.4	1.02	1.01	.96	1.02
2453	13425	265	182.6	134	82.7	264.5	181.8	132.7	82.2	1.00	.99	1.01	.99
2453	17900	287	195	141	86.6	280.6	191.3	138.7	84.9	.98	.98	.99	.98
2453	22375	305	205.6	148	89.8	293.4	198.9	143.6	87.4	.96	.97	.98	.97
3270	8950	247	171.7	127	79.5	252	174.7	128.4	80.4	1.02	1.01	.97	1.01
3270	13425	277	189.5	138	85.7	279.6	190.6	138.3	84.7	1.00	1.00	1.01	.99
3270	17900	301	204.4	148	90.4	301.8	204.1	147	89.2	1.00	1.00	1.00	.98
3270	22375	324	217.4	156	94.4	320.1	215.4	154.6	93.6	.98	.99	.99	.99
4088	8950	252	175	130	81.1	258.1	178.2	130.5	81.2	1.02	1.02	1.00	1.00
4088	13425	285	194.7	142	87.9	291	197.5	142.7	86.9	1.02	1.01	1.00	.98
4088	17900	313	211.5	153	93.2	318	214.5	154.1	93.4	1.01	1.01	1.00	1.00
4088	22375	339	226.2	162	97.9	342	229.7	164.4	99.9	1.00	1.01	1.01	1.02
SR						0.037	0.05	0.06	0.087				
b						0.036	0.025	0.017	0.0057				
n						1.335	1.54	1.79	2.635				

number of experimental works carried out by previous investigators (Wood, 1952; Rosenhaupt, 1962; Burhouse, 1969; Stafford Smith et. al., 1978; Annamalai et. al., 1984 and Ranjit, 1992) of wall-beam structure dealing with above parameter are also very limited.

Now it is important to derive a straight forward single equation for moment coefficient from the curves shown in Fig. 9.3. As a step to normalise these curves, an initial value of K1 denoted by K1n for each curve was extrapolated for a common value of $c_1 = 2$ in the equation of each of the curves in Fig. 9.3. It is evident from Fig. 9.3 that the values K1n will depend on support width and depth of supporting beam denoted by non dimensional terms 'FR' and 'SR' respectively. The variation of K1n with 'SR' for different values of 'FR' is shown in Fig. 9.4. The normalised values of K1 denoted by K1nn ($= K1/K1n$) for each of beam depth and support width are again plotted against c_1 . The relation of K1nn with c_1 is given by a generalised expression $y = 1 + bx^n$ (where, $y = K1nn$ and $x = c_1$). The values of the constants 'b' and 'n' obtained for each curve were found to vary with the support

Table 9.2(c) Comparison of K1 (FE Vs. Design Equation, Eqn. 9.3) (cont.)

$$FR = 0.846 \quad c_2 = 6.41, 7.45, 8.32, 9.85 \quad K1n = 185, 142, 111.6, 76$$

Em	Eb	K1 from FE				K1 (Design)				K1 (Design)/K1(FE)			
		Depth of Beam (mm)				Depth of Beam (mm)				Depth of Beam (mm)			
		75	100	125	175	75	100	125	175	75	100	125	175
1635	8950	228	160.2	118	74	231.2	163.3	121.8	78	1.01	1.02	1.03	1.05
1635	13425	248	172.1	126	78.24	244.5	170.5	125.9	79.5	.98	.99	1.03	1.01
1635	17900	264	181	132	81.09	254	175.8	129	80.7	.96	.97	.99	.99
1635	22375	277	188.6	136	83.3	261	179.8	131.4	81.6	.94	.95	.97	.98
2453	8950	239	167.2	124	77.3	243.6	170	125.6	79.4	1.02	1.01	.96	1.02
2453	13425	265	182.6	134	82.7	264.5	181.8	132.7	82.2	1.00	.99	1.01	.99
2453	17900	287	195	141	86.6	280.6	191.3	138.7	84.9	.98	.98	.99	.98
2453	22375	305	205.6	148	89.8	293.4	198.9	143.6	87.4	.96	.97	.98	.97
3270	8950	247	171.7	127	79.5	252	174.7	128.4	80.4	1.02	1.01	.97	1.01
3270	13425	277	189.5	138	85.7	279.6	190.6	138.3	84.7	1.00	1.00	1.01	.99
3270	17900	301	204.4	148	90.4	301.8	204.1	147	89.2	1.00	1.00	1.00	.98
3270	22375	324	217.4	156	94.4	320.1	215.4	154.6	93.6	.98	.99	.99	.99
4088	8950	252	175	130	81.1	258.1	178.2	130.5	81.2	1.02	1.02	1.00	1.00
4088	13425	285	194.7	142	87.9	291	197.5	142.7	86.9	1.02	1.01	1.00	.98
4088	17900	313	211.5	153	93.2	318	214.5	154.1	93.4	1.01	1.01	1.00	1.00
4088	22375	339	226.2	162	97.9	342	229.7	164.4	99.9	1.00	1.01	1.01	1.02
SR						0.037	0.05	0.06	0.087				
b						0.036	0.025	0.017	0.0057				
n						1.335	1.54	1.79	2.635				

number of experimental works carried out by previous investigators (Wood, 1952; Rosenhaupt, 1962; Burhouse, 1969; Stafford Smith et. al., 1978; Annamalai et. al., 1984 and Ranjit, 1992) of wall-beam structure dealing with above parameter are also very limited.

Now it is important to derive a straight forward single equation for moment coefficient from the curves shown in Fig. 9.3. As a step to normalise these curves, an initial value of K1 denoted by K1n for each curve was extrapolated for a common value of $c_1 = 2$ in the equation of each of the curves in Fig. 9.3. It is evident from Fig. 9.3 that the values K1n will depend on support width and depth of supporting beam denoted by non dimensional terms 'FR' and 'SR' respectively. The variation of K1n with 'SR' for different values of 'FR' is shown in Fig. 9.4. The normalised values of K1 denoted by K1nn ($= K1/K1n$) for each of beam depth and support width are again plotted against c_1 . The relation of K1nn with c_1 is given by a generalised expression $y = 1 + bx^n$ (where, $y = K1nn$ and $x = c_1$). The values of the constants 'b' and 'n' obtained for each curve were found to vary with the support

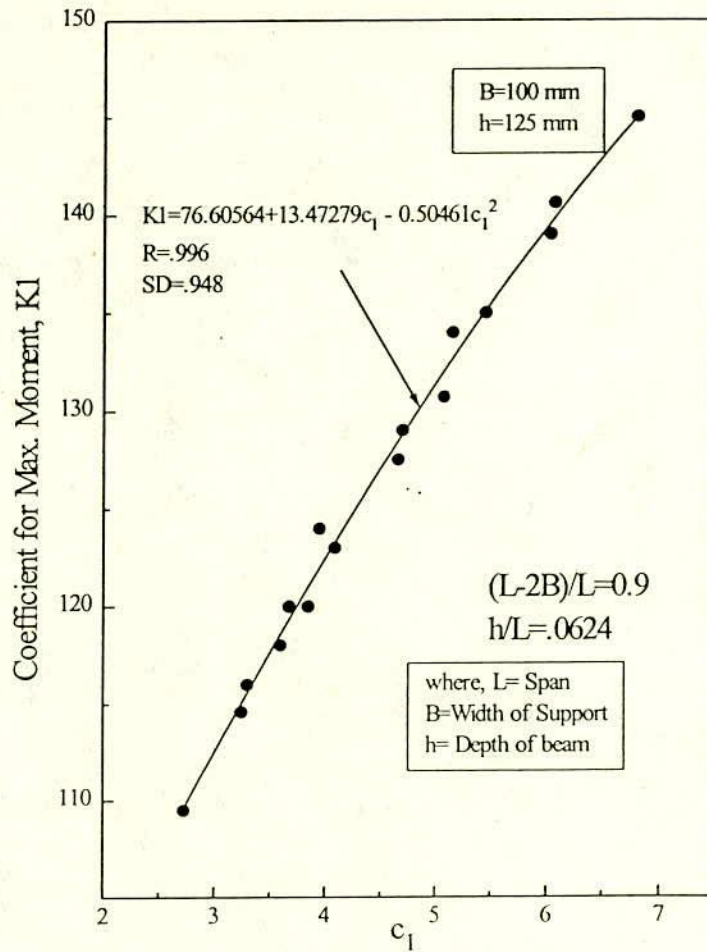


Fig. 9.2 Coefficient for Max. Moment ($K1$) Vs. Characteristics Parameter c_1

width and depth of supporting beam. Therefore, these two constants, b and n are related to the non dimensional parameter c_2 as shown in Fig. 9.5 and c_2 is derived from Eqn. 9.2. Therefore, we get the expression $K1n^n = (K1/K1n) = (1 + bc_1^n)$ where from the coefficient for maximum moment is given by,

$$K1 = K1n (1 + bc_1^n) \quad (9.3)$$

In this equation, ' $K1n$ ' is obtained from Fig. 9.4 and constants ' b ' and ' n ' are obtained from Fig. 9.5. Two non dimensional characteristic parameters c_1 and c_2 are deduced before by Eqn. 9.1 and Eqn. 9.2.

Here it should be mentioned that the horizontal shear developed at the interface of the wall and the beam has not been considered in the computation of bending moment in the supporting beam. The inclusion of shear in this computation will cause even more reduction of bending moment in the beam which will provide extra factor of safety. The coefficient for maximum moment considering the horizontal shear force at wall-beam interface as obtained from finite element analyses can be seen from Table A V.1 in Appendix V.

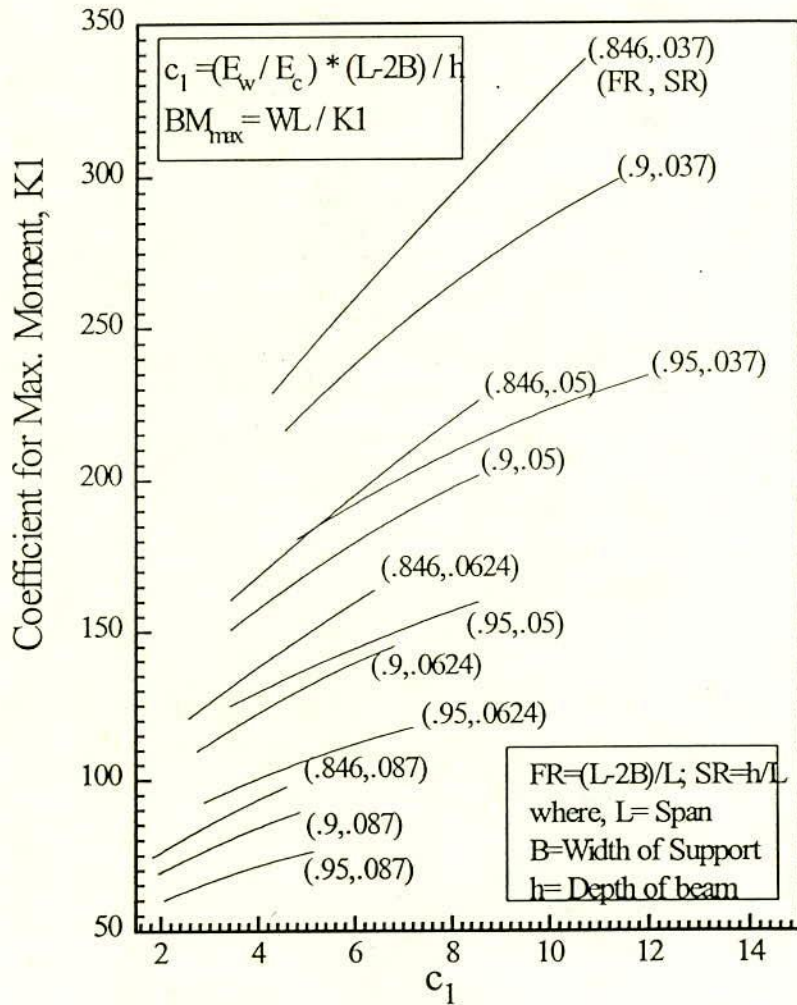


Fig. 9.3 Variation of K1 with c1 (when FR = .85 to .95 and SR = .037 to .087)

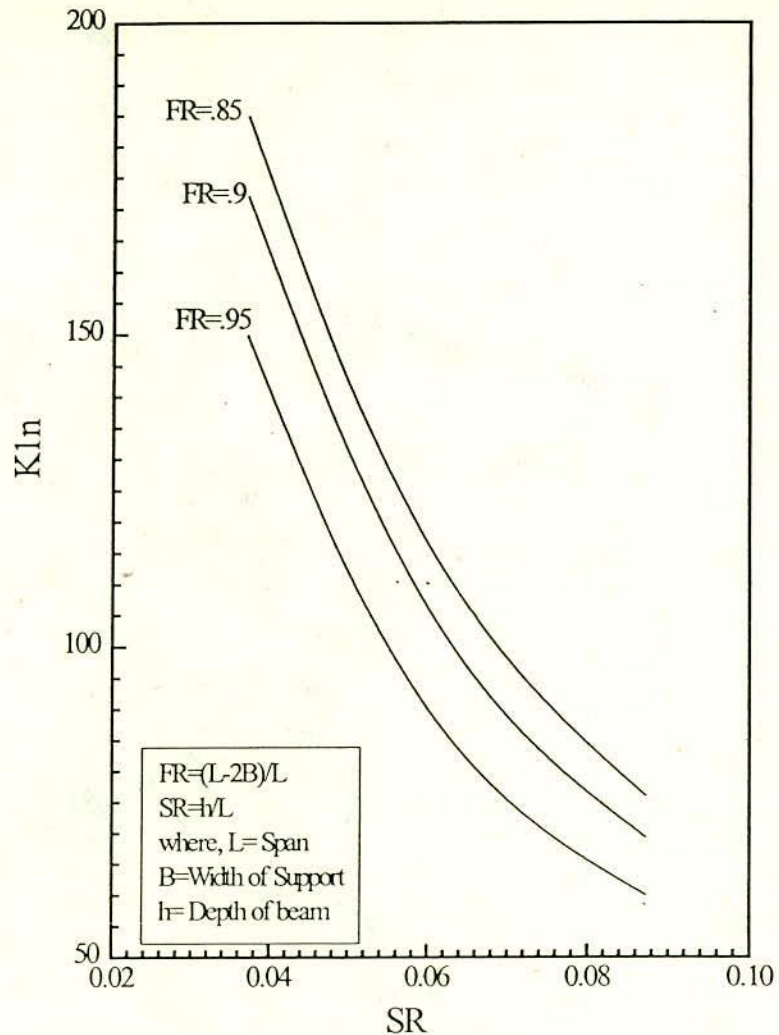


Fig. 9.4 Variation of KIn with SR and FR

9.4.3 Tie Force in Supporting Beam.

The tie force in the supporting beam is calculated in subroutine MOMAX by algebraic summation of horizontal forces acting at elements down the vertical section and within the thickness of the supporting beam. The number of sections are equal to the number of elements in the direction of the span considering half of its length. These tie forces, calculated at different sections are stored in an array from which the maximum tie force and its location are obtained. The variation of K with respect to elastic properties, support width and depth of supporting beam as obtained from finite element analyses can be seen from Table 9.3(a) to Table 9.3(c).

To derive the equation for maximum tie force in the supporting beam the same approaches of the previous article have been adopted. The maximum tie force is expressed by $T = W/K$, where, W is the total load on the top of the wall and K is known as the coefficient for maximum tie force which is given by,

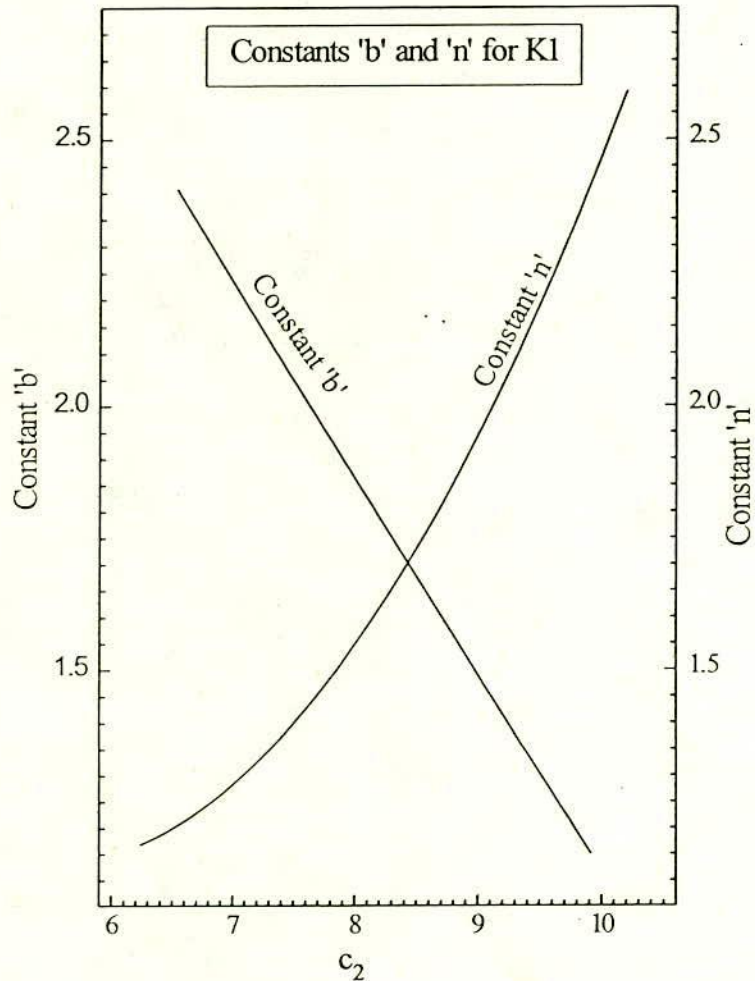


Fig. 9.5 Constants 'b' and 'n' for Max. Moment Coefficient

$$K = K_n (1 + bc_1^n) \quad (9.4)$$

where, K_n is obtained from Fig. 9.6 and constants b and n are obtained from Fig. 9.7 and the non dimensional characteristic parameters c_1 and c_2 are explained before.

9.4.4 Maximum Vertical Stress in Wall.

As it reveals from the elastic analysis that due to arching action in the wall-beam the load applied at the top of the wall-beam concentrates towards the support. Parametric study reveals that the vertical stress is the maximum at bottom corner of wall and depends on support width and beam depth more than elastic properties of the constituent materials. The vertical stress is generally expressed as the vertical

Table 9.3 (a) Comparison of K (FE Vs. Design Equation, Eqn. 9.4)

$$FR=.95 \quad c_2=6.236, 7.25, 8.1, 9.58 \quad Kn= 4.32, 4.2, 3.95, 3.91$$

Em	Eb	K from FE				K (Design)				K (Design)/K(FE)			
		Depth of beam (mm)				Depth of beam (mm)				Depth of beam (mm)			
		75	100	125	175	75	100	125	175	75	100	125	175
1635	8950	5.8	5.07	4.58	4.1	5.9	5.1	4.5	4.13	1.9	1.00	.98	1.00
1635	13425	6.3	5.41	4.82	4.22	6.3	5.3	4.67	4.22	1.00	.98	.97	1.00
1635	17900	6.62	5.67	5.0	4.32	6.57	5.5	4.79	4.29	.99	.97	.96	.99
1635	22375	6.85	5.86	5.16	4.41	6.77	5.6	4.9	4.35	.98	.95	.95	.98
2453	8950	6.1	5.28	4.76	4.22	6.28	4.29	4.65	4.22	1.03	.81	.97	1.00
2453	13425	6.68	5.75	5.09	4.42	6.87	5.7	4.93	4.38	1.03	.99	.97	.99
2453	17900	7.06	6.04	5.36	4.57	7.32	6	5.14	4.52	1.04	.99	.96	.99
2453	22375	7.4	6.26	5.58	4.71	7.66	6.2	5.3	4.63	1.03	.99	.95	.98
3270	8950	6.29	5.43	4.9	4.31	6.5	5.5	4.77	4.28	1.03	1.01	.97	.99
3270	13425	6.9	5.94	5.3	4.55	7.3	5.98	5.12	4.51	1.05	1.00	.96	.99
3270	17900	7.35	6.27	5.62	4.75	7.89	6.37	5.42	4.71	1.07	1.01	.96	.99
3270	22375	7.71	6.55	5.84	4.93	8.37	6.69	5.66	4.89	1.08	1.02	.97	.99
4088	8950	6.43	5.53	4.96	4.37	6.69	5.6	4.85	4.33	1.04	1.01	.98	.99
4088	13425	7.06	6.07	5.42	4.65	7.6	6.19	5.27	4.61	1.07	1.02	.97	.99
4088	17900	7.53	6.44	5.74	4.87	8.32	6.66	5.64	4.87	1.10	1.03	.98	1.00
4088	22375	7.89	6.73	5.99	5.1	8.9	7.08	5.95	5.12	1.12	1.05	.99	1.00
SR						0.037	0.05	0.06	0.087				
b						0.06	0.044	0.032	0.015				
n						1.16	1.25	1.4	1.85				

stress concentration and is given by $Vc = \frac{\sigma_y}{w}$ where, σ_y = vertical stress at the wall-beam interface and 'w' is the intensity of uniformly distributed load on the top of the wall. The maximum vertical stress concentration, 'Vc' is directly obtained from subroutine MOMAX and its variation with respect to support width, depth of supporting beam and elastic properties as obtained from finite element analyses can be seen from Table 9.4(a) to Table 9.4(c).

The similar mode of approaches and steps adopted in the previous articles were chronologically followed for deriving the equation for maximum vertical

Table 9.3 (b) Comparison of K (FE Vs. Design Equation, Eqn. 9.4) (contd.)

FR=.9 c_2 =6.41, 7.45, 8.32, 9.85 K_n = 5.06, 4.79, 4.62, 4.45

Em	Eb	K from FE				K (Design)				K (Design)/K (FE)			
		Depth of beam (mm)				Depth of beam (mm)				Depth of beam (mm)			
		75	100	125	175	75	100	125	175	75	100	125	175
1635	8950	6.39	5.63	5.1	4.59	6.7	5.73	5.18	4.6	1.05	1.01	1.01	1.00
1635	13425	6.94	6	5.4	4.72	7.1	5.98	5.35	4.7	1.02	.99	.99	.99
1635	17900	7.36	6.29	5.6	4.82	7.38	6.16	5.47	4.8	1.00	.98	.97	.99
1635	22375	6.72	6.53	5.7	4.9	7.58	6.29	5.57	4.88	1.13	.96	.97	.99
2453	8950	6.69	5.84	5.3	4.68	7.07	5.96	5.34	4.74	1.05	1.02	1.00	1.01
2453	13425	7.41	6.34	5.6	4.87	7.68	6.36	5.6	4.91	1.03	1.00	1.00	1.00
2453	17900	8	6.74	5.9	5.04	8.1	6.66	5.8	5.05	1.01	.98	.98	1.00
2453	22375	8.5	7.1	6.2	5.18	8.5	6.89	6	5.17	1.00	.97	.97	.99
3270	8950	6.9	6	5.41	4.75	7.32	6.12	5.4	4.81	1.06	1.02	.99	1.01
3270	13425	7.73	6.57	5.8	5	8.11	6.64	5.8	5.04	1.05	1.01	1.00	1.00
3270	17900	8.44	7.06	6.2	5.21	8.73	7.05	6.12	5.26	1.03	.99	.98	1.00
3270	22375	9.06	7.5	6.5	5.4	9.2	7.37	6.37	5.45	1.01	.98	.98	1.00
4088	8950	7.05	6.08	5.5	4.81	7.5	6.24	5.53	4.86	1.06	1.02	1.00	1.01
4088	13425	7.94	6.74	6	5.1	8.43	6.85	5.97	5.15	1.06	1.01	.995	1.00
4088	17900	8.78	7.31	6.37	5.34	9.2	7.37	6.36	5.43	1.04	1.00	.99	1.01
4088	22375	9.44	7.82	6.7	5.57	9.8	7.79	6.68	5.69	1.04	.99	.99	1.02
SR						0.037	0.05	0.06	0.087				
b						0.056	0.042	0.029	0.013				
n						1.16	1.26	1.425	1.94				

Table 9.3 (c) Comparison of K (FE Vs. Design Equation, Eqn. 9.4) (contd.)

FR=.846 c_2 = 6.61, 7.68, 8.58, 10.16 K_n = 5.5, 5.39, 5.23, 5.09

Em	Eb	K from FE				K (Design)				K (Design)/K (FE)			
		Depth of beam (mm)				Depth of beam (mm)				Depth of beam (mm)			
		75	100	125	175	75	100	125	175	75	100	125	175
1635	8950	7.05	6.24	5.7	5.19	7.14	6.33	5.79	5.25	1.01	1.01	1.01	1.01
1635	13425	7.65	6.65	6	5.32	7.56	6.59	5.99	5.32	.98	.99	.99	1.00
1635	17900	8.12	7	6.21	5.41	7.84	6.78	6.12	5.39	.96	.97	.98	.99
1635	22375	8.52	7.24	6.39	5.5	8.05	6.92	6.23	5.44	.94	.95	.97	.99
2453	8950	7.36	6.46	5.86	5.26	7.53	6.57	5.97	5.32	1.02	1.01	1.01	1.01
2453	13425	8.15	7	6.25	5.45	8.15	6.99	6.28	5.46	1.00	.99	1.00	1.00
2453	17900	8.79	7.45	6.56	5.63	8.63	7.31	6.53	5.59	.98	.98	.99	.99
2453	22375	9.35	7.83	6.84	5.78	8.99	7.56	6.73	5.69	.96	.96	.98	.98
3270	8950	7.58	6.6	6	5.32	7.78	6.74	6.09	5.37	1.02	1.02	1.01	1.01
3270	13425	8.49	7.24	6.45	5.57	8.6	7.29	6.51	5.58	1.01	1.00	1.00	1.00
3270	17900	9.26	7.78	6.8	5.79	9.24	7.73	6.86	5.77	.99	.99	1.01	.99
3270	22375	9.94	8.26	7.2	6	9.74	8.08	7.15	5.94	.98	.98	.99	.99
4088	8950	7.74	6.72	6.06	5.37	7.97	6.86	6.18	5.41	1.03	1.02	1.02	1.00
4088	13425	8.75	7.42	6.56	5.66	8.92	7.51	6.69	5.67	1.02	1.01	1.02	1.00
4088	17900	9.62	8.03	7	5.92	9.71	8.06	7.13	5.93	1.01	1.00	1.02	1.00
4088	22375	10.4	8.6	7.4	6.16	10.37	8.52	7.52	6.1	.99	.99	1.01	.99
SR						0.037	0.05	0.06	0.087				
b						0.054	0.038	0.026	0.009				
n						1.18	1.31	1.52	2.08				

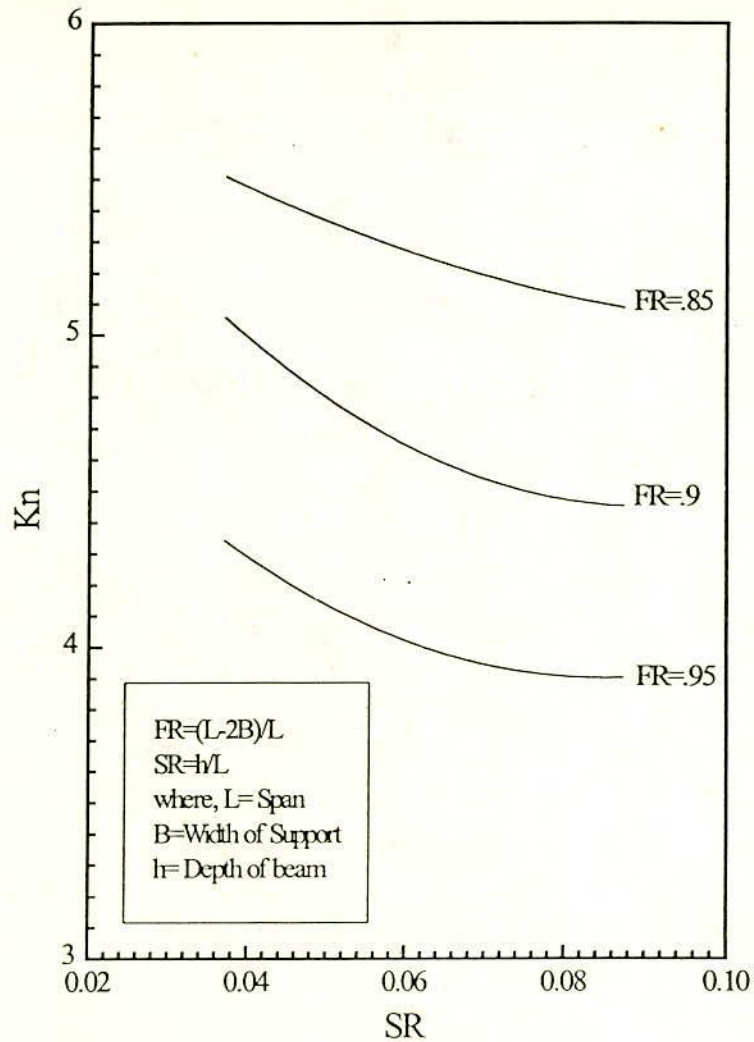


Fig. 9.6 Variation of Kn with SR and FR

stress concentration, V_c and is given by

$$V_c = V_{cn}(1 + bc_1^n) \quad (9.5)$$

where, V_{cn} is obtained from Fig. 9.8 and constants b and n are obtained from Fig. 9.9 and the non dimensional characteristic parameters c_1 and c_2 are explained before.

9.4.5 Maximum Shear Stress in Wall

The discussion made in the previous article (9.4.4) is equally applicable for shear stress in the wall. The shear stress is expressed by shear stress concentration and is given by $Sc = \tau_{xy}/w$, where, τ_{xy} = shear stress at wall-beam interface and

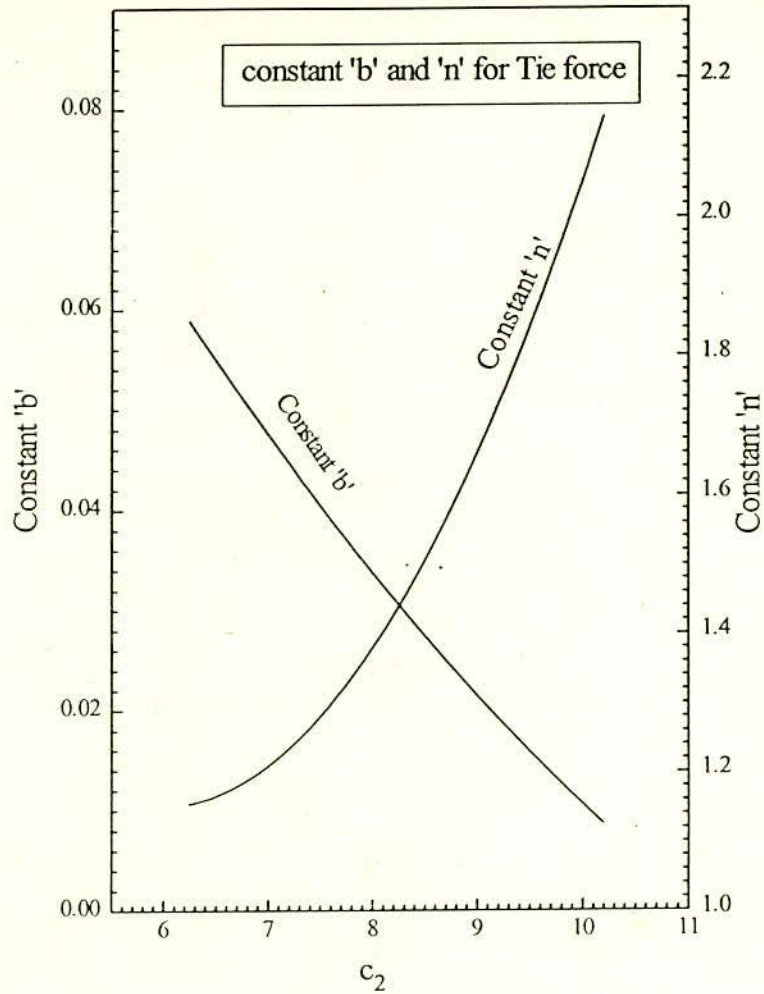


Fig. 9.7 Constants 'b' and 'n' for Coefficient (K) for Max. Tie Force

w is the intensity of uniformly distributed load on the top of the wall. The maximum shear stress concentration 'Sc' is directly obtained from subroutine MOMAX and its variation with respect to elastic properties, support width and depth of supporting beam as obtained from finite element analyses are given in Table 9.5(a) to Table 9.5(c).

The similar mode of approaches and steps adopted in the previous articles were chronologically followed for deriving the equation for maximum shear stress concentration Sc and is given by

$$Sc = Scn(1 + b(\gamma c_1)^n) \quad (9.6)$$

where, S_{cn} is obtained from Fig. 9.8 and constants 'n' and 'b' are obtained from Fig. 9.10 and Fig. 9.11 respectively. The non-dimensional parameter c_1 is explained before and $\gamma = E_m/E_w$.

Table 9.4 (a) Comparison of V_c (FE Vs. Design Equation, Eqn. 9.5)

$$FR=.95 \quad c_2=6.236, 7.25, 8.1, 9.58 \quad V_{cn} = 8 \text{ (for all values of SR)}$$

Em	Eb	Vc from FE				Vc Design				Vc Design/Vc FE			
		Depth of Beam (mm)				Depth of Beam (mm)				Depth of Beam (mm)			
		75	100	125	175	75	100	125	175	75	100	125	175
1635	8950	9.26	9.25	8.78	7.62	9.18	8.88	8.68	8.38	.99	.96	.99	1.09
1635	13425	9.52	9.4	8.87	7.65	9.4	9.06	8.83	8.49	.98	.96	.99	1.1
1635	17900	9.67	9.48	8.92	7.65	9.55	9.18	8.94	8.5	.98	.97	1.00	1.11
1635	22375	9.75	9.5	8.93	7.64	9.66	9.27	9.02	8.6	.99	.97	1.01	1.12
2453	8950	9.67	9.66	9.15	7.89	9.39	9.05	8.82	8.48	.97	.94	.96	1.07
2453	13425	10	9.86	9.27	7.95	9.7	9.32	9.06	8.6	.97	.94	.98	1.08
2453	17900	10.2	10	9.34	7.97	9.94	9.51	9.24	8.8	.974	.95	.99	1.1
2453	22375	10.3	10	9.37	7.97	10.11	9.66	9.37	8.9	.98	.97	1.0	1.11
3270	8950	10	9.89	9.3	8.05	9.52	9.16	8.9	8.5	.95	.93	.96	1.05
3270	13425	10.3	10.14	9.47	8.11	9.92	9.5	9.23	8.79	.96	.94	.97	1.08
3270	17900	10.5	10.3	9.56	8.15	10.22	9.76	9.46	8.9	.97	.94	.99	1.09
3270	22375	10.7	10.4	9.6	8.15	10.45	9.96	9.65	9.1	.97	.95	1.00	1.11
4088	8950	10	10.05	9.5	8.15	9.62	9.24	8.99	8.6	.962	.92	.95	1.05
4088	13425	10.5	10.3	9.7	8.22	10.1	9.63	9.35	8.8	.96	.93	.96	1.07
4088	17900	10.7	10.4	9.76	8.26	10.43	9.94	9.64	9.13	.97	.95	.98	1.10
4088	22375	10.9	10.6	9.8	8.28	10.73	10.2	9.88	9.3	.98	.96	1.00	1.12
SR						0.037	0.05	0.06	0.087				
b						0.0355	0.0305	0.026	0.0175				
n						0.91	1.0	1.115	1.38				

9.5 COMPARISON OF RESULTS OBTAINED FROM THE PROPOSED DESIGN FORMULA

In the previous articles the empirical relations have been developed from the regression analysis of a large volume of data obtained from finite element analyses. Due to simplifications made in the regression analysis the empirical formulae are approximate and may not represent the finite element results exactly. It is therefore necessary to compare the results obtained from empirical equations with those of finite element analysis and the similar existing formulae prepared by previous investigators. Such comparisons of the equations derived for maximum bending moment and tie force in the supporting beam and maximum vertical and shear stress at the interface of wall-beam structure are carried out in the following sections.

Table 9.4 (b) Comparison of Vc (FE Vs. Design Equation, Eqn. 9.5)

FR=.9 c₂=6.41, 7.45, 8.32, 9.85 Vcn= 4.75 (for all values of SR)

Em	Eb	Vc from FE				Vc Design				Vc Design/Vc FE			
		Depth of Beam (mm)				Depth of Beam (mm)				Depth of Beam (mm)			
		75	100	125	175	75	100	125	175	75	100	125	175
1635	8950	5.57	4.88	5	5.31	5.41	5.24	5.11	4.95	.97	1.07	1.02	.93
1635	13425	5.72	5.03	5.1	5.39	5.54	5.3	5.2	5.01	.97	1.05	1.02	.93
1635	17900	5.81	5.12	5.24	5.4	5.62	5.41	5.26	5.06	.97	1.05	1.00	.94
1635	22375	5.87	5.18	5.3	5.46	5.68	5.46	5.31	5.10	.96	1.05	1.00	.93
2453	8950	5.82	5.08	5.2	5.51	5.53	5.33	5.19	5.01	.95	1.05	.99	.91
2453	13425	5.98	5.26	5.37	5.61	5.71	5.49	5.33	5.12	.95	1.04	.99	.91
2453	17900	6.09	5.37	5.5	5.67	5.84	5.60	5.43	5.19	.96	1.04	.98	.91
2453	22375	6.15	5.45	5.5	5.7	5.94	5.69	5.5	5.26	.96	1.04	1.00	.92
3270	8950	5.98	5.2	5.3	5.6	5.61	5.40	5.25	5.05	.94	1.04	.99	.9
3270	13425	6.15	5.4	5.5	5.7	5.83	5.59	5.42	5.19	.95	1.03	.98	.9
3270	17900	6.26	5.53	5.6	5.8	6.0	5.74	5.55	5.31	.96	1.04	.99	.91
3270	22375	6.34	5.62	5.7	5.89	6.13	5.85	5.66	5.40	.97	1.04	.99	.92
4088	8950	6.09	5.28	5.35	5.7	5.66	5.44	5.29	5.08	.93	1.03	.99	.89
4088	13425	6.28	5.5	5.57	5.8	5.92	5.67	5.49	5.25	.94	1.03	.98	.9
4088	17900	6.39	5.64	5.72	5.9	6.13	5.85	5.65	5.39	.96	1.04	.98	.91
4088	22375	6.47	5.74	5.82	5.93	6.29	6.00	5.78	5.51	.97	1.04	.99	.93
SR						0.037	0.05	0.06	0.087				
b						0.0346	.0296	.0245	.0165				
n						0.92	1.02	1.14	1.44				

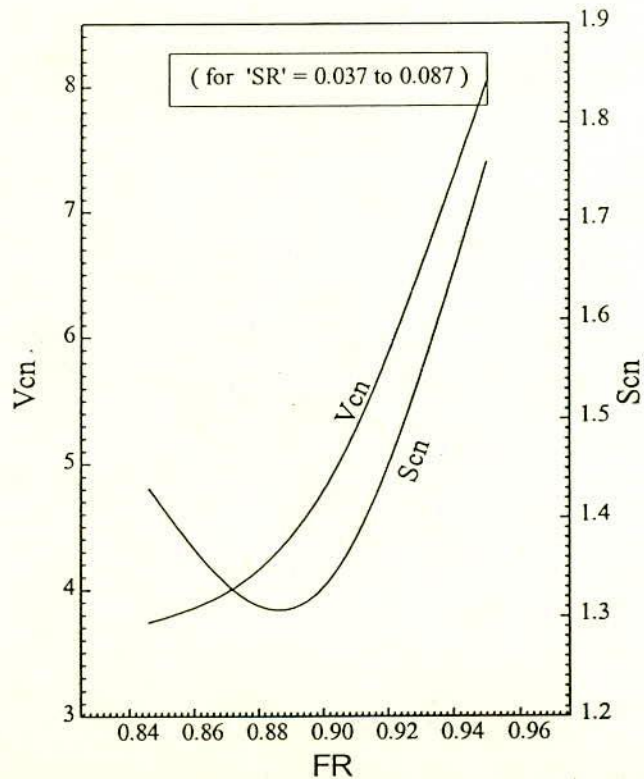


Fig. 9.8 Variation of Vcn and Scn with FR(.037 ≤ SR ≤.087)

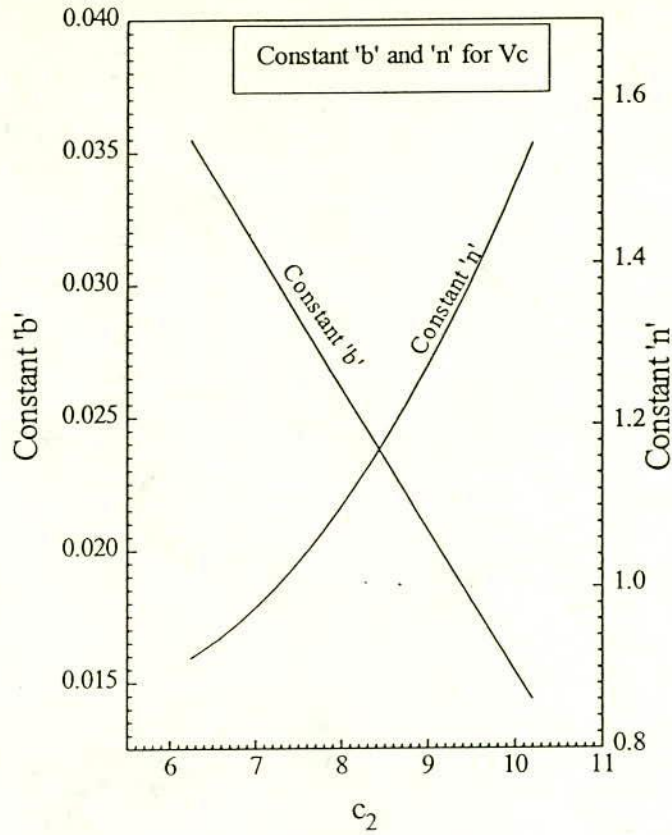


Fig. 9.9 Constants 'b' and 'n' for Max. Vertical Stress Concentration, Vc

Table 9.4 (c) Comparison of Vc (FE Vs. Design Equation, Eqn. 9.5)
 FR=.846 $c_2 = 6.61, 7.68, 8.58, 10.16$ $V_{cn} = 3.8$ (for all values of SR)

Em	Eb	Vc from FE				Vc Design				Vc Design/Vc FE			
		Depth of Beam (mm)				Depth of Beam (mm)				Depth of Beam (mm)			
		75	100	125	175	75	100	125	175	75	100	125	175
1635	8950	4.86	4.16	3.67	3.37	4.29	4.16	4.06	3.95	.88	1.0	1.10	1.17
1635	13425	4.95	4.26	3.77	3.48	4.39	4.24	4.13	4.00	.88	.99	1.09	1.15
1635	17900	5	4.3	3.84	3.51	4.46	4.30	4.18	4.03	.89	1.0	1.09	1.14
1635	22375	5.04	4.34	3.88	3.54	4.5	4.34	4.21	4.06	.89	1.0	1.08	1.14
2453	8950	5.03	4.3	3.74	3.47	4.39	4.24	4.12	3.99	.87	.98	1.10	1.14
2453	13425	5.14	4.4	3.91	3.58	4.53	4.36	4.29	4.07	.88	.99	1.09	1.13
2453	17900	5.2	4.47	3.99	3.65	4.63	4.45	4.30	4.14	.89	.99	1.07	1.13
2453	22375	5.23	4.52	4.04	3.7	4.71	4.51	4.36	4.19	.9	.99	1.08	1.13
3270	8950	5.13	4.37	3.85	3.53	4.45	4.29	4.17	4.03	.86	.98	1.08	1.14
3270	13425	5.25	4.49	4	3.65	4.62	4.44	4.3	4.14	.88	.98	1.07	1.13
3270	17900	5.31	4.57	4.07	3.73	4.75	4.55	4.40	4.23	.89	.99	1.08	1.13
3270	22375	5.34	4.63	4.1	3.79	4.86	4.65	4.49	4.31	.91	1.00	1.09	1.13
4088	8950	5.19	4.42	3.91	3.57	4.48	4.32	4.19	4.05	.86	.97	1.07	1.13
4088	13425	5.32	4.56	4.05	3.7	4.69	4.50	4.35	4.18	.88	.98	1.07	1.12
4088	17900	5.38	4.64	4.14	3.78	4.85	4.64	4.48	4.3	.9	1.0	1.08	1.13
4088	22375	5.41	4.7	4.19	3.85	4.98	4.75	4.59	4.4	.92	1.01	1.09	1.14
SR						0.037	0.05	0.06	0.087				
b						.0335	.0283	.0225	.0146				
n						.94	1.05	1.2	1.51				

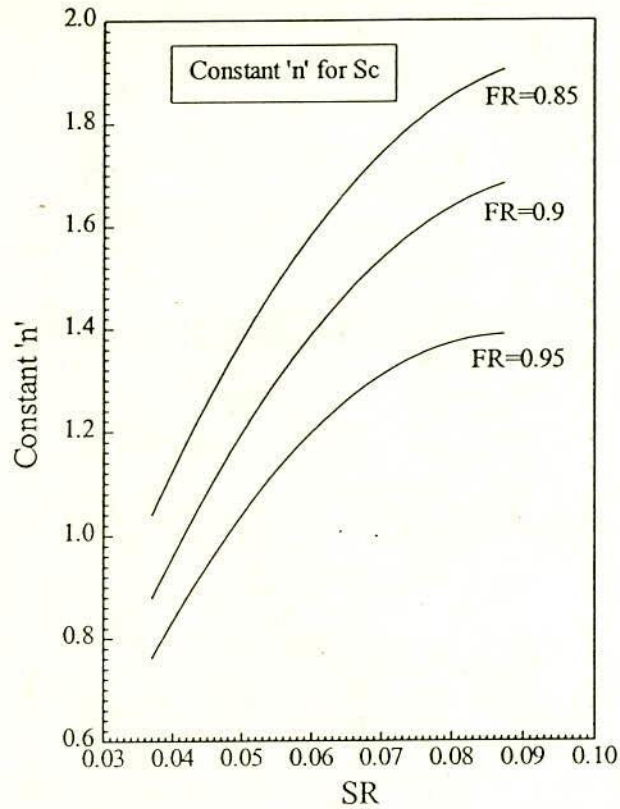


Fig. 9.10 Constant 'n' for Max. Shear Stress Concentration, Sc

9.5.1 Comparison of Proposed Empirical Formulae with Finite Element Analysis

The calculation procedure of bending moment and tie force in the supporting beam and maximum stresses at the interface of the wall-beam structure from the graphs obtained from the results of finite element analysis has been discussed in the previous articles. The equations are valid for a practical range of support width, beam depth and elastic properties of masonry constituents. The coefficients for maximum moment obtained from Eqn. 9.3 are compared with those obtained from finite element analysis and are presented in Table 9.2(a) to Table 9.2(c). The agreement has been found to be excellent.

Similarly, the coefficient for maximum tie force in the supporting beam obtained from Eqn. 9.4 are compared with those obtained from finite element analyses and are given in 9.3(a) to Table 9.3(c). In this case also the agreement is found to be excellent.

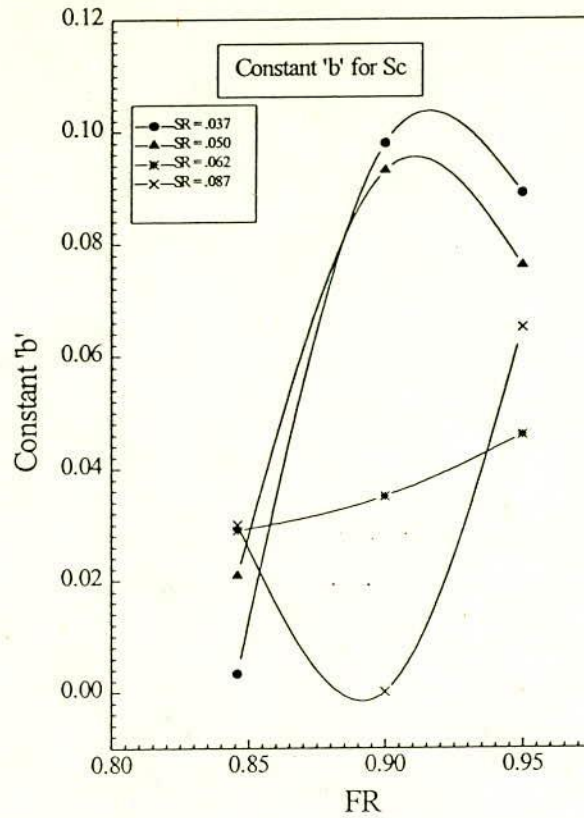


Fig. 9.11 Constant 'b' for Max. Shear Stress Concentration

Table 9.5 (a) Comparison of Sc (FE Vs. Design Equation, Eqn. 9.6)
FR=.95 Scn = 1.75 (for all values of SR)

Em	Eb	Sc from FE				Sc Design				Sc Design/Sc FE			
		Depth of Beam (mm)				Depth of Beam (mm)				Depth of Beam (mm)			
		75	100	125	175	75	100	125	175	75	100	125	175
1635	8950	2.21	1.95	1.78	1.55	1.95	1.89	1.844	1.790	.88	.97	1.03	1.15
1635	13425	2.18	1.96	1.81	1.58	1.95	1.89	1.845	1.791	.89	.96	1.02	1.13
1635	17900	2.17	1.95	1.81	1.59	1.95	1.89	1.845	1.791	.89	.97	1.02	1.12
1635	22375	2.14	1.93	1.8	1.59	1.96	1.89	1.845	1.791	.91	.98	1.02	1.12
2453	8950	2.32	2.04	1.86	1.61	2.03	1.97	1.904	1.821	.88	.96	1.02	1.13
2453	13425	2.31	2.05	1.9	1.65	2.03	1.97	1.903	1.821	.88	.96	1.00	1.10
2453	17900	2.3	2.05	1.9	1.68	2.03	1.97	1.902	1.820	.88	.96	1.00	1.08
2453	22375	2.3	2.03	1.9	1.67	2.03	1.974	1.904	1.822	.88	.97	1.00	1.09
3270	8950	2.38	2.08	1.9	1.63	2.09	2.136	1.963	1.853	.88	1.02	1.03	1.13
3270	13425	2.39	2.11	1.9	1.69	2.09	2.049	1.965	1.855	.87	.97	1.03	1.09
3270	17900	2.37	2.1	1.9	1.72	2.09	2.05	1.966	1.855	.88	.97	1.03	1.08
3270	22375	2.35	2.1	1.9	1.72	2.10	2.052	1.967	1.856	.89	.98	1.03	1.08
4088	8950	2.42	2.11	1.9	1.65	2.16	2.134	2.031	1.892	.89	1.01	1.07	1.14
4088	13425	2.44	2.14	2	1.72	2.16	2.134	2.035	1.895	.88	.99	1.01	1.10
4088	17900	2.42	2.13	2	1.74	2.16	2.131	2.033	1.894	.89	1.00	1.01	1.09
4088	22375	2.4	2.12	2	1.75	2.16	2.134	2.034	1.894	.90	1.00	1.01	1.08
SR						0.037	0.05	0.06	0.087				
b						0.089	0.076	0.064	0.045				
n						0.76	1.06	1.12	1.38				

Table 9.5 (b) Comparison of S_c (FE Vs. Design Equation, Eqn. 9.6)
 $FR=.9$ $Scn= 1.33$ (for all values of SR)

Em	Eb	Sc from FE				Sc Design				Sc Design/Sc FE			
		Depth of Beam (mm)				Depth of Beam (mm)				Depth of Beam (mm)			
		75	100	125	175	75	100	125	175	75	100	125	175
1635	8950	1.74	1.48	1.34	1.22	1.502	1.456	1.365	1.33	.86	.98	1.02	1.09
1635	13425	1.69	1.46	1.3	1.25	1.503	1.457	1.365	1.33	.89	.99	1.05	1.06
1635	17900	1.65	1.44	1.32	1.25	1.503	1.457	1.365	1.33	.91	1.01	1.03	1.06
1635	22375	1.61	1.42	1.31	1.25	1.504	1.458	1.366	1.33	.93	1.02	1.04	1.06
2453	8950	1.84	1.58	1.37	1.22	1.578	1.537	1.392	1.331	.86	.97	1.01	1.09
2453	13425	1.81	1.55	1.36	1.24	1.576	1.535	1.392	1.331	.87	.99	1.02	1.07
2453	17900	1.77	1.52	1.35	1.25	1.575	1.534	1.392	1.331	.89	1.00	1.03	1.06
2453	22375	1.73	1.49	1.33	1.25	1.578	1.537	1.393	1.331	.91	1.03	1.04	1.06
3270	8950	1.94	1.64	1.4	1.21	1.645	1.617	1.421	1.332	.84	.98	1.01	1.10
3270	13425	1.91	1.6	1.4	1.23	1.647	1.619	1.422	1.165	.86	1.01	1.01	.95
3270	17900	1.86	1.57	1.4	1.23	1.648	1.62	1.423	1.332	.88	1.03	1.01	1.08
3270	22375	1.82	1.54	1.37	1.23	1.648	1.620	1.423	1.332	.9	1.05	1.04	1.08
4088	8950	2.01	1.67	1.45	1.19	1.717	1.709	1.456	1.332	.85	1.02	1.00	1.12
4088	13425	1.97	1.64	1.45	1.22	1.721	1.714	1.467	1.332	.87	1.04	1.01	1.09
4088	17900	1.93	1.6	1.42	1.22	1.721	1.714	1.457	1.332	.89	1.07	1.02	1.09
4088	22375	1.88	1.56	1.4	1.21	1.722	1.715	1.456	1.332	.91	1.10	1.04	1.10
SR						0.037	0.05	0.06	0.087				
b						0.098	0.092	0.035	0.002				
n						0.89	1.21	1.4	1.68				

Table 9.5 (c) Comparison of S_c (FE Vs. Design Equation, Eqn. 9.6)
 $FR=.846$ $Scn = 1.41$ (for all values of SR)

Em	Eb	Sc from FE				Sc Design				Sc Design/Sc FE			
		Depth of Beam (mm)				Depth of Beam (mm)				Depth of Beam (mm)			
		75	100	125	175	75	100	125	175	75	100	125	175
1635	8950	1.73	1.55	1.38	1.12	1.414	1.438	1.436	1.423	.82	.93	1.04	1.27
1635	13425	1.7	1.56	1.4	1.19	1.414	1.438	1.436	1.423	.83	.92	1.02	1.19
1635	17900	1.67	1.55	1.4	1.17	1.414	1.438	1.436	1.423	.84	.93	1.02	1.21
1635	22375	1.65	1.54	1.39	1.17	1.414	1.438	1.436	1.423	.85	.93	1.03	1.21
2453	8950	1.75	1.6	1.42	1.15	1.417	1.460	1.46	1.438	.81	.91	1.03	1.25
2453	13425	1.72	1.6	1.45	1.19	1.417	1.459	1.459	1.437	.82	.91	1.00	1.2
2453	17900	1.68	1.58	1.45	1.21	1.417	1.459	1.459	1.437	.84	.92	1.00	1.18
2453	22375	1.65	1.56	1.44	1.21	1.417	1.460	1.460	1.438	.86	.93	1.01	1.18
3270	8950	1.74	1.6	1.44	1.17	1.420	1.483	1.486	1.456	.81	.92	1.03	1.24
3270	13425	1.71	1.61	1.46	1.21	1.420	1.484	1.487	1.457	.83	.92	1.02	1.20
3270	17900	1.67	1.59	1.46	1.23	1.420	1.484	1.488	1.457	.85	.93	1.02	1.18
3270	22375	1.63	1.57	1.4	1.23	1.420	1.485	1.488	1.457	.87	.94	1.06	1.18
4088	8950	1.79	1.6	1.44	1.18	1.424	1.511	1.52	1.481	.79	.94	1.05	1.25
4088	13425	1.74	1.61	1.47	1.22	1.425	1.520	1.531	1.49	.82	.94	1.04	1.22
4088	17900	1.69	1.6	1.47	1.24	1.424	1.512	1.521	1.482	.84	.945	1.03	1.19
4088	22375	1.65	1.57	1.46	1.24	1.424	1.513	1.522	1.482	.86	.963	1.04	1.19
SR						0.037	0.05	0.06	0.087				
b						0.002	0.021	0.028	0.028				
n						1.4	1.41	1.58	1.88				

Likewise, the comparison of maximum vertical stress concentration obtained from Eqn. 9.5 has been made with those obtained from finite element analyses. The results are presented in Table 9.4(a) to Table 9.4(c). Similarly the maximum shear stress concentration obtained from Eqn. 9.6 has been compared with those obtained from finite element analyses. The results are presented in Table 9.5(a) to Table 9.5(c). In both cases the agreement is satisfactory.

9.5.2 Comparison Between Proposed Empirical Formulae and the Existing Formulae

Unlike other researchers the effect of support width has been considered in this study and the design equations and the design curves derived before (Eqn. 9.3 to Eqn 9.6) consider the support widths having different practical dimensions. When the wall-beam has knife edged support (i. e. support width, $b = 0$), as it was the case in the past (Wood, 1952; Stafford Smith and Riddington, 1977 and Davies and Ahmed, 1978), the design coefficients derived before (Eqn. 9.3 to Eqn 9.6) need to be modified. This has become necessary for the purpose of comparison between the results of the proposed formulae and the existing formulae. The finite element program used in this study is flexible enough to allow this modification by slight change in the input data file. For this purpose a total of 48 analyses was carried out. A summary of the parameters considered and the finite element results can be seen from Table A V.2 in Appendix V

The modified curves for $K1n$ and constants b and n (see Fig. 9.12 and 9.14) have been obtained from the results of the parametric study. The general equation for coefficient for maximum bending moment, ($K1 = K1n (1 + bc_1^n)$) is valid in this case also. The constant $K1n$ is obtained from Fig. 9.12; constants b and n from Fig. 9.13 and characteristics parameter c_1 from Eqn. 9.1 with $b = 0$. Similarly, the value of the constants for tie force, vertical stress and shear stress can be obtained if necessary.

The coefficient for maximum bending moment $K1$ in the supporting beam, obtained from present finite element analyses along with the value suggested by other authors (Wood, 1952; Stafford Smith and Riddington, 1977 and Davies and Ahmed, 1978) are presented in Table 9.6. The comparison is shown in Table 9.7. It is seen from Table 9.6 and Table 9.7 that coefficient for maximum moment obtained from the proposed equation agrees favourably with the finite element results. The coefficients for maximum bending moment as derived by Davies and

Ahmed (1978) for flexible beams ($5 < R < 7$) are found to agree favourably with the results obtained from proposed formula. With the increase of 'R', i. e., when the beam becomes more flexible the difference between the results of Davies's formula and the proposed formula increases but still agrees reasonably well on the conservative side. The coefficients for maximum moment as derived by Stafford Smith and Riddington are very high in comparison to the present finite element analysis and the Davies's formula. The expression for moment proposed by Stafford Smith and Riddington does not clearly indicate whether or not the reduction of bending moment due to induced horizontal shear at the interface has been considered. In the computations of total bending moment in the supporting beam, the reduction of moment due to horizontal shear at wall-beam interface has been shown in Davies's expression and is not considered in this comparison. The better agreement for moment coefficient has been observed between the present finite element analysis and the formulae proposed by Davies and Ahmed (1978) and Stafford Smith and Riddington (1977) in case of stiffer beams. The coefficients for maximum moments from Table 9.6 are shown graphically in Fig. 9.14 wherein the foregoing observations are clearly demonstrated. The diagonal solid line represents the coefficients for maximum moments obtained from present finite element analyses and the different symbols represent the values calculated by equation proposed by different authors. It is seen that within a particular range of SR ($SR = 0.037$ to 0.087) Eqn. 9.3 truly represent the values obtained from present finite element analysis. Equation proposed by Davies and Ahmed is reasonably good for wall-beams with stiffer supporting beam ($SR \geq .06$; or $R \leq 7$). For more flexible beams the coefficients become smaller leading to higher moment ($M = WL/K1$) in the beam resulting in a conservative estimate of the materials. Equation proposed by Stafford Smith and Riddington overestimates the value of $K1$ resulting in lower values of bending moment leading to nonconservative estimate of the materials.

Table 9.6
Coefficients K1 from Analyses, Design Eqn. and Other Authors

Modulus of Elasticity for Brickwork = E_w

Maximum Bending Moment = $WL / K1$ where K1 is Coeff. for Max. Bending Moment

END SUPPORTED BEAM ($B = 0$)

Ew	K1(Davies) h (mm)=			K1(Stafford) h (mm)=			K1(Design) h (mm)=			K1 (Analysis) h (mm)=		
	75!!	125!!	175!	75	125	175	75	125	175	75	125	175
5408	100.6	61.44	48.9	140.4	84.2	60	109.8	68.7	50.1	108.6	67.5	48.5
6531	105.2	73.64	51.02	149.5	89.7	64.1	113.3	70.5	51.1	112.2	70.0	50.5
7287	107.9	75.51	52.3	155.0	93.0	66.5	115.6	71.7	51.9	114	71.2	51.6
7831	109.8	76.78	53.15	158.8	95.3	68.1	117.3	72.6	52.5	115.6	72.3	52.5
6450	104.9	73.42	50.88	148.9	89.3	63.8	113.0	70.4	51.0	114.7	70.8	51
8113	110.7	77.40	53.57	160.7	96.4	68.9	118.2	73.1	52.9	119.3	73.8	53.5
9314	114.4	79.91	55.27	168.3	101.0	72.1	121.9	75.2	54.4	122	75.6	55
10222	116.9	81.64	56.45	173.6	104.1	74.4	124.8	76.9	55.6	124.2	77.1	56.1
7135	107.4	75.15	52.04	154.0	92.4	66.0	115.2	71.5	51.8	118.4	72.8	52.5
9230	114.1	79.74	55.16	167.8	100.7	71.9	121.6	75.0	54.2	123.9	76.4	55.4
10816	118.5	82.72	57.18	176.9	106.1	75.8	126.6	78.0	56.5	127.1	78.6	57
12060	121.6	84.83	58.61	183.4	110.0	78.6	130.7	80.3	58.5	129.5	80	58.3
7623	109.1	76.30	52.82	157.4	94.4	67.5	116.6	72.3	52.3	121.9	74.3	53.6
10061	116.5	81.34	56.25	172.7	103.6	74.0	124.3	76.6	55.4	127.1	78.2	56.6
11977	121.4	84.70	58.52	183.0	109.8	78.4	130.3	80.2	58.4	130.6	80.5	58.5
13521	124.9	87.12	60.15	190.5	114.3	81.7	135.1	83.2	61.1	133.4	82.1	59.8

! $5 < R < 7$: $r = 0.25$ and $\lambda = 0.33$; !! $R > 7$: $r = 0.33$ and $\lambda = 0.5$

$$K1 \text{ (Davies and Ahmed)} = \frac{4\lambda(1 + \beta R)}{r} \text{ where } R^4 = \frac{E_w t H^3}{EI};$$

$$K1 \text{ (Stafford Smith and Riddington)} = 4K^{4/3} \text{ where } K^4 = \frac{E_w t L^3}{EI}$$

$$K1 \text{ (Eqn. 9.3)} = K1n(1 + bc_1^n) \text{ where } c_1 = \frac{E_w}{E_c} \cdot \frac{L - 2B}{h}$$

The characteristics parameter K first proposed by Stafford Smith and Riddington (1976,1977) was given by $K^4 = \frac{E_w t L^3}{EI}$ and they proposed maximum bending moment = $W_w L / 4K^{4/3}$ where W_w is total load on top of wall, E_w = modulus of elasticity of wall t = thickness of wall and E , I and L are the modulus of elasticity, second moment of area and span of the beam respectively. (in this case $t=114$ mm, $L=2004$ mm, $E = E_c = 28600$ Mpa) Therefore, the moment coefficient is $K1 = 4K^{4/3}$

Davies and Ahmed (1978) proposed a characteristics parameter similar to that of Stafford Smith and Riddington by replacing L by H and is known as flexural stiffness parameter, R which is given by $R^4 = \frac{E_w t H^3}{EI}$ where, H = height of brick wall only (= 1230 mm constant for all three depth of beam 75, 125,

175 mm. $L=2004$ mm). And they also proposed bending moment as, $M_v = \frac{W L r}{4\lambda(1 + \beta R)}$ due to vertical load and was assumed to be maximum at central region. Therefore, the moment coefficient considering

vertical load is $K1 = \frac{4\lambda(1 + \beta R)}{r}$

Three cases were considered according to magnitude of stiffness parameter R .

Case 1 $R \leq 5$ stiff beam : $r = 0.2$ and $\lambda = 0.25$.

Case 2 flexible beam $5 < R < 7$: $r = 0.25$ and $\lambda = 0.33$.

Case 3 Very flexible beam $R > 7$: $r = 0.33$ and $\lambda = 0.5$.

Table 9.7
Comparison of Moment Coefficient, K1 used by Other Authors
with proposed design equation (Eqn. 9.3)

Modulus of Elasticity of Brickwork = E_w

Maximum Bending Moment = WL/K_1 where K_1 is the Coefficient for Maximum Bending Moment

END SUPPORTED BEAM ($B=0$)

L-2b	Em	Eb	Ew	K1 (FE)/K1(Design)			K1(Eq)/K1(S. Smith)			K1(Eq.)/K1(Davies)		
				h (mm)			h (mm)			h (mm)		
				75	125	175	75	125	175	75	125	175
2004	1635	8950	5408	.99	.98	.97	.78	.81	.84	1.09	1.12	1.02
		13425	6531	.99	.99	.99	.75	.78	.79	1.07	.96	1.00
		17900	7287	.99	.99	.99	.74	.77	.78	1.07	.95	.99
		22375	7831	.98	.99	1	.74	.76	.77	1.07	.94	.99
	2453	8950	6450	1.01	1.00	1	.76	.79	.80	1.07	.96	1.00
		13425	8113	1.00	1.01	1.01	.74	.76	.77	1.07	.94	.99
		17900	9314	1.00	1.00	1.01	.72	.74	.75	1.06	.94	.98
		22375	10222	.99	1.00	1.00	.72	.74	.75	1.07	.94	.98
	3270	8950	7135	1.03	1.02	1.01	.75	.77	.78	1.07	.95	.99
		13425	9230	1.02	1.02	1.02	.72	.74	.75	1.06	.94	.98
		17900	10816	1.00	1.01	1.01	.72	.74	.74	1.07	.94	.99
		22375	12060	.99	.996	.99	.71	.73	.74	1.07	.95	1.00
	4088	8950	7623	1.04	1.02	1.02	.74	.76	.77	1.07	.95	.99
		13425	10061	1.02	1.02	1.02	.72	.74	.75	1.07	.94	.98
		17900	11977	1.00	1.00	1.00	.71	.73	.74	1.07	.95	.99
		22375	13521	.98	.99	.98	.71	.73	.75	1.08	.95	1.01

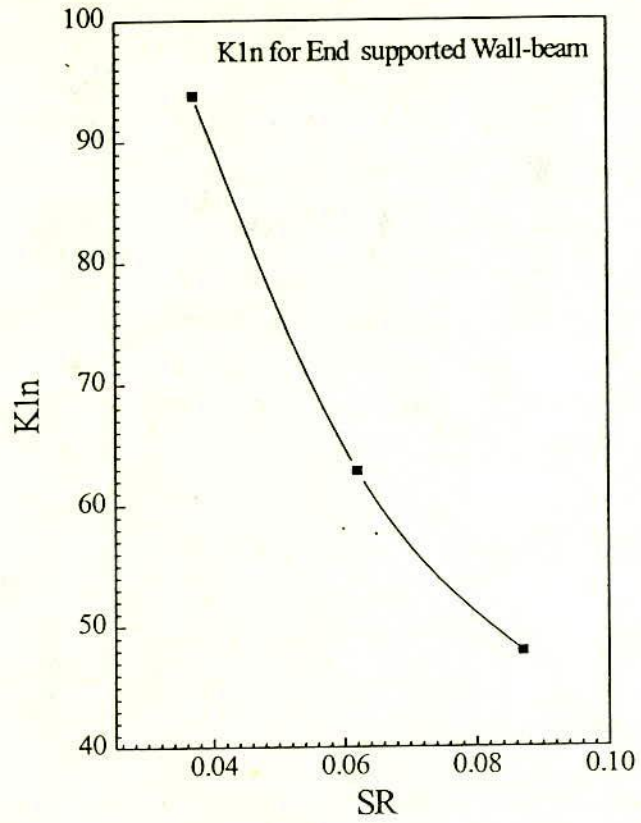


Fig. 9.12 Variation of K1n with SR (End supported wall-beam)

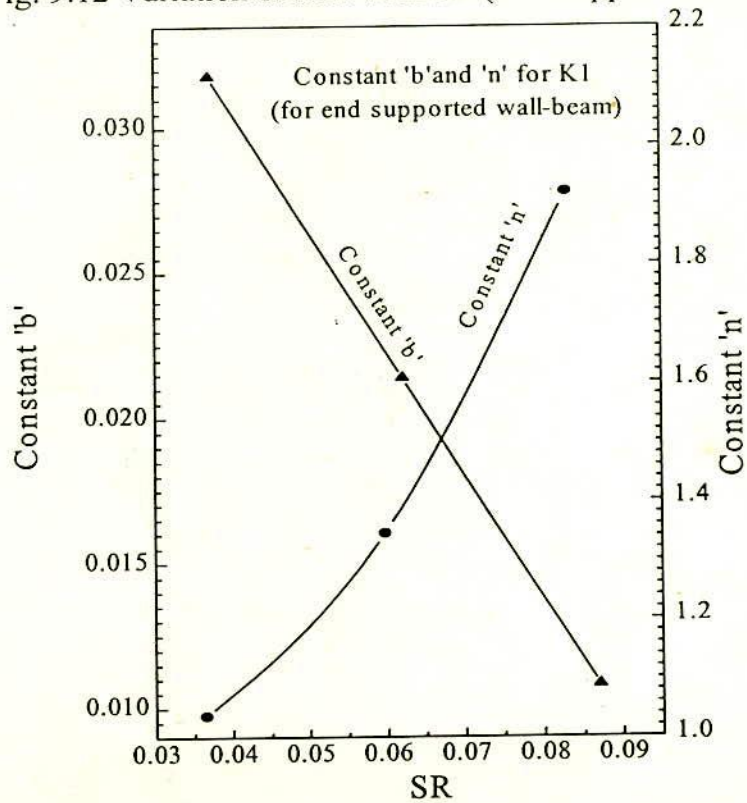


Fig. 9.13 Constant 'b' and 'n' for max. Moment Coefficient (K1) (End supported wall-beam)

From results of experimental tests, Wood (1952) proposed that when brick wall is supported on reinforced concrete beam, the beam reinforcement may be designed for a bending moment of $WL/100$ either for plane walls or for plane walls with central opening only. In a comparison made by Male and Arbon (1969) it was noted that for the modular ratio ($m = E_b/E_m$) of 5.35 corresponding to burnt brick wall the agreement between the finite element analysis made by him (Maximum Moment = $WL/116$) and that proposed by Wood (Maximum Moment $WL/100$) is very good but for a modular ratio of 30 corresponding to light weight concrete block wall, the moment by finite element is considerably higher ($WL/43$) than the value suggested by Wood ($WL/100$). In a broader sense the moment coefficient method of Wood makes no allowance for variations of the wall/beam stiffness due to change in elastic properties and/or beam section. As a result, the constant moment coefficient of $WL/100$ as proposed by Wood, irrespective of other parameters, will lead to either very large moment for flexible beams or very low moment for stiffer beams. This observations are clearly shown in Fig. 9.14.

The limiting moment arm method proposed initially by Navier for freely supported deep beam walls was applied by Wood to brick wall supported on a concrete beam. In this method the tension is considered to be concentrated on the beam acting at a distance $2/3$ rd of the overall depth from the 'centre of compression' with a limit of 0.7 times the span. From the analytical and experimental results described before, it is clear that the stress distributions in the beam are generally far from uniform. Furthermore, the moment makes no allowance for variations of the wall/beam stiffness due to change in elastic properties and beam section. Therefore, the use of limiting moment arm method will again result in either very large moment for flexible beams or very low moment for stiffer beams.

However with the foregoing discussion it can be concluded that the equation proposed in this study (Eqn. 9.3) can be recommended as a reasonable one which can accommodate most of the important parameters.

9.6 THE DESIGN PROBLEM

The use of wall-beam concept in building structure is getting popularity since 1952. It is also possible to use this concept in the design of transfer girder at the base of the building. Thus replacement of the traditional RCC girder can save huge amount of concrete and steel. Therefore, it is important

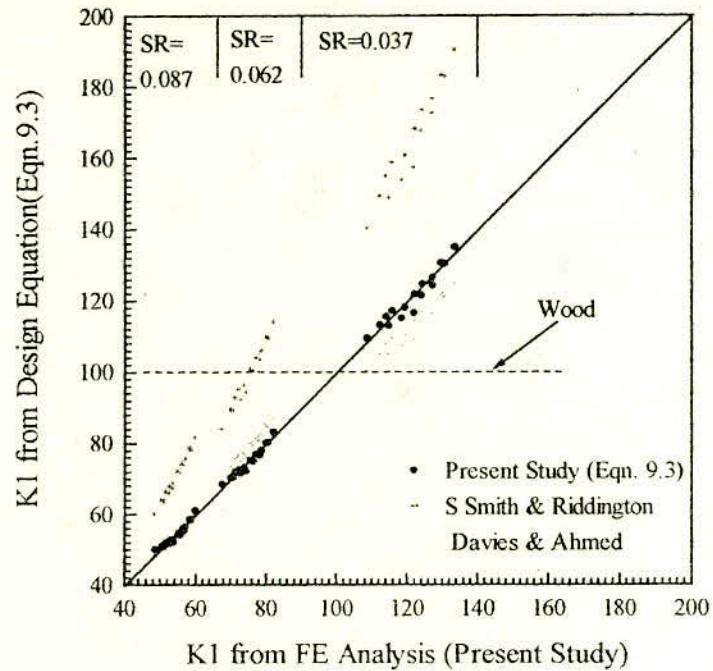


Fig. 9.14 Comparison of Empirical Equations for Coefficient of Max Moment (for end supported wall-beam Structure)

to recognise more accurately the consequences of the arching effect in the wall-beam structure and to incorporate them into design method.

In practice the thickness and material of a wall are often determined by considerations other than those of structural adequacy, for example, acoustic or aesthetic requirements and commercial size of the brick unit. One of the criteria for the design of a wall or beam structure is the limiting beam deflection. A value often adopted in practice is a maximum deflection of $L/300$. In a series of full scale test conducted by Burhouse (1969) the largest deflection recorded at failure was $L/840$. It is therefore clear, that in the majority of design cases the deflection will not be critical. In such cases the problem reduces to the selection of the minimum size of the supporting beam which is strong enough to support the bending moments induced in it by the wall and the super imposed load carried by it. The beam should also be stiff enough to maintain the wall stresses within allowable limits.

9.6.1 Estimate of critical actions.

(a) Knife edged support.

To illustrate the design formulae and its usefulness the wall-beam shown in Fig. 9.15 is considered.

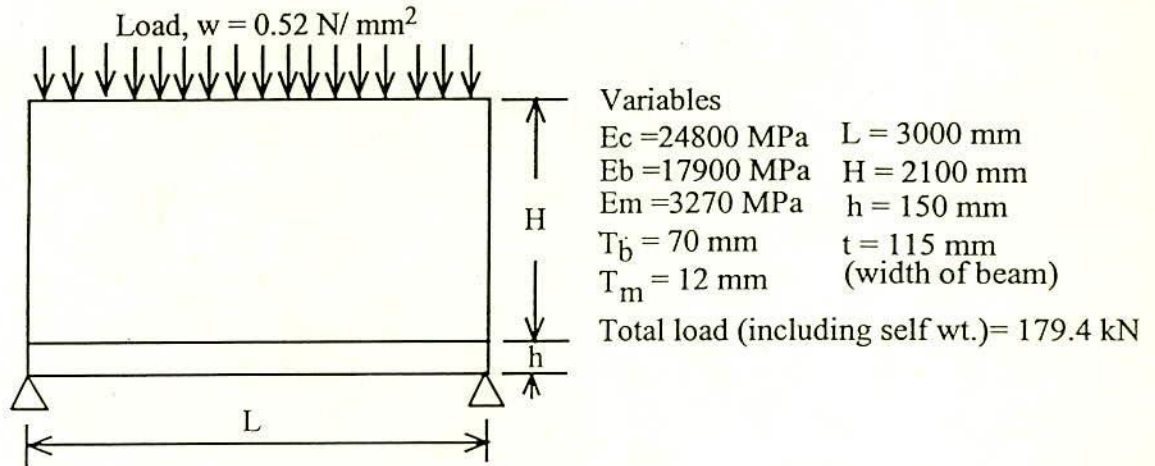


Fig. 9.15

Calculation of coefficient for maximum moment, K_1 ($M = WL/K_1$)

Coefficient for maximum Moment (K_1) from Eq. 9.3 is $K_1 = K_1 n (1 + bc_1^n)$

and $c_1 = \frac{E_w}{E_c} \cdot \frac{L - 2b}{h}$ where $E_w = \frac{E_b}{(\mu + \beta\phi)}$; $\mu = \frac{\alpha}{1 + \alpha}$; $\phi = \frac{1}{1 + \alpha}$; $\beta = \frac{E_b}{E_m}$;

$\alpha = \frac{T_b}{T_m}$ and $b =$ width of support = 0 in this case.

By assigning proper values from Fig. 9.15 one can get

$\alpha = 5.83$; $\beta = 5.47$; $\phi = 0.146$; $\mu = 0.85$, therefore, $E_w = 10857 \text{ MPa}$ and $c_1 = 8.756$

Taking values of $K_1 n = 75.9$ from Fig. 9.12 and $b = .0265$, $n = 1.17$ from Fig. 9.13, the value of $K_1 = 75.9 (1 + .0265 \cdot 8.756^{1.17}) = 95.6$

To determine the coefficient for maximum tie force in the supporting beam, maximum vertical stress concentration and maximum shear stress concentration for the end supported wall-beam the related curves may be drawn from the finite element results summarised in Table A V.2 of Appendix V.

(b) Considering support width

In all practical cases the end condition of wall-beam must provide some bearing area through which it will transfer the load downward. Thus the top of pile, pile cap, column or load bearing wall do provide a finite width of support for the wall-beam. It has been seen in the parametric study that this support width if considered in the design can provide a considerable amount of beneficial effects in different aspects of wall-beam. To illustrate the use of design formulae proposed for wall-beam system the panel shown in Fig. 9.15 with 150 mm support width is considered.

i) Calculation of coefficient for maximum moment, K_1 ($M = WL/K_1$)

Coefficient for maximum Moment (K_1) from Eq 9.3 is $K_1 = K_1 n (1 + bc_1^n)$

'SR' = h/L , 'FR' = $(L-2B)/L$ and $c_2 = \sqrt{(1000 \cdot SR/FR)}$

SR = $150/3000 = .05$ FR = $2700/3000 = 0.9$ and $c_2 = 7.45$. Using these values we get $K_1 n = 132$ from Fig. 9.4 and $b = .0285$, $n = 1.47$ from Fig. 9.5 and $c_1 = 7.88$ computed as before with $B = 150$ mm. Thus with the above values $K_1 = 132 (1 + .0285 \cdot 7.88^{1.47}) = 210$.

Thus this calculation reveals that keeping all other variables constant the consideration of support width just reduces the moment to at least half of the value calculated by moment coefficient method proposed by Wood (1952). It seems that due to this factor of safety his design procedure became remarkably popular. It is claimed that although there have been numerous applications in practice no case of failure has been reported (Wood and Simms, 1969).

ii) Calculation of coefficient for maximum tie force, K ($T = W/K$)

Coefficient for maximum Tie force (K) from Eq. 9.4 is $K = Kn (1 + bc_1^n)$, where, SR, FR, c_1 and c_2 are same as before. With these values, using Fig. 9.6, the value of $Kn = 4.8$ and using Fig. 9.7, $b = .041$ and $n = 1.27$. Thus with the above values, $K = 4.8(1 + .041 \cdot 7.88^{1.27}) = 7.51$.

iii) Calculation of maximum vertical stress concentration, V_c ($= \frac{\sigma_y}{w}$)

Coefficient for maximum vertical stress concentration (V_c) from Eq. 9.5 is $V_c = V_c n (1 + bc_1^n)$. The values of 'SR', 'FR', c_1 and c_2 are same as before. With these values and from Fig. 9.8 we get $V_c n = 4.8$. From Fig. 9.9 we get $b = .029$ and $n = 1.13$. Thus with these values $V_c = 4.8(1 + .029 \cdot 7.88^{1.13}) = 6.23$.

iv) Calculation of maximum shear stress concentration, $S_c (= \tau_{xy}/w)$

Coefficient for maximum shear stress concentration (S_c) from Eq. 9.6 is

$S_c = S_{cn}(1+b(\gamma c_1)^n)$. The values of 'SR', 'FR', and c_1 are same as before and $\gamma = E_m/E_w = 0.3$. With these values and using Fig. 9.8 we get $S_{cn} = 1.33$. Using Fig. 9.10 we get $n = 1.24$ and using Fig. 9.11 we get $b = .086$. Thus with the above values $S_c = 1.33(1+.086 * (.3*7.88)^{1.24}) = 1.66$.

9.6.2 Adequacy of Beam Section and Reinforcement

The calculations presented in the previous sections are carried out in terms of imposed loads and are to be compared with the design strengths of the material in compression, tension and shear. The design of supporting beam would be carried out in accordance with the relevant code of practice.

(i) Bending strength of beam

In designing the beam of a wall-beam structure it is important to ensure the strength and stiffness of the beam against bending. The coefficient for maximum moment in the beam of Fig. 9.15 (with support width of 150 mm) has been found to be 210. Therefore, maximum moment in the supporting beam in this case, $M_m = WL/K_1 = 179400*3000/210 = 25.63 \times 10^5$ N mm. With only 2 no 10 mm diameter reinforcing steel having 345 MPa yield strength and concrete of 27.6 MPa crushing strength having an assumed size (115 mm x 150 mm) of the supporting beam is strong enough to withstand this bending moment.

The location of the maximum moment is not so important for the design purpose, since the reinforcement has to be continued for full length of the beam. However, the maximum moment is found to occur not at the middle but approximately at quarter distance from the support.

(ii) Design of axial tie force in beam (T)

This force is maximum at the centre and can be determined using the equation $T = W/K$, where K = coefficient for maximum tie force. The coefficient for maximum tie force in the beam of Fig. 9.15 (with support width of 150 mm) has been found to be 7.51. Therefore, $T = 179400/7.51 = 23888$ N. The beam is acted upon by this axial tension in addition to the tensile stress due to bending. The

additional reinforcement required in this case will be 69 mm^2 . Therefore, 2 no 12 mm diameter reinforcing steel at the bottom is sufficient to resist both tie action and bending action.

(iii) Design for crushing failure of masonry

Due to arching action in wall-beam the load applied on the top of wall concentrates towards the support. The concentration is maximum over the supports and many times more than the intensity of the applied load at the top of the wall. This concentration often results crushing failure at the corner. This maximum vertical stress in wall (f_m) can be determined using the equation $f_m = V_c \times w$, where V_c is the maximum vertical stress concentration as calculated in the previous article. The maximum vertical stress concentration in the beam of Fig. 9.15 (with support width of 150 mm) has been found to be 6.23. Therefore, $f_m = 6.23 \times 0.52 = 3.24 \text{ MPa}$. The load carrying capacity ceases when the value of f_m exceeds the maximum permissible compressive stress of masonry. However, the depth of beam may be increased to maintain desired level of factor of safety. The use of higher strength brick unit near the supports is also reported to carry higher load under such circumstance (Burhouse, 1969).

(iv) Design for sliding along interface

The maximum interface shear stress (τ_m) occurs near the support and can be determined as $\tau_m = S_c \times w$ where S_c is the maximum shear stress concentration as derived in the previous article. The maximum shear stress concentration in the beam of Fig. 9.15 (with support width of 150 mm) has been found to be 1.66 in this case. Therefore, the maximum shear stress developed on the horizontal interface is $\tau_m = 1.66 \times 0.52 = .863 \text{ MPa}$ which has to be compared with shear strength of masonry and is given by the friction type formula,

$$f_s = f_{bs} + \mu \sigma_y$$

in which f_{bs} is the shear bond strength, μ is the coefficient of internal friction and σ_y is the compressive stress perpendicular to the bedding plane. When the masonry rests on concrete beam the conservative estimate of μ is 0.5. The value of f_{bs} in this study is 0.594 MPa. And the vertical stress corresponding to the location of maximum shear stress is assumed to be the maximum vertical stress as calculated in step (iii).

$$f_s = .594 + .5 \times 3.24 = 2.21 \text{ MPa} > 0.863 \text{ MPa}$$

(v) Vertical shear in the supporting beam

The shear in the supporting beam can be assumed to be critical at a distance 'h' from the face of the support. This is equal to half the vertical load on the total span minus the load on the left of critical section for shear. For the latter calculation the maximum vertical stress concentration at wall-beam interface is assumed to be occupied over a length of (B + h) from end of the beam. For the example in Fig. 9.15 with support width of 150 mm the maximum vertical stress is calculated as 3.24 MPa. Therefore, the maximum shear can be calculated as

$$V = W/2 - V_c * w * t * (B + h)$$

$$\therefore V = 179400/2 - 3.24 * 115 * 300 = 67620 \text{ N}$$

$$\therefore \text{Shear stress developed} = 67620/115/150 = 3.92 \text{ M Pa} > 0.87$$

Shear reinforcement has to be provided as per rule. Allowable shear stress without web reinforcement = 0.87 MPa from concrete. Shear capacity of the masonry part of wall-beam if considered can significantly reduce the developed shear stress in the beam.

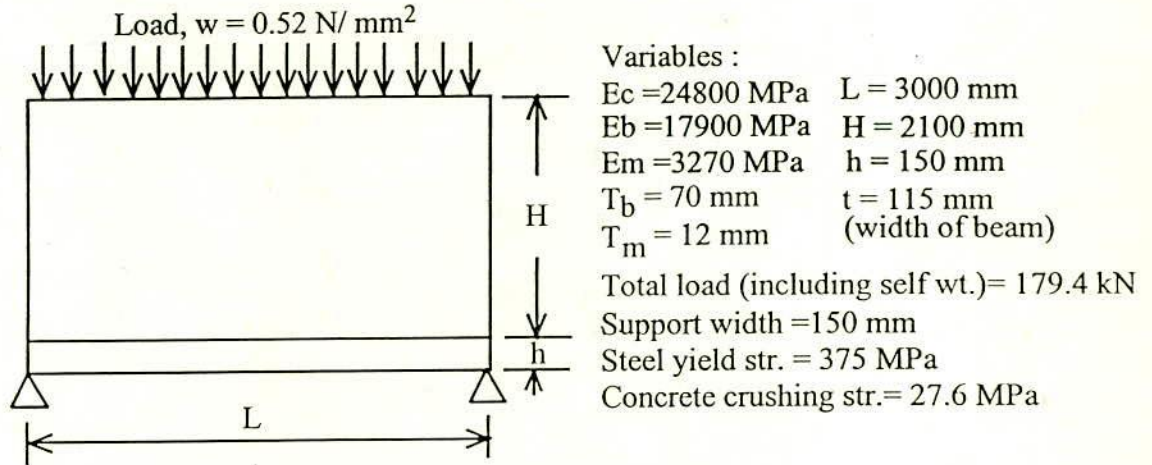
(vi) In addition to these forces and bending moment the supporting beam should be designed as a beam to carry the loading at the construction stage before composite action develops and any loading from the floor slabs if supported directly on it.

9.6.3 Illustration of Economy in Design of Wall-beam Structure.

The most significant effects in a wall-beam structure which result from the arching behaviour are the compressive and shear stresses in the masonry wall, and bending moment and tie action in the supporting beam. The combined result of these effects reduces the bending moment in the supporting beam.

The supporting beam of typical wall-beam structure as shown below is to be designed to illustrate the comparison between wall-beam analysis and conventional analysis. The interaction forces in supporting beam and wall are calculated below according to design aids proposed in this study. It may be mentioned that the maximum vertical and shear stress developed in the wall are respectively 6.23 and 1.66 times higher than the load intensity applied on the top of the wall. Considering the requirement for moment in the supporting beam the comparison is made for

material consumption (see Table 9.8). The comparison reveals that significant economy to the tune of 50% for concrete and 60% for reinforcing steel can be achieved by considering the composite action of wall-beam structure.



- Max. moment = 2.557 kN M (see Eq. 9.3; Fig. 9.4 and Fig. 9.5)
- Max. tie force = 23.83 kN (see Eq. 9.4; Fig. 9.6 and Fig. 9.7)
- Max. $\sigma_y = 3.24 \text{ MPa}$ (see Eq. 9.5; Fig. 9.8 and Fig. 9.9)
- Max. $\tau_{xy} = 0.86 \text{ MPa}$ (see Eq. 9.6; Fig. 9.10 and Fig. 9.11)

Table 9.8 Economy in Design of Wall-beam Structure

Method of Analysis	Effects in Beam		Effects in Wall		Material Required	
	Moment (kN-M)	Tie force (kN)	Vertical Stress MPa	Shear Stress MPa	Concrete M ³	Steel 12 mm ϕ
Wall-beam	2.557	23.83	3.24	0.86	.05	4 No
Conventional!	60.4	—	—	—	0.1	10 No
Economy					50 %	60 %

! Designed according to BNBC, 1993

9.6.4 Some Additional Practical Considerations for Composite Action of Wall-beam Structures

1. Practically the ends of a wall-beam structure do not rest on knife edged supports, but are almost always (a) built in, or (b) if the beam is a part of the framed structure, its connection to the column will probably have some degree of rigidity, or (c) in other cases beam and wall may be continuous over one or more intermediate supports. From these practical considerations the coefficients for the design equations were derived from the analyses of wall-beams having variable support widths. In all the above cases (a to c) a rotational restraint acts on the ends of the beam thereby producing lower wall stresses.
2. If the composite action is to be developed between the wall and the supporting beam acting as an arch, the presence of doors or window openings can not be allowed in the arching region of the wall.
3. It should also be noted that in the design method it is assumed that the weight of the wall and any superimposed load is uniformly distributed along the wall. However, if the weight of the wall or the applied load is distributed eccentrically the proposed design method would be inappropriate.
4. An important practical consideration to ensure the composite action between wall and the beam is the construction of the wall on the supporting beam. If a wall is built on an unpropped beam, the bond between wall and the supporting beam may be weak due to variation of curvature caused by bending. This effect will eventually produce a weak interface. Due to this weak interface the shear transfer between wall and the supporting beam may not be ensured which is very important for composite action. Therefore, the beam should be propped during construction until the wall is fully cured.

9.7 SUMMARY

In formulating design recommendations for uniformly distributed load on wall-beam structure, simplifications are usually made because of the difficulty in obtaining sufficient experimental data and/or realistically analysing the behaviour of wall-beam.

A study of previous research reveals that some significant experimental work has been carried out, but with very limited data for the formulation of a rational design basis. Theoretical research in this area is also lacking. The prediction of failure of wall-beams subjected to uniformly distributed load using

numerical technique is very complex due to large number of parameters. The lack of suitable material models and efficient numerical procedures were also major drawback for theoretical research in the past. Since, the finite element model developed in this investigation is directly applicable to this problem, it has been used to prepare some limited design information for solid brick wall-beam structure subjected to uniformly distributed load.

A parametric study of the behaviour of storey-height wall-beam with varying support width, beam depth and elastic properties was performed. A total of 240 walls were analysed. The following conclusions can be drawn from the study.

1. The finite element model has provided a complete solution to the wall-beam interaction problem.
2. From finite element analysis the influence of some significant parameters was investigated with the aim of formulating simple design procedure.
3. From the results of the parametric study, design rules to estimate the maximum bending moment, maximum tie force in the supporting beam, maximum vertical stress and maximum shear stress within the masonry wall have been proposed.
4. The moment coefficient method proposed by Wood (1952) gives higher moments for relatively flexible beams and lower moments for stiffer beams. The moment calculation suggested by Stafford Smith and Riddington (1977) is nonconservative. However the design method proposed by Davies and Ahmed (1978) can be a good alternative provided proper interaction between brick and mortar joint is considered in the evaluation of modulus of elasticity of brickwork (E_w).
5. The maximum bending moment in the beam occurs very near to the supports and not at the middle of the span.
6. To ensure arch action the door or window opening should be away from the ends of the wall-beam.
7. The proposed design formulae are valid for uniformly distributed load. However, the proposed finite element model can be used for wall-beam having other types load as well.
8. The beam should be propped until the wall is cured.

CHAPTER 10

CONCLUSIONS AND RECOMMENDATIONS

This thesis has developed finite element program which can be used to analyse wall-beam structure subjected to uniformly distributed and concentrated loads. The proposed model considers brick masonry to be a composite of bricks set in a non-linear mortar matrix. The non-linear response of brick masonry is produced by a combination of non-linear deformation characteristics and progressive failure of the masonry constituents (with the latter effect being the major contributing factor).

Linear elastic finite element models have been used in chapter 3 to establish the critical parameters which influence the behaviour of wall-beam structure subjected to uniformly distributed loads. Two types of two-dimensional finite element analyses were used. One assumed masonry to be a homogeneous continuum, the other considered masonry to be an assemblage of elastic bricks and joints, each with differing properties. The finite element model which treats bricks and joints separately is more effective, since it reflects the influence of the varying stiffness of its constituents. The linear elastic finite element model used in this chapter is limited in its use and can study the nature of stress distributions only. It cannot be used to predict the failure and crack propagation.

The derivation of material parameters needed to define the finite element model have been described in chapter 4. Finite element model for masonry in which bricks and mortars are considered separately requires brick and mortar properties individually and preferably in in-situ condition along with the bond parameters between bricks and joints. Results of the material properties obtained in this chapter are important for 'micro' modelling of masonry structures and thus make it possible to study the localised failure in wall-beam structures.

Chapter 5 described the constitutive relations for brick, concrete, steel and mortar joints before and after failure. Failure criteria for joint bond failure and tensile and compressive failure of bricks, concrete, steel and mortar joints have been presented, as well as appropriate techniques for crack modelling. Consideration has also been given to the manner in which the local stresses in the fractured regions are redistributed. The possibility of crack closing, opening and formation of secondary cracks have also been considered. In wall-beam like other

masonry structures progressive cracking is major source of non-linearity in comparison to deformation characteristics of component materials.

The non-linear finite element program and some of the important components which govern the performance and efficiency of the computer programs have been described in chapter 6. A four noded rectangular linear element has been used as it is the most suited to the geometric nature of the bricks and joints. Finer mesh was used in regions of high stress gradients for better accuracy of the solution. The program is incremental and iterative in nature allowing material non-linearity and progressive cracking. The crack propagation was simulated by smeared crack modelling technique.

Experimental verification of the theoretical model has been described in chapter 7 in which the failure loads and different failure modes were verified by tests on different types of wall-beams. The predicted failure loads reasonably agreed with the experimental results but were consistently lower. The gradual release of stresses in the region of a crack ("strain softening" model) realistically reflects the propagation of the crack. The finite element model was found to be capable of predicting initial cracking load, failure load and failure pattern with reasonable accuracy and was considered representative for analysis of wall-beam structure with uniformly distributed load. The verification also confirms that the material model developed in chapter 4 and chapter 5 is realistic.

A sensitivity analysis of parameters which influence the non-linear fracture analysis of wall-beam structure was carried out in chapter 8. This study revealed that the Young's modulus of elasticity of the masonry constituents have considerable influence on the load carrying capacity of the wall-beam panel. And the strength parameters specially the tensile strengths of brick and mortar are of prime importance to predict the failure load. This sensitivity analysis suggests the relative importance of different aspects of the material model derived in chapter 4. Sensitivity analysis also suggests that influence of non-linear deformation characteristics of constituents materials and bond property of mortar joints are not significant to ultimate load.

A comprehensive parametric study of the behaviour of storey high wall-beam has been carried out in chapter 9. From the results of this parametric study design rules to estimate the maximum bending moment and tie force in the

supporting beam, and maximum vertical stress and shear stress within the masonry wall have been proposed for uniformly distributed load.

Even though the validity and potentials of the finite element model (and hence the material model) have been demonstrated, the limitations of the study must be clearly defined. The material model has not considered time dependant behaviour or the possibility of cyclic loading. The results are only applicable to solid masonry wall-beam subjected to uniformly distributed load which extends over the complete wall thickness.

Despite these limitations, the proposed finite element model offers major advantages over previous analyses. It is an ideal research tool, since each of the components of wall-beam structure is modelled separately, and the properties of these individual components can therefore be varied conveniently. This is in marked contrast to most previous models which have considered brick masonry as a continuum with average properties. The model can be used to prepare design information for any static load, and can be used as a realistic substitute for any experimental investigation. Since material parameters required for the finite element model can be determined from relatively simple tests, it can be readily adopted to any brick-mortar combination built in any bond pattern.

SUGGESTIONS FOR FURTHER RESEARCH

The present study has been concerned with the investigation of interaction of wall-beam structure considering the support width, beam depth and elastic properties of masonry constituents where the wall is made of burnt clay solid brick. Clearly there is a scope of further investigation on wall-beam structures made of hollow or light weight brick unit with reinforced concrete beam or steel beam. In this investigation only vertical in-plane load has been considered. The finite element program is also capable of modelling racking type loading which could be investigated in future. The boundary conditions of the wall-beam structures other than those considered in design aids indicated to have influence on the wall-beam interaction. These could be confirmed by further analytical and experimental works and may covered by the followings:

- The effect of vertical edge ties or stanchions.
- The behaviour of walls on continuous beams.
- The effect of loading at the beam level.
- The influence of fixity of supports.
- The influence of off set openings.

From the elastic analysis of wall-beam with a central opening, it may be concluded that apart from slight increase in the vertical stress concentration over the supports the influence of a central door or window opening on the interaction between wall and beam is insignificant. However, for an opening near a support, the stress flow is influenced by the geometry of that opening. An offset door opening gives rise to concentrated load effect along the span and hence induces vertical stress concentration in the wall and substantial bending moment and deflection in the supporting beam. A detailed analytical and experimental investigation should be carried out for wall-beam structure with such off set opening. Therefore, the design aids proposed in this study should not be adopted for the design of wall-beam structure with opening near the support.

REFERENCES

- Achyutha, (1971), "Discussion of the Paper by Ramesh et. al.", **Indian Concrete Journal**, Vol 45, No. 5.
- Ahmed, E. A., (1977), "A Study of the Composite Action Between Masonry Panels and Supporting Beams", **Ph. D. Thesis**, University of Edinburgh.
- Ali, S. S., (1987), "Concentrated Loads on Solid Masonry", **Ph.D. Thesis**, University of Newcastle.
- Al-Mahaidi, R.H.S. and Nilson, A.H., (1979) "Non-Linear Finite Element Analysis of Reinforced Concrete Deep Members", **Report No. 79-1, Dept. of Structural Engineering**, Cornell University, Ithaca, N.Y.
- Anand, S.C. and Shaw, R.H., (1980), "Mesh-Refinement and substructuring technique in Elastic-Plastic Finite Element Analysis", **Comput. and Struct.**, Vol. 11, pp.13-21.
- Anderson, G.W., (1969) "Small Specimens of Brickwork as Design and Construction Criteria", **Civil Engg. Transactions, Instn. of Engrs.**, Australia, pp. 150-156.
- Annamalai, G., Jayaraman R. and Madhava Rao, A. G., (1984), "Experimental investigation of the composite behaviour of reinforced brickwork thin lintels", **Indian Concrete Journal**, June 1984, pp. 154-161
- Anthoine. A. (1992) "In-plane Behaviour of Masonry: A Literature Review" , **Report EUR 13840 EN**, Commission of the European Communities, JRC - Institute for Safety Technology, Ispra, Italy.
- ASTM C109 (1980), "Test Method for Compressive Strength of Hydraulic Cement Mortars (using 2-in or 50mm cube specimens)
- ASTM C1006 (1984), "Test Method for Splitting Tensile Strength of Masonry Units".
- Bangladesh National Building Code (BNBC) (1993), "Specified Compressive Strength for Masonry, f_m ", Art. 4.2.3, p 6-95
- Bathe, K. J. and Ramaswamy, S., (1979), "On Three-dimensional Non-linear analysis of Concrete Structures", **Nuclear Engng. and Design**, Vol. 52, No. 3, pp. 385-409.

BDS 208(1980), "Bangladesh Standard Specification for Common Building Clay Bricks", BSTI, First Revision 1984.

Beech, D.G., Everill, J.B. and West, H.W.H, (1973) "Effect of Size of Packing Material on Brick Crushing Strength", **Proc. British Ceram. Soc., Load Bearing Brick Work (4)**, No. 21, pp. 1-6.

Bergan, P. G. and Clough, R. W., (1972), "Convergence Criteria for Iterative Processes", **AIAA J.**, Vol. 10, pp. 1107-1108.

Bergan, P. G. and Soreide, T. H., (1973), "A Comparative Study of Different Solution Techniques as Applied to a Non-linear Structural Problem", **Comput. Meth. Appl. Mech. Engng.**, Vol. 2, pp. 185-210.

Bergan, P. G. and Holand, I., (1979), "Non-linear Finite Element Analysis of Concrete Structures", **Comput. Meth. Appl. Mech. Engng.**, Vol. 17, pp. 443-463.

Brebbia, C.A. and Ferrante, A.J. (1978), "Computational Methods for the Solution of Engineering Problems ", **Pentech Press Ltd.**

Burhouse, P., (1969), "Composite action between brick panel walls and their supporting beams", **Proc. Instn. of Civil Engrs.**, Vol. 43, pp. 175-194.

Buyukozturk, O., (1977), "Non-linear Analysis of Reinforced Concrete Structures", **Comput. and Struct.**, Vol. 7, pp. 149-156. Pergamon Press 1977. Printed in Great Britain.

Chandrashekhara, K. and Jacob, K. A., "Photoelastic Analysis of Composite Action of Walls Supported on Beams", **Building and Environment**, Vol 11, 1976, pp. 139-144

Chen, W.F. and Saleeb, A. F., (1982), "Constitutive Equations for Engineering Materials", Vol. 1, **John Willey and Sons.**

Colbourne, J. R., (1969), "Studies in Composite Construction: An Elastic Analysis of Wall/Beam Structures", **CP 15/69, Building Research Station**, pp.1-10.

Cook, R.D., (1981), "Concept and Applications of Finite Element Analysis", 2nd Ed. **John Wiley and Sons Inc.**

Coull, A., (1966), "Composite Action of Walls Supported on Beams", **Building Science**, Vol 1, pp 259-270

- Davies, S. R. and Ahmed, A. E., (1978), "An approximate method for analysing composite wall-beams", **Proc. British Ceram. Soc.**, No. 27, pp. 305-320 (London).
- Davies, S. R. and Ahmed, A. E., (1980), "A graphical solution of composite wall-beams", **International Journal of Masonry Construction**, Volume 1 No.1, pp.29-33.
- Desai, C.S. and Abel, J.F., (1972), "Introduction to the Finite Element Method - A Numerical Method for Engineering Analysis", **Von Nostrand Reinhold**.
- Dhanasekar, M., Page, A.W. and Kleeman, P.W., (1984), "A Finite Element Model for the In-Plane Behaviour of Brick Masonry", **Proc. 9th Aus. Conf. on the Mech. of Struct. and Mat.**, Sydney, pp. 262-267.
- Dhanasekar, M., (1985), "The Performance of Brick Masonry Subjected to in-Plane Loading ", **Ph.D. Thesis**, The Univ. of Newcastle, Australia.
- Dhanasekar, M., Page, A.W. and Kleeman, P.W., (1985), "The Failure of Brick Masonry Under Biaxial Stresses", **Proc. Instn. of Civil Engineers.**, Part 2, 79, pp.295-313.
- Dhanasekar, M., Kleeman, P.W., and Page, A.W., (1985) "Biaxial Stress-Strain Relations for Brick Masonry ", **J. of Struct. Dvn., ASCE**, Vol. 111, No. 5, pp.1085-1100.
- Duncan, W. and Johnarry, T., (1979), "Further Studies on the Constant Stiffness Method of Non-linear Analysis of Concrete Structures", **Proc. Instn. of Civ. Engrs.**, Part 2, Vol. 67, pp. 951-969.
- Farrar. N.S., (1971) "The Influence of Platen Friction on the Fracture on Brittle Materials", **J. of Materials**, Vol. 6, No. 4, pp.889-910.
- Francis, A.M., (1969), "The S.A.A. Brickwork Code: The Research Background", **Civil Engg. Trans., Instn. of Engrs.**, Australia, Vol. CE II, No.2, pp.165-176.
- Gallagher, R. H., (1973), "Element and Global Formulations and Solution Algorithms for Geometrically Non-linear Analysis", **ICCAD Course Advanced Topics in Finite Element Analysis**, Italy,, Lecture Series No. 1/74, Chapter 12.
- Govindan, P. and Santhakumar, A. R., (1985), "Composite action of reinforced concrete beams with plane masonry infills ", **Indian Concrete Journal**, August, pp. 204-208.

- Green, D. R., (1970) "The Stress Analysis of Shear Walls ", **Ph. D. Thesis**, University of Glasgow.
- Green, D. R., (1972) "The Interaction of Solid Shear Walls and their Supporting Structures", **Build. Sci.**, Vol. 7, pp. 239-248.
- Grimm, C.P., (1975) "Strength and Related Properties of Brick Masonry", **J. of Struct. Dvn.**, ASCE, Vol. 101 No.1, pp.217-232.
- Hamid, A. A. and Drysdale, R. D., (1980) "Concrete Masonry Under Combined shear and Compression Along the Mortar Joints", **J. of Am. Conc. Inst.**, Vol. 77, No.5, pp.314-320.
- Harding, J.R., Laird, R.T. and Beech, D.G., (1973) "Effect of Rate of Loading and Type of Packing on Measured Strength of Bricks", **Proc. British Ceram. Soc.**, Load Bearing Brickwork (4), No 21, pp.7-21.
- Hegemier, G.A., Arya S.K., Krishnamoorthy, G., Nachbar, W. and Furgerson, R., (1978), "On the Behaviour of Joint in Concrete Masonry", **Proc. North Am. Mas. Conf.**, Boulder, Colorado, pp.4.1-4.21.
- Hendry, A.W. and Sinha, B.P., (1971), "Shear Tests on Full Scale Single Story Brick Work Structures Subjected to Precompression", **Civil Engg. and Public Works Review**, Vol. 66, No. 785.
- Hendry, A.W., (1981), "Structural Brickwork", The **Macmillan Ptes Ltd.**, London.
- Hendry, A. W., Sinha, B. P., and Davies, S.R., (1981), "An Introduction to Load Bearing Brick Work Design ", **John Wiley and Sons**.
- Hilsdorf, K. H., (1969), "Investigation in to the Failure Mechanism of Brick Masonry Loaded in Axial Compression ", **Designing Engg. and Constructing with Mas. Products**, Gulf Publishing Co., Texas, pp.34-41.
- Hinton, E. and Owen, D.R.J., (1977), "Finite Element Programming", **Academic Press**.
- Hrennikoff, A., (1941), "Solutions of Problems of Elasticity by the Framework Methods ", **Journal of Applied Mechanics**, ASME, December, p A-169.
- Irons, B., and Ahmad, S., (1980) "Techniques of Finite Elements ", **Ellis HorWood Ltd.**

- Johnson, F.B. and Thompson, J.N., (1969), "Development of Diametral Testing Procedure to Provide a Measure of Strength Characteristics of masonry Assemblages", **Designing, Engg. and Constructing with Mas. Products**, Gulf Publishing Co., Texas, pp. 51-57.
- Kamal, H. R., (1990), "Finite Element Study of Wall-beam Structures", **M. Sc. Thesis**, Bangladesh University of Engineering and Technology, Dhaka.
- Kawsar, A. M., (1991), "Behaviour of Brick Masonry Under Compressive Loading", **M. Sc. Thesis**, Bangladesh University of Engineering and Technology, Dhaka.
- Khoo, C. L., (1972), "A Failure Criterion for Brickwork in Axial Compression", **Ph. D. Thesis**, University of Edinburgh.
- Khoo, C.L., and Hendry, A.W., (1973), "A Failure Criterion for Brickwork in Axial Compression", **Proc. 3rd Int. Brick Mas. Conf**, Essen. pp, 141-145.
- Khoo, C.L. and Hendry, A.W., (1973) "Strength Test on Brick and Mortar Under Complex Stresses for The Development of a Failure Criterion for Brickwork in Compression", **Proc. British Ceram. Soc.**, Load Bearing Brickwork (4), No. 21, pp.51-66.
- Kupfer, H.B., Hilsdorf, K.H. and Rusch, H., (1969), "Behaviour of Concrete Under Biaxial Stresses", **Proc. Am. Conc. Inst.**, Vol.66, pp.656-666.
- Lenczner, D., (1971)," Creep in Brickwork", **Proceedings of the Second International Brick masonry Conference** (Stoke-on-Trent), pp. 44-9.
- Lenczner, D., (1973), "Creep in Brickwork with and without Damp Proof Course", **Proc. Br. Ceram., Soc.**, 21, pp. 39-49.
- Lenczner, D., Salahuddin, J. and Wyatt, K., (1975), "Effect of Stress on Creep in Brickwork Piers", **Proc., Br., Ceram. Soc.**, 24, pp. 1-10.
- Lenczner, D. and Salahuddin, J., (1976), "Creep and Moisture Movement in Masonry Piers", **Proceedings of the First Canadian Masonry Symposium** (Calgary), pp. 72-86.
- Levy, M and Spira, E., (1973) "Analysis of Composite Walls with and Without Openings", **International Association for Bridges and Structural Engineers**, Vol 33-I, pp 143-166.

Logcher, R. D., Conner, J. J. and Nelson, M. F., "ICES STRUDL-II, The Structural Design Language ", **Engineering Users Manual, Vol 2**, Massachusetts Institute of Technology, Cambridge, Massachusetts.

Lourenco, P.B., (1994) "Analysis of Masonry Structures with Interface Elements: Theory and Applications" Report 03-21-22-0-01, Delft University of Technology, Delft, The Netherlands.

Lourenco, P.B., (1996) "Computational Strategies for Masonry Structures", **Ph. D. Thesis**, Delft University of Technology, Delft, The Netherlands.

Mainstone, R. J., (1960), "Studies in Composite Construction, Part III, Test on the New Government Offices, Whitehall Gardens", **National Building Studies**, Research Paper No 28.

Male, D. J. and Arbon, P. F., (1969), "A Finite Element Study of Composite Action in Walls", **Second Australian Conference on Mechanics of Structures and Materials**, Univ., of Adelaide, Aug., pp. 14.1-14.23.

Male, D. J. and Arbon, P. F., (1971) "A Finite Element Study of Composite Action in Walls Supported on Simple Beams", **Building Science**, Vol 6, pp 151-159.

Nelissen, L. J. M., (1972), "Biaxial Testing of Normal Concrete", **HERON**, Vol. 18, No.1, Delft, pp. 90.

Newman, K. and Lachance, L., (1964), "The Testing of Brittle Materials Under Uniform Uniaxial Compressive Stress", **Proc. Am. Soc. for Testing of Mat., ASTEA**, Vol. 64, pp. 1044-1067.

Ortega, J. M. and Rheinboldt, W. C., (1970), "Iterative Solution of Non-linear Equations in Several Variables", **Academic Press**, New York

Owen, D. R. J. and Hinton, E., (1980), "Finite Elements in Plasticity: Theory and Practice", **Pineridge Press Ltd.**

Page, A.W., (1978), "Finite Element Model for Masonry", **Journal of the Struct. Div., Proc. of ASCE** Vol. 104, No ST8, Aug, pp. 1267-1285.

Page, A. W., (1979), "A non-linear analysis of the composite action of masonry walls on beams", **Proc. Instn. Civ. Engrs., Part2**, 67, Mar., pp. 93-110.

Page, A. W., (1981), "The Biaxial Compressive Strength of Brick Masonry", **Proc. Instn. of Civil Engrs., Part 2**, Vol. 71, pp. 893-906.

Page, A. W., and Marshal, R., 1985, "The Influence of Brick and Brickwork Prism Aspect Ratio on the Evaluation of Compressive Strength ", **Proc. 7th. Int. Brick Mas. Conf., Melbourne**, pp 653-664.

Page, A.W., Samarasinghe, W. and Hendry, A.W., (1982), "The In-Plane Failure of Masonry A Review", **Proc. British Ceram. Soc., Load Bearing Brickwork (7)**, No. 30, pp.90-100.

Page, A.W., (1983), "The Strength of Brick Masonry under Biaxial Tension-Compression", **Int. J. of Mas. Constn.**, Vol. 3, No. 1, pp. 26-31.

Page, A. W., (1984), "A Study of the Influence of Brick Size on the Compressive Strength of Calcium silicate Masonry", **Engineering Bulletin CE13**, University of Newcastle.

Plowman, J.M., (1965), "The Modulus of Elasticity of Brickwork", **Proc. Br. Ceram. Soc.**, 4 pp. 37 - 44.

Plowman, J.M., Sutherland, R. J. M. and Couzens, M. L., (1967), "The Testing of Reinforced Brickwork and Concrete Slabs Forming Box Beams", **Structural Engineer**, Vol 45, pp 379-393.

Powell, B., and Hodgkinson, H.R., (1976), "The Determination of Stress/Strain Relationship of Brickwork ", **Proc. of the 4th. Int. Brick Mas. Conference (Brugge)**, paper 2.a.5.

Raab, A. R., (1964), "Discussion of the Papers by Rosenhaupt^{2.91} ", **Proc. ACI**, Vol 61, pp. 1685-1688.

Ramesh, C. K., David, P. S., and Anjanayulu, E., (1970) "A Study of Composite Action in Brick Panel Wall Supported on Reinforced Concrete Beams", **Indian Concrete Journal**, Vol 44, October, pp. 442-448.

Ranjit, K. R., (1992), "Composite Behaviour of Wall-Beam Structure", **M. Sc. Thesis**, Bagladesh University of Engineering and Technology, Dhaka.

Riddington, J. R., (1974), "The Composite Behaviour of Walls Interacting with Flexural Members", **Ph. D. Thesis**, University of Southampton.

Riddington, J. R. and Stafford Smith, B., (1978), "Composite method of design for heavily loaded wall-beam structure", **Proc. Instn Civ. Engrs**, Part 1, 64, Feb., pp.137-151.

- Rosenhaupt, S., (1961) "Elastic Analysis of Composite Walls - A General Theory", **Bulletin Research Council of Israel**, Vol 10c, pp 62-77
- Rosenhaupt, S., (1962), "Experimental study of masonry walls on beams", **Jr. of Struc. Div., Proc., of ASCE**, June, pp. 137-166.
- Rosenhaupt, S and Muellor, G., (1963), "Openings in Masonry Walls on Settling Supports", **Proc ASCE No ST3**, June, pp 107-131
- Rosenhaupt, S., (1964), "Stresses in Point Supported Composite Walls", **Journal of the American Concrete Institute**, July, pp. 795-809.
- Rosenhaupt, S., and Sokal, Y., (1965), "Masonry walls on continuous beams", **Jr. Struc. Div. Proc. of ASCE**, Feb., pp.155-171.
- Rosenhaupt, S., Beresford, F. D. and Blakey, F. A., (1967), "Test of a Post-Tensioned Concrete Masonry Wall", **Proc. ACI**, Vol 64, pp 829-837.
- Sahlin, S., (1971), "Structural Masonry ", (**Prentice-Hall**, Englewood Cliffs, N. J. pp. 59-61.
- Samarasinghe, W., (1980), "The In-Plane Failure of Brickwork", **Ph.D. Thesis**, University of Edinburgh.
- Saw, C. B., (1974) "Linear Elastic Finite Element Analysis of Masonry Walls on Beams", **Build. Sci.** Vol. 9, pp. 299-307.
- Saw, C. B., (1975), "Composite Action of Masonry Walls on Beams", **Proc. of Britain Ceramic Society**, 24, PP. 139-146.
- Scrivener, J.C. and Willams, D., (1971) "Compressive of Behaviour Masonry Prism", **Proc. 3rd Aus. Conf. on Mech. of Struct. and Mat.**, Auckland.
- Scordelis, A., (1972) "Finite Element Analysis of Reinforced Concrete Structures", **Proceedings of the McGill, Engineering Institute of Canada Speciality Conference on Finite Element Methods in Civil Engineering**, McGill University, Montreal, June, pp. 71-114.
- Sinha, B.P., (1967), "Model Studies Related to Load Bearing Brickwork", **Ph. D. Thesis**, University of Edinburgh.
- Sinha, B.P. and Hendry, A.W., (1969), "Racking Tests on Story Height Shear Wall Structures with Opening Subjected to Precompression", **Design Engg. and Constn. with Mas.Products**, Gulf Pub. Co., Texas, pp. 192-199.

Sinha, B.P. and Pederasty, R., (1983), "Compressive Strength and Some Elastic properties of Brickwork", **Int. J. of Mas. Constn.**, Vol. 3, No. 1, pp. 19-25.

Stafford Smith, B., Carter, C. and Choudhury, J. R., (1970) "The Diagonal Tensile Strength of Brickwork ", **The Structural Engineer**, June, No 6, Vol 48, pp 219-225.

Stafford Smith, B. and Rahman, K. M. K., (1972), "The Variation of Stresses in Vertically Loaded Brickwork Walls ", **Proc. Instn Civ. Engrs**, Part 2, Vol 51, pp. 689-700.

Stafford Smith, B. and Riddington, J. R., (1973) "The Design for Composite Action of Brickwork Walls on Steel Beams", **3rd International Brick-Masonry Conference**, Essex, April.

Stafford Smith, B. and Riddington, J. R., (1976), "The Composite Behaviour of Masonry Wall on Steel Beam Structures", **Proc. First Canadian Masonry Symposium**, Univ. of Calgary, Alberta, pp. 292-303

Stafford Smith, B. and Riddington, J. R., (1977), "The composite behaviour of elastic wall-beam system", **Proc. Instn Civ. Engrs**, Part 2, 63, June, pp. 377-391.

Stafford Smith, B., Khan, M. A. H. and Wickens, H. G. (1978), "Tests on wall-beam structures", **Proc. Britain Ceramic Society**, 27, pp. 289-303.

Thomas, K. and O' Leary, D.C., (1970), "Tensile Strength Tests on Two Types of Bricks ", **Proc. 2nd Int. Brick Mas. Conf., Stoke-on-Trent**, England, pp. 69-74.

Timoshenko, S. P. and J. N. Goodier (1970), "Theory of Elasticity", 3rd. Ed., **McGraw-Hill**, New York.

West, H.W.H., (1968), "The Performance of Walls Built of Wirecut Bricks With and Without Perforations. Part 1-Basis of Experimentation", **Transactions of British Ceram. Soc.**, Vol. 67, pp. 421-434.

West, H.W.H., Hodgkinson, H.R., Beech, D.G. and Davenport, S.T.E.,(1968), "The Performance of Walls Built of Wirecut Bricks With and Without Perforations: Part II Strength Tests", **Transactions of British Ceram. Soc.**, Vol. 67, pp.434-461.

Wood, R.H, (1952), "Studies in Composite Construction, Part 1, The Composite Action of Brick Panel Walls Supported on Reinforced Concrete Beams", **National Building Studies**, Research Paper No 13.

Wood, R. H. and Simms, L. G., (1969), "A tentative design method for the composite action of heavily loaded brick panel walls supported on reinforced concrete beams", **Building Research Station**, CP 26/69, July, pp. 1-6.

Wyatt, K., Lenczner, D. and Salahudin, J., (1975) "The Analysis on Creep Data in Brickwork ", **Proc. Br. Ceram. Soc.**, 24, 11-21.

Yettram, A. L. and Hirst, M. J. S., (1971), " An Elastic Analysis for the Composite Action of Walls Supported on Simple Beams", **Build. Sci.** Vol. 6, pp. 151-159.

Yettram, A. L. and Hirst, M. J. S., (1974) "An Elastic Analysis for the Composite Action of Walls Supported on Encastre Beams and Portal Frames", **Building Science**, Vol 9, pp 233-241.

Yisun, G., Tingwei, J., Zhonglian, Y., Baoin, Z., Jiashuen, Y and Wenzheng, M., (1985), "Application of the finite element method to the design of wall-beam", **Proc. of the 7th ICBM** Feb., Australia, pp. 501-508.

Zienkiewicz, O.C., Valliappan, S., and King, I. P., (1969), "Elasto-Plastic Solutions of Engineering Problems INITIAL STRESS' Finite Element Approach", **Intn. J. of Num. Meth. in Engg.**, Vol. 1, No. 1, pp. 75-100.

Zienkiewicz, O.C., (1977), "The Finite Element Method", McGraw-Hill, (Third Edition).

APPENDIX I

RECTANGULAR ELEMENT (4-NODED)

Rectangular element is one of the popular and simple type of element. It is convenient to relate its local co-ordinate axes with the global axes by its inclination angle. Considering the local reference system and using an undetermined parameters expansion, the displacements are approximated by

$$\begin{aligned} u &= \alpha_1 + \alpha_2 x + \alpha_3 y + \alpha_4 xy \\ v &= \alpha_5 + \alpha_6 x + \alpha_7 y + \alpha_8 xy \end{aligned} \quad (\text{AI.1})$$

This gives linear variation for the displacements on the element boundary, but a slightly non-linear one inside the element, due to the presence of the term xy . Also, due to this term this element gives much better result than the simple triangle. The problem is however that it can only be used for integration domains of rectangular shape, unless the finite element mesh could be constructed mixing triangular and rectangular elements. However, for wall-beam structure, where the bricks and mortars are predominantly of rectangular shape this element is considered suitable.

The displacements within an element are adequately described by a polynomial. Rayleigh-Ritz solution uses interpolation to express the displacement of each point within the element in terms of the d.o.f. of that element. These d.o.f. are found by solving simultaneous algebraic equations.

Displacement $\{f\} = \{u \ v \ w\}$ in an element are interpolated from element nodal d.o.f. $\{d\}$ by assumed fields and can be given by the relation,

$$\{f\} = [N] \{d\} \quad (\text{AI.2})$$

where $[N]$ is the shape function matrix. The strain displacement matrix $[B]$ operates on $\{d\}$ to produce strains for plane and solid elasticity problem, as given by,

$$\{\varepsilon\} = [B] \{d\} \quad \text{where } [B] = \begin{bmatrix} \partial/\partial x & 0 \\ 0 & \partial/\partial y \\ \partial/\partial y & \partial/\partial x \end{bmatrix} [N] \quad (\text{AI.3})$$

In bending problems such as beams and plates it is customary to express strain energy in terms of curvature. Then $\{\kappa\} = [\mathbf{B}]\{d\}$ where $\{\kappa\}$ is an array of curvature and $[\mathbf{B}]$ is derived from $[\mathbf{B}] = \frac{d^2}{dx^2}[\mathbf{N}]$. However in either case $[\mathbf{B}]$ is derived from $[\mathbf{N}]$.

The total potential energy of a body of volume V and surface area S is given by,

$$\prod_p = \int_v U_0 dV - \int_v \{f\}^T \{F\} dV - \int_s \{f\}^T \{\Phi\} dS - \{\delta\}^T \{P\} \quad (\text{AI.4})$$

In the above equation surface integral, $\{f\}$ is evaluated on S . Forces $\{P\}$ are concentrated loads not included in the surface integral, and $\{\delta\}$ are their displacements. They can be related as, $\{\delta\}^T \{P\} = \delta_1 P_1 + \delta_2 P_2 + \dots$. Usually the P_i and D_i are nodal forces and displacements. They are considered positive in the same sense. Strain energy per unit volume U_0 , is given by

$$U_0 = \frac{1}{2} \{\varepsilon\}^T [\mathbf{D}] \{\varepsilon\} - \{\varepsilon\}^T [\mathbf{D}] \{\varepsilon_0\} + \{\varepsilon\}^T \{\sigma_0\} \quad (\text{AI.5})$$

For the case of plane stress or plane strain, $[\mathbf{D}]$ becomes 3 by 3. and is respectively defined by,

$$[\mathbf{D}] = \frac{E}{1-\nu^2} \begin{bmatrix} 1 & \nu & 0 \\ \nu & 1 & 0 \\ 0 & 0 & \frac{1-\nu}{2} \end{bmatrix} \quad \text{and} \quad [\mathbf{D}] = \frac{E}{(1+\nu)(1-2\nu)} \begin{bmatrix} 1-\nu & \nu & 0 \\ \nu & 1-\nu & 0 \\ 0 & 0 & \frac{1-2\nu}{2} \end{bmatrix}$$

Plane stress and plane strain conditions is to be prevailed in the xy plane and the xy plane must be a plane of elastic symmetry.

Substitution of values of $\{f\}$ and $\{\varepsilon\}$ from Eqn.(AI.2) and Eqn.(AI.3) in to Eqn. (AI.4) yields,

$$\prod_p = \frac{1}{2} \sum_1^{\text{numel}} \{d\}^T [\mathbf{k}] \{d\} - \sum_1^{\text{numel}} \{d\}^T \{r\} - \{\delta\}^T \{P\} \quad (\text{AI.6})$$

in which

$$[k] = \int_v [B]^T [D][B] dV \quad (\text{AI.7})$$

$$\begin{aligned} \{r\} = & \int_v [B]^T [D]\{\varepsilon_0\}dV - \int_v [B]^T \{\sigma_0\}dV \\ & + \int_v [N]^T \{F\}dV + \int_s [N]^T \{\Phi\}dS \end{aligned} \quad (\text{AI.8})$$

where V denotes the volume of an element and S its surface. In the surface integral, $[N]$ is evaluated on S . The summation signs in Eqn. AI.6 say that contribution from all numel elements of the structure have been included. $[k]$ is identified as the element stiffness and $\{r\}$ as loads applied by an element to its nodes. When specific displacement field is assumed they yield specific $[k]$ and $\{r\}$ matrices.

Every d.o.f. in an element vector $\{d\}$ also appears in the structure vector $\{\delta\}$. Therefore $\{\delta\}$ replaces $\{d\}$ if $[k]$ and $\{r\}$ are expanded to structure size.

$$\text{Thus Eqn. AI.6 becomes, } \prod_p = \frac{1}{2} \{\delta\}^T [K] \{\delta\} - \{\delta\}^T \{R\} \quad (\text{AI.9})$$

$$\text{where, } [K] = \sum_1^{\text{numel}} [k], \quad \text{and } \{R\} = \{P\} + \sum_1^{\text{numel}} \{r\} \quad (\text{AI.10})$$

Summations indicate the assembly of element matrices. Now \prod_p is a function of generalised co-ordinates $\{\delta\}$, so static equilibrium prevails when $\{\delta\}$ satisfies the equation

$$[K]\{\delta\} = \{R\} \quad (\text{AI.11})$$

Eqn. AI.11 is obtained by differentiating Eqn. AI.9. The element stiffness matrix (Eqn. AI.7) is symmetric because $[D]$ is symmetric.

Formulation of element stiffness:

The eight d.o.f. element of Fig. AI.1(a) has the assumed displacement field,

$$\begin{Bmatrix} u \\ v \end{Bmatrix} = \begin{bmatrix} 1 & x & y & xy & 0 & 0 & 0 & 0 \\ 0 & 0 & 0 & 0 & 1 & x & y & xy \end{bmatrix} \{a_1 a_2 \dots a_8\} \quad (\text{AI.12})$$

where a_i are the i th nodal displacements in Fig. AI.1(a). This field and this element are some times called bilinear because, coefficients in the matrix come from the product of two linear expressions $(1+x)$ times $(1+y)$. But like the constant strain triangle, the element is 'linear' because sides remain straight when the element deforms. For example if $y = c$ then u and v are linear in x so edge 3-4 is always straight. Adjacent elements are therefore compatible with one another. The desired shape function can be found directly from Lagrange's interpolation formula as shown in Fig. AI.1(b).

$$\text{We have,} \quad \{u \ v\} = [N]\{d\} \quad (\text{AI.13})$$

$$\text{where, } [N] = \begin{bmatrix} N_1 & 0 & N_2 & 0 & N_3 & 0 & N_4 & 0 \\ 0 & N_1 & 0 & N_2 & 0 & N_3 & 0 & N_4 \end{bmatrix}$$

$$\text{and } \{d\} = \{u_1 \ v_1 \ u_2 \ v_2 \ u_3 \ v_3 \ u_4 \ v_4\}$$

and N_i are shown in Fig. AI.1(b), such that $N_i = 1$ if co-ordinates of node i are inserted, and $N_j = 0$ if $i \neq j$.

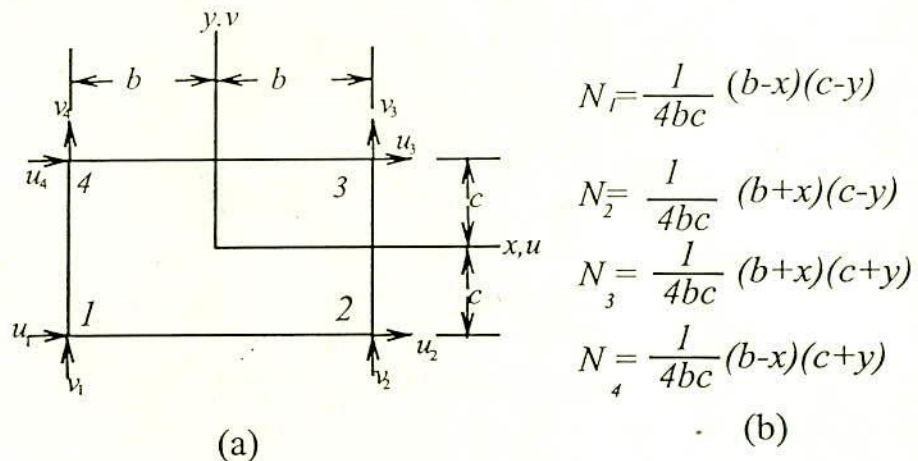


Fig. AI.1. (a) Eight d.o.f. linear (also called bilinear) element. (b) Shape function of the element

Substituting the appropriate values in Eqn. AI.2 (for plane elasticity), yields the value of strain displacement matrix, $[B]$.

$$[B] = \frac{1}{4bc} \begin{bmatrix} -(c-y) & 0 & (c-y) & 0 & \text{etc.} \\ 0 & -(b-x) & 0 & -(b+x) & \text{etc.} \\ -(b-x) & -(c-y) & -(b+x) & (c-y) & \text{etc.} \end{bmatrix} \quad (\text{AI.14})$$

It is seen that ϵ_x depends on y , ϵ_y depends on x , and γ_{xy} depends on both x and y . Now with the $[B]$ known it is ready to evaluate the stiffness matrix

$$[k] = \int_{-c}^c \int_{-b}^b [B]^T [D] [B] t \, dx \, dy \quad (\text{A1.15})$$

where t is the element thickness.



QM6 - ELEMENT

Linear elements are attractive because they are simple and have only corner nodes. But in bending they are too stiff. Consider the element in Fig. AI.2(a) is rectangular, so $\xi = 2x/L$ and $\eta = 2y/H$. If displacements \bar{u} are imposed, the element must respond as Fig. AI.2(b) because its sides must remain straight. Its deformation field is

$$u = \bar{u}\xi\eta \quad \text{and} \quad v = 0 \quad (\text{AI.16})$$

The *correct* shape under pure bending, Fig. AI.2(c), after Timoshenko (1970) is

$$u = \bar{u}\xi\eta \quad \text{and} \quad v = \frac{L\bar{u}}{2H}(1-\xi^2) + v\frac{H\bar{u}}{2L}(1-\eta^2) \quad (\text{AI.17})$$

Eqn. AI.17 yield correct value of shear strain ($\gamma_{xy} = 0$), but Eqn. AI.16 do not. So to impose displacements \bar{u} on the element, we must apply a moment big enough to overcome shear resistance as well as bending resistance. Thus the element is too stiff in bending mode. This effect is called *parasitic shear*. Its influence is disastrous if L/H is large.

The improvement scheme proposed by Cook (1981) was done by using global-local formulation of nodeless d.o.f. is outlined below. And coefficient of element stiffness matrix for QM-6 element is given at the end of this Appendix.

Nodeless D.O.F Global-Local Formulation

In addition to conventional stiffness matrix $[k]$ which operates on nodal d.o.f. $\{d\}$ another stiffness matrix $[k_a]$ which operates on generalised co-ordinates $\{a\}$ can simultaneously operate provided an element can have d.o.f. $\{d\}$ and $\{a\}$ at the same time. However in this context $\{a\}$ represents *additional* element d.o.f. and is not another way of representing $\{d\}$. These a_i are called *internal* or *nodeless* d.o.f. These can be associated with the displacement field of a four-node plane quadrilateral by :

$$u = \sum_1^4 N_i u_i + N_5 a_1, \quad \text{and} \quad v = \sum_1^4 N_i v_i + N_5 a_2 \quad (\text{AI.18})$$

where the individual shape functions are

$$N_1 = \frac{1}{4}(1-\xi)(1-\eta) \quad N_2 = \frac{1}{4}(1+\xi)(1-\eta)$$

$$N_3 = \frac{1}{4}(1+\xi)(1+\eta) \quad N_4 = \frac{1}{4}(1-\xi)(1+\eta) \quad (\text{AI.19})$$

$$N_5 = (1-\xi^2)(1-\eta^2) \quad \text{where } N_5 \text{ is the "bubble function".}$$

The fifth mode has no effect in displacements along element edges. The d.o.f.

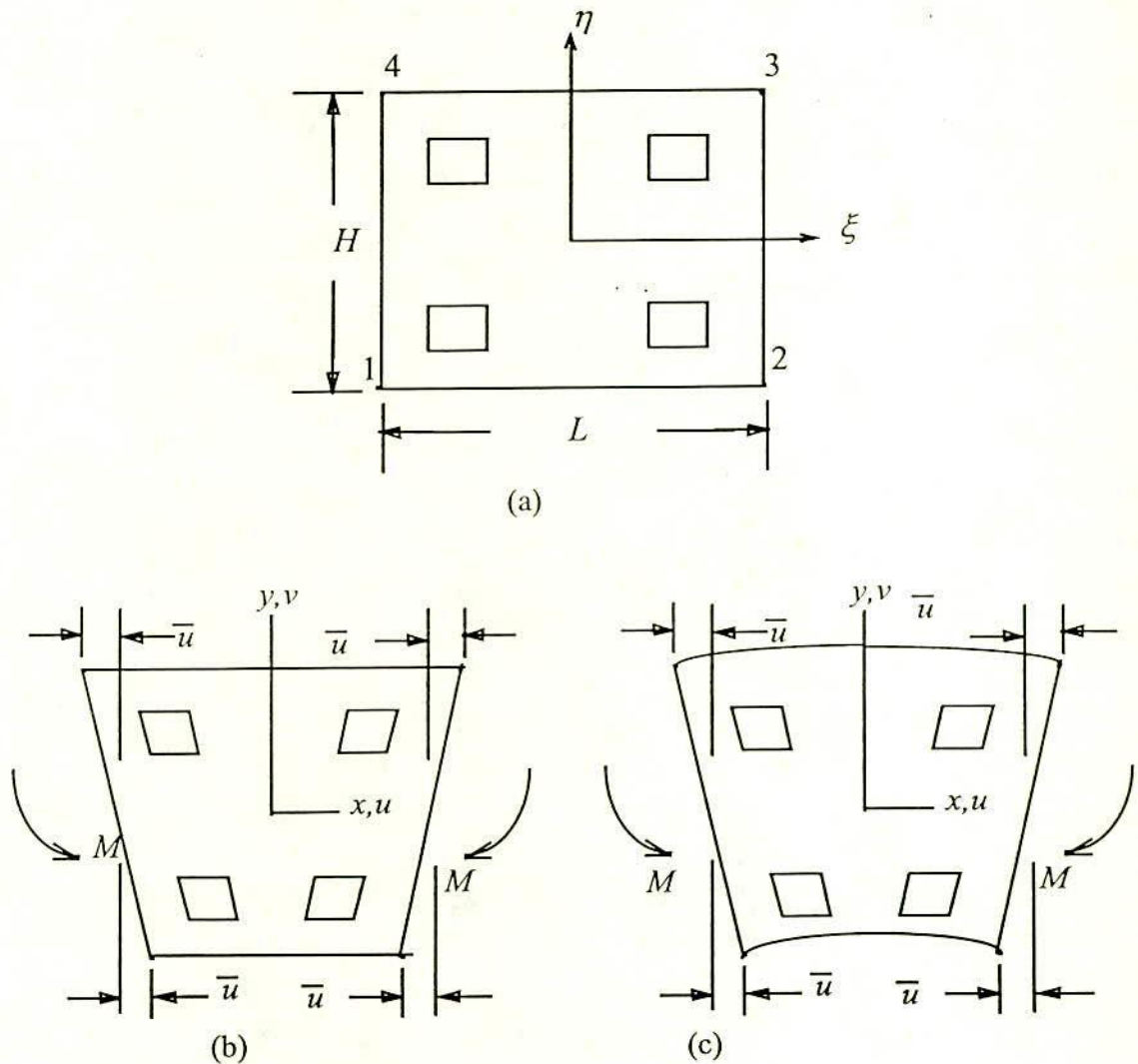


Fig. AI.2 A rectangular Linear Element. Quadrilaterals within the element represent initial and deformed shapes at Gauss Points of 2X 2 quadrature rule. (a) Undeformed shape. (b) Prescribed d.o.f. deform the element in bending mode. (c) The correct shape of beam segment in bending

a_1 and a_2 are internal to the element and are not associated with node. They can be regarded as u and v displacements at $\xi = \eta = 0$ relative to the displacements at $\xi = \eta = 0$ produced by the corner d. o. f. u_i and v_i .

Although $\{a\}$ is now present, arguments associated with formulas for element matrices for rectangular linear element (Eqn. AI.2 to Eqn. AI.8) require no change. But now displacement and strain fields are augmented.

$$\{f\} = [N \quad N_a] \{d \quad a\}, \quad \{\varepsilon\} = [B \quad B_a] \{d \quad a\} \quad (\text{AI.20})$$

Adopting the notation

$$\begin{aligned} [k_{rr}] &= \int_V [B]^T [D] [B] dV \\ [k_{er}]^T &= [k_{re}] = \int_V [B]^T [D] [B_a] dV \\ [k_{ee}] &= \int_V [B_a]^T [D] [B_a] dV \end{aligned} \quad (\text{AI.21})$$

Matrix $[k_{rr}]$ is the usual stiffness matrix that would appear if $\{a\}$ were absent and $\{r_r\}$ are the corresponding nodal loads as stated by Eqn. AI.8. Loads $\{r_e\}$ are those associated with the use of $[N_a]$ and $[B_a]$ instead of $[N]$ and $[B]$ in Eqn. AI.8.

The element stiffness equation is

$$[k'] \{d \quad a\} = \{r_r \quad r_e\} \quad (\text{AI.22})$$

where $[k']$ is given by assembling Eqn. AI.21 in the format of Eqn. AI.23

$$\begin{bmatrix} k_{rr} & k_{re} \\ k_{er} & k_{ee} \end{bmatrix} \begin{Bmatrix} d_r \\ d_e \end{Bmatrix} = \begin{Bmatrix} r_r \\ r_e \end{Bmatrix} \quad (\text{AI.23})$$

where $\{d_r\}$ are boundary d.o.f. to be retained and $\{d_e\}$ are internal d.o.f. to be eliminated. Eq. 3.24 regarded as a 'fragment' of the structural equations, so the right side represents loads applied to nodes by elements. The lower partition of Eq. 3.25 is solved for $\{d_e\}$.

$$\{d_e\} = -[k_{ee}]^{-1} ([k_{er}] \{d_r\} - \{r_e\}) \quad (\text{AI.24})$$

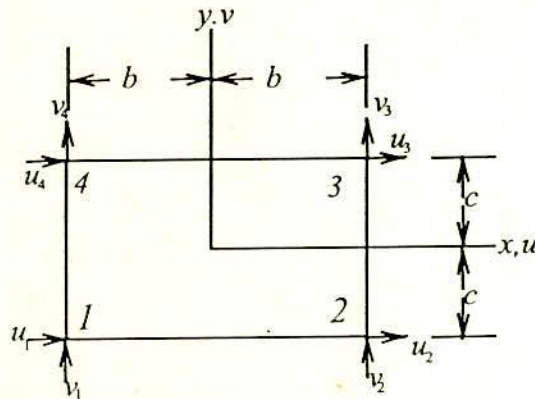
This expression for $\{d_e\}$ is substituted into the upper partition of Eq. 3.24. Thus the element stiffness equation is $[k]\{d_r\} = \{r\}$ in which

$$\begin{aligned} [k] &= [k_{rr}] - [k_{re}][k_{ee}]^{-1}[k_{er}] \\ \{r\} &= \{r_r\} - [k_{re}][k_{ee}]^{-1}\{r_e\} \end{aligned} \tag{A1.25}$$

Here, $[k]$ is the element stiffness matrix for Q M6 element.

Stiffness matrix for QM6 Element

The condensed stiffness matrix proposed by Cook (1981) for a plane, isotropic, rectangular QM6 element of constant thickness t is shown below.



Element dimension and co-ordinates

$$\left[\mathbf{k}_{8 \times 8} \right] = \frac{Qt}{12(1-m^2)} \begin{bmatrix} A_1 & C_1 & A_2 & -C_2 & A_4 & -C_1 & A_3 & C_2 \\ & B_1 & C_2 & B_3 & -C_1 & B_4 & -C_2 & B_2 \\ & & A_1 & -C_1 & A_3 & -C_2 & A_4 & C_1 \\ & & & B_1 & C_2 & B_2 & C_1 & B_4 \\ & & & & A_1 & C_1 & A_2 & -C_2 \\ & & & & & B_1 & C_2 & B_3 \\ & & & & & & A_1 & -C_1 \\ & & & & & & & B_1 \end{bmatrix}$$

Symmetric

In plane stress : $Q = E$, $m = \nu$

In plane strain : $Q = \frac{E}{1-\nu^2}$, $m = \frac{\nu}{1-\nu}$

$$A_1 = (4 - m^2)c/b + 1.5(1 - m)b/c$$

$$A_2 = -(4 - m^2)c/b + 1.5(1 - m)b/c$$

$$A_3 = (2 + m^2)c/b - 1.5(1 - m)b/c$$

$$A_4 = -(2 + m^2)c/b - 1.5(1 - m)b/c$$

$$C_1 = 1.5(1 + m) \quad \text{and} \quad C_2 = 1.5(1 - 3m)$$

$B_1 - B_4$ are obtained from $A_1 - A_4$ by interchanging b and c

APPENDIX II

BRICK, MORTAR AND BRICK MASONRY PROPERTIES

Contents

- Table AII.1 Compressive and Tensile Strength of Brick
- Table AII.2 Compression Test on Brick (Loaded Parallel to Bed Joint)
- Table AII.3 Compression Test on Stack bonded Prism (Normal
Stress-Strain reading for Brick)
- Table AII.4 Average of Lateral Strain Reading of Brick and Mortar
- Table AII.5 Compressive and Tensile Strength of Mortar
- Table AII.6 Compressive Test on Mortar Cylinders
- Table AII.7 Compression Test on Stack bonded Prism (Normal
Stress-Strain Reading for Brickwork)
- Table AII.8 Compression Test on Stack bonded Prism (Normal
Stress-Strain Reading for Mortar)
- Table AII.9 Shear Deformation of Shear Couplets (Shear
Stress-Strain Reading for Brickwork)
- Table AII.10 Shear Deformation of Shear Couplets (Shear
Stress-Strain Reading for Mortar Joint)
- Table AII.11 Constants for Stress-Plastic Strain Equation for Mortar
- Table AII.12 Tensile Bond Strength of Vertical Joint
(from Splitting Test on Brick Masonry Prism)
- Table AII.13 Shear Test on Brick Masonry Triplet (for Shear
Bond Strength of Mortar Joint)
- Table AII.14(a) Lateral Strain Reading for Bricks
(from Uniaxial compression tests on bricks)
- Table AII.14(b) Lateral Strain Reading of Bricks from Prism Test
- Fig. AII.1 Normal Stress-Strain Curves for Individual Bricks
(a) Load Parallel to bed
(b) Prism Test
- Fig. AII.2 Semi-Logarithmic Plot of Plastic Normal Strain vs. Normal Stress
- Fig. AII.3 Semi-Logarithmic Plot of Plastic Shear Strain vs. Shear Stress
- Fig. AII.4 Construction of Control Specimens

Table AII.1
Compressive and Tensile Strength of Brick
(All values are in MPa)

Specimen No	Compressive Strength			Tensile Strength (indirect test)
	Load Normal to Bed Joint	Load Parallel to the Bed Joint	Standard Test	Split Tensile
1	75.6	39.12	55.35	3.53
2	56.7	47.77	71.96	3.75
3	54.0	46.33	58.12	2.86
4	81.0	36.86	66.42	3.57
5	77.0	36.04	77.49	2.68
6	52.65	47.77	60.89	3.80
7	67.5	32.54	74.73	3.51
8	64.8	36.04	60.89	2.68
9	54.0	35.42	69.19	3.35
10	45.9	44.07	66.42	2.68
\bar{X}	62.91	40.20	66.15	3.24
S	11.41	5.44	6.94	0.44
C. of V (%)	18	13.50	11	13.6

\bar{X} = Mean, S = Standard Deviation, C. of V. = Coefficient of Variation

Note: Ratio of compressive strength, using load parallel to bed to compressive strength using standard test is 0.60.

Table AII.2
 Compression Test on Brick (Load Parallel to Bed Joint)
 (Strain Reading on 30 mm Gauge Length, $\times 10^{-6}$)

Stress MPa	Specimen No										\bar{X}	S	C of V %
	1	2	3	4	5	6	7	8	9	10			
4.12	243	246	232	304	304	172	354	228	250	240	257	48	19
8.24	385	466	372	541	541	366	616	368	415	388	446	85.6	19.2
12.36	614	719	491	723	811	564	892	698	810	650	697	115.8	16.6
16.47	883	881	941	974	1096	701	1165	912	1011	875	944	122.4	13
20.59	1130	1162	1112	1243	1369	850	1470	1169	1201	1145	1185	155.5	13.1
24.71	1386	1382	1265	1480	1656	1012	1768	1413	1619	1384	1437	203	14.1
28.83	1596	1597	1405	1718	1910	1170	1946	1641	1817	1580	1638	221	13.5
32.95	1790	1800	1592	1957	2224	1372		1877		1800	1802	234	13
37.07	1970	2032	1691			1528					1805	205	11
41.18		2321	1897			1698					1972	260	13
45.30		2574											
ϵ_{cu} (10^{-5})	208.8	274.2	238.7	240.8	239.4	205.1	219.0	202.2	224.9	221.7	227.5	20.56	9.0
E_0 (Gpa)	19.27	17.76	19.41	16.18	15.00	23.50	13.43	18.55	16.94	18.95	17.90	2.63	14.7
E_{cs} (Gpa)	18.74	17.42	19.40	15.31	15.00	23.30	13.43	17.83	15.75	18.95	17.51	2.68	15.3

\bar{X} = Mean, S = Standard Deviation, C. of V. = Coefficient of Variation

E_0 = Initial Modulus of Elasticity; E_{cs} = Secant Modulus of Elasticity at ϵ_{cu} and ϵ_{cu} is the strain at f'_c .

Table AII. 3
 Compression Test on Stack Bonded Prism (Load Normal to bed joint)
 (Normal stress-strain reading* for Brick X 10⁻⁶)

Stress Mpa	Prism No										\bar{X}	S	C.of V %
	1	2	3	4	5	6	7	8	9	10			
1.2	114	58	60	136	147	88	148	83	91	137	106	33	31
2.4	241	162	133	114	225	244	158	265	185	179	273	54	27
3.6	210	214	177	312	378	246	372	302	324	400	293	74	25
4.8	312	303	246	408	530	348	488	405	405	536	398	90	22.5
6.0	351	402	316	501	683	454	603	516	539	671	504	119	23.6
7.2	426	517	386	590	821	572	711	632	747	810	621	144	23
8.4	532	603	446	682	969	748	821	744	976	935	745	174	23.4
9.6	648	689	511	784	1132	926	925	852	1210	1060	874	210	24
10.8	780	776	573	887	1287	975	1028	957	1500	1186	995	257	25.8
12.0	927	867	650	995	1442		1123	1064	1488	1299	1100	260	23.4
13.3	1036	952	727	1101	1586		1202	1157	1582	1449	1200	270	22
14.5	1172	1037	804	1211	1715			1247	1573	1515	1280	280	22
15.7	1309	1130	884		1855				1671	1600	1410	330	23
16.9	1455	1187			1994				1895	1742	1655	2960	18
18.1	1625	1251			2124				2123		1780	340	19
19.3		1329			2203				2278		1937	43	22
20.5		1448			2225								
f_{pm} (MPa)	19.0	21.2	16.8	14.8	21.2	19.3	15.7	16.3	18.8	18.4	18.16	2.1	11
E_0 (GPa)	16.3	15.9	19.3	11.2	9.4	14.3	9.3	12.3	12.3	9.0	12.93	3.28	25

Note: E_0 = Initial Tangent Modulus of Brick when load is normal to bed
 (obtained from prism test)

* Measured in the middle height of middle brick in the direction of the load
 applied in the Prism Test

Table AII. 4
Average of Lateral Strain Reading of Brick and Mortar !

Brick				Mortar	
Stress (MPa)	Lateral strain $\times 10^{-6}$ (Load parallel to bed)	Stress (MPa)	Lateral strain $\times 10^{-6}$ (Load normal to bed)*	Stress (MPa)	Lateral strain $\times 10^{-6}$ (Mortar cylinder)
4.12	36.4	1.2	23.4	0.98	17
8.24	62	2.4	37.8	1.96	34
12.36	92.2	3.6	59	2.94	64
16.47	126.3	4.8	79.3	3.92	93
20.59	163.7	6.0	99.4	4.90	117
24.71	200	7.2	119.6	5.88	141
28.83	231.9	8.4	144	6.86	166
32.95	253.8	9.6	172	7.84	190.3
		10.8	201	8.82	246
		12.0	233	9.8	302.3
		13.3	266		
		14.5	323		
		15.7	404		
		16.9	386		

* Measured in the midheight of middle brick in the direction transverse to the direction of the load applied in the Prism Test

! Details can be seen from Table AII.14(a) and Table AII.14(b)

Table AII. 5
Compressive and Tensile Strength of Mortar
(All values of strength are in MPa)

Specimen	Compressive Strength**		Tensile Strength*
	No	2 in. cube	6 in. cylinder
1	12.80	11.68	0.971
2	12.40	11.76	0.960
3	12.30	11.68	1.017
4	12.42	12.58	0.914
5	13.27	12.58	0.937
6	13.52		0.994
7	11.56		1.000
8	11.24		0.971
9	12.59		0.902
10	12.74		1.017
\bar{X}	12.5	12.0	0.97
S	0.66	.043	0.038
C. of V (%)	5.0	4.0	4.0

Note: ** Determined from tests on 2 in. cube and 3 in. X 6 in. cylinder at 28 days

* Determined from Splitting test on 100 mm X 50 mm X 40 mm prism
at 28 days

Table AII. 6
 Compressive Test on Mortar Cylinder
 (Normal stress-strain reading for Mortar, $\times 10^{-6}$)

Stress (MPa)	Mortar Cylinder			\bar{X}	S	C. of V %
	1	2	3			
0.98	91	95	98	94.7	2.8	3
1.96	182	190	196	189.3	5.7	3
2.94	276	302	428	335.3	66.4	20
3.92	369	413	659	480.3	127.6	26
4.90	473	521	784	592.7	136.7	23
5.88	577	629	909	705	145.8	20.6
6.86	711	818	954	827.7	99.4	12
7.84	845	1006	999	950	74.3	8
8.82	1051	1280	1207	1179.3	95.5	8
9.8	1256	1554	1414	1408	121.7	8
E_0 (GPa)	11.0	10.4	7.37	9.59	1.58	16

Table AII. 7
Compressive Test on Stack Bonded Prism
(Normal stress-strain reading for Brickwork, X 10⁻⁵)

Stress	Prism No										\bar{X}	S	C. of V %
	1	2	3	4	5	6	7	8	9	10			
1.2	18.2	9.1	27.3	18.0	18.2	9.1	15.9	13.6	13.7	14.8	15.8	5.0	31
2.4		20.5	36.4	29.5	29.5	31.8	34.1	29.5	25.0	29.5	29.0	4.4	15
3.6	43.2	36.4	47.3	50.0	43.2	52.3	61.4	47.7	40.9	47.7	47.0	6.5	14
4.8	65.9	52.3	65.9	75.0	63.6	75.0	88.6	70.5	52.3	70.5	67.9	10.3	15
6.0	88.6	70.5	72.7	102	84	102	129	95.5	71.6	95.5	91.3	17.2	19
7.2	118	88.6	81.8	134	111	136	152	125	100	123	117	20.9	18
8.4	146	111	111	171	136	171	186	159	132	152	147	23.7	16
9.6	180	134	143	209	171	211	223	191	168	184	181	27.3	15
10.8	205	161	148	252	205	268	264	230	214	221	217	38.0	18
12.0	246	189	221	307	243	296	293	264	266	259	258	34.2	13
13.3	282	223	266	371	284	352	355	311	321	302	307	43.0	14
14.5	323	259	311	434	327	405	409	366	377	348	356	50.2	14
15.7	382	291	366		377	459	520	514	459	407	420	70.7	17
16.9	432	339	518		425				568	450	452	67.8	15
18.1	507	418			471	580			659		527	84.5	16
19.3		484			525	666			746		605	105	17
20.5		550			616						583	32.6	5
f'_{pm}	19.0	21.2	16.8	14.8	21.2	19.3	15.7	16.3	18.8	18.4	18.2	2.1	11
E_{0pm}	8.56	9.89		7.37	8.48	6.82	6.01	7.73	10	7.76	8.07	1.25	15

Note: f'_{pm} = Prism Strength in MPa and
 E_{0pm} = Initial Tangent Modulus of Prism in GPa

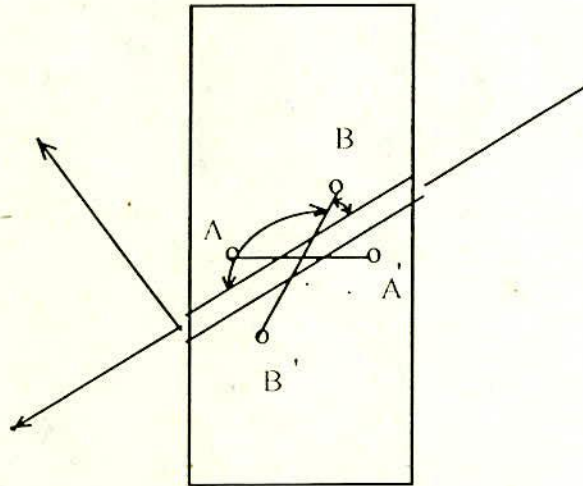
Table AII. 8
Compressive Test on Stack Bonded Prism
(Normal stress-strain reading for Mortar Joint, $\times 10^{-5}$)

Stress MPa	Prism No									\bar{X}	S	C. of V %
	1	2	3	4	5	6	7	8	9			
1.2	54	26.5	41	37	10.7	21.8	41.8	38	20.4	32	12	7
2.4	71.5	58.2	66.8	56.4	117	74.3	87.6	62.5	41.4	62.7	28.4	45
3.6	160	115	149	71.6	199	189	140	86	88.6	127	52.8	42
	249	168	256	220	288	299	229	115	160	209	66.2	32
6.0	372	230	378	168	403	496	327	165	245	309	107	35
7.2	518	284	531	266	555	581	452	234	343	418	129	31
8.4	633	381	711	345	676	738	607	313	463	541	157	30
9.6	786	479	900	473	839	911	750	418	597	684	183	27
10.8	873	604	1117	606	1170	1114	937	550	756	859	228	26
12.0	1053	728	1403	766		1249	1095	885	942	1050	218	21
13.3	1225	897	1747	948		1593	1346	1178	1134	1258	276	22
14.5	1409	1080	2089	1150			1641	1540	1385	1471	312	21
15.7	1708	1136		1391				2002	1711	1590	298	19
16.9	1945	1501		1619				2570	1908	1908	37	19
18.1	2327	1967		1834				3021		2287	460	20
19.3		2340		2137				3481		2653	592	22
20.5		2692		2695						2694	1.8	.06
f'_{pm}	19.0	21.2	14.8	21.2	19.3	15.7	16.3	18.9	18.4	18.3	2.16	11.8
E_0	2.67	3.54	2.80	4.36	2.48	2.66	2.74	4.18	3.99	3.27	0.70	21

\bar{X} = Mean, S = Standard Deviation, C. of V. = Coefficient of Variation

Note: f'_{pm} = Prism Strength in MPa and E_0 = Initial Tangent Modulus of Mortar (in situ) in GPa

Strain Transformation Equations



Measured Strain: $AA' = \epsilon_A$
 $BB' = \epsilon_B$

Strain at angle is :

$$\epsilon_{\theta} = \epsilon_X \cos^2 \theta + \epsilon_Y \sin^2 \theta + \gamma_{XY} \sin \theta \cos \theta$$

in which ϵ_x, ϵ_y are normal strains and γ_{xy} the shear strain i.e.

$$\begin{aligned} \epsilon_A &= \epsilon_X \cos^2 \theta + \epsilon_Y \sin^2 \theta + \gamma_{XY} \sin \theta \cos \theta \\ \epsilon_B &= \epsilon_X \cos^2 \theta' + \epsilon_Y \sin^2 \theta' + \gamma_{XY} \sin \theta' \cos \theta' \end{aligned}$$

Substitute $\theta' = 180 - \theta$ and subtract (2) from (1),

$$\therefore \gamma_{XY} = \frac{\epsilon_A - \epsilon_B}{\sin 2\theta}$$

Table AII. 9
 Shear Deformation of Shear Couplets ($\theta = 40^\circ$)
 (Shear stress-strain reading for brickwork ($\times 10^{-5}$))

Stress MPa	Couplet no			\bar{X}	S	C of V %
	1	2	3			
0.79	13.2	16	18	15.7	2	13
1.57	21	40	40	33.7	9	27
2.37	38	95	83	72	24	33
3.15	55	150	127	106	39	37
3.94	75	207	183	155	57	37
4.73	101	262	263	208.7	76	36
5.62	140		353			
6.3	200					
7.1	296					

Table AII.10
 Shear Deformation of Shear Couplets ($\theta = 40^\circ$)
 (Shear stress-Strain reading for mortar joint ($\times 10^{-5}$))

Stress MPa	Couplet no			\bar{X}	S	C of V %
	1	2	3			
0.79	32.7	47.5	58.0	46	10.3	22
1.57	37.3	137.7	137.7	104.2	47.3	45
2.37	89.6	391.0	327.4	266	128	48
3.15	142.8	645.0	447.8	411.8	206	50
3.94	211.4	909.2	782.3	634.3	303	47
4.73	311.7	1162.8	1168	881	402	45
5.62	476.1		1602			
6.3	761.4					
7.1	1231					
G	2838	1342.4	1271	1817	722	40

Table AII. 11
 Constants for Stress-Plastic Strain Equations for Mortar

Specimen No	Normal Stress-Strain		Shear Stress-Strain	
	a_n	b_n	a_s	b_s
1	-7.36	0.198	-10.76	.825
2	-8.48	0.243	-8.676	.90
3	-8.94	0.275	-8.821	.81
4	-8.59	0.358		
5	-7.21	0.224		
6	-9.03	0.346		
7	-8.07	0.249		
\bar{X}	-8.24	0.27	-9.42	.845
S	-0.67	.05	-.95	.04
C. of V (%)	8.1	18	10	5

Table AII. 12
 Tensile Bond Strength of Vertical Joints (Splitting Test on Brick Masonry Prism)

Specimen No	Ultimate Vertical. load (kN)	Tensile Bond Strength (MPa)
1	17.7	1.43
2	16.0	1.29
3	15.4	1.24
4	20.0	1.62
5	19.4	1.57
6	15.8	1.28
7	17.6	1.42
8	20.5	1.66
9	18.7	1.51
10	17.5	1.41
\bar{X}	17.86	1.443
S	1.69	0.138
C. of V (%)	9.46	10

\bar{X} = Mean, S = Standard Deviation, C. of V. = Coefficient of Variation

Table AII.13
Shear Test on Brick Masonry Triplet

Specimen No	Ultimate Load (kN)	Shear Stress (MPa)
1	6.672	0.54
2	6.672	0.54
3	6.583	0.53
4	9.341	0.76
5	7.739	0.63
6	6.850	0.55
7	7.117	0.57
8	9.163	0.74
9	6.138	0.49
10	7.117	0.57
\bar{X}	7.339	0.594
S	1.04	0.09
C. of V (%)	14.2	15

\bar{X} = Mean, S = Standard Deviation, C. of V. = Coefficient of Variation

Table AII.14(a)
Lateral Strain Reading of Bricks ($\times 10^{-6}$)
(obtained from uniaxial compression test on brick, Load parallel to bed)

Stress in MPa	Brick No									\bar{X}	S	CF V
	1	2	3	4	5	6	7	8	10			
4.12	85	34	35	15	25	25	60	39	10	36.4	22	60
8.24	113	54	56	40	55	55	80	68	37	62	21.8	35
12.36	150	77	76	83	67	91	105	102	79	92.2	23.5	25
16.47	203	96	145	105	74	130	150	124	110	126.3	35.2	27.8
20.59	252	128	174	155	94	170	190	176	161	163.7	40.9	25
24.71	301	148	197	210	116	210	225	205	219	200	49	24.5
28.83	341	161	219	259	138	249	250	242	265	232	56.8	24.5
32.95	374	177	258		145	304	277	270		254	71.1	28
37.07	447	207	271				315	301		308	78.7	25.5
41.18		313	309									
45.30		373										
Fail	39.1	47.8	46.3	35.42	36.86	36.04	44.1	47.8	32.5	40.2	5.44	13.5

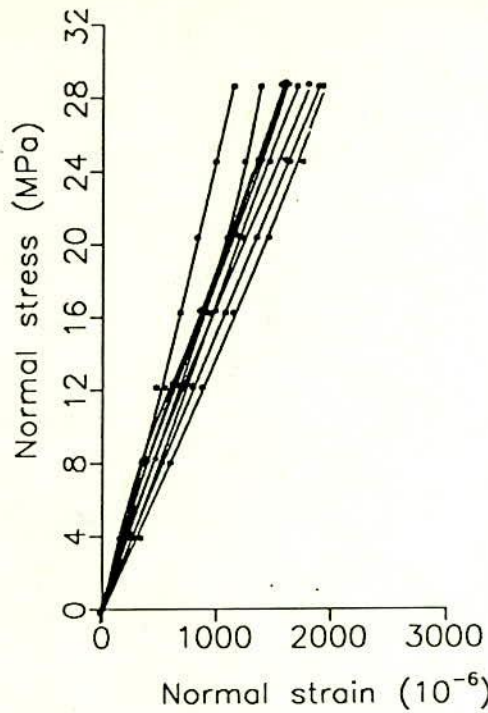
Note : The strain recorded at the end of each brick is the maximum tensile lateral strain at the specified load corresponding to the last strain recorded . On averaging these strains the maximum tensile strain can be assumed to be 30.2×10^{-5}

Table AII.14(b)
Lateral Strain Reading of Bricks ($\times 10^{-6}$) from Prism Tests
(Measured in Transverse Direction of Loading, i. e, Load Normal to Bed)

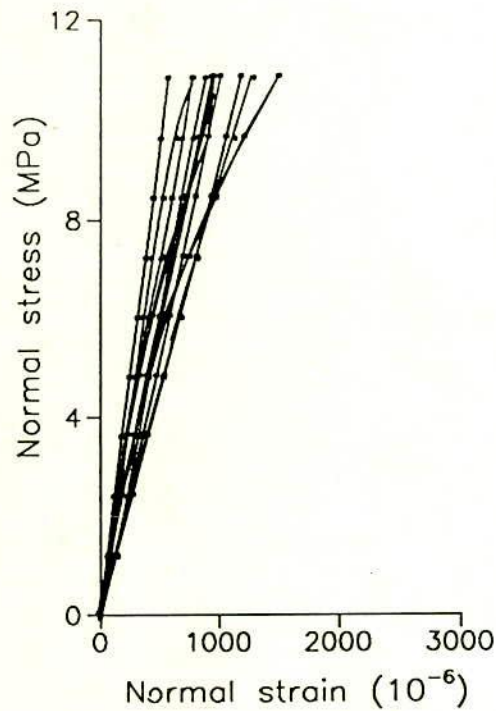
Stress in MPa	Prism No										\bar{X}	S	C of V
	1	2	3	4	5	6	7	8	9	10			
1.2	39	36	20	-35	19	12	28	21	15	21	23.4	8.6	36
2.41	117	58	31	-26	30	21	58	41	25	39	37.8	13	34
3.62	196	78	47	-12	50	34	90	63	53	57	59	16.7	28
4.82	249	101	60	5	71	48	121	84	68	81	79.3	21.7	27
6.03	343	115	75	24	93	65	152	108	85	101	99.4	25	25
7.23	409	130	93	48	113	82	185	133	93	128	120	30.6	25
8.44	452	165	110	72	138	100	220	156	108	155	144	37	26
9.64	487	203	130	97	170	120	259	180	127	183	172	43.6	25
10.9	530	237	147	124	202	139	305	206	156	216	201	51.4	25
12.1	568	273	166	157	235	159	350	237	190	251	233	58.6	25
13.3	609	309	184	189	263	175	389	282	229	297	266	65.7	25
14.5	664	349	202	211	292	187	392	388	432	338	323	83	26
15.7	722	382	223		326		462		626	404	404	124	30
16.9	777	419	283		368					475	386	70	18
18.1	732	439			406								
Fail	19.0	21.2	16.9	14.8	21.2	19.3	15.7	16.3	18.9	18.4	18.2	21	11

Note: In the Prisms 2,6,8,9 10 the lateral strain decreases due to on set of cracks at loads corresponding to the last strain entry. Therefore the average tensile strain at which the brick starts cracking can be assumed to be 42.3×10^{-5} in comparison to max. compressive strain (227.5×10^{-5}) obtained from uniaxial tests on bricks loaded parallel to the bed joint.

Note: Prism no 1 and 4 was not considered due to very high and low reading respectively.



(a) Stress-Strain diagram for bricks
(Load parallel to bed)



(b) Stress-Strain diagram for brick
(from Prism test)

Fig. AII.1 Normal Stress-Strain Curve for Individual Bricks
(Uniaxial Compression Test and Prism Test)

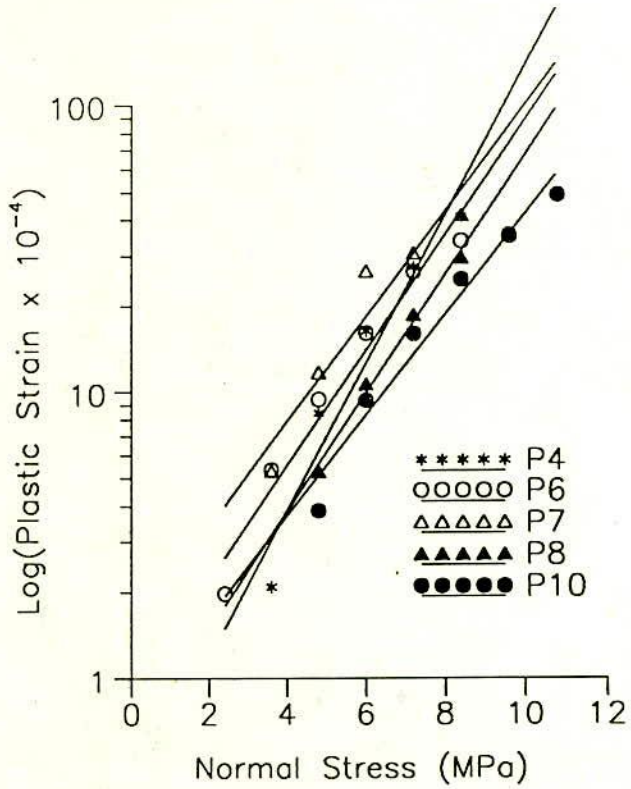
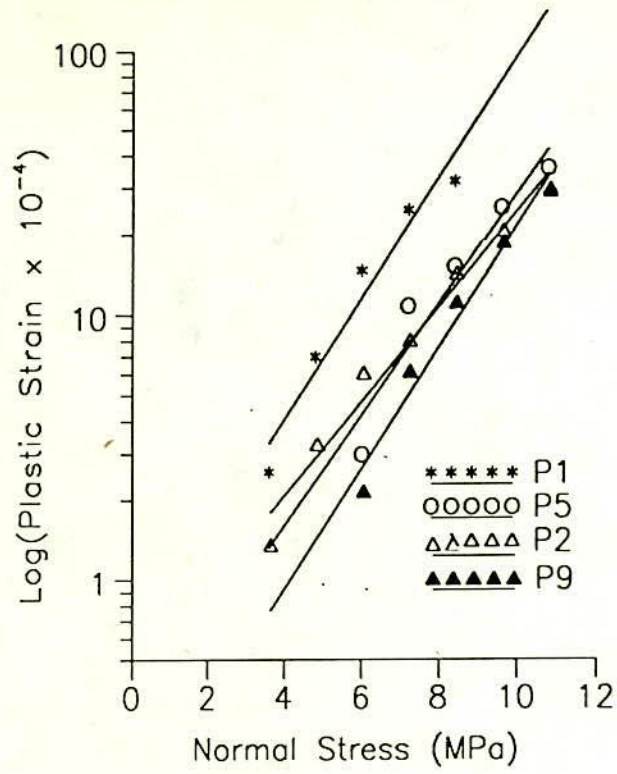


Fig. AII.2 Semi Logarithmic Plot of Plastic Normal Strain Vs. Normal Stress

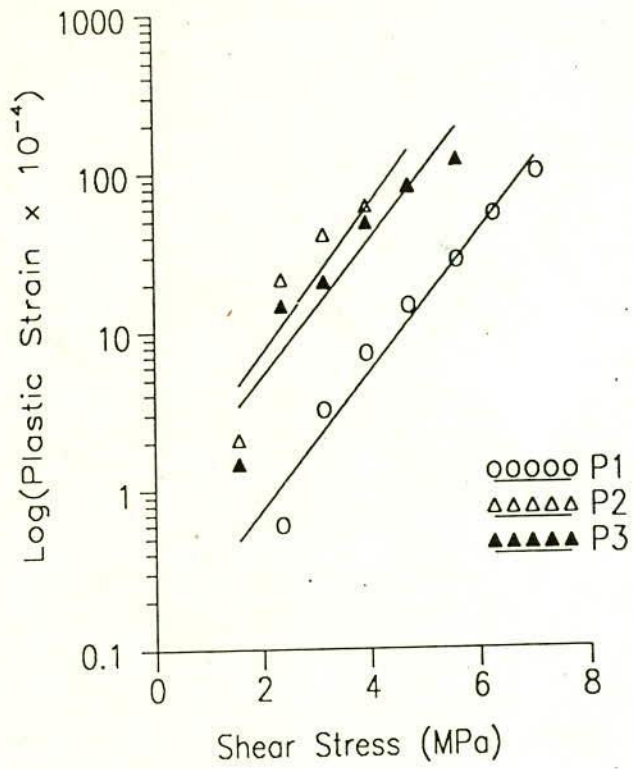


Fig. AII.3 Semi Logarithmic Plot of Plastic Shear Strain Vs. Shear Stress

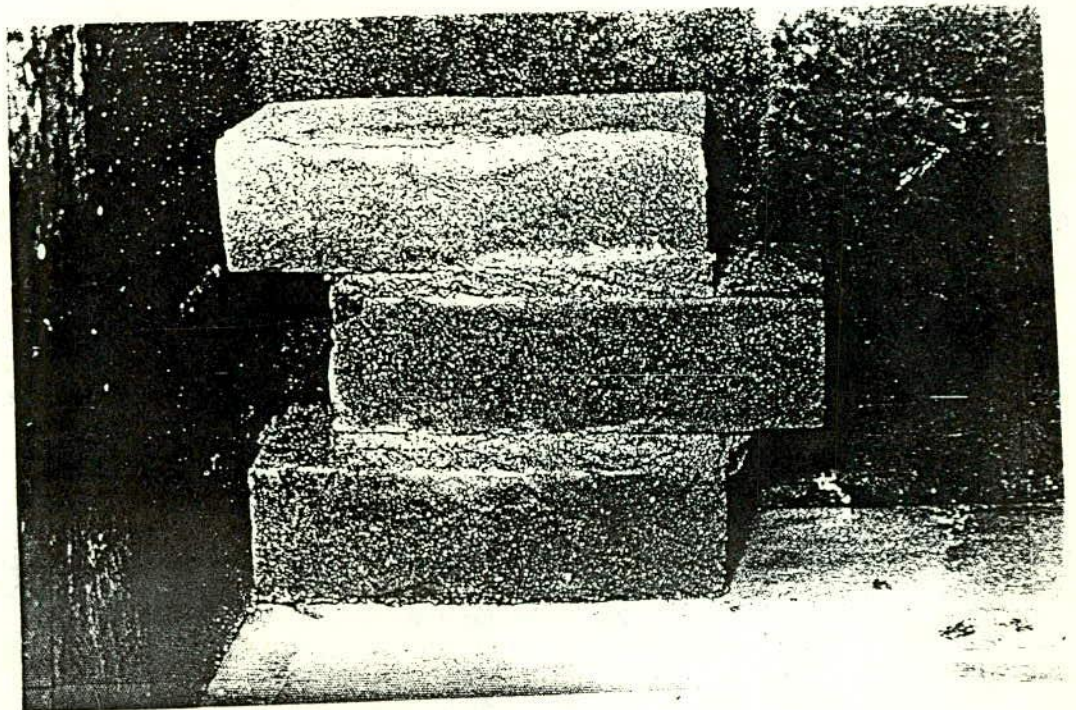


Fig. AII.4 Construction of Control Specimens

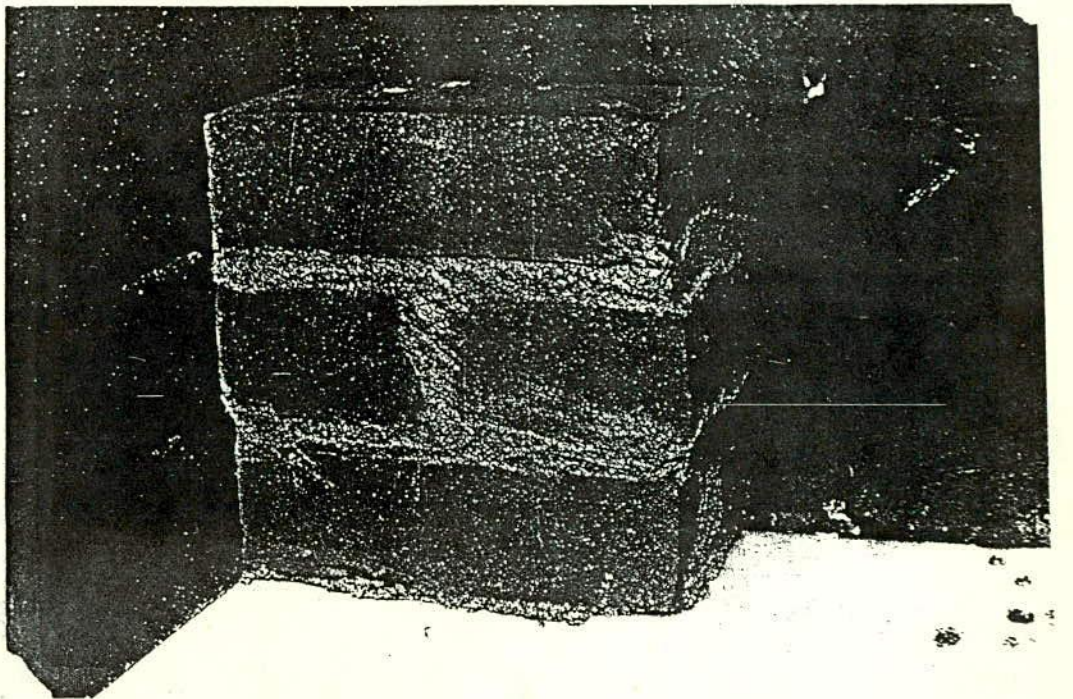
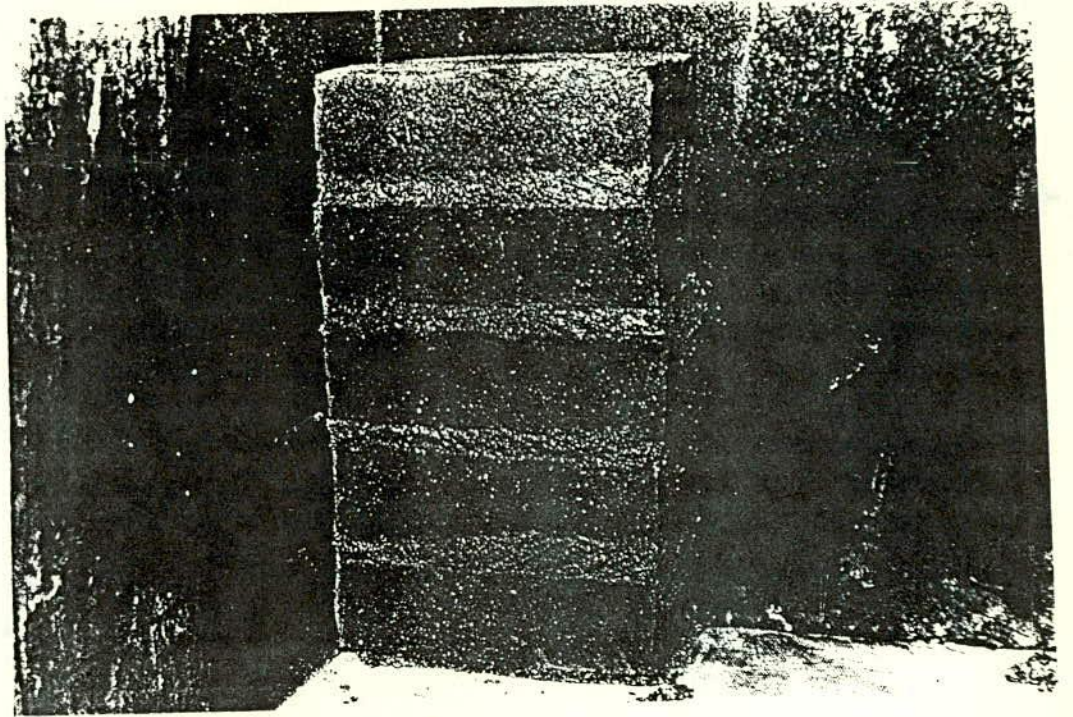


Fig. AII.4 Construction of Control Specimens

APPENDIX III

PROGRAM "WBMGEN"

Content

Description of Major Subroutines

Table AIII.1 Error Code for Checks for Input Data

Table AIII.2 Various Options of Output

Table AIII.3 Codes of Different Modes of Failure

Sample Data File

Sample out-put file

Program structure for new or modified subroutines

Description of major Subroutines :SUBROUTINE "PROBTP"

This subroutine mainly determines the following:

1. Type of bond failure to be used for the mortar joint.
2. Type of softening model to be used
3. Type of fracture analysis to be performed

SUBROUTINE "INPUT"

This subroutine accepts data for the finite element subdivision and the material properties. The data necessary is generated by the subroutine "GENER" and "CORDEN".

SUBROUTINE "GENER"

This subroutine generates the finite element mesh using a 4 noded element. This subroutine gives the same material number to all the elements.

SUBROUTINE "REDATA"

This subroutine gives the option to change the data on the load factor (FACTO) and solution algorithm (NALGO) if the crack forms within the wall-beam structure. Due to formation of crack the convergence becomes very slow. So to make convergence quicker the load can be applied in smaller increments and the solution technique also can be changed. (NALGO = 3 represents initial stiffness method and NALGO = 1 represents modified Newton-Raphson method).

SUBROUTINE "CENTRE"

This subroutines calculates the co-ordinates of the centre, the height and width of the 4 noded rectangular element and stores in vectors XCEN(IELEM) YCEN(IELEM), AX(IELEM) and BX(IELEM) respectively. These are required for plotting purposes.

SUBROUTINE "DIMEN"

This subroutine carries out "dynamic dimensioning" of various arrays used in the program. With dynamic dimensioning, variable names are assigned to the parameters controlling the size of the program (such as the maximum number of nodes, maximum number of elements, maximum front width, etc.).

SUBROUTINE "DIFMAT"

This subroutine is called when the wall-beam structure is modelled as a non-homogeneous material. This subroutine accepts data on the number of elements to be provided per course and on different levels of brickwork where the vertical joints are to be assigned. The subroutine assigns the correct material number and the orientation number for the joint elements.

SUBROUTINE "CHECK1"

This subroutine checks any obvious errors in the input of main control data. The errors diagnosed by this subroutine are given in Table AIII.1.

SUBROUTINE "CHECK2"

This subroutine checks any obvious errors in the input data related with finite element mesh generation. The errors diagnosed by this subroutine are given in Table AIII.1.

SUBROUTINE "LOADPS"

This subroutine accepts the data on the applied loads. The applied loads are stored in an array RLOAD(IELEM, IEVAV) in which IELEM ranges over the number of elements and IEVAB ranges over the degrees of freedom of the element.

SUBROUTINE "ZERO"

This subroutine initialises single and dimensional variables. This is necessary because many variables are cumulative in the incremental iterative program.

SUBROUTINE "INCREM"

This subroutine accepts data on the load factor "FACTO" by which the applied load must be incremented, tolerance factors "TOLFR" for force criteria and "TOLDS" for displacement criteria, maximum number of iterations permitted "MITFR" and output controlling parameter "NOUTP". FACTO is cumulative and allows for unequal increments of load to be applied. TOLFR and TOLDS allows the degree of accuracy desired in and increment to be varied.

SUBROUTINE "ALGOR"

This subroutine controls the method of solution. The controlling parameter of the solution process is KRESL. If the stiffness matrices of the elements are reformulated, KRESL is assigned a value 1; if not, KRESL assigned a value 2 and the initial stiffness matrices are used for the solution process.

SUBROUTINE "DBFAL"

This subroutine modifies the [D] matrix for the cracking or crushing type of failure in the materials. For cracking type of failure, materials only loses its strength perpendicular to the crack whereas for crushing type of failure, material loses its strength completely.

SUBROUTINE "DJFAL"

This subroutine modifies the [D] matrix for the bond type of failure. Bond type of failure occurs when the normal stress is tensile.

SUBROUTINE "DIFFEL"

This subroutine evaluates the linear elastic stiffness matrix for the representative elements and stores them in a 3-D array. Unless the element is either plasticised or fractured, the stiffness matrix for the element is taken from this array. Element representation array is IELEM(IELEM).

SUBROUTINE "STIFFP"

This subroutine is called from the subroutine FRONT when KRESL =1. The main purpose of this subroutine is to inform, whether the element IELEM is elastic, plastic or fractured. If the element is in the elastic limit, takes the stiffness matrix from 3-D array STOCK(IEVAB, JEVAB, KLEM), otherwise the subroutine recalculates the stiffness matrix for the element.

SUBROUTINE "FRONT"

The frontal solution is a very efficient direct solution process in which the active life of a node lasts from the time in which it first appears in an element to the time in which it last appears in an element. The main idea of frontal solution is to assemble the equations and eliminate the variables at the same time. As soon as the coefficient of the equation are completely assembled from the contribution of all relevant elements, the corresponding variable can be eliminated. Therefore the complete structural stiffness matrix is never formed as such, since after elimination the reduced equations immediately transferred to back-up file. During the assembly/elimination process the elements are considered each in turn according to a prescribed order. The maximum size of problem which can be solved is governed by the "maximum front width". Whenever a new element is called in, its stiffness coefficients are read from memory and summed either in to existing equations if the nodes are already active, or into new equations which have to be included in the front if the nodes are being activated for the first time. If some nodes are appearing for the last time, the corresponding equations can be eliminated and stored away on a file and are thus deactivated. In so doing they free space in the front which can be employed during assembly of the next element. The displacement are obtained by back substitution in reverse order. In this study the frontal solution subroutine is treated as "black box" and the details can be found elsewhere (Hinton and Owen, 1977).

SUBROUTINE "GAPCOM"

This subroutine accepts data for different physical aspects of wall-beam structure e.g., supporting beam, lintel/top beam, end or intermediate column, opening in the wall-beam and support details. This subroutine assigns material number for concrete beam and column with the provision of interface mortar between concrete and wall. The subroutine also accepts data to assign material number for reinforcement in the supporting beam.

SUBROUTINE "MOMAX"

This subroutine utilises the array STRSG(I, IELEM), AX(IELEM) and BX(IELEM) to calculate forces (horizontal, vertical and shear) acting on the elements in supporting beam. By summing horizontal forces acting on elements along a vertical section the tension at that section of the supporting beam is calculated. These are stored in an array AXIAL(NLEMY). From this array maximum tension in the beam is scanned. Similarly the vertical force at wall-beam interface level and at reaction nodes are obtained to calculate moment in sections along the span and is stored in an array WBTMOM(IM) from where maximum moment without considering shear force at interface is scanned. Provision for calculating moment considering shear force is also present in this subroutine. In the same way maximum vertical stress concentration and maximum shear stress concentration is obtained.

SUBROUTINE "BFSTRS"

The role of this subroutine is to monitor the cracking and crushing type of failure of the elements. This subroutine also releases the stresses according to the degree of softening (NRELS) used in the materials. For brittle collapse model, subroutine STRELT is called to release the stresses. For strain softening, subroutine BSTREL is called to release the stresses gradually.

SUBROUTINE "FJOINT"

The purpose of this subroutine is to monitor the bond type of failure of the mortar joint. The subroutine releases according to the degree of softening (NRELS) used in the mortar joint. For releasing the stresses, the subroutine XJSTRL is called. For bringing the stresses to the failure surface, the subroutine DUCT is called.

SUBROUTINE "RESIDU"

The function of this subroutine is to evaluate the stress in various elements allowing for non-linear deformation and post-failure behaviour. When the elements are fractured, the subroutine RESD is called to calculate the residual forces. The nodal forces thus determined are stored in the array ELOAD which is used for a latter check on convergence and as a load for the next iteration. Subroutine REDUCT is called to evaluate the stresses according to the constitutive relations before fracture of the materials. Whereas, the subroutine BFSTRS is called to check the violation of fracture criteria and to evaluate the stresses according to the constitutive relations after fracture of the materials. The subroutine REDJON is called to evaluate the stresses for joint elements before bond type of failure whereas the subroutine FJOINT is called to evaluate the stresses according to the constitutive relations after bond type of failure in the mortar joint. Of the stresses exceeding the initial failure surface, the "excess" stresses are removed suddenly or gradually. The nodal forces are evaluated from these excess stresses which is applied further to correct the displacements. The subroutine CRACK is called to check the status of the crack (closed or reopened).

SUBROUTINE "CONVER"

The role of this subroutine is to check whether or not the solution process is converging. Force as well as displacement convergence criteria has been used. For force criterion, the residual nodal forces in the array ELOAD (evaluated in the subroutine RESIDU), are compared against the total external load-reaction system TLOAD (accumulated through the process of iteration). If the ratio of the sum of the squares of the residual forces (ϕ) to the sum of the squares of the external forces (F) is less than the prescribed tolerance limit (TOLER), the process is assumed to have converged. Stated mathematically for convergence to occur,

$$\sum_{i=1}^N \frac{(\phi_i^r)^2}{(F_i^T)^2} \leq \text{TOLER}$$

Similarly for displacement criteria

$$\sum_{i=1}^N \frac{(\Delta\delta_i)^2}{(\delta_i^T)^2} \leq \text{TOLER}$$

where ϕ_i is the residual force; F_i^T is the total load; $\Delta\delta_i$ is the incremental displacement and δ_i^T is the total displacement for the iteration i . N is the total number of nodal points of the structure. If the solution process is found to have not converged, it could be either converging or diverging depending on the values of the residual forces in the i th iteration. A parameter NCHEK, defining the nature of the solution process is assigned different values depending on the stage of the solution process. For a converged solution NCHEK

is zero; for converging process NCHEK is one and for a diverging process a value "999" is assigned. The convergence code is printed out at every iteration.

SUBROUTINE "OUTPUT"

This subroutine is called if the solution process has converged at a given load increment to print out the various segment of output specified by input parameter NOUTP. The codes of parameter NOUTP and its interpretation are given in Table AIII.2. The subroutine PLOTIGLAST is called to make the data file for plotting purposes and the subroutine CRFUL is called to check whether or not the crack has propagated through the height of the wall-beam.

Table AIII.1 Error Code for Checks for Input Data

ERROR CODE	INTERPRETATION
1	Total number of structure nodes less than or equal to zero
2	The possible maximum total number of nodal points in the structure is less than the specified number of structure nodes
3	The number of restrained nodes is less than two or greater than the number of structures nodes
4	The total number of load increments is less than 1
5	The total number of nodes per element is less than 4 or greater than 9
6	The number of degrees of freedom per node is less than 2
7	The number of different materials is less than 1 or greater than the number of elements
8	The number of Gauss integration points in each direction is less than 2 or greater than 3
9	Two nodes have identical co-ordinates
10	The material number of element is less than 1 or greater than the number of different materials
11	Nodal number of the element is zero
12	Nodal number of the elements is less than 1 or greater than the total number of nodal points
13	Repetition of a node number within an element
14, 15	Co-ordinates of an unused node have not been specified
16	Unused node number is a restrained node
17	Required front width is greater than the front width available in the program
18	Restrained node number is less than or equal to zero or greater than the total number of nodal points
19	Restrained code is missing for restrained nodes
20	Two identical restrained nodes

Table AIII.2 Various Options of Output

OUTPUT CODE	INTERPRETATION
0	No output necessary
1	Print only the displacements of nodes
2	Print displacements of nodes and reaction at supports
3	Print displacements of nodes, reaction at supports and stresses at each sampling point of the element

Table AIII.3 Codes of Different Modes of Failure

OUTPUT CODE	INTERPRETATION
11	Bond type of failure for the joint. Cracking type of failure for the brick and concrete
22	Crushing type of failure for brick, mortar and concrete
33	Cracking type of failure for the mortar
11	Yielding of steel

Sample Data File

The sample data was produced for a Wall-beam of following physical aspects :-

Span=1290 mm,

Height=784.5 mm

Beam Depth=45 mm

Beam Width=100 mm

At Support 6 Nodes are Restrained in Y- Direction

Idealised Vertical and Horizontal Mortar=7.5 mm

Prediction by Strain Softening Model gave the following main results :-

$P_c = 29.64$ kN AT 4th increment (the crack opens for the first time)

$P_u = 2 \times 96.3$ kN AT 19th increment, failed of converge within specified number of iterations (i.e., Numerical Failure)

Data File

```

70 0 0 1 1 0 3 .10000 .500
0.522 0.154 -0.808 -0.924 -0.179 0.834
6.
1848 1848 1760 62 4 7 2 3 2 40 33 56 0 0
0 0 0 0 0 0 0 1 1 1 0
0 5
0
1 33 65 97 129
000.00 14.44 28.88 43.32 57.75 65.25 84.50
103.75 123.00 130.50 159.375 188.25 195.75 224.625
253.50 261.00 289.875 318.75 326.25 355.125 384.00
391.50 420.375 449.25 456.75 485.625 514.50 522.00
550.875 579.75 587.25 616.125 645.00
000.00 12.50 19.50 32.00 45.00 52.50 70.50
88.50 96.00 114.00 132.00 139.50 157.50 175.50
183.00 201.00 219.00 226.50 244.50 262.50 270.00
288.00 306.00 313.50 331.50 349.50 357.00 375.00
393.00 400.50 418.50 436.50 444.00 462.00 480.00
487.50 505.50 523.50 531.00 549.00 567.00 574.50
592.50 610.50 618.00 636.00 654.00 661.50 679.50
697.50 705.00 723.00 741.00 748.50 766.50 784.50
4 2 6 9 5 15 12 21 18 27
24 32 30 3 3 3 3 3 3 3
3 1 3
1 0
33 5 1 5
0
1 1
2 0 2
1 01 0.000 0.0000
2 01 0.000 0.0000
3 01 0.000 0.0000
4 01 0.000 0.0000
5 01 0.000 0.0000
6 01 0.000 0.0000
33 10 0.000 0.0000

```


Sample Output File

MAXIMUM FRONT WIDTH USED = 70
 INDICATOR FOR SUB STRUCTURING TECHNIQUE = 0
 TYPE OF BOND FAILURE CRITERION USED = 0
 TYPE OF FRACTURE ANALYSIS = 1
 TYPE OF COLLAPSE MODEL = 1
 INDICATOR FOR INTERNAL EQUILIBRIUM CHECK = 0
 POST FRACTURE SOLUTION ALGORITHM TYPE = 3
 AGGREGATE INTERLOCK FACTOR = 0.1000
 LOAD FACTOR AFTER FRACTURE INITIATES = 0.5000

CONVENTIONAL FINITE ELEMENT ANALYSIS
 TOTAL NUMBER OF STRUCTURE NODES = 1848
 TOTAL NUMBER OF ELEMENTS = 1760
 TOTAL NUMBER OF BOUNDARY NODES = 62
 NUMBER OF NODES PER ELEMENT = 4
 TOTAL NUMBER OF DIFF. MATERIALS = 7
 ORDER OF GAUSS QUADRATURE RULE = 2
 TOTAL D.O.F. OF ELEMENT = 8
 TYPE OF THE ALGORITHM = 3
 TYPE OF YIELD CRITERION = 2
 NUMBER OF LOAD INCREMENTS = 40

ELEMENT CONNECTIVITY DATA :
 (out put cancelled to minimise space)

IDENTIFICATION CODES :
 --- * --- 10 : CONCRETE BRICK
 --- * --- 20 : BED JOINT
 --- * --- 30 : HEADER JOINT

ELEM.NO. MATERIAL PROP. ID NO. ELEMENT NODAL NUMBERS
 (out put cancelled to minimise space)

NODAL COORDINATES IN MM :
 NODE NO. X-AXIS Y-AXIS
 (out put cancelled to minimise space)

SUPPORT INFORMATION :
 **** 10 - FIXED ALONG X AXIS ****
 **** 01 - FIXED ALONG Y AXIS ****
 **** 11 - FIXED ALONG X&Y AXES****

NODE NO.	CODE	FIXED VALUES(MM)	
1	1	0.00000	0.00000
2	1	0.00000	0.00000
3	1	0.00000	0.00000
4	1	0.00000	0.00000
5	1	0.00000	0.00000
6	1	0.00000	0.00000
33	10	0.00000	0.00000
66	10	0.00000	0.00000
99	10	0.00000	0.00000
*	*	*	*
*	*	*	*


```

*      *      *      *
1782  10  0.00000  0.00000
1815  10  0.00000  0.00000
1848  10  0.00000  0.00000

```

MATERIAL PROPERTIES:
(out put cancelled to minimise space)

MAXIMUM FRONTWIDTH ENCOUNTERED = 70

NUMBER OF NODAL LOADS= 1
NUMBER OF BODY FORCES= 0
NUMBER OF EDGE FORCES= 0

```

1816  0.0000E+00  -0.8300E-01
1817  0.0000E+00  -0.1660E+00
1818  0.0000E+00  -0.1660E+00
*      *      *
*      *      *
*      *      *
1846  0.0000E+00  -0.2090E+00
1847  0.0000E+00  -0.3320E+00
1848  0.0000E+00  -0.1660E+00

```

INCREMENT NUMBER= 1

LOAD FACTOR = 1.000
CONVERGENCE TOLERANCE = 1.000
MAXIMUM NO.OF ITERATION = 20
INITIAL OUTPUT PARAMETER = 0
FINAL OUTPUT PARAMETER = 0

CURRENT ITERATION NO.= 1

ELEMENTS THAT HAVE JUST FAILED
EL. NO. MAT NO. ID NO. FAILURE CODE XX-STRESS YY-STRESS XY STRESS STRN-XX
STRN-YY STRN-XY

CONVERGENCE CODE= 1
NORM. OF RESIDUAL SUM RATIO= 0.1000E+03
MAXIMUM RESIDUAL= 0.4719E-03

CURRENT ITERATION NO.= 2

ELEMENTS THAT HAVE JUST FAILED
EL. NO. MAT NO. ID NO. FAILURE CODE XX-STRESS YY-STRESS XY STRESS STRN-XX
STRN-YY STRN-XY

CONVERGENCE CODE= 0
NORM. OF RESIDUAL SUM RATIO= 0.0000E+00
MAXIMUM RESIDUAL= 0.0000E+00

LOAD APPLIED EXTERNALLY ----- 7.409472KN
CPU TIME USED = 355.769

INCREMENT NUMBER= 2
LOAD APPLIED EXTERNALLY ----- 14.818944KN

LEVEL---- 33 NO. ELEMENT
 LEVEL---- 65 NO. ELEMENT

```

      *           *           *           *           *           *
      *           *           *           *           *           *
      *           *           *           *           *           *
    
```

INCREMENT NUMBER= 5

LOAD FACTOR = 4.500
 CONVERGENCE TOLERANCE = 1.000
 MAXIMUM NO.OF ITERATION = 20
 INITIAL OUTPUT PARAMETER = 0
 FINAL OUTPUT PARAMETER = 0

CURRENT ITERATION NO.= 1

ELEMENTS THAT HAVE JUST FAILED

EL. NO.	MAT NO.	ID NO.	FAILURE CODE	XX-STRESS	YY-STRESS	XY STRESS	STRN-XX	STRN-YY	STRN-XY
261	3	30	11	0.2118E+00	-0.1543E+01	-0.6123E+00	0.4044E+00	-0.1735E+01	0.1625E+03
293	3	30	11	0.2644E+00	-0.1431E+01	-0.5643E+00	0.4350E+00	-0.1602E+01	0.1632E+03

CONVERGENCE CODE= 1
 NORM. OF RESIDUAL SUM RATIO= 0.1111E+02
 MAXIMUM RESIDUAL= 0.2360E-03

CURRENT ITERATION NO.= 2

ELEMENTS THAT HAVE JUST FAILED

EL. NO.	MAT NO.	ID NO.	FAILURE CODE	XX-STRESS	YY-STRESS	XY STRESS	STRN-XX	STRN-YY	STRN-XY
261	3	30	11	0.2374E+00	-0.1555E+01	-0.6115E+00	0.4262E+00	-0.1743E+01	0.1628E+03
293	3	30	11	0.2978E+00	-0.1444E+01	-0.5641E+00	0.4645E+00	-0.1611E+01	0.1635E+03

CONVERGENCE CODE= 0
 NORM. OF RESIDUAL SUM RATIO= 0.9202E-02
 MAXIMUM RESIDUAL= 0.1075E-05

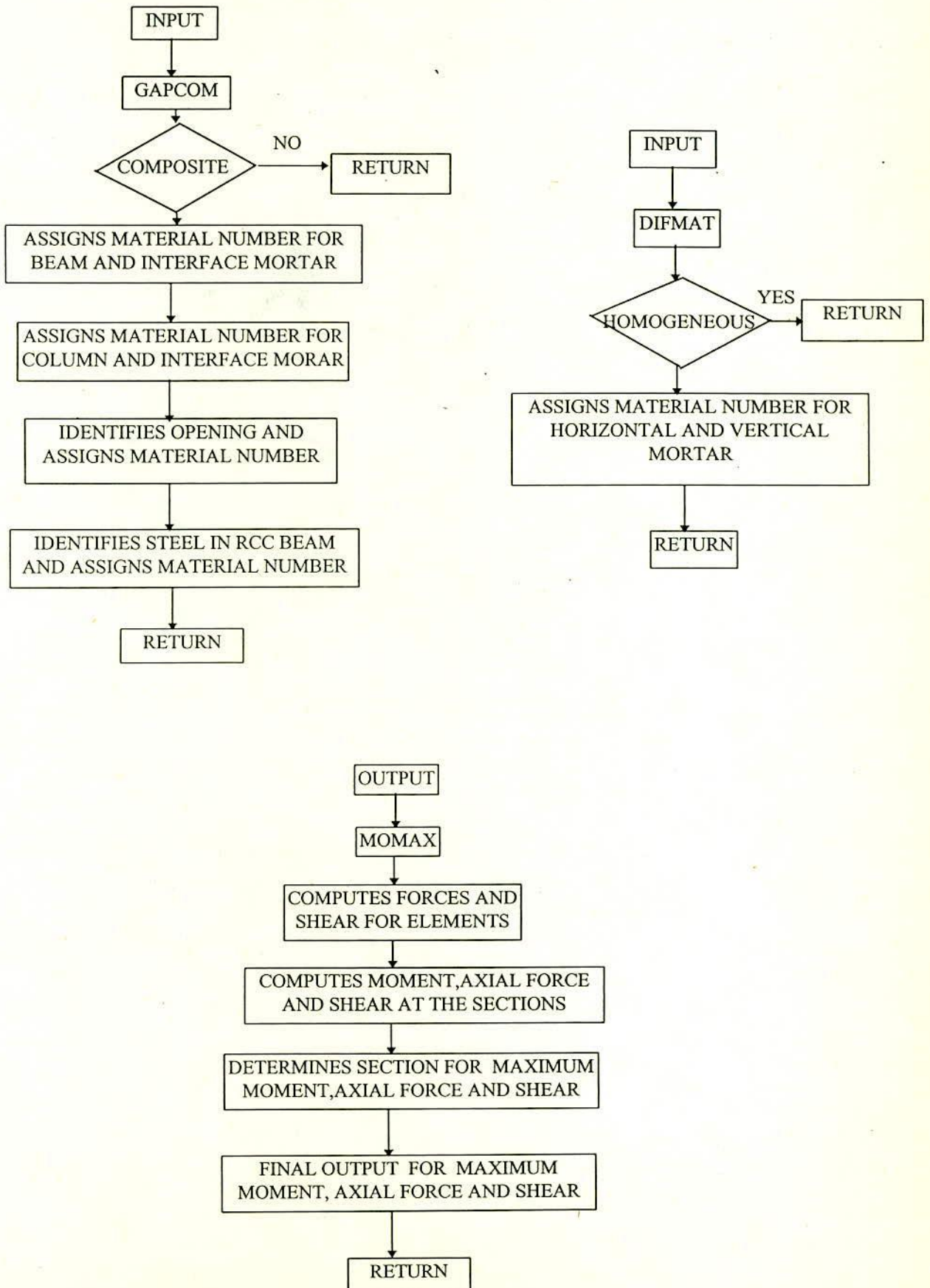
LOAD APPLIED EXTERNALLY ----- 33.342625KN
 * * *
 * * *

INCREMENT NUMBER= 6

```

      *           *           *
      *           *           *
    
```

Program structure for new or modified subroutines



APPENDIX IV

EXPERIMENTAL VERIFICATION OF THEORETICAL MODEL

Content

Comparison of Non-linear Analysis with Elastic Analysis

Fig. AIV.1 Horizontal Strain Through Mid Vertical Section of Plane Wall-beam :

(a) At the Load of 44.5 kN.

(b) At the Load of 112 kN.

(c) At the Load of 290 kN.

(d) At the Load of 312 kN.

(e) At the Load of 424 kN.

Fig. AIV.2(a) Failure of Wall-beam Panel with Opening (back side)

Fig. AIV.2(b) Failure of Wall-beam Panel with Frame (back side)

Fig. AIV.2(c) Failure of Plane Wall-beam Panel (back side)

Fig. AIV.3 Vertical Strain in Brick at Bottom Corner of Panels with
Progress of Load (Experimental)

Table AIV.1 28 Day Compressive Strength of 50 mm Mortar Cubes

NON-LINEAR ANALYSIS vs. ELASTIC ANALYSIS

For this purpose the analysis of a plane wall-beam (see Fig. 7.4(c)) carried out by model "B" (Non-linear analysis with softening, abbreviated as "NLA") was compared with elastic analysis, abbreviated as "EA". In the latter case the specified load was not applied in incremental steps. The finite element discretization and elastic properties of constituent materials are same for both cases. Comparison gives an indication of the degree of stress redistribution taking place due to progressive failure of the elements and non-linear material properties. Horizontal strains at the mid vertical section of the panel at different loads are shown in Fig. AIV.1(a to e). At load of 44.5 kN and 112 kN (which is about 10 % and 24 % of the ultimate test load), a stage before the onset of initial crack, there is practically very little difference between the horizontal strain predicted by the non-linear fracture analysis and the elastic analysis (see Fig. AIV.1(a, b)). The difference becomes more pronounced at greater loads. Significant stress redistribution occurs in the non-linear model due to progressive cracking and local failure. This results reduction in the compressive stresses in the lower half of the panel and an increase in the compressive stresses near the top of the panel in comparison to those obtained from elastic analysis having the same load on the top of the wall. At higher loads the higher horizontal strain near the top of the panel (see Fig. AIV.1(c to e)) corresponds to the increase in the arching action between the supports with the increase of the applied load. This is because at higher loads the cracks in progress continuously shifts the neutral axis in up ward direction until the crack fails to penetrate in the arching zone under highly biaxial compressive state of stress. High tensile strain encountered in the wall above the supporting beam at mid span is representative to the failure pattern of the plane wall-beam (see Fig. 7.4(c)).

The changing behaviour of the composite panel as predicted by non-linear analysis is shown by the strain distribution in the section through the centre span. Once wall-beam separation occurs or the mortar elements at the interface of wall and beam fail (at a load level approximately 60 - 70 % of the test load) there is a marked change in the stress distribution within the supporting beam (see Fig. AIV.1(e)). With partial loss of composite action, the bottom reinforcement of the supporting beam undergoes a sudden increase in tensile force. While in the elastic solution composite action is assumed throughout the load history which predicts considerably lower tensile force in the bottom steel. Therefore, the discussion reveals that for heavy loads the proportioning of the reinforcement for the supporting beam should be governed by non-linear fracture analysis.

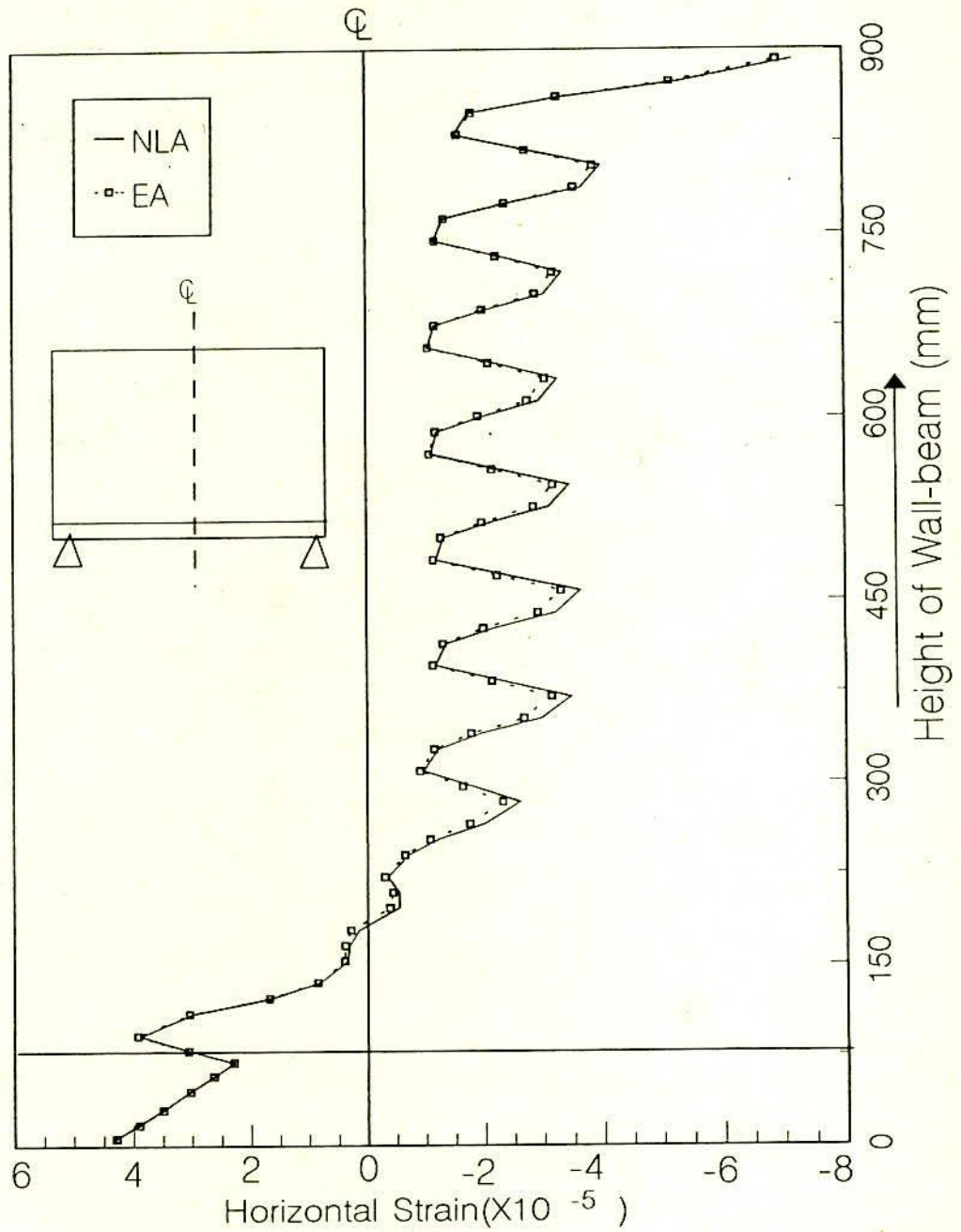


Fig. AIV.1(a)-Horizontal Strain at Mid Vertical Section at the Load of 44.5 kN..
(Plane Wall-beam)

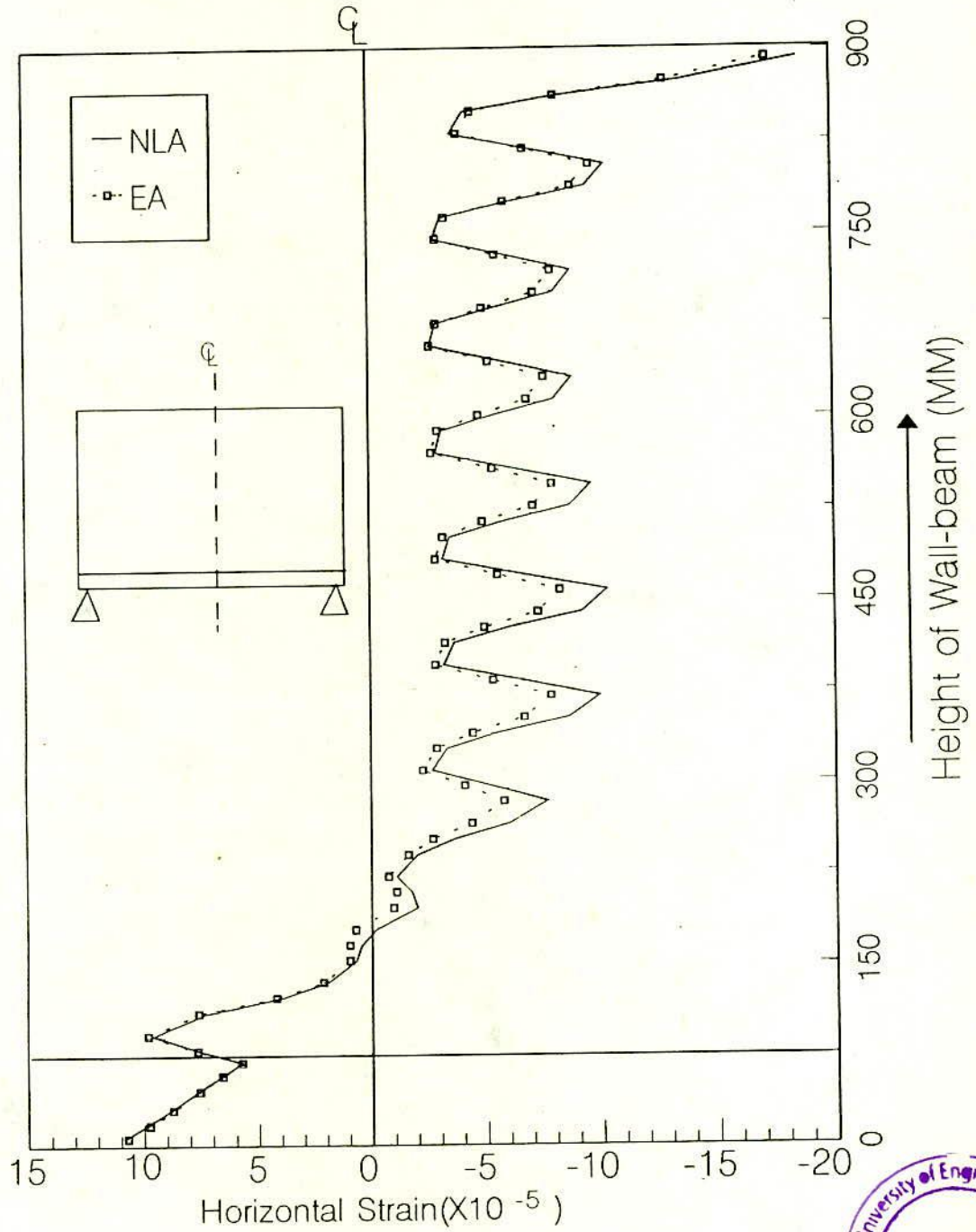


Fig. AIV.1(b)-Horizontal Strain at Mid Vertical Section at the Load of 112 kN..
(Plane Wall-beam)



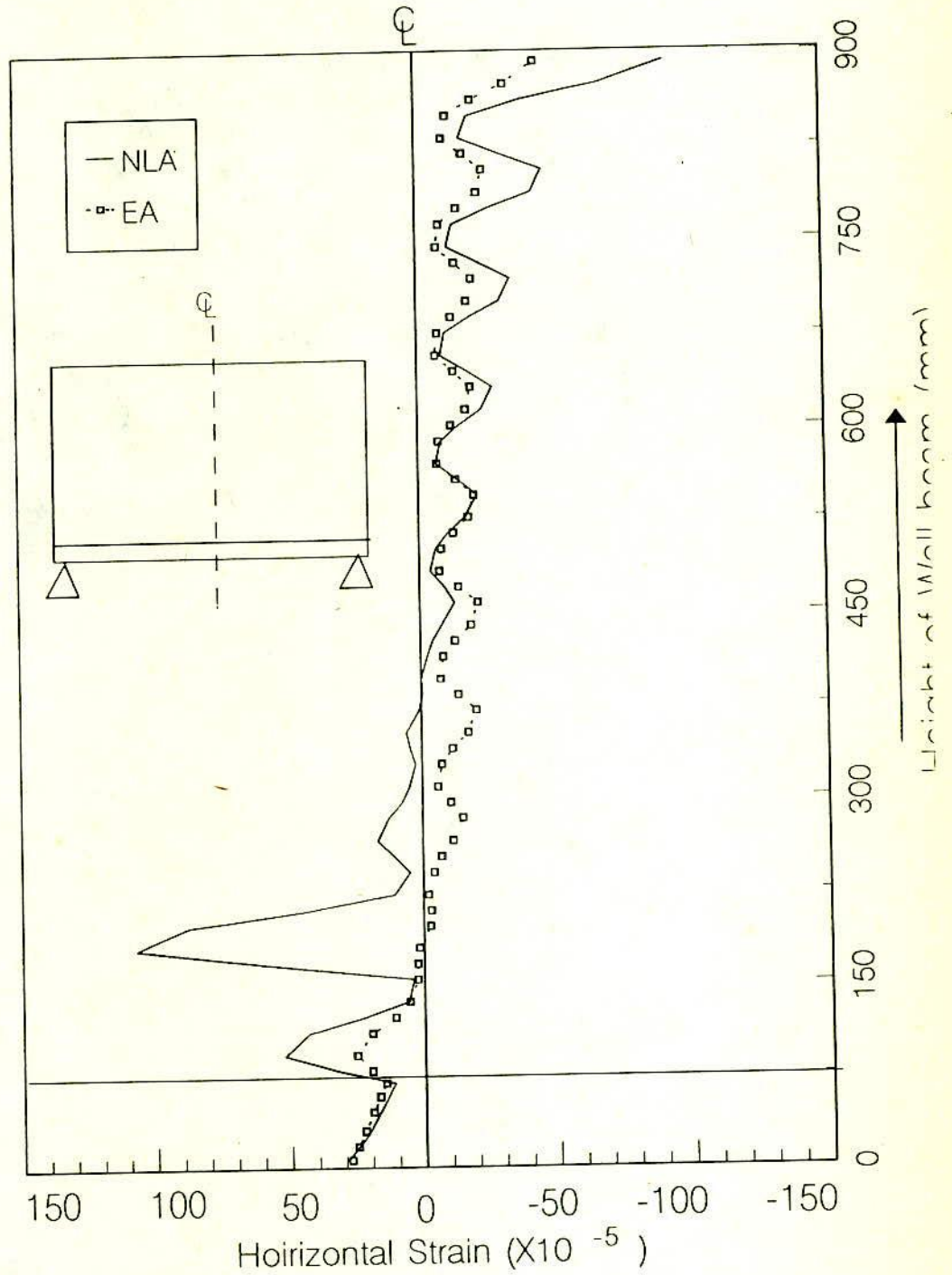


Fig. AIV.1(c)-Horizontal Strain at Mid Vertical Section at the Load of 290 kN..
(Plane Wall-beam)

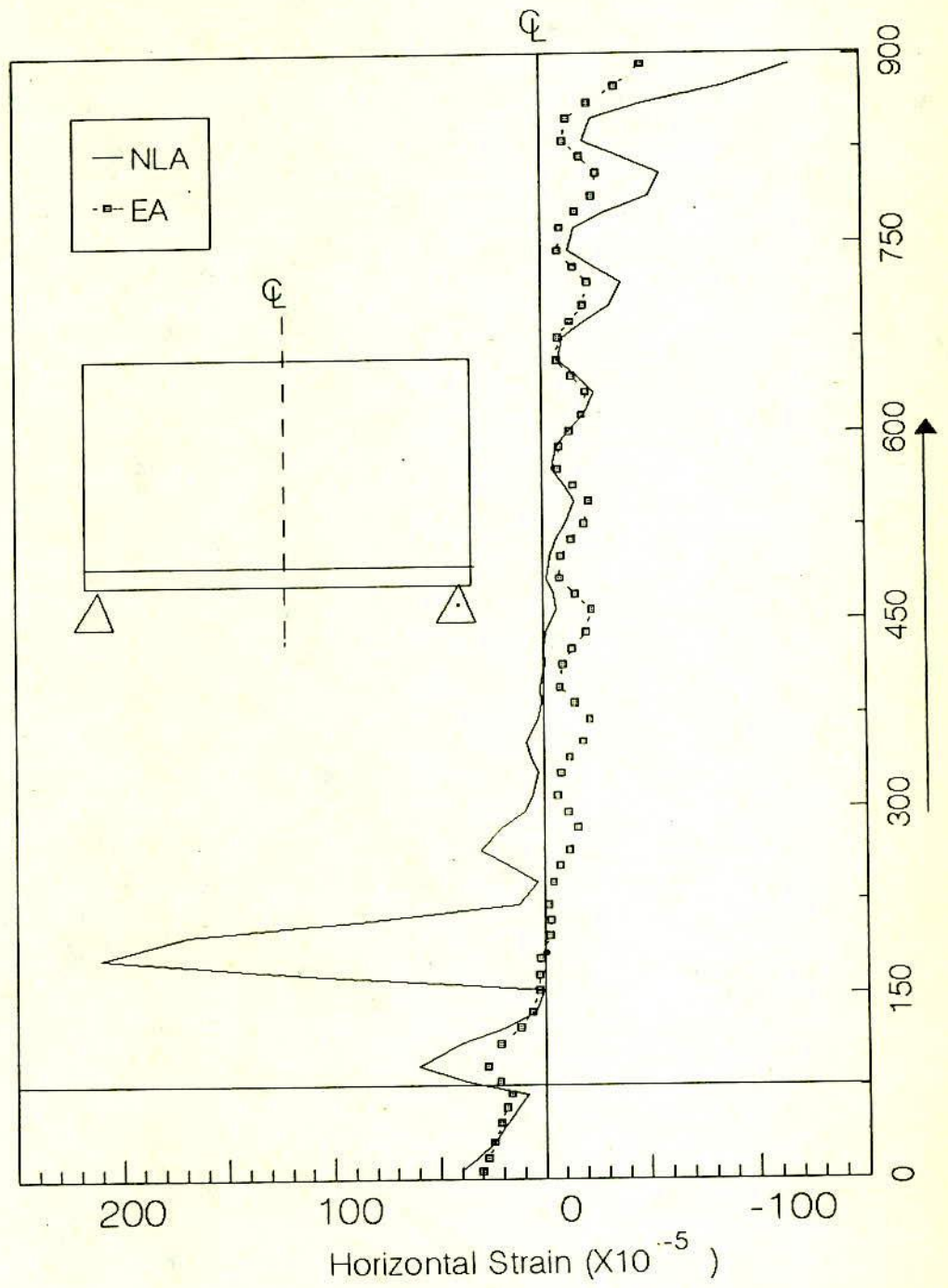


Fig. AIV.1(d)-Horizontal Strain at Mid Vertical Section at the Load of 312 kN..
(Plane Wall-beam)

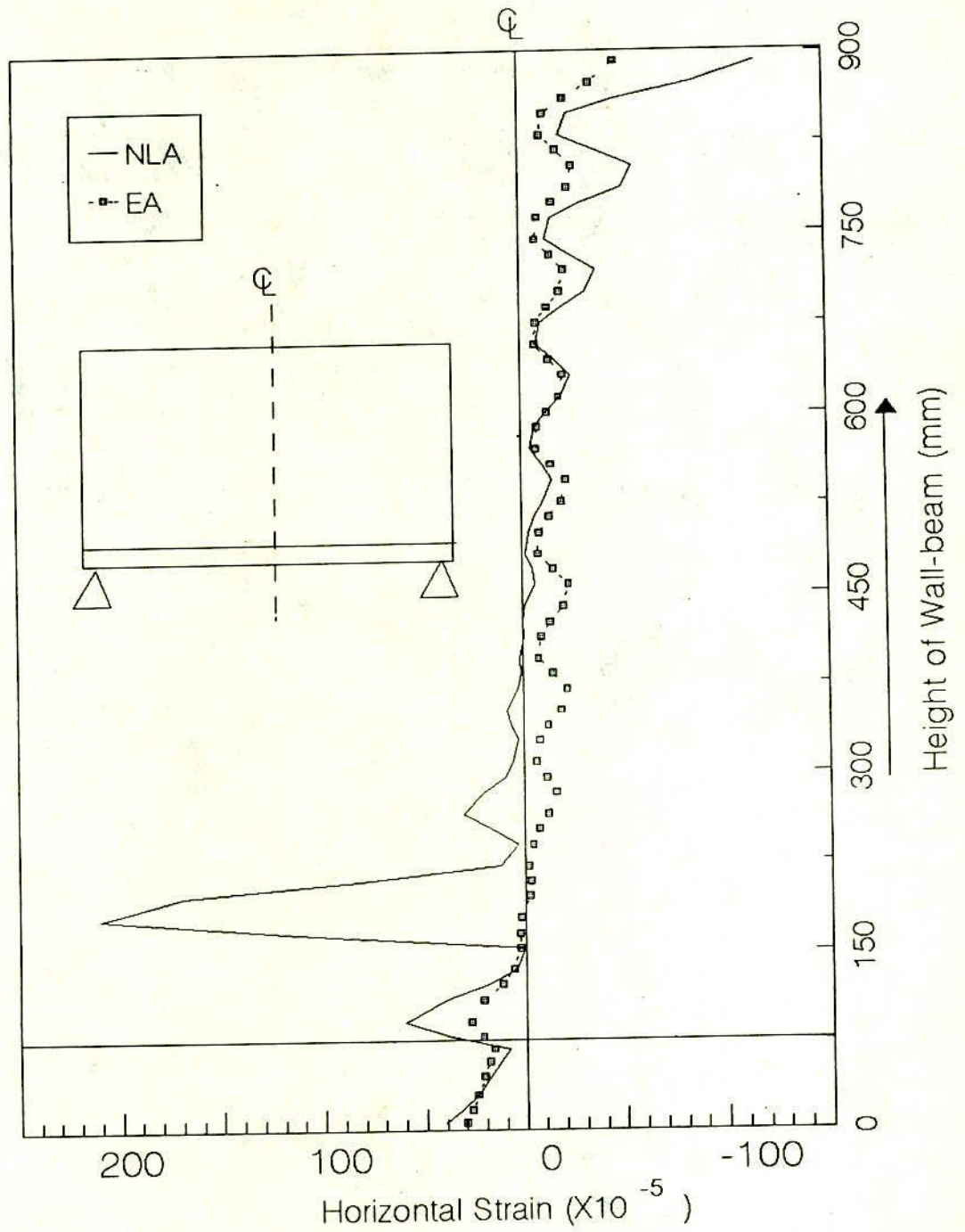


Fig. AIV.1(e)-Horizontal Strain at Mid Vertical Section at the Load of 424 kN..
(Plane Wall-beam)

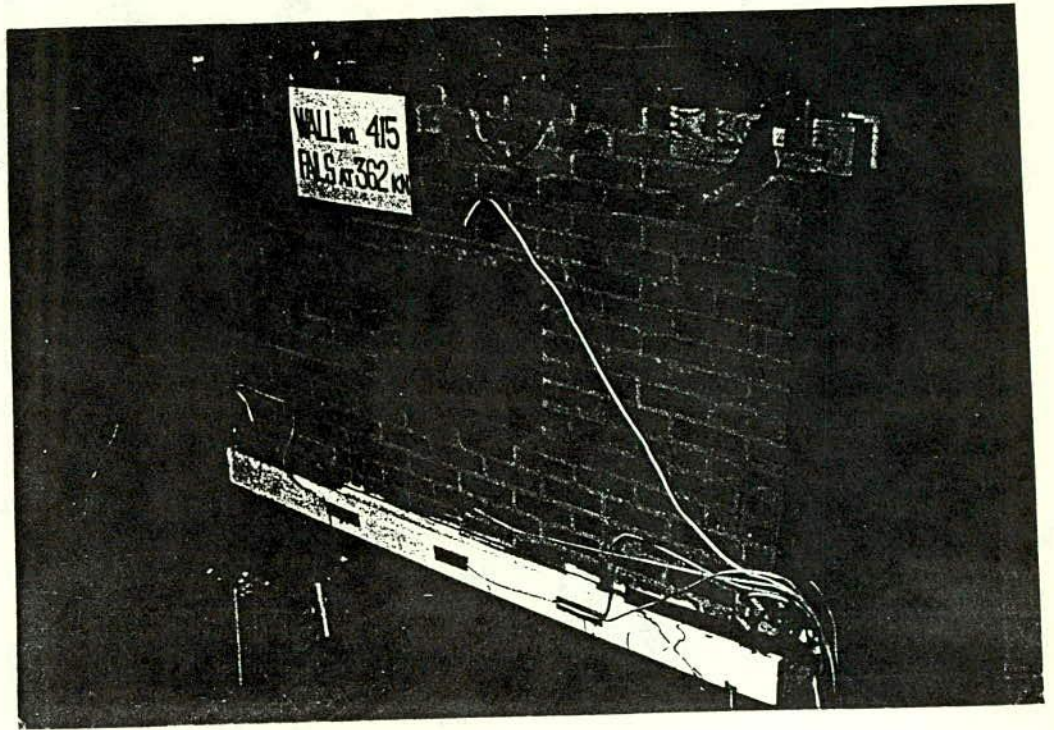


Fig. AIV.2(a) Failure of Wall-beam Panel with opening (back side)

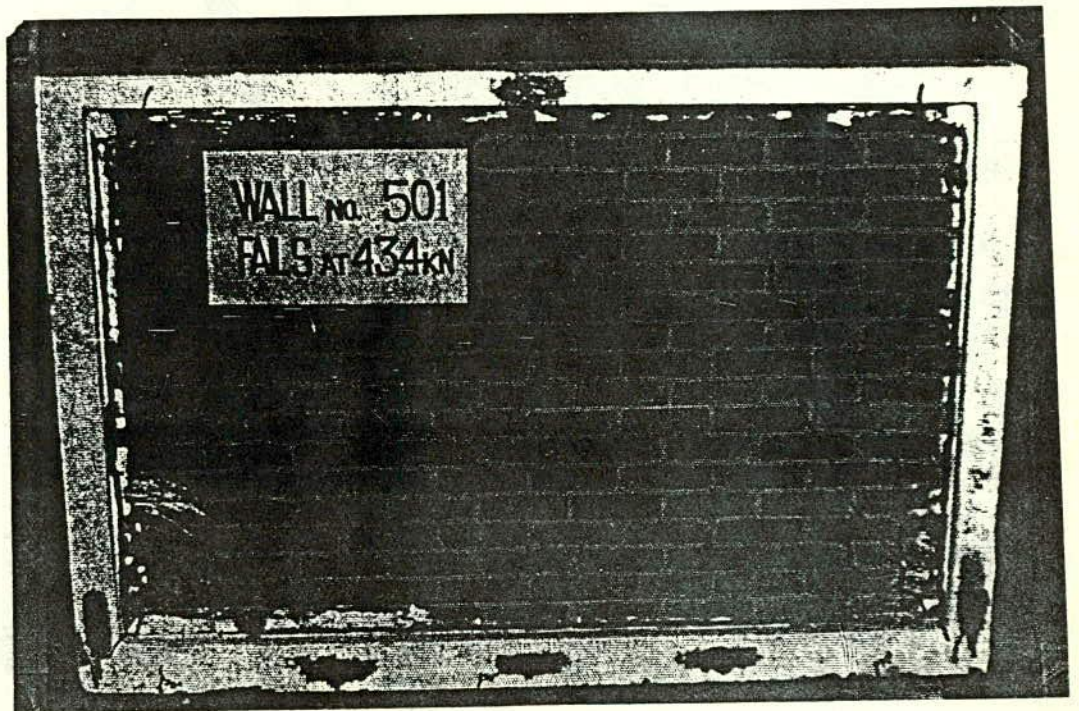


Fig. AIV.2(b) Failure of Wall-beam Panel with frame (back side)

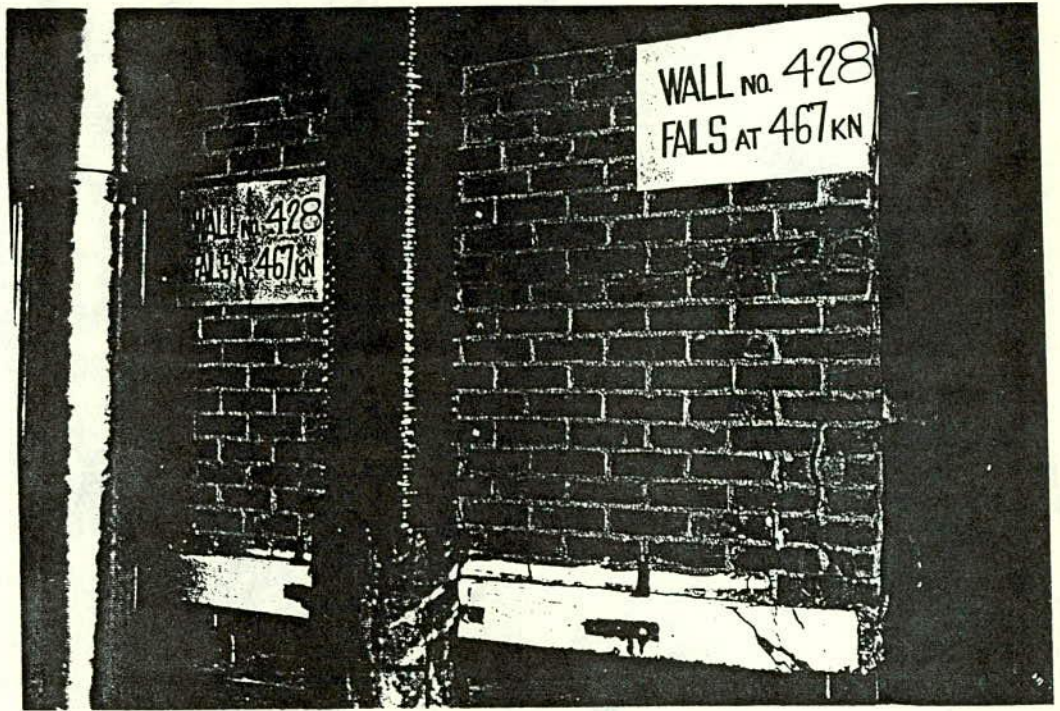


Fig. AIV.2(c) Failure of Plane Wall-beam Panel (back side)

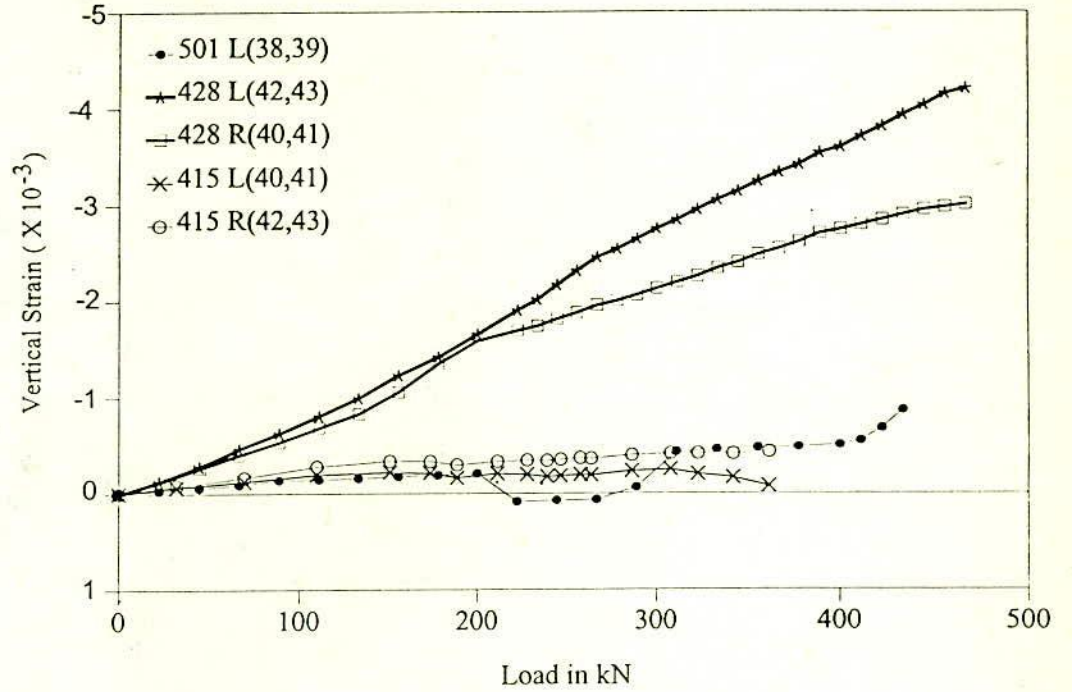


Fig. AIV.3 Vertical Strain in Brick at Bottom Corner of Panels with Progress of Load (Experimental)

Table AIV.1

28 Day Compressive Strength of 50mm Mortar Cubes

Sp. No.	Batch No.	Mortar Cubes	
		Ultimate Load (kN)	Comp. Str. (MPa)
1	1	31.5	12.6
2	"	31	12.4
3	"	32.4	12.9
4	2	35	14
5	"	33.3	13.3
6	"	32.4	12.9
7	3	32	12.8
8	"	34	13.5
9	"	34.5	13.8
— x s	•	32.9	13.13
C. of V (%)		1.38	.55
		4.2	4.2

APPENDIX V

PARAMETRIC STUDY AND DESIGN RECOMMENDATIONS

Contents

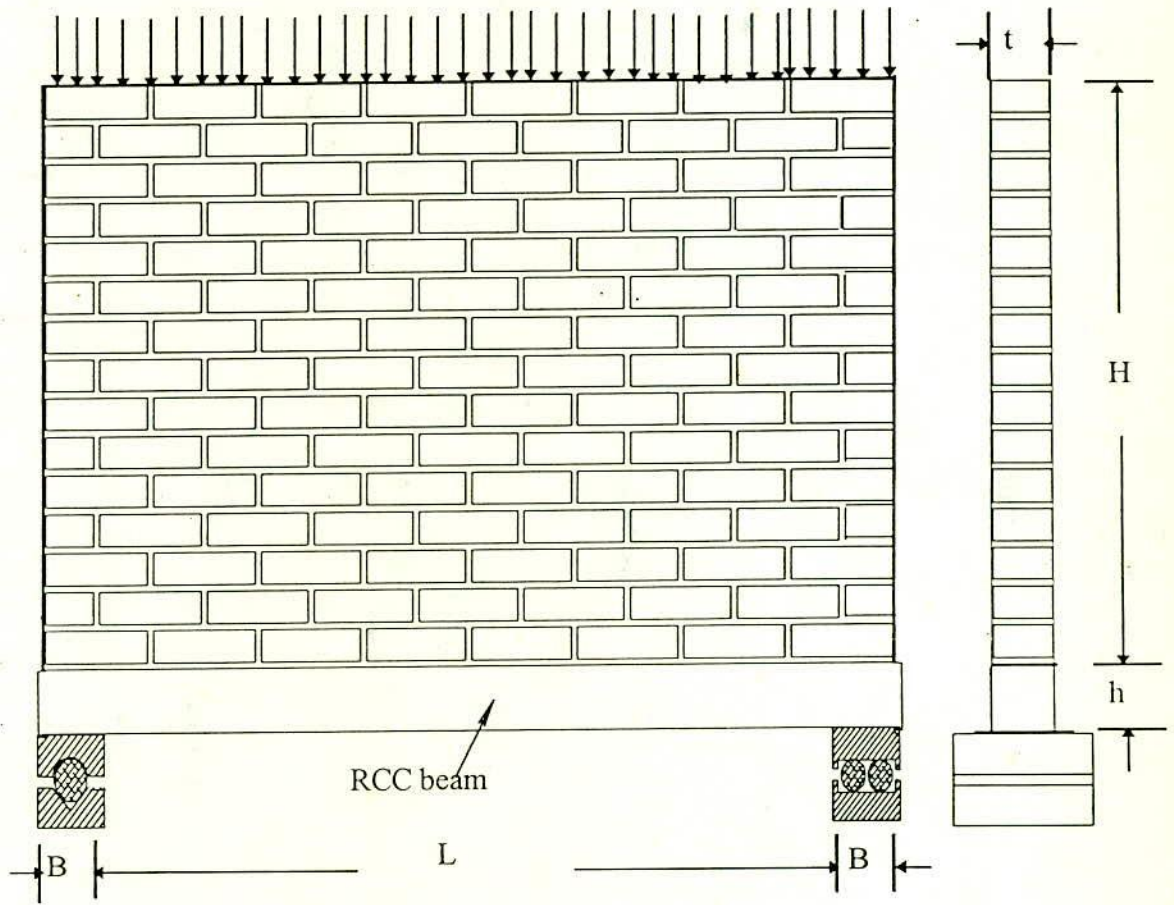
Fig. AV.1 Storey High Wall-beam for Parametric Study

Fig. AV.2 Finite Element Mesh with Different Number of Elements

Table A V.1 Coefficient for Max. Moment K_2

(considering shear at wall/beam interface)

Table A V.2 Summary of Elastic Analyses of End Supported Wall-beam.



$B= 50$ to 150 mm; $h=75$ to 175 mm; $H=1230$ mm; $L=2000$ mm; $t=115$ mm

Fig. AV.1 Storey High Wall-beam for Parametric Study

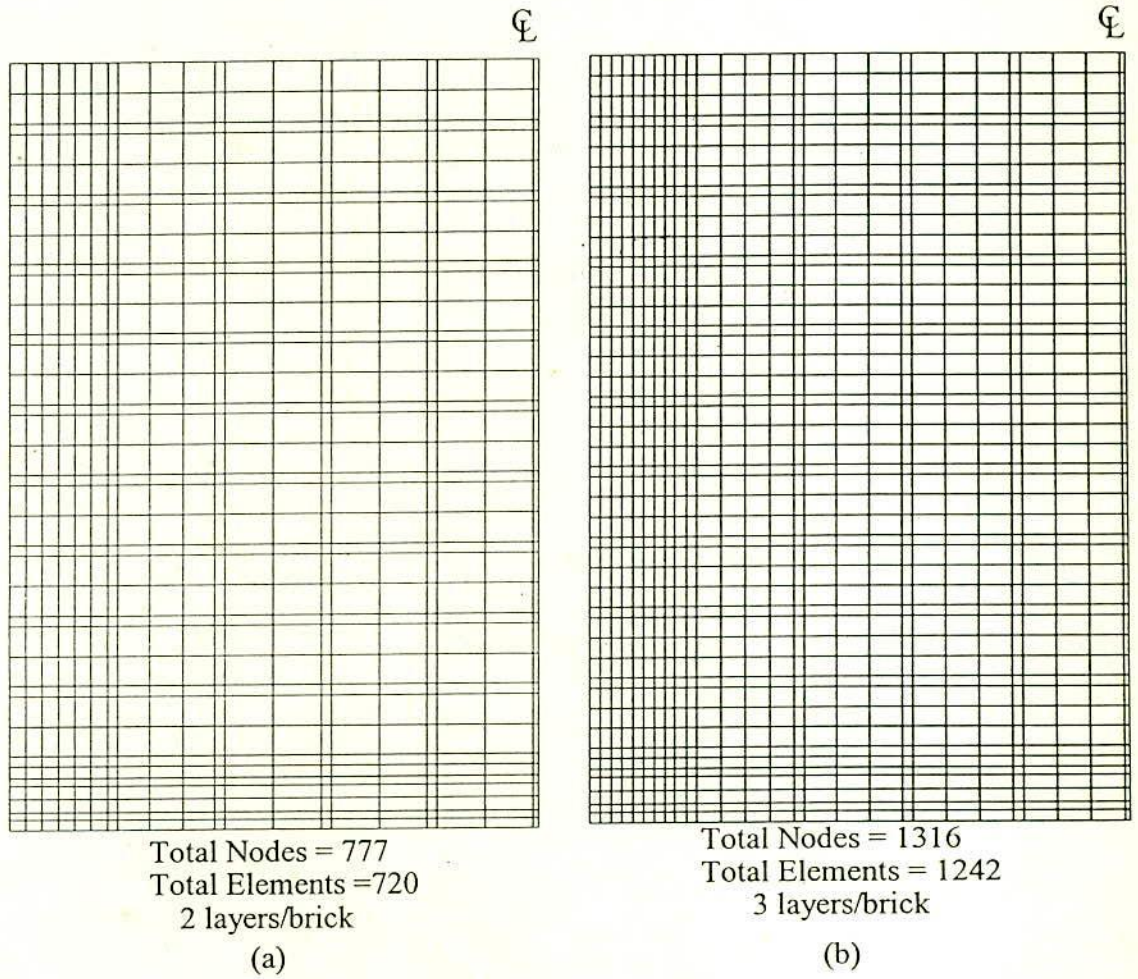


Fig. AV.2 Finite Element Mesh with Different Number of Elements

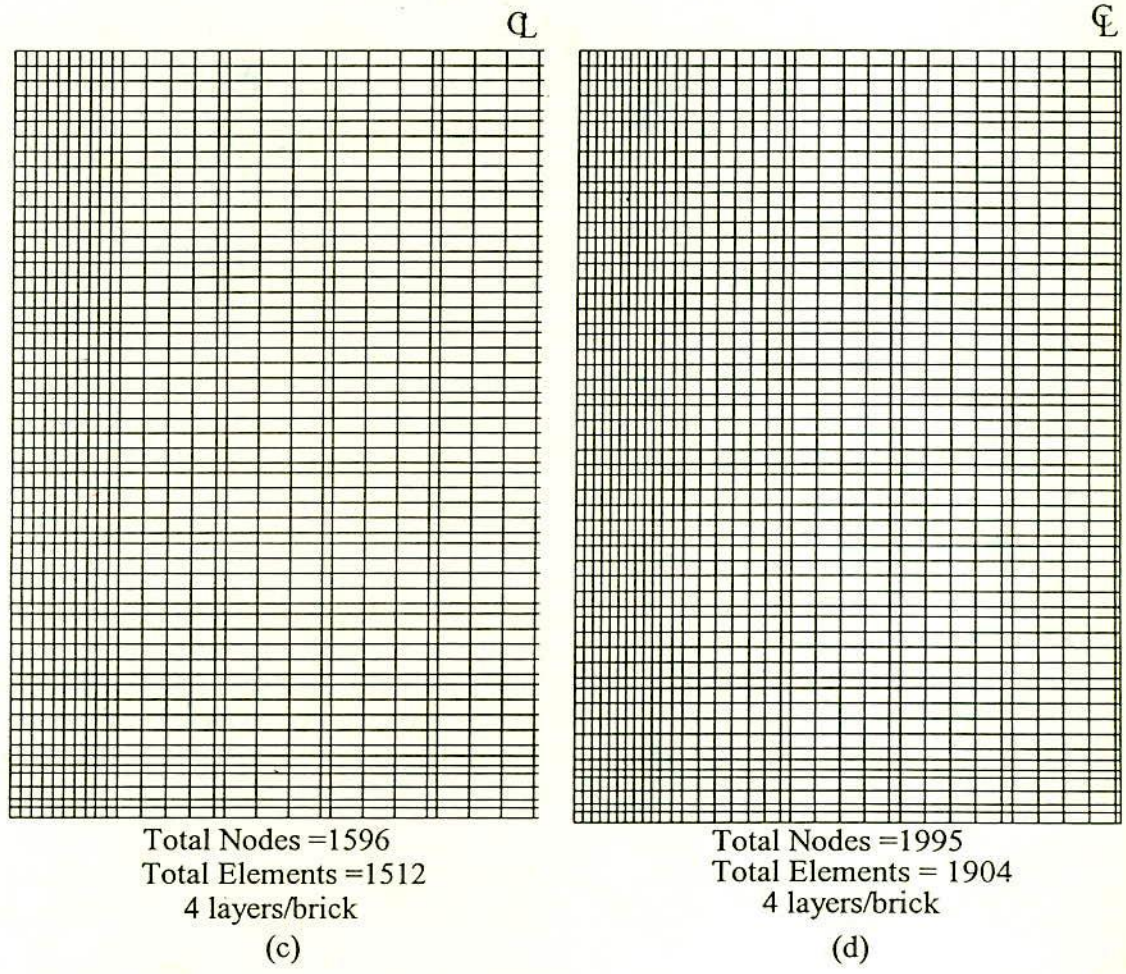
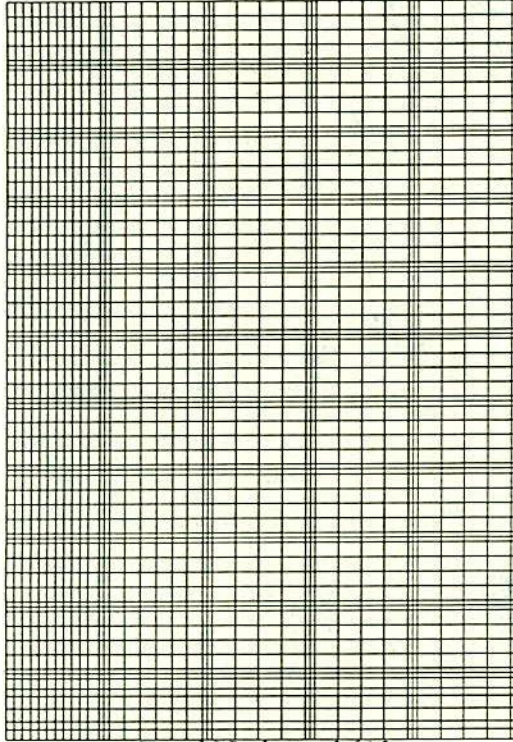
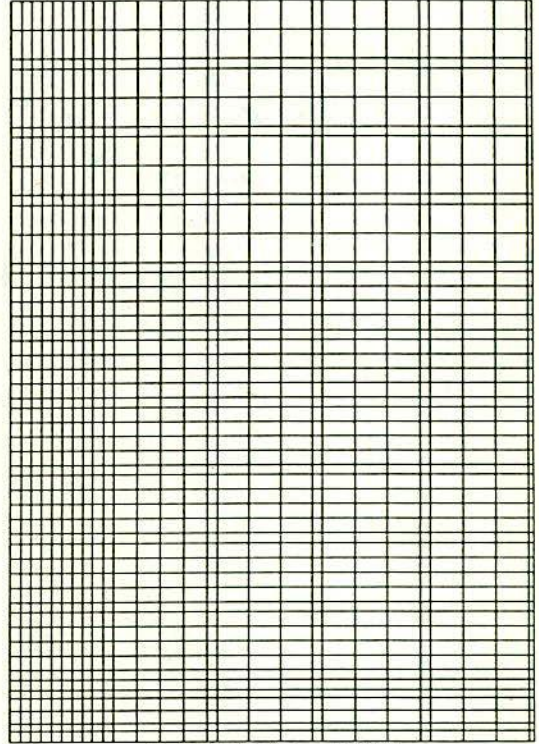


Fig. AV.2 Finite Element Mesh with Different Number of Elements

℄



Total Nodes = 2613
Total Elements = 2508
4 layers/brick
2 layers/bed joint
(e)



Total Nodes = 1372
Total Elements = 1296
4 layers/brick
2 layers/brick at top 1/3 rd
(f)

Fig. AV.2 Finite Element Mesh with Different Number of Elements

Table A V.2 Summary of Elastic Analyses of End Supported Wall-beam.

Maximum bending moment = WL / K1

K1= Coefficient of maximum bending moment

K2= Coefficient of max. bending moment considering shear force at wall-beam interface

Characteristic parameter $c_1 = \frac{E_w L - 2b}{E_c h}$

$E_w = \frac{E_b}{(\mu + \beta\Phi)}$ where, $\beta = \frac{E_b}{E_m}$, $\alpha = \frac{T_b}{T_m}$, $\Phi = \frac{1}{1 + \alpha}$, $\mu = \frac{\alpha}{1 + \alpha}$ $\mu=0.8536$, $\Phi=.1464$

L-2b	Em	Eb	β	Ew	Kc			K1			K2		
					75	125	175	75	125	175	75	125	175
2004	1635	8950	5.474	5408	5.05	3.03	2.16	108.6	67.5	48.5	168.4	108	81.7
		13425	8.211	6531	6.1	3.66	2.62	112.2	70	50.5	173.4	112	85.8
		1790	10.95	7287	6.81	4.08	2.92	114	71.2	51.6	175.8	115	87.4
		22375	13.68	7831	7.31	4.39	3.13	115.6	72.3	52.5	177.9	117	88.6
	2453	8950	3.648	6450	6.03	3.62	2.58	114.7	70.8	51	182.2	116	87.4
		13425	5.473	8113	7.58	4.55	3.25	119.3	73.8	53.5	189.3	122	90.8
		17900	7.297	9314	8.70	5.22	3.73	122	75.6	55	193	124	92.8
		22375	9.121	10222	9.55	5.73	4.09	124.2	77.1	56.1	196	126	94.3
	3270	8950	2.737	7135	6.67	4.00	2.86	118.4	72.8	52.5	191.7	121.4	90.1
		13425	4.105	9230	8.62	5.17	3.69	123.9	76.4	55.4	200.4	127	94.1
		17900	5.474	10816	10.1	6.06	4.33	127.1	78.6	57	203.8	130	96.3
		22375	6.842	12060	11.3	6.76	4.83	129.5	80	58.3	206.5	132	98.1
	4088	8950	2.189	7623	7.12	4.27	3.05	121.9	74.3	53.6	198.7	125	92
		13425	3.284	10061	9.4	5.64	4.03	127.1	78.2	56.6	207.4	131	96.4
		17900	4.378	11977	11.2	6.71	4.80	130.6	80.5	58.5	211.5	134	99
		2237	5.473	13521	12.6	7.58	5.41	133.4	82.1	59.8	214.6	137	101

Table A V.2 contd.

K = Coefficient of tie force in the supporting beam

Vc = Vertical stress concentration

Sc = Shear Stress Concentration

L-2b	Em	Eb	β	Ew	K			Vc			Sc		
					75	125	175	75	125	175	75	125	175
2004	1635	8950	5.474	5408	4.79	4.13	3.73	19.26	12.82	9.72	3.85	2.79	2.15
		13425	8.211	6531	4.94	4.29	3.85	19.33	12.84	9.72	3.86	2.74	2.22
		17900	10.95	7287	5.03	4.38	3.94	19.38	12.8	9.71	3.88	2.77	2.25
		22375	13.68	7831	5.14	4.47	4.02	19.34	12.8	9.67	3.89	2.77	2.26
	2453	8950	3.648	6450	4.84	4.28	3.86	20.23	13.38	10.1	4.16	2.79	2.23
		13425	5.473	8113	5.08	4.48	4.04	20.34	13.45	10.13	4.16	2.86	2.32
		17900	7.297	9314	5.21	4.6	4.17	20.48	13.48	10.14	4.16	2.9	2.36
		22375	9.121	10222	5.32	4.72	4.29	20.48	13.46	10.10	4.15	2.9	2.38
	3270	8950	2.737	7135	4.94	4.37	3.94	20.82	13.7	10.31	4.38	2.8	2.28
		13425	4.105	9230	5.17	4.6	4.14	21.04	13.8	10.36	4.38	2.94	2.38
		17900	5.474	10816	5.31	4.7	4.33	21.17	13.86	10.38	4.36	2.98	2.43
		22375	6.842	12060	5.44	4.87	4.44	21.2	13.86	10.36	4.35	2.98	2.45
	4088	8950	2.189	7623	4.99	4.43	4.01	21.22	13.93	10.45	4.56	2.9	2.3
		13425	3.284	10061	5.22	4.66	4.26	21.48	14.05	10.51	4.55	3.0	2.41
		17900	4.378	11977	5.38	4.83	4.42	21.64	14.11	10.53	4.53	3.03	2.47
		22375	5.473	13521	5.53	4.97	4.85	21.69	14.12	10.52	4.5	3.04	2.49

END